



HAL
open science

A novel, evolutionarily conserved transcription factor that regulates the inflammatory response

Alexia Pavlidaki

► **To cite this version:**

Alexia Pavlidaki. A novel, evolutionarily conserved transcription factor that regulates the inflammatory response. Human health and pathology. Université de Strasbourg, 2021. English. NNT : 2021STRAJ026 . tel-04213508

HAL Id: tel-04213508

<https://theses.hal.science/tel-04213508v1>

Submitted on 21 Sep 2023

HAL is a multi-disciplinary open access archive for the deposit and dissemination of scientific research documents, whether they are published or not. The documents may come from teaching and research institutions in France or abroad, or from public or private research centers.

L'archive ouverte pluridisciplinaire **HAL**, est destinée au dépôt et à la diffusion de documents scientifiques de niveau recherche, publiés ou non, émanant des établissements d'enseignement et de recherche français ou étrangers, des laboratoires publics ou privés.



UNIVERSITÉ DE STRASBOURG

ÉCOLE DOCTORALE DES SCIENCES DE LA VIE ET DE LA SANTÉ
INSTITUT DE GÉNÉTIQUE ET DE BIOLOGIE MOLÉCULAIRE ET CELLULAIRE

THÈSE

présentée par:

PAVLIDAKI ALEXIA

Soutenue le: 30 août 2021

Pour obtenir le grade de: **Docteur de l' Université de Strasbourg**

Mention: Sciences de la Vie et de la Santé

Discipline/S spécialité: Génétique, Biologie Moléculaire et Cellulaire

**UN NOUVEAU FACTEUR DE TRANSCRIPTION, CONSERVÉ AU COURS DE
L' ÉVOLUTION, QUI RÉGULE LA RÉPONSE INFLAMMATOIRE**

THÈSE dirigée par:

Mme GIANGRANDE Angela Directeur de recherche, IGBMC, Illkirch, France

RAPPORTEURS EXTERNES:

M KNOBELOCH Klaus-Peter Directeur de recherche, Institute of Neuropathology, Freiburg, Germany

M BIRMAN Serge Directeur de recherche, ESPCI, Paris, France

RAPPORTEURS INTERNE:

Mme GOLZIO Christelle Directeur de recherche, IGBMC, Illkirch, France

Σὰ βγεῖς στὸν πηγαμὸ γιὰ τὴν Ἰθάκη,
νὰ εὔχεσαι νᾶναι μακρὸς ὁ δρόμος,
γεμάτος περιπέτειες, γεμάτος γνώσεις.

...

Ἡ Ἰθάκη σ' ἔδωσε τ' ωραῖο ταξίδι.
Χωρὶς αὐτὴν δεν θάβγαινες στὸν δρόμο.
Ἄλλα δεν ἔχει νὰ σε δώσει πια.

Κι αν πτωχικὴ τὴν βρεις, ἡ Ἰθάκη δεν σε γέλασε.
Ἔτσι σοφὸς που ἔγινες, με τόση πείρα,
ἤδη θα το κατάλαβες ἡ Ἰθάκες τι σημαίνουν.

Ἰθάκη Κ. Π. Καβάφης

**As you set out for Ithaka
hope the voyage is a long one,
full of adventure, full of knowledge.**

...

**Ithaka gave you the marvellous journey.
Without her you would not have set out.
She has nothing left to give you now.**

**And if you find her poor, Ithaka won't have fooled you.
Wise as you will have become, so full of experience,
you will have understood by then what these Ithakas mean.**

Ithaka, K.P. Kavafis

Acknowledgments

The participation and guidance of many people led my exciting PhD journey to reach the desired accomplishment. A total of 4 years have passed filled with hard work, patience, determination and unforgettable memories, where I gained the best experience and enjoyed excellent science at the University of Strasbourg and the IGBMC. First of all, I would like to express my sincere gratitude to my advisor Dr. Angela Giangrande for her continuous guidance, motivation and support during my PhD. Without her comments and advice, I would not have reached my goals.

I would also like to express my special appreciation to my jury members: Dr Klaus-Peter Knobloch, Dr Serge Birman and Dr. Christelle Golzio for accepting to read and judge my work. Your achievements in the research field have broadened scientific knowledge.

To my lab colleagues, I will never forget all the joyful moments in the lab but also outside of it. To Dr. Pierre Cattenoz, I would like to thank him for his advice, support and guidance all throughout my PhD. To Mrs. Celine Riet, I would like to thank her for all the help during these four years. Without her support, many experiments would not have been accomplished. I would especially like to thank my good colleagues and friends, Dr Sara Monticelli and Rosy Sakr, for their continuous support during these years. I would also like to thank Mrs Claude Delaporte and Mrs Holy Andriamampianina for all their help during my *Drosophila* experiments. Finally, I would like to thank former lab member Dr. Yoshihiro Yuasa for all the help in the beginning.

Additionally, I would like to thank all my friends from Greece and France for standing by my side. During my stay in France, I gained not only friends but also people that I would consider as family. I would especially like to thank my best friends Despina Tzoumaka and Melanie Koumendea, for all their emotional support throughout. They are the sisters I never had and without them my life would not have been as interesting.

Finally, I would like to thank my family, whom I love so much, and to whom I dedicate my work. This includes my parents who continuously encourage me to follow my dreams, as well as my partner Benjamin March for all his support and emotional help over the last two years. Last but not least I would like to thank my bunnies, Pinkman and Dexter, for always making me smile after a hard day at the lab.

Also, I would like to thank the IGBMC and the Labex for supporting my PhD studies.

Table of Contents	
List of abbreviation	6
Résumé en Français	10
Summary in English.....	22
Introduction.....	34
Introducing the immune system.....	34
The transcription factor Gcm.....	37
Gcm is important for the development of the immune system of <i>Drosophila</i>	38
Activation of the immune system in <i>Drosophila melanogaster</i> and the role of Gcm in the immune response.....	40
Conservation of Gcm in evolution	43
The role of Gcm in the development of macrophages	46
Role of Gcm in the development of the immune system of invertebrates	47
Role of <i>Gcm</i> in the development of the immune system of vertebrates	48
Hematopoiesis in mammals.....	51
Microglia	Error! Bookmark not defined.
Microglia Development.....	54
Microglia functions during development and homeostasis	56
Microglia functions during an immune response	60
Microglia during aging	63
Microglia during autoimmune and neurodegenerative diseases.....	66
Materials and Methods.....	76
Mouse lines	76
Genotyping.....	76
Weight measurements and body composition.....	77
Metabolic cages	78
P1 primary CNS cultures	78
Tissue dissections.....	79
Phagocytosis Assay	79
Migration Assay	80
Immunolabelling	80
Confocal Imaging.....	82
Image Analysis.....	82
Fly strains	84
Hemocyte counting.....	85
Hemocyte Immunolabelling.....	85

Larval hemocyte RNA extraction and qPCR	86
Wasp survival and encapsulation assays	86
Paraquat Assay.....	87
Adult CNS dissection	87
Phagocytosis assay.....	88
Adhesion assay.....	88
Statistical analysis	88
Chapter I	92
Characterisation of the mGcm2 expression profile in mice	92
Introduction	92
Results.....	93
Characterisation of the mGcm2 expression profile during development	93
Characterisation of the mGcm2 expression profile during life span	94
.....	95
Characterisation of the mGcm1 and mGcm2 expression in CNS cultures.....	96
Discussion.....	100
mGcm2 is expressed during the primitive hematopoietic wave	101
mGcm2 is expressed again during aging in the microglia.....	101
Chapter II.....	105
Characterisation of the mGcm2 conditional knock out in CX3CR1-cre expressing cells	105
Introduction	105
Results.....	106
mGcm2 cko mice show increased weight compared to the controls.....	106
Neonatal and young adults mGcm2 cko mice have increased number of microglia	115
Microglia of mGcm2 cko mice have an activated morphology under basal conditions.....	117
mGcm2 cko animals have a pro-inflammatory profile	121
Discussion.....	125
mGcm2 cko animals show an increased weight compared to the controls	125
mGcm2 cko animals have increased microglia populations.....	126
mGcm2 cko animals show a more pro-inflammatory profile in the aged brain compared to the controls	127
Chapter III.....	130
Functional characterisation of mGcm2 <i>in vitro</i>	130
Introduction	130
Results.....	132
mGcm2 is decreased upon bead exposure but it does not control their phagocytosis	132

mGcm2 is not implicated in the migration of microglia <i>in vitro</i>	135
Discussion.....	137
Chapter IV	142
Study of Gcm expression during neuroinflammation in <i>Drosophila melanogaster</i>	142
Introduction	143
Results.....	146
<i>Gcm</i> is not re-expressed in the aged brain of <i>Drosophila</i>	146
<i>Gcm</i> is re-expressed in hemocytes upon α -Syn overexpression	149
Hemocytes enter the <i>Drosophila</i> CNS upon paraquat exposure.....	151
Discussion.....	153
Chapter V	155
Characterisation of Shot in the immune cells of <i>Drosophila melanogaster</i>	155
Introduction	156
Results.....	160
Evaluation of the transgenic lines of Shot	160
Shot actively participates during the encapsulation of wasp eggs.....	165
Discussion.....	166
Discussion and Perspectives	171
References	179

List of abbreviations

Abbreviation	Acronym
AD	Alzheimer's disease
AGM	Aorta-Gonad-Mesonephros
AIDS	Acquired immunodeficiency syndrome
AMP	Antimicrobial peptides
APOE	Apolipoprotein E
Arg-1	Arginase 1
BBB	Blood Brain Barrier
CAT	Catalase
CNS	Central Nervous System
CR3	Complement Receptor 3
CSF	Cerebrospinal Fluid
CSF1R	Colony Stimulating Factor 1 Receptor
CSPQ@CM	coated Cu ²⁺ -xSe-PVP-Qe
CX3CR1	CX3C motif Receptor 1
DAM	Damage Associated Microglia
DAMP	Damage Associated Molecular Pattern
DIO	Diet Induced Obesity
DMT	Disease Modifying Therapies
E(x)	Embryonic Day x
EAE	Experimental Autoimmune Encephalomyelitis
EMP	Embryonic Myeloid Progenitors
FcγRIIIB	Fc gamma receptor IIB
FOG	Friends Of GATA
Gcm/Glide	Glial cells missing/ Glial deficiency
GFP	Green Fluorescent Protein
GOF	Gain of Function
GPx	Glutathione Peroxidase
GWAS	Genome Wide Associated Studies
HFD	High Fat Diet
HSC	Hematopoietic Stem Cells
Iba-1	Ionized calcium Binding Adaptor molecule 1
IL	Interleukin
Imd	Immune deficiency
INF-γ	Interferon γ
iNOS	induced Nitric Oxygen Species
IRF8	Interferon Regulatory Factor
JAK/STAT	Janus kinases (JAKs) /Signal Transducer and Activator of Transcription proteins (STATs)
LB	Lewis Bodies
LCA	Leukocyte Common Antigen
LOF	Loss of Function
LRRK2	Leucine Rich Repeat Kinase 2
Lz	Lozange
MBP	Myelin Basic Protein
MHC II	Major Histocompatibility Class II

MiCs	MANF immunoreactive cells
MOG	Myelin Oligodendrocyte Glycoprotein
MS	Multiple Sclerosis
Nf-KB	Nuclear Factor kappa-light-chain-enhancer of activated B cells
NO	Nitrogen Oxygen
NPC	Neuronal Precursor Cells
NRF-2	Nuclear factor erythroid 2-related factor 2
P(x)	Postnatal Day x
PD	Parkinson's disease
PGRP-LG	peptidoglycan recognition protein-LC
PINK1	PTEN-induced kinase 1
PLP	proteolipid protein
PPO	Pro-Phenol Oxidase
PQ	Paraquat
ROS	Reactive Oxygen Species
scRNA sec	single cell RNA sequencing
SFA	Saturated Fatty Acids
SNpc	Substantia Nigra pars compacta
SOD	Superoxide Dismutase
Srp	Serpent
TBX1	T-Box 1
Th2	T helper cells type 2
TLR	Toll like Receptor
TMEM119	Transmembrane Protein 119
TNF- α	Tumor Necrosis Factor α
TREM-2	Triggering receptor expressed on myeloid cells 2
Ush	U-shaped
VTA	Ventral Tegmental Area
YFP	Yellow Fluorescent Protein
α -Syn	α -Synuclein

1. Introduction :

La défense contre le non-soi est une fonction ancienne des organismes vivants et les voies moléculaires contrôlant le développement des cellules immunitaires ou l'hématopoïèse sont extrêmement conservées (Evans, Hartenstein, & Banerjee, 2003). Typiquement, les facteurs de transcription des familles GATA, Notch, et RUNX contrôlent l'hématopoïèse tout au long de l'évolution (Avet-Rochex et al., 2010). En outre, un certain nombre de voies immunitaires telles que la voie JAK/STAT et la signalisation TLR sont également conservées au cours de l'évolution (Liongue, O'Sullivan, Trengove, & Ward, 2012; Song, Jin, Qin, Chen, & Ma, 2012). Ainsi, l'analyse de la réponse immunitaire de la drosophile constitue un grand avantage pour étudier les voies qui sont des acteurs clés de l'inflammation.

Le facteur de transcription *Glide/Gcm* est exprimé et requis dans la glie de la mouche ainsi que dans les hémocytes, les macrophages agissant à l'intérieur et à l'extérieur du système nerveux central (SNC), respectivement (Bernardoni, Vivancos, & Giangrande, 1997; Cattenoz & Giangrande, 2013, 2015; Jacques, Soustelle, Nagy, Diebold, & Giangrande, 2009). Notre laboratoire a caractérisé le rôle de *Glide/Gcm* dans les hémocytes, comme inhibiteur de la voie pro-inflammatoire JAK/STAT (Bazzi et al., 2018) et de la voie TOLL (en préparation). Le rôle et la conservation évolutive du gène *gcm* en font une cible intéressante pour analyser son rôle au cours de la neuroinflammation. Mon objectif est de transposer les résultats obtenus chez les mouches aux vertébrés.

Deux gènes orthologues sont présents chez les mammifères jusqu'à l'homme, *GCM1* et *GCM2*. Chez la souris, le knock out de *mGcm1* ou *mGcm2* est létal en raison de rôles cruciaux dans le placenta (*mGcm1*) et dans le développement des parathyroïdes (*mGcm2*), deux fonctions qui sont conservées dans les gènes *GCM* humains (Hashemolhosseini & Wegner, 2004).

Cependant, aucun rôle n'a été détecté dans le développement des cellules gliales et aucune étude n'a été réalisée dans le système immunitaire. Étant donné la forte conservation évolutive des voies immunitaires, j'ai émis l'hypothèse que les gènes Gcm pourraient avoir un rôle dans la modulation de la réponse immunitaire. Pour établir le profil d'expression de mGcm1 et mGcm2 dans les cellules immunitaires de la souris, nous avons d'abord analysé leurs niveaux de transcription par PCR quantitative dans les tissus adultes. La protéine mGcm2 est exprimée dans les trois principaux tissus hématopoïétiques : la moelle osseuse, la rate et le thymus. La protéine mGcm1 est exprimée à un niveau beaucoup plus faible. Des analyses par qRT-PCR sur des cellules triées ont révélé une large distribution d'expression de mGcm2 dans les cellules du système immunitaire, y compris les cellules microgliales.

Les cellules microgliales sont les cellules immunitaires innées du SNC. Ces cellules sont issues de la vague hématopoïétique primitive qui a lieu dans le sac vitellin au début de l'embryogenèse. Les progéniteurs de la microglie migrent ensuite dans le SNC en développement et finissent par se différencier. Contrairement à tous les autres macrophages spécifiques des tissus, la microglie est la seule population de macrophages résidents qui ne sera pas remplacée par d'autres macrophages issus de la vague hématopoïétique définitive. Cela fait de la microglie une population idéale pour étudier l'effet de la mGcm2 car chez la drosophile l'orthologue est spécifiquement exprimée dans la vague hématopoïétique primitive.

2. Objectifs :

- Caractériser le profil d'expression de mGcm2 (Immunomarquage anti-mGcm2 sur des embryons entiers et des sections de tissus adultes).
- Analyser le rôle de la mGcm2 dans la cellule microgliaie en phénotypant une lignée knock-out conditionnel (cko) (prolifération de la microglie, morphologie, expression de marqueurs inflammatoires et analyse phénotypique).
- Caractériser le rôle de la mGcm2 dans la cellule microgliaie *in vitro* en utilisant des culture primaires de souris néonatales cko (tests de phagocytose et de migration).
- Caractériser l'expression de Gcm chez la drosophile dans des conditions neuroinflammatoires.
- Caractériser l'expression de *short stop (shot)* dans les hémocytes de *Drosophila melanogaster* pendant l'homéostasie et lors d'une infestation par des guêpes.

3. Résultats :

mGcm2 est exprimée tôt au cours du développement dans le sac vitellin et dans les cellules de la cellule microgliaie du SNC des animaux âgés.

J'ai caractérisé le profil d'expression de la mGcm2 au cours du développement (de E7.5 à E16.5). Des cellules positives pour mGcm2 ont été observées dans le sac vitellin des embryons de E7.5 avec des marqueurs spécifiques des macrophages. Ce marquage est absent à d'autres stades développementaux. Ces résultats suggèrent que mGcm2 est exprimé de manière précoce et transitoire dans le système hématopoïétique, de manière similaire à ce qui a été décrit pour l'orthologue de la mouche.

Ensuite, j'ai caractérisé le profil d'expression de la mGcm2 dans différents tissus (cerveau, rate, tissu adipeux pulmonaire etc.) et groupes d'âge (postnatal 0 P0, P14, et 2,12 et 24 mois). Les résultats ont montré une expression dans les cerveaux de 12 et 24 mois mais pas chez les animaux de 2 mois. De plus, le double marquage de mGcm2 et CD45 (un marqueur courant de macrophages) n'a montré aucune expression dans les autres macrophages résidant dans les tissus. Ainsi, mGcm2 est exprimé uniquement dans le SNC des animaux âgés.

Les souris cko mGcm2 présentent une augmentation de poids

J'ai caractérisé la lignée cko mGcm2 *in vivo*. Pour cela, j'ai créé une cohorte initiale pour étudier la durée de vie des animaux cko. Tous les animaux ont été gardés à l'Institut Clinique de la Souris (ICS) sous un régime alimentaire normal. Afin de créer la lignée cko mGcm2 de cellules microgliales, j'ai utilisé la lignée CX3CR1-Cre. En tant que témoin, j'ai utilisé CX3CR1-Cre/+;mGcm2^{fllox/+}. De plus, tous les animaux ont été pesés une fois par semaine. Il n'y a pas de différence dans la durée de vie mais, de façon frappante, les animaux cko montrent une augmentation de poids par rapport aux témoins.

Pour confirmer ce phénotype, j'ai créé une deuxième cohorte. Ces souris ont été pesées une fois par semaine et ont subi des tests métaboliques. Plus précisément, j'ai effectué un test de composition corporelle et des cages métaboliques pendant 24h. Le premier test donne des informations sur le tissu maigre, la teneur en graisse et les fluides corporels libres. Ces tests n'ont révélé aucune différence entre les deux génotypes, même si le groupe cko avait un poids significativement plus élevé que le groupe témoin. Les cages métaboliques permettent de mesurer simultanément la dépense énergétique, l'activité ambulatoire ainsi que la consommation de nourriture et d'eau. Les résultats ont révélé une tendance à une plus grande consommation de nourriture et à moins de mouvements chez les souris cko, bien que les résultats ne soient pas statistiquement significatifs. Pour cette raison, il serait intéressant d'induire l'obésité chez les animaux cko et de voir si dans ces conditions les paramètres seront statistiquement significatifs. Même si le rôle de la microglie a été lié à l'hyperphagie et à l'obésité, mes données suggèrent pour la première fois que l'expression de mGcm2 dans la cellule microgliaie est impliquée dans l'homéostasie métabolique.

La perte de mGcm2 conduit à un état pro-inflammatoire de la microglie

J'ai caractérisé la population de la microglie *in vivo*. Tout d'abord, j'ai compté la population de cellules microgliales dans différentes régions et à différents stades (souris âgées de P0, P14, 4 et 24 mois), en collaboration avec le Dr Katrin Kierdorf de l'Université de Freiburg. Les cellules ont été marquées avec le marqueur spécifique de la microglie, Iba-1, et des comptages cellulaires ont été effectués dans différentes régions du cerveau. Les cerveaux cko présentent un nombre plus élevé de microglie à P14 et 4 mois par rapport aux témoins, ce qui pourrait indiquer un environnement pro-inflammatoire.

Mon objectif suivant était de voir si la cellule microgliaie des souris mutantes mGcm2 présente également des caractéristiques inflammatoires. Les microglies de surveillance ont une morphologie ramifiée avec des processus longs et fins. Au cours d'une inflammation ou du vieillissement, la microglie montre des signes d'une morphologie activée, moins ramifiée. Le marquage avec le marqueur spécifique de la microglie Iba-1 a montré que les animaux cko âgés de 2 et 12 mois n'ont pas une morphologie différente de celle des témoins. En revanche, les animaux cko âgés de 24 mois présentent moins de ramifications et une moindre zone de couverture. Dans l'ensemble, ces données suggèrent que l'absence de mGcm2 a un impact significatif sur la morphologie et l'état de la microglie.

La perte de mGcm2 dans la microglie entraîne une augmentation du nombre de cellules pro-inflammatoires positives.

Pour renforcer les données morphologiques, j'ai marqué le SNC de 2, 12 et 24 mois avec des marqueurs indicatifs d'un état inflammatoire. Les états d'activation des microglies/macrophages sont classés comme pro-inflammatoires (ou M1) ou anti-inflammatoires (ou M2). J'ai choisi induced Nitrogen Oxygen Species (iNOS) pour l'état M1 et Arginase-1 (Arg-1) pour l'état M2, deux marqueurs qui ont déjà été utilisés pour caractériser l'état de la microglie *in vivo* (Lisi et al., 2017 ; Cherry et al., 2017). J'ai évalué l'expression de ces deux marqueurs dans les microglies co-marquées avec Iba-1. Les animaux cko âgés de 24 mois ont significativement plus de microglies positives à iNOS par rapport aux témoins du même âge. De plus, les animaux cko âgés de 24 mois présentent une diminution significative des microglies positives à l'Arg-1 par rapport aux animaux cko âgés de 12 mois, alors que les animaux témoins d'âge comparable ne présentent pas de différence significative dans le marquage de l'Arg-1. Ces données suggèrent que les animaux cko ont plus de microglies

polarisées vers le phénotype M1 que les animaux témoins. Ceci valide mon hypothèse selon laquelle mGcm2 a un rôle anti-inflammatoire conservé au cours de l'évolution dans les cellules immunitaires de la vague hématopoïétique primitive.

Gcm est exprimé dans les hémocytes de *Drosophila melanogaster* dans des conditions neuroinflammatoires.

L'étape suivante consistait à examiner si le rôle de Gcm spécifiquement pendant la neuro-inflammation était conservé au cours de l'évolution. Chez les adultes de *Drosophila melanogaster*, Gcm est exprimé uniquement dans un sous-ensemble de neurones, mais il n'est pas exprimé dans la glie ni dans les hémocytes. J'ai d'abord suivi l'expression de Gcm au cours du vieillissement en utilisant une lignée transgénique qui retrace la lignée de toutes les cellules qui, à un moment donné de la vie adulte, expriment Gcm. En dehors du sous-ensemble de neurones déjà caractérisé, Gcm n'est pas exprimé dans le SNC des mouches âgées. Cependant, comme la durée de vie des mouches est beaucoup plus courte que celle des mammifères, j'ai émis l'hypothèse que le vieillissement pourrait ne pas être suffisant pour induire une expression *de novo* de Gcm dans un cerveau par ailleurs normal.

Pour cette raison, j'ai induit une réponse inflammatoire dans le SNC de mouches adultes en utilisant une lignée qui surexprime l' α -Synucléine dans tous les neurones en utilisant le système Lex A. La Synucléine- α est une protéine neuronale qui régule le trafic des vésicules synaptiques et la libération ultérieure de neurotransmetteurs. L'agrégation de cette protéine est liée à plusieurs maladies neurodégénératives telles que la maladie de Parkinson. La surexpression de la Synucléine- α a révélé l'existence de cellules positives à Gcm dans le SNC. Les cellules n'expriment ni marqueurs neuronaux ni marqueurs gliales, mais elles expriment des marqueurs hémocytaires. L'ensemble de ces données suggère que, lors d'une réponse neuro-inflammatoire, les hémocytes adultes expriment Gcm et pénètrent la barrière hémat-

encéphalique (BHE). L'invasion des hémocytes a également été confirmée par test paraquat (PQ). D'autres expériences devraient viser à confirmer si ces hémocytes ré-expriment également Gcm. Ainsi, Gcm s'avère être un nouveau facteur de la réponse immunitaire innée dans le SNC.

Caractérisation de la microglie mGcm2 cko *in vitro*

Mon objectif final était de relier l'expression de mGcm2 à une fonction du système immunitaire inné. La microglie, comme la plupart des cellules de l'immunité innée, a deux fonctions majeures : la phagocytose et la migration sur le site de l'inflammation. Au cours de mon doctorat, j'ai caractérisé l'expression de mGcm2 pendant la phagocytose ainsi que pendant la migration dans des cultures primaires de SNC et j'ai utilisé des animaux cko pour découvrir tout changement phénotypique.

J'ai d'abord évalué l'expression de mGcm2 dans les conditions basales des cultures et j'ai révélé sa présence spécifique dans un sous-ensemble de microglies de forme ronde (30% du nombre total de cellules rondes). Lors de la stimulation avec des billes de latex, les microglies phagocytent les billes à la fin de l'essai (t=120 min.). Le marquage des cultures de microglie stimulées montre une diminution significative des niveaux de la protéine mGcm2 tôt après la stimulation (t=20 min.), qui revient aux niveaux basaux (t=0 min.) après 120 min. Ceci m'incite à proposer que le processus de phagocytose affecte l'expression de mGcm2.

Afin d'évaluer si les niveaux de mGcm2 ont un impact sur la phagocytose, j'ai effectué le même test sur des cultures primaires de microglie mGcm2 cko. Pour effectuer une analyse quantitative, j'ai mesuré l'intensité de la fluorescence dans les cellules, qui reflète l'activité phagocytaire. Je n'ai trouvé aucune différence dans la capacité phagocytaire des microglies entre les animaux expérimentaux et les animaux témoins. Ce résultat me permet de proposer que mGcm2 ne contrôle pas la phagocytose des billes de latex.

En outre, lors d'une activation due à une blessure ou à des agents pathogènes, la microglie migre rapidement vers la zone enflammée et phagocyte les débris cellulaires ou les neurones endommagés. Pour mieux évaluer les rôles possibles de mGcm2 dans la microglie, j'ai supposé qu'il pouvait avoir un impact sur la migration et j'ai donc réalisé un test de migration par rayage en utilisant les mêmes cultures primaires de cellules microgliales que ci-dessus. La migration dans la cicatrice ouverte a été documentée par des microphotographies à différents moments après le grattage. Les résultats n'ont pas montré d'expression de mGcm2 dans les cellules de la microglie migrant vers la cicatrice. En outre, les cultures ont été évaluées pour leur capacité à fermer la plaie et pour savoir si l'absence de mGcm2 a un impact sur le processus de guérison. Je n'ai trouvé aucune différence entre les cellules cko et les cellules témoins, ce qui indique que mGcm2 n'affecte pas la migration de la microglie *in vitro*.

Caractérisation de l'expression de *short stop (shot)* dans les hémocytes de *Drosophila melanogaster* pendant l'homéostasie et lors d'une infestation par des guêpes parasitoïdes

En parallèle, j'ai travaillé dans l'effort d'équipe pour caractériser la population d'hémocytes de *Drosophila melanogaster* avec le séquençage de cellules uniques. Ma principale contribution au projet a été de relier les deux populations distinctes d'hémocytes, résidente et circulante, et de caractériser l'expression des marqueurs hémocytaires lors d'un défi immunitaire avec une infestation par des guêpes parasitoïdes. Les résultats de ce dernier ont révélé un nouveau marqueur pour les hémocytes et leur forme activée, les lamellocytes, *short stop (shot)*. Ce gène code pour un membre de la famille des spectraplakines, de grandes molécules de liaison du cytosquelette. Shot se lie à l'actine et aux microtubules, ainsi qu'aux protéines d'échafaudage, à certains facteurs de signalisation et au calcium. En outre, cette protéine joue un rôle dans le

développement et le maintien de plusieurs tissus du système nerveux, de l'épiderme, aux attaches musculaires, intestin antérieur, aile, trachées et ovocytes.

Mon projet a tenté de disséquer le rôle de Shot dans les hémocytes dans des conditions homéostatiques ainsi que lors d'un challenge immunitaire (infestation par des guêpes parasitoïdes). Les résultats montrent que Shot participe à l'adhésion des hémocytes *in vitro* et dans des conditions homéostatiques. Plus précisément, l'extinction de Shot en utilisant ARNi nuit à l'adhésion des hémocytes, tandis que sa surexpression entraîne une augmentation de l'adhésion par rapport aux témoins *in vitro*. L'extinction de Shot entraîne également une réduction de l'expression de la protéine N-Cadherin. Enfin, j'ai démontré que Shot joue un rôle central dans la réponse de la mouche à l'infestation par les guêpes, car les animaux n'exprimant pas Shot montrent une encapsulation réduite de l'œuf de guêpe 24 heures après l'infestation. Tous ces résultats suggèrent que Shot est un nouvel acteur dans l'adhésion entre les hémocytes et dans la formation de jonctions entre les cellules.

4. Conclusions

Mon travail met en évidence mGcm2 comme un nouveau facteur de transcription fonctionnant dans les cellules immunitaires présentes dans le SNC des mammifères. J'ai découvert que ce facteur de transcription est exprimé dans le sac vitellin de la souris, ce qui est similaire à l'expression précoce de Gcm pendant l'hématopoïèse embryonnaire chez *Drosophila melanogaster*. Les macrophages des mammifères de la vague hématopoïétique précoce migrent vers différents organes et donnent naissance aux macrophages résidents des tissus. Contrairement à toutes les autres populations résidentes des tissus, la cellule microgliaie est le seul type de cellule qui n'est pas remplacé par les nouvelles populations de macrophages de la vague hématopoïétique définitive. De plus, la cellule microgliaie est le seul type de cellule qui exprime mGcm2 au cours du vieillissement, un processus qui ressemble beaucoup à une réponse immunitaire. Enfin, j'ai montré que l'absence de mGcm2 conduit *in vivo* à un état pro-inflammatoire des cellules de la microglie. Ces données suggèrent un rôle important de mGcm2 dans le contexte de la neuro-inflammation et une conservation de sa fonction au cours de l'évolution. Je pense que mes travaux permettront de mieux comprendre la réponse immunitaire innée du SNC. A long terme, cela pourrait aider à comprendre les mécanismes physiopathologiques qui sous-tendent les maladies humaines telles que les maladies auto-immunes ou neurodégénératives, qui représentent un lourd fardeau pour nos sociétés.

Summary in English

1. Introduction:

The defence against non-self is an ancient function of living organisms and the molecular pathways controlling the development of immune cells or hematopoiesis are extremely conserved (Evans, Hartenstein, & Banerjee, 2003). Typically, the transcription factors of the GATA, Notch, and RUNX families control hematopoiesis throughout evolution (Avet-Rochex et al., 2010). In addition, a number of immune pathways such as the JAK / STAT pathway and TLR signalling are also conserved during evolution (Liongue, O'Sullivan, Trengove, & Ward, 2012; Song, Jin, Qin, Chen , & Ma, 2012). Thus, the analysis of the *Drosophila* immune response constitutes a great advantage for studying the pathways which are key players in inflammation.

The *Glide/Gcm* transcription factor is expressed and required in fly glia as well as in the hemocytes, the macrophages acting inside and outside the central nervous system (CNS), respectively (Bernardoni, Vivancos, & Giangrande, 1997; Cattenoz & Giangrande, 2013, 2015; Jacques, Soustelle, Nagy, Diebold, & Giangrande, 2009). Our laboratory has characterised the role of *Glide/Gcm* in hemocytes, as an inhibitor of the pro-inflammatory JAK / STAT pathway (Bazzi et al., 2018) and of the TOLL pathway (in preparation). The role and the evolutionary conservation of the *gcm* gene makes it an interesting target to analyse its role during neuroinflammation. My goal is to transpose the results obtained in flies to vertebrates.

Two orthologous genes are present in mammals up to humans, GCM1 and GCM2. In mice, the knockout of mGcm1 or mGcm2 is lethal due to crucial roles in the placenta (mGcm1) and in parathyroid development (mGcm2), two functions that are conserved in human GCM genes (Hashemthosseini & Wegner, 2004). However, no role has been detected in the development of glial cells and no studies have been performed in the immune system. Given the strong

evolutionary conservation of the immune pathways, I hypothesized that the Gcm genes could have a role in the modulation of the immune response. To establish the expression profile of mGcm1 and mGcm2 in mouse immune cells, our lab first analysed their transcription levels by quantitative PCR in adult tissues. The mGcm2 is expressed in the three main hematopoietic tissues: bone marrow, spleen and thymus. The mGcm1 is expressed at a much lower level. Analysis by qPCR on sorted cells revealed a wide distribution of expression of mGcm2 including microglia cells.

Microglia cells are the innate immune cells of the CNS. These cells originate from the primitive hematopoietic wave that takes place in the yolk sac at the start of embryogenesis. The microglia progenitors then migrate into the developing CNS and eventually differentiate. Unlike all other tissue-specific macrophages, microglia are the only resident macrophage population that is not replaced by other macrophages from the definitive hematopoietic wave. This makes the microglia an ideal population to study the effect of mGcm2 because as in *Drosophila* the ortholog is specifically expressed in the primitive hematopoietic wave.

2. Objectives:

- Characterise the expression profile of mGcm2 (anti-mGcm2 immunostaining on whole embryos and sections of adult tissues).
- Analyse the role of mGcm2 in the microglia cell by phenotyping a conditional knock-out (cko) line (microglia proliferation, morphology, expression of inflammatory markers and phenotypic analysis).
- Characterise the role of mGcm2 in the microglia cell *in vitro* using primary cultures of neonatal cko mice (phagocytosis and migration assays).
- Characterise the expression of Gcm in *Drosophila* under neuroinflammatory conditions.
- Characterise the expression of *short stop (shot)* in *Drosophila melanogaster* hemocytes during homeostasis and during wasp infestation.

3. Results:

mGcm2 is expressed early in the yolk sac and in microglia cells of the CNS of aged animals.

I characterised the expression profile of mGcm2 during development (from E7.5 to E16.5). Cells positive for mGcm2 were observed in the yolk sac of E7.5 embryos with macrophage-specific markers. This marking was absent at other developmental stages. These results suggest that mGcm2 is expressed early and transiently in the hematopoietic system, similar to what has been described for the fly orthologue.

Next, I characterised the expression profile of mGcm2 in different tissues (brain, spleen, white adipose tissue) and age groups (postnatal 0 P0, P14, and 2.12 and 24 months). Results showed expression in 12- and 24-month-old brains but not in 2-month-old animals. In addition, double labelling of mGcm2 and CD45 (a common marker of macrophages) showed no expression in other tissue resident macrophages. Thus, mGcm2 is expressed only in the CNS of aged animals.

Cko mGcm2 mice show increased weight

I then characterised the cko mGcm2 line *in vivo*. For this, I created a first cohort to study the lifespan of cko animals. All animals were kept at the Institut Clinique de la Souris (ICS) under a normal chow fed diet. In order to create the cko mGcm2 microglia cell line, I used the CX3CR1-Cre line. As a control I used CX3CR1-Cre / +; mGcm2^{fllox/+}. In addition, all animals were weighed once a week. There is no difference in lifespan, but strikingly the cko animals show an increase in weight compared to controls.

To confirm this phenotype, I created a second cohort. These mice were weighed once a week and underwent metabolic testing. Specifically, I performed a body composition test and

metabolic cages test for 24 hours. The first test gives information about lean tissue, fat content, and free body fluids. These tests revealed no difference between the two genotypes, even though the cko group had a significantly higher weight than the control group. Metabolic cages make it possible to simultaneously measure energy expenditure, ambulatory activity as well as food and water consumption. The results revealed a tendency for higher food consumption and less movement in cko mice, although the results were not statistically significant. For this reason it would be interesting to induce obesity in the cko animals and see whether under these conditions the parameters will be statistically significant. Even though the role of microglia has been linked with hyperphagia and obesity, my data for the first time suggest that the expression of mGcm2 in the microglia cell is involved in metabolic homeostasis.

The loss of mGcm2 leads to a pro-inflammatory state of the microglia

Since I knew the mGcm2 expression profile in microglia I decided to characterise the microglia population *in vivo*. First, I counted the microglia cell population in different regions and at different stages (mice aged P0, P14, 4 and 24 months), together with Dr Katrin Kierdorf from the University of Freiburg. The cells were labelled with the specific marker for microglia, Iba-1, and cell counts were performed in different regions of the brain. Cko brains show a higher number of microglia at P14 and 4 months compared to controls, which could indicate a pro-inflammatory environment.

My next goal was to see if microglia of mGcm2 mutant mice also exhibits inflammatory features. Resting microglia have a branched morphology with long, thin processes. During inflammation or aging, the microglia show signs of an activated, less branched morphology. Labelling with the specific marker for microglia Iba-1 showed that the cko animals aged 2 and 12 months did not have a different morphology from that of the controls. In contrast, 24 month

old cko animals show less branching and less coverage. Overall, these data suggest that the absence of mGcm2 has a significant impact on the morphology and thus the of the microglia.

The loss of mGcm2 in the microglia leads to an increase in the number of positive pro-inflammatory cells.

To reinforce the morphological data, I marked the 2, 12 and 24 month CNS with markers indicative of an inflammatory state. Microglia / macrophage activation states are classified as pro-inflammatory (or M1) or anti-inflammatory (or M2). I chose induced Nitrogen Oxygen Species (iNOS) for the M1 state and Arginase-1 (Arg-1) for the M2 state, two markers that have already been used to characterise the state of microglia *in vivo* (Lisi et al., 2017; Cherry et al., 2017). I then evaluated the expression of these two markers in the microglia co-labelled with Iba-1. 24 month old cko animals had significantly more iNOS positive microglia compared to controls of the same age. In addition, 24 month old cko animals showed a significant decrease in Arg-1 positive microglia compared to 12 month old cko animals, while comparable age control animals did not show a significant difference in labelling of Arg-1. These data suggest that cko animals have more microglia polarized towards the M1 phenotype than control animals. This validates my hypothesis that mGcm2 has an anti-inflammatory role conserved during evolution in immune cells of the primary hematopoietic wave.

Gcm is expressed in *Drosophila melanogaster* hemocytes under neuroinflammatory conditions.

The next step was to examine whether the role of Gcm specifically during neuroinflammation is conserved during evolution. In adults of *Drosophila melanogaster*, Gcm is expressed only in a subset of neurons, but it is not expressed in glia or in hemocytes. I first followed the

expression of Gcm during aging using a transgenic line which traces the lineage of all cells which, at some point in adult life, express Gcm. Apart from the subset of neurons already characterised, Gcm is not expressed in the CNS of old flies. However, since the lifespan of flies are much shorter than that of mammals, I hypothesised that aging might not be sufficient to induce *de novo* expression of Gcm in an otherwise normal brain.

For this reason, I induced an inflammatory response in the CNS of adult flies using a line that overexpresses a-Synuclein in all neurons using the Lex A system. a-Synuclein is a neuronal protein that regulates trafficking synaptic vesicles and the subsequent release of neurotransmitters. The aggregation of this protein is linked to several neurodegenerative diseases such as Parkinson's disease. a-Synuclein overexpression revealed the presence of Gcm positive cells in the CNS, which do not express neuronal markers or glial markers, but they express hemocyte markers. All these data suggest that, during a challenge, adult hemocytes express Gcm and penetrate the blood-brain barrier (BBB). Invasion of hemocytes was also confirmed by paraquat assay (PQ). Further experiments should aim to confirm whether these hemocytes also express Gcm. Thus, Gcm could be a novel factor in the innate immune response in the CNS.

Characterisation of mGcm2 cko microglia *in vitro*

My final goal was to link the expression of mGcm2 to a function of the innate immune system. Microglia have two major functions: phagocytosis and migration to the site of inflammation. During my PhD, I characterised the expression of mGcm2 during phagocytosis as well as during migration in primary cultures of CNS and used cko animals to discover any phenotypic changes.

I first evaluated the expression of mGcm2 under the basal conditions of the cultures and revealed its specific presence in a subset of round-shaped microglia (30% of the total number of round cells). During stimulation with latex beads, the microglia phagocytose the beads at the end of the test (t = 120 min.). Staining of the stimulated microglia cultures shows a significant decrease in mGcm2 protein levels soon after stimulation (t = 20 min.), which returns to basal levels (t = 0 min.) after 120 min. This prompts me to suggest that the phagocytosis process affects the expression of mGcm2.

In order to assess whether mGcm2 levels impact phagocytosis, I performed the same test on primary cultures of mGcm2 cko microglia. To perform a quantitative analysis, I measured the intensity of fluorescence in the cells, which reflects phagocytic activity. I did not find any difference in the phagocytic capacity of the microglia between the cko animals and the control animals. This result allows me to propose that mGcm2 does not control phagocytosis of latex beads.

In addition, upon activation due to injury or pathogens, the microglia quickly migrate to the inflamed area and phagocytose cell debris or damaged neurons. To better assess the possible roles of mGcm2 in microglia, I assumed that it might impact migration and therefore performed a scratch migration assay, a widely used assay, using the same primary cultures of microglia cells as above. Migration into the open scar was documented by microphotographs at various times after scratching. The results did not show expression of mGcm2 in the microglia cells migrating to the scar. In addition, the cultures were evaluated for their ability to close the wound and whether the absence of mGcm2 had an impact on the healing process. I did not find any difference between cko cells and control cells, indicating that mGcm2 does not affect microglia migration *in vitro*.

Characterisation of *short stop (shot)* expression in *Drosophila melanogaster* hemocytes during homeostasis and during infestation by parasitoid wasps

In parallel, I contributed to the team effort to characterise the *Drosophila melanogaster* hemocyte population by single cell RNA sequencing. My main contribution to the project was to link the two distinct populations of hemocytes, resident and circulating, and to characterise the expression of hemocyte markers during an immune challenge through infestation by parasitoid wasps. The results of the latter revealed a new marker for hemocytes and their activated form, lamellocytes, *short stop (shot)*. This gene codes for a member of the spectraplakins family, large cytoskeletal binding molecules. Shot binds to actin and microtubules, as well as scaffold proteins, certain signalling factors, and calcium. In addition, this protein plays a role in the development and maintenance of several tissues of the nervous system, epidermis, muscle attachments, foregut, wing, trachea and oocytes.

My project tried to dissect the role of Shot in hemocytes in homeostatic conditions as well as during an immune challenge (infestation by parasitoid wasps). The results show that Shot participates in the adhesion of hemocytes *in vitro* and under homeostatic conditions. More precisely, silencing of Shot by using RNAi construct decreases the adhesion of hemocytes, while its overexpression results in an increase in adhesion compared to controls *in vitro*. Shot silencing also results in reduced expression of the N-Cadherin protein. Finally, I demonstrated that Shot plays a central role in the fly response to wasp infestation, as animals not expressing Shot show reduced encapsulation of the wasp egg 24 hours after the infestation. All these results suggest that Shot is a new player in adhesion between hemocytes and in the formation of junctions between cells.

4. Conclusions

My work highlights mGcm2 as a novel evolutionary conserved transcription factor of innate immune cells originating from the primitive wave. I found that this transcription factor is expressed in the mouse yolk sac, which is similar to the early expression of Gcm during embryonic hematopoiesis in *Drosophila melanogaster*. Early hematopoietic waves in mammals produce macrophages which migrate to different organs and give rise to tissue resident macrophages. Unlike all other tissue resident populations, microglia are the only cell type that are not replaced by the new macrophage populations of the definitive hematopoietic wave. Additionally, microglia is the only type of cell that expresses mGcm2 during aging, a process that closely resembles an immune response. Finally, I have shown that the absence of mGcm2 leads *in vivo* to a pro-inflammatory state of the cells of the microglia. These data suggest an important role of mGcm2 in the context of neuroinflammation and conservation of its function during evolution. I believe that my work will provide a better understanding of the innate immune response of the CNS. In the long term, this could help to understand the pathophysiological mechanisms underlying human diseases such as autoimmune or neurodegenerative diseases, which represent a heavy burden on our societies.

Introduction

Introducing the immune system

The immune system constitutes a network of biological processes that protects an organism from foreign bodies. It detects and responds to a wide variety of pathogens, from viruses to parasitic worms, as well as cancer cells and foreign objects, distinguishing them from the organism's own healthy tissue. Almost all organisms have a form of a defence mechanism. Even bacteria have a primary immune response in the form of enzymes that protect against viral infections (Dunin-Horkawicz, Kopec, & Lupas, 2014; Loureiro & da Silva, 2019). Multicellular organisms such as insects and mammals have further developed anatomical barriers, specialised cells and humoral responses which provide a preconfigured reaction to a variety of stimuli (Desjardins, Berchiche, Haddad, & Heveker, 2007). These mechanisms together comprise the innate immune system. Vertebrates have an additional set of highly specialised immune cells and cellular responses that comprise the adaptive immune system (Kasahara, Suzuki, & Pasquier, 2004). Adaptive immunity creates immunological memory after an initial response to a specific pathogen, thus leading to an enhanced response to future encounters with the same pathogen. Characteristics of innate and adaptive immune responses can be found in **Figure 1**.

Innate immune system	Adaptive immune system
• Non-specific response	• Pathogen specific response
• Immediate response	• Takes time to be activated
• Found in almost all forms of life	• Immunological memory
	• Only in vertebrates

Figure 1. Characteristics of the innate and adaptive immune system.

Generally, the aim of the immune system is to defend the host against pathogens and then promote tissue repair and healing. Early response includes a complex and highly coordinated chain of events at a molecular, cellular and physiological level (Cooper, 2010). These events lead to the production of soluble mediators, such as cytokines and chemokines, by resident immune cells (macrophages, dendritic cells etc.) and non-immune cells (endothelial cells, fibroblasts, etc.). Next, the chemokines attract cells of the innate immune system, a relatively broad - acting but highly effective defence that is largely preoccupied with the elimination of infectious agents. The actions of the innate immune system are also responsible for alerting the cells of the adaptive immune system in vertebrates.

The ability of the immune system to respond to pathogens is diminished throughout the host's lifespan, with immune responses beginning to decline with aging due to immunosenescence. Immunodeficiency is a state in which the immune system's ability to fight infectious diseases is compromised or entirely absent (Chinen & Shearer, 2010). Immunodeficiencies could be due to genetic mutations such as severe combined immunodeficiency or acquired such as acquired immunodeficiency syndrome (AIDS) due to HIV infection (Fischer, Hacein-Bey Abina, Touzot, & Cavazzana, 2015). On the other hand, overreaction of the immune system could lead to autoimmunity. Here, the immune system fails to properly distinguish between self and non-self, and attacks part of the body. Thus, a fine tuning of the immune system is of imperative importance and is regulated by transcription factors.

The Glial deficiency / Glial cells missing (Glide/Gcm) transcription factor is expressed and required in fly glia as well as in the hemocytes, the macrophages acting inside and outside the central nervous system (CNS), respectively (Bernardoni, Vivancos, & Giangrande, 1997). Our laboratory has characterised the role of Gcm in hemocytes as an inhibitor of the pro-inflammatory Janus Kinases / Signal Transducer and Activator of Transcription Proteins (JAK

/ STAT) pathway (Bazzi et al., 2018). The role and the evolutionary conservation of the *gcm* gene makes it an interesting target to analyse during inflammation in mammals.

The CNS, which in vertebrates contains the brain and the spinal cord, is isolated from the rest of the organism by the blood brain barrier (BBB). For this reason, inflammation in the CNS is orchestrated by the resident tissue macrophages, that are known as microglia, and later by infiltration of peripheral immune cells (Jurga, Paleczna, & Kuter, 2020). Sources of neuroinflammation can be due to injury or infection, such as a virus that can penetrate the BBB. Dysregulation of the immune system could lead to autoimmune or neurodegenerative disorders such as Multiple Sclerosis (MS), Parkinson's disorder (PD) and Alzheimer's disease (AD). During neuroinflammation microglia play a pivotal role in either promoting or suppressing the inflammatory response and for this reason many studies target those immune cells to develop new therapeutic strategies.

The transcription factor Gcm

Gcm is an atypical zinc finger transcription factor (Akiyama, Hosoya, Poole, & Hotta, 1996; Cohen et al., 2002; Schreiber, Sock, & Wegner, 1997). It was first characterised as an essential factor for the differentiation of the glia cells in the *Drosophila* embryo (Akiyama et al., 1996; S. Vincent, Vonesch, & Giangrande, 1996). In *Drosophila*, a functional nervous system requires the correct specification and precise organization of many neural cell types. Neural cells can be classified into two distinct groups, neurons and glia (Freeman, 2015). Neurons play a leading role in processing and transmitting information, while glia play a supporting role, nourishing and insulating neurons. One general rule that has emerged from lineage analysis of neurogenesis is that both neurons and glia are generated from multipotent neural progenitors (Bossing, Udolph, Doe, & Technau, 1996; Udolph, Prokop, Bossing, & Technau, 1993). Gcm Loss of function (LOF) showed that embryos are devoid of glial cells, with neural progenitors producing essentially neurons (**Figure 2**). Conversely, embryos expressing *gcm* throughout the nervous system (Gcm Gain of function (GOF) embryos) present supernumerary glial cells with neuroblasts producing essentially glia (Hosoya, Takizawa, Nitta, & Hotta, 1995; B. W. Jones, Fetter, Tear, & Goodman, 1995; S. Vincent et al., 1996). Due to its significant role in glia development, Gcm was first described and named as the master regulator of glia differentiation and indeed ectopic expression of Gcm is adequate to induce the expression of glial markers even in the epidermis and in the mesoderm (Akiyama-Oda, Hosoya, & Hotta, 1998; Bernardoni, Miller, & Giangrande, 1998).

In *Drosophila*, a second *gcm* gene was identified (Alfonso & Jones, 2002; Kammerer & Giangrande, 2001). This *gcm2/glide2* gene is the result of a recent gene duplication event and assists *gcm/glide* in its function during gliogenesis.

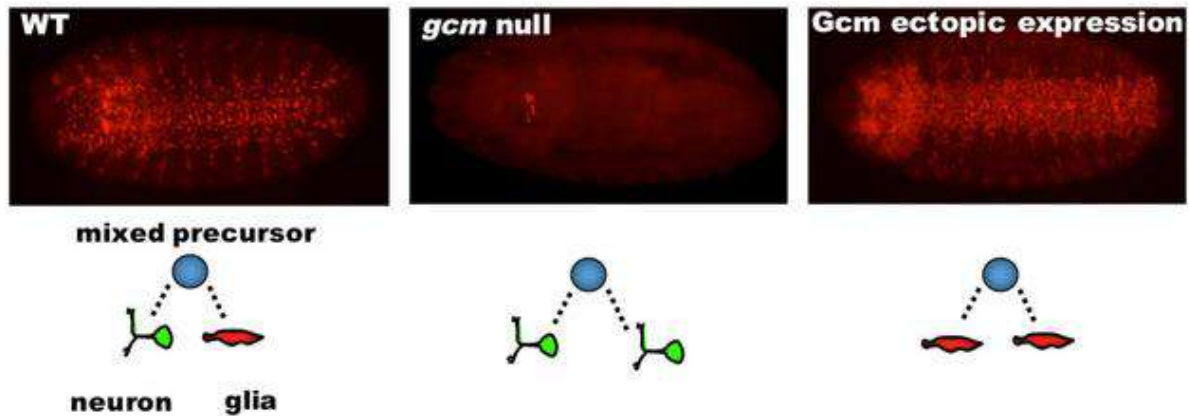


Figure 2. *gcm* acts as a binary switch for glia (red) versus neurons (green in the schematic) in *Drosophila*. Phenotypes are shown for a neural progenitor that gives rise to a neuron and a glia in a wild-type animal, *Gcm* loss-of-function mutant animal (null), and *Gcm* gain-of-function mutant animal in which a transgenic construct drives ectopic *gcm* expression in presumptive neurons (modified from A.Giangrande <http://www.stemcells-live.fr/giangrande.html>).

Gcm is important for the development of the immune system of *Drosophila*

Hematopoiesis in the fly model has been well documented along with all the signalling cascade required for the differentiation of hemocytes. The hematopoietic process is divided into two waves (**Figure 3**). The first wave is of mesodermic origin and derives from the procephalic region of the embryo. These cells give rise to prohemocytes, which are a defined number of blood cell progenitors (Tepass, Fessler, Aziz, & Hartenstein, 1994). Prohemocytes differentiate into plasmatocytes, the functional orthologue of the mammalian macrophages. Plasmatocytes are able to phagocytose pathogens and debris. They also secrete extracellular matrix during development and contribute to the humoral response by producing antimicrobial peptides (AMPs) (Martinek, Shahab, Saathoff, & Ringuette, 2008; Tepass et al., 1994). A small fraction of prohemocytes give rise to crystal cells, a cell population specialised for the melanisation process during inflammation (Lebestky, Chang, Hartenstein, & Banerjee, 2000). The third type of hemocytes are the lamellocytes which are only present upon challenge. During an inflammatory response, plasmatocytes transdifferentiate into lamellocytes. These cells are able to encapsulate large foreign bodies such as the eggs from parasitic wasps (Markus et al., 2009).

The second wave derives from the lymph gland, a hematopoietic organ that arises in the embryo independently of the embryonic prohemocytes (**Figure 3**) (Lebestky, Jung, & Banerjee, 2003; Rizki & Rizki, 1978). The lymph gland keeps growing during the larval stages and hystolyses upon metamorphosis to release a second pool of hemocytes that co-exist with those of the primitive wave (Grigorian, Mandal, & Hartenstein, 2011). Interestingly, the second wave of hematopoiesis is independent of Gcm, thus highlighting the specificity of Gcm within the primitive wave (Bazzi et al., 2018). This is the only known case of a wave-specific transcriptional pathway, suggesting that the embryonically derived hemocytes display specific epigenetic, transcriptional and functional features.

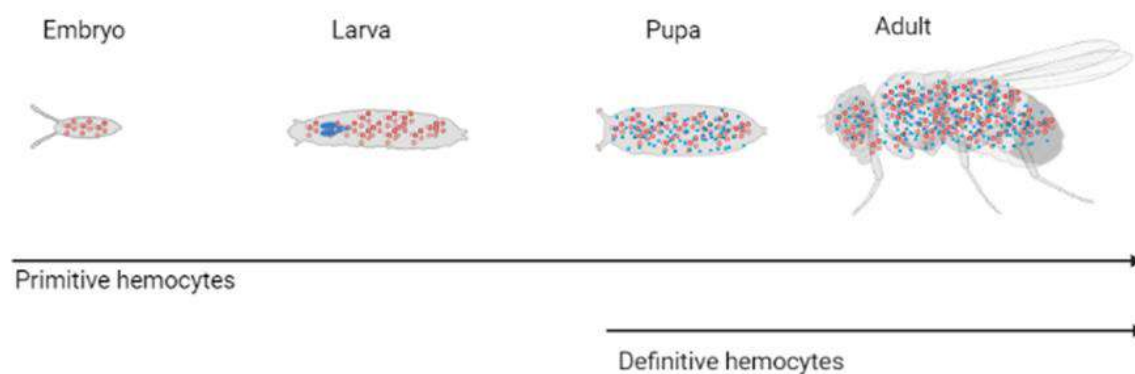


Figure 3. The hematopoiesis of *Drosophila melanogaster*. The first primitive wave originates in the embryo (red) and the second definitive wave derives from the lymph gland (blue).

The fate of prohemocytes is determined by specific transcription factors (**Figure 4**). Prohemocytes of the primitive wave express the transcription factor Serpent (Srp), a member of the GATA family, which activates the expression of the U-shaped (Ush) transcription factor (member of the Friend of GATA (FOG) family). Together these two factors activate the expression of the Gcm transcription factor 1 and 2. Activation of the Gcm1 and Gcm2 induces

the expression of plasmatocyte specific genes (Fossett et al., 2001). The Gcm factor is so vital that its ectopic expression leads to conversion of crystal cells into plasmatocytes (Fossett & Schulz, 2001). Finally, prohemocytes that express the Runt protein Lozenge (Lz) differentiate into crystal cells.

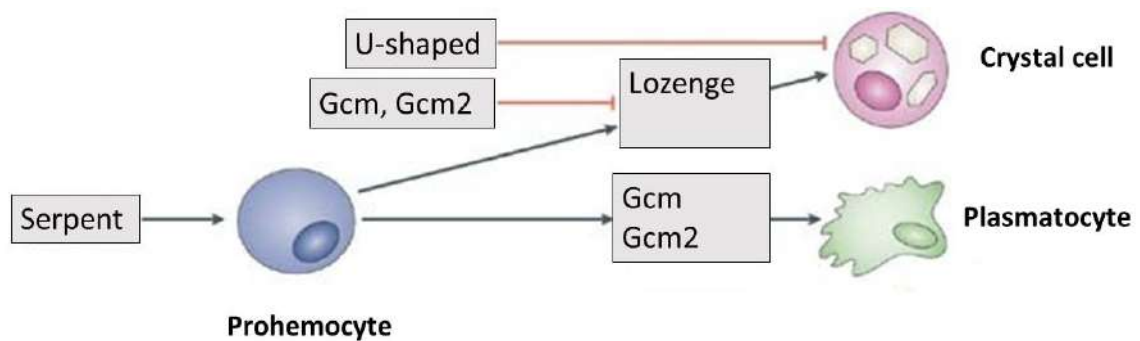


Figure 4. Many factors that regulate the primitive haematopoiesis in *Drosophila melanogaster* have been identified. Serpent is required for the specification of the haemocyte in the embryo. The specification of plasmatocytes (green) requires the transcription factors glial-cells missing (Gcm) and Gcm2. Differentiation of crystal cells (pink) requires the expression of the transcription factor Lozenge. GCM, GCM2 and the *D. melanogaster* friend-of-GATA homologue U-shaped antagonize crystal-cell development in the embryo (modified from Wood & Jacinto, 2007).

Activation of the immune system in *Drosophila melanogaster* and the role of Gcm in the immune response

The absence of adaptive immune response in *Drosophila* provides as a powerful model to study the aspects of the innate immune system that might otherwise be masked by the adaptive immune response. *Drosophila* defend itself against a range of parasites and microbes by invoking a variety of innate immune responses, some of which are clearly shared with vertebrates such as the NF- κ B and the JAK/STAT pathways (Hoffmann, 2003; Hultmark & Ekengren, 2003).

Flies with mutations for genes of the NF- κ B pathway are impaired in their ability to fight bacterial or fungal infections. Genetic studies of those mutant animals demonstrated that flies

could discriminate between classes of surface molecules on pathogens. Two distinct NF- κ B pathways, the Toll and the Immune deficiency (Imd), control AMP production by recruiting the transcription factors Dorsal/Dif and Relish respectively (Manfrulli, Reichhart, Steward, Hoffmann, & Lemaitre, 1999). The Toll pathway is responsible for resistance to fungal and Gram-positive bacterial infections (Hoffmann, 2003; Hultmark, 2003; Tanji & Ip, 2005) and the Imd is responsible for Gram-negative bacteria (Lemaitre & Hoffmann, 2007; Martinelli & Reichhart, 2005). The mammalian orthologues of these proteins also regulate similar innate immune responses thus, highlighting the conservation of the innate immune pathways throughout evolution (Govind, 2008).

In addition to the Toll and Imd pathways, other signalling cascades complement and contribute to the core circuitry in order to have a strong immune response. The JAK/STAT cascade is among the simplest of the conserved metazoan signalling pathways (**Figure 5**) (Myllymaki & Ramet, 2014). The binding of extracellular ligand, such as the cytokines Upd2 and Upd3, leads to pathway activation via changes to the receptor Domeless (Dome) which in turn permits the associated intracellular JAKs to phosphorylate one another. Events downstream of Dome are carried out by the JAKs and the transcription factor STAT92E.

A recent study from our lab revealed that down-regulation of Gcm specifically in embryonic hemocytes show enhanced larval phenotypes. This was induced by over-expressing the pro-inflammatory JAK/STAT pathway, either through expression of the Hop^{Tum1} dominant Gain of function allele, which lead to formation of melanotic tumours, or by wasp infestation (**Figure 5**). More specifically, the role of Gcm is to prevent the state of chronic inflammation induced by the JAK/STAT pathway. Gcm induces the expression of Ptp61F, Socs36E and Socs44A, which inhibit this pathway. In so doing, Gcm prevents the production of the Upd2 and Upd3 pro-inflammatory cytokines, whose over-expression is sufficient to induce the inflammatory response (Bazzi et al., 2018). These interesting data suggested that Gcm expression during

development orchestrates the inflammatory response later in larva. Even though the Gcm cascade has been most extensively studied in flies, studies in other animal models show that this transcription factor is conserved throughout evolution.

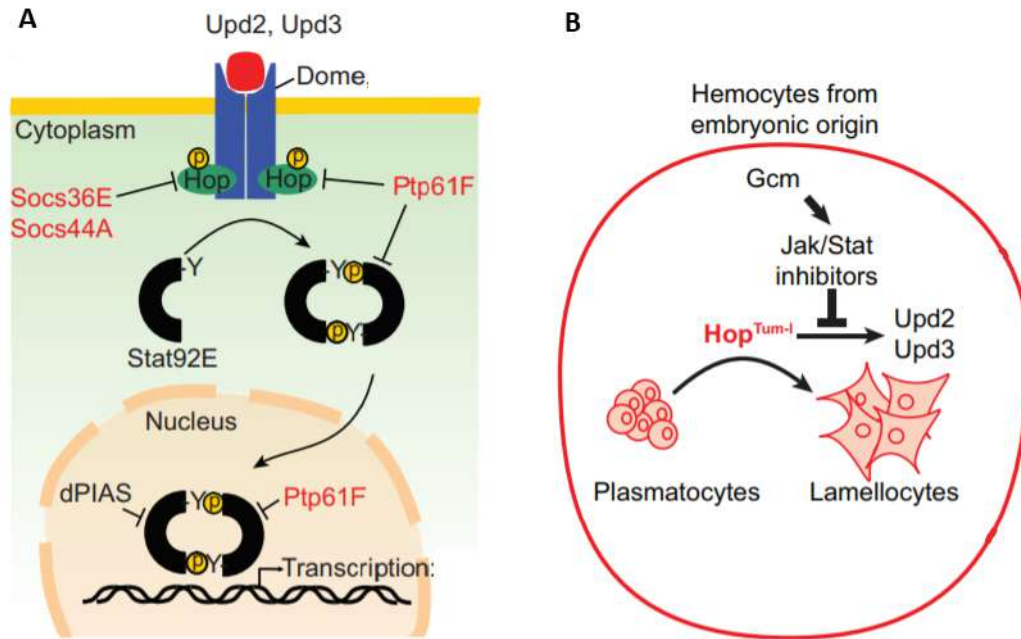


Figure 5. The signalling pathway of JAK/STAT (A) JAK/STAT pathway: inhibitors of the pathway that are regulated by Gcm are in red.(B) *gcm*> *hop*^{Tum-1} activates the JAK/STAT pathway exclusively in the hemocytes at embryonic stage. This leads to the production of the Upd2/Upd3 pro-inflammatory cytokines in those cells and to the activation of the Jak/Stat pathway (modified from Bazzi et al., 2018).

Conservation of Gcm in evolution

As many other transcription factors, Gcm is also conserved throughout evolution (**Figure 6**). More specifically, in all the known Gcm proteins the DNA binding site is highly conserved, thus indicating a possible immune role of Gcm in the immune response (Hashemolhosseini & Wegner, 2004). Gcm proteins have been identified and characterised in other species such as the *Gallus gallus*, the *Xenopus laevis*, the *Strongylocentrotus purpuratus*, the *Fugu rubripes*, and the *Danio rerio* (Hashemolhosseini, Schmidt, Kilian, Rodriguez, & Wegner, 2004; Hashemolhosseini & Wegner, 2004). In mammals, there are two orthologues of *Drosophila gcm*, which are named in humans hGCM1 and hGCM2, and mGcm1 and mGcm2 in mice.

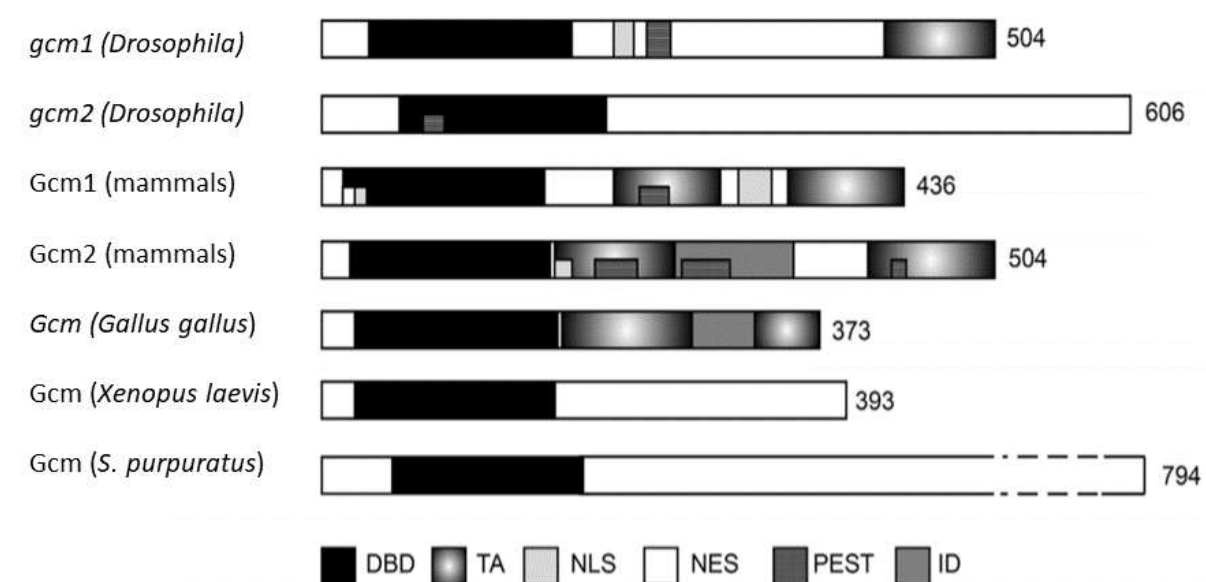


Figure 6. Overview and domain topology of GCM proteins. Numbers to the right indicate amino acid residues in each GCM protein. At the bottom, differently patterned squares corresponding to different functional domains are shown (DBD, DNA-binding domain; TA, transactivation domain; NLS, nuclear localization signal; NES, nuclear export signal; PEST, proline-glutamine-serine-threonine rich motif; ID, inhibitory domain) (modified from Hashemolhosseini and Wegner, 2004)

In mammals, Gcm1 genes are required for differentiation of trophoblasts in the developing placenta (Basyuk et al., 1999). In mice, mGcm1 drives the placenta development in three distinct phases and it is important for nutrient and gas exchange between the foetus and the

bloodstream of the mother through the labyrinth cells (Basyuk et al., 1999; Stecca et al., 2002). Similarly, hGCM1 is necessary for nutrient/gas exchange between syncytio- and cytotrophoblasts of the human placenta (Nait-Oumesmar, Copperman, & Lazzarini, 2000). Mutation and complete deletion of mGcm1 leads to severe placenta defects and thus early embryonic lethality (Anson-Cartwright et al., 2000; Schreiber et al., 2000). Gcm2 is expressed and required mainly in the parathyroid glands, (Gordon, Bennett, Blackburn, & Manley, 2001; J. Kim et al., 1998) where it is necessary for the survival and differentiation of precursor cells (Gordon et al., 2001; Gunther et al., 2000; J. Kim et al., 1998; Z. Liu, Yu, & Manley, 2007). mGcm2 knock out mice are also embryonically lethal (Anson-Cartwright et al., 2000; Gunther et al., 2000).

Many studies have tried to link the expression of the Gcm genes with gliogenesis in mammals. Initially, overexpression studies supported a function of mammalian Gcm proteins in nervous system development. Gcm1 disrupts neurogenesis or induced gliogenesis when ectopically expressed in the nervous system of *Drosophila* and mammals (J. Kim et al., 1998; Nait-Oumesmar et al., 2000; Reifegerste, Schreiber, Gulland, Ludemann, & Wegner, 1999). Furthermore, Gcm1 and Gcm2 are involved in the epigenetic regulation of Hes5, a transcription factor that participates in the neocortical development (Hitoshi et al., 2011). However, none of studies detect significant amounts of Gcm1 or Gcm2 in the mammalian nervous system. These data suggest that Gcm does not participate in the gliogenesis but raise the question of whether there is a common cascade that Gcm acts on.

Due to lack of known Gcm1 and Gcm2 target genes, a study identified a conserved Gcm cascade on the mammalian orthologues (Cattenoz et al., 2016). A Gene Ontology term enrichment analysis identified orthologues that are associated with the parathyroid gland or the placenta as well as new potential targets of the Gcm genes in mammals. Moreover, the results showed that there is enrichment for the motif ATGCGGG at the loci bound by Gcm. This motif

is closely related to most of the Gcm binding sites (GBSs) previously described (Akiyama et al., 1996; Miller, Bernardoni, & Giangrande, 1998; Ragone et al., 2003; Schreiber et al., 1997). Overall, the data indicated that even though the main sites of *gcm* expression may be different in mammals and *Drosophila*, the Gcm cascade is at least partially conserved through the DNA binding sites. Although, mammalian Gcm does not participate in gliogenesis, another cascade maybe conserved in evolution.

The role of Gcm in the development of macrophages

Gcm was first discovered as a pivotal transcription factor in the development of the CNS in *Drosophila melanogaster*. In flies, neurons and glia are descendants of the same precursor cells and Gcm acts on those precursors to give rise to glia cells (Reichert, 2011; S. Vincent et al., 1996). Glia cells are present in all Deuterostomia as well as many Protostomia. But glia evolution most probably happened at different stages, thus neurogenesis in flies and mammals is not under the control of the same transcription factors (**Figure 7**). However, studies in anthozoan cnidarians, such as *Nematostella vectensis*, that completely lack glia cells, show Gcm expression during development of immune cells (Sullivan et al., 2008). Since the existence of *gcm* precedes that of glia, this transcription factor could act in a more ancestral function (**Figure 7**).

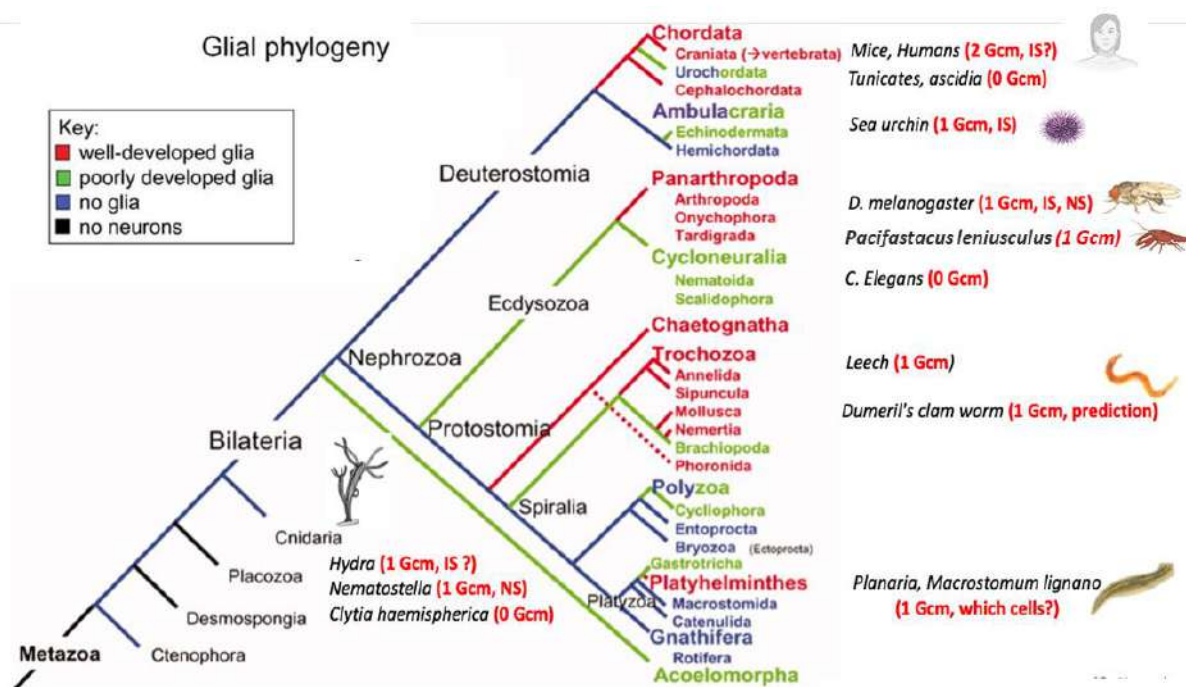


Figure 7. Phylogenetic tree of various living taxa, coded for absence of glia (blue), poorly developed glia (green), well-developed glia (red) and the known species that have the *gcm* gene, Immune system (IS), Nervous System (NS) (modified from (Hartline, 2011)).

Role of Gcm in the development of the immune system of invertebrates

Hematopoiesis maintains most transcription factors throughout evolution. In *Drosophila*, early hemocyte precursors express Srp which leads to Gcm expression and thus, differentiation of these precursors into plasmatocytes (Wood & Jacinto, 2007). In addition to the developmental role, Gcm has a striking impact on the immune response. Hemocyte specific Gcm mutants appear to have a normal phenotype with the appearance of few lamellocytes (Bazzi et al., 2018; Gupta, Kumar, Cattenoz, VijayRaghavan, & Giangrande, 2016). However, combination of Gcm mutants with an immune challenge gives rise to a severe inflammatory response in the mutants compared to the controls (Bazzi et al., 2018).

In Deuterostomia, Gcm plays a pivotal role in the development of the immune system. Most published data are in the sea urchin and a peculiar macrophage population called pigment cells (**Figure 7**). As hemocytes in *Drosophila*, these cells are committed early in development through Gcm expression (E. H. Davidson et al., 2002; Ransick & Davidson, 2006, 2012). Such cells are involved in the immune defence by pigment production which has anti-microbial properties (Rast, Smith, Loza-Coll, Hibino, & Litman, 2006). More specifically, the presence of foreign molecules leads to rapid pigment release which protects the animal. In the same animal model, Gcm mutants are less resistant to challenging environmental conditions portrayed with a decreased survival rate when compared to the controls (E. H. Davidson et al., 2002; Ransick & Davidson, 2006, 2012). Interestingly, Gcm mutants are albinos which suggests that it is important for the differentiation of pigment cells and for pigment production in general (Wessel, Kiyomoto, Shen, & Yajima, 2020). This was the second animal model that highlighted the role of Gcm in the immune system.

Since then, more and more data suggest that the Gcm cascade is highly conserved in the development and function of the innate immune system. A recent study showed that a *gcm* orthologue is expressed in the freshwater crayfish *Pacifastacus leniusculus* (Junkunlo,

Soderhall, & Soderhall, 2020). The *P. leniusculus gcm* only transcript is expressed exclusively in the CNS (**Figure 7**), and by *in situ* hybridization the study showed that the expression is restricted to a small number of large cells. Furthermore, they showed that the expression of Gcm coincides with the expression of a Repo homologue, thus resembling the gliogenesis in *Drosophila*. Interestingly, the Gcm transcript was increased shortly and transiently after injection of cystamine, a paralytic substance. This increase in expression of Gcm after the injection could mean that Gcm induces the expression of other genes that are important for restoring homeostasis, thus linking Gcm with innate immune responses of the CNS.

Role of *Gcm* in the development of the immune system of vertebrates

The role of *Gcm* in the immune system of vertebrates is more complicated to study since both Gcm1 and Gcm2 are embryonically lethal (Nait-Oumesmar et al., 2000). Given the complexity of studying a gene expression when its mutants are lethal, the role of *Gcm* in the development of the immune system was not further explored. However, unpublished data show that Gcm is present in the immune system of *Danio rerio* (zebrafish) (**Figure 8**, data provided from the lab of S. Kucenas, experiment performed by Laura Fontenas, University of Virginia). Similar to mammals, primitive hematopoiesis in zebrafish occurs in the extraembryonic yolk sac blood islands and predominantly generates erythroid cells (A. J. Davidson & Zon, 2004). Those primitive macrophages are born in the yolk sac at 22 hours post fertilization (hpf) and then proliferate and migrate to peripheral tissues (Herbomel, 1999; Herbomel, Thisse, & Thisse, 2001). The present data suggest that Gcm is expressed during the primitive hematopoietic wave in zebrafish and that its role in glia development in flies as well as placenta/parathyroid development in mammals came later in the evolution. Thus, studying the role of Gcm during the development and innate immune response could shed light into the conserved cascade of this transcription factor.

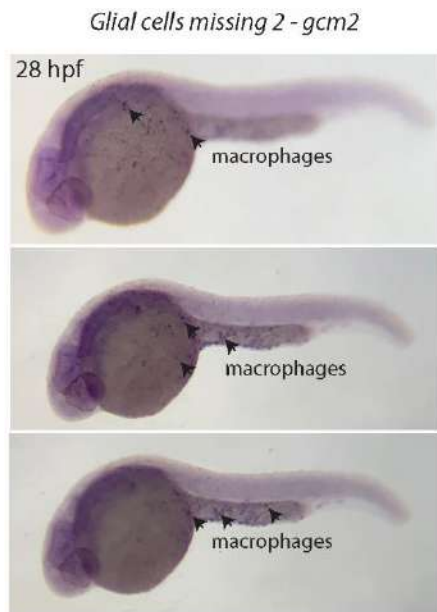


Figure 8. *In situ* expression of *gcm2* in the yolk sac during the development of macrophages in zebra fish as indicated by the arrows.

To establish the expression profile of mGcm1 and mGcm2 in the mouse immune cells, our lab performed quantitative PCR (qPCR) analysis in adult tissues. mGcm2 is expressed in the three major hematopoietic tissues: bone marrow, spleen and thymus. mGcm1 is expressed at a much lower level. qPCR assays on sorted cells also revealed a wide distribution of mGcm2 expression in myeloid as well as lymphoid lineages: T cells, plasmacytoid dendritic cells (pDC), B cells and microglia (**Figure 9**, Y. Yasha unpublished data). From those cell types, microglia, the innate immune cells of the CNS were the most attractive candidate. First of all, microglia are the only cell population that derives directly from the primitive wave in the yolk sac and do not get replaced by monocytes of the other hematopoietic waves (Ginhoux et al., 2010). Furthermore, microglia closely resemble the glia cells and hemocytes of *Drosophila* as well as the glia cells in the crayfish where Gcm plays a pivotal role during development and immune responses. Further analysis of both mGcm1 and mGcm2 showed that only the latter was expressed albeit at low levels (**Figure 9**). During my PhD, I chose to address the question of whether or not the expression of mGcm2 has an impact on the development and homeostasis of microglia.

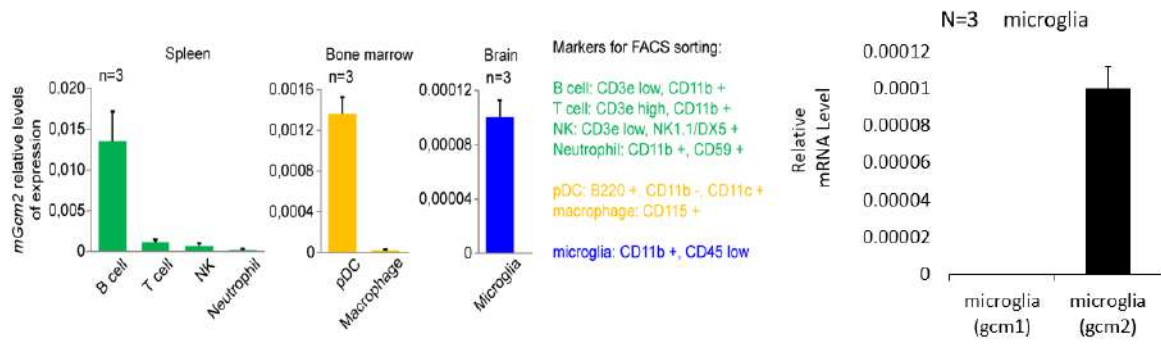


Figure 9. mGcm2 expression profile in sorted cells of adult wild type mice. qRT-PCR assays were performed on 6-7 week-old animals.

Hematopoiesis in mammals

Similar to *Drosophila*, hematopoiesis in mammals occurs in several waves. During embryonic development of mammals, macrophages are one of the first blood cell lineages to emerge. In mice, macrophages originate from three distinct waves of hematopoiesis: primitive hematopoiesis, hematopoiesis in the fetal liver and definitive hematopoiesis (**Figure 10**). Each wave differs but also overlaps temporally and spatially (Davies, Jenkins, Allen, & Taylor, 2013).

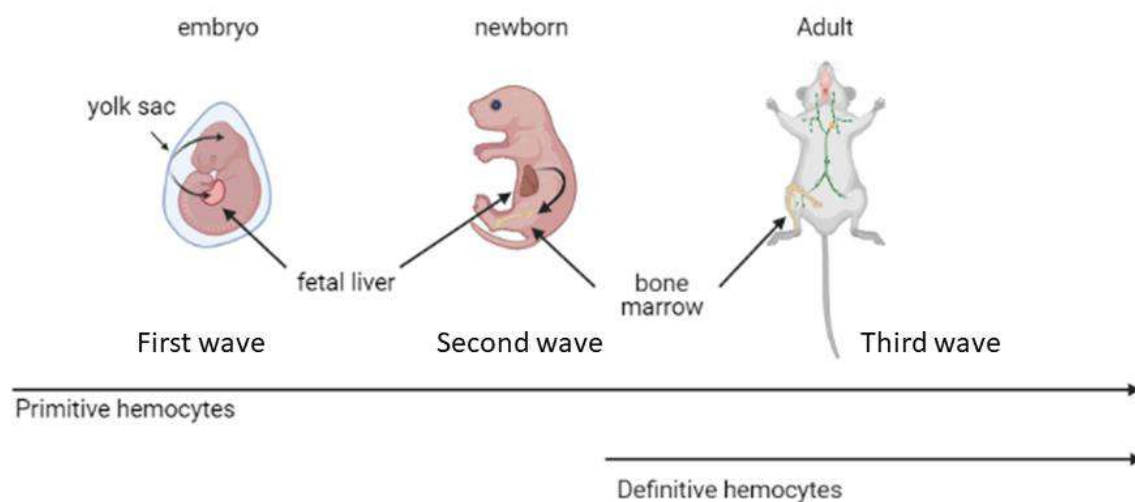


Figure 10. The hematopoietic waves in mammals.

In mice, primitive hematopoiesis begins around embryonic day E7.25 (Palis, 2016). The process occurs in distinct clusters of cells in the extra-embryonic yolk sac, called blood islands. Blood islands are composed of primitive hematopoietic cells in the center and sparse endothelial cells in the periphery (Hoeffel & Ginhoux, 2018). In the blood islands, unipotent myeloid progenitors are generated from erythromyeloid progenitors (EMPs) and can give rise to the macrophage lineage but not leukocytes (Hoeffel & Ginhoux, 2018). These progenitors remain in the blood islands until they are released during the onset of blood circulation at E8.0. Then, they circulate throughout the embryo (Hoeffel & Ginhoux, 2018). The first embryonic-

derived macrophages are detected in the yolk sac at E9.0 (**Figure 10**) (Naito, Yamamura, Nishikawa, & Takahashi, 1989; Takahashi, Yamamura, & Naito, 1989). Yolk sac-derived macrophages continue to proliferate and colonise the developing brain by E9.5 and the rest of the embryonic tissues by E12.5 until further diluted and replaced by macrophages generated from later waves (Hoeffel et al., 2015; McGrath, Frame, Fegan, et al., 2015; Palis, 2016; Schulz et al., 2012).

The second wave of macrophage generation also arises from the EMPs in the yolk sac around E8.25 (Hoeffel et al., 2015) and seed the developing fetal liver by E10.5 (**Figure 10**) (McGrath, Frame, & Palis, 2015; Palis & Yoder, 2001). There, they produce the first enucleated erythrocytes and give rise to bipotent granulocyte/macrophage progenitors and mast cells (Bertrand et al., 2005; McGrath, Frame, Fegan, et al., 2015; Palis, Robertson, Kennedy, Wall, & Keller, 1999). However, EMPs of the second wave are short-term progenitors, since transplantation of E10.5 EMPs into adult mouse recipients produce erythroid cells, with very limited myeloid cells or platelets (McGrath, Frame, Fegan, et al., 2015; McGrath, Frame, & Palis, 2015). Due to lack of long-term potential in adults, the second wave of hematopoiesis is also called “transient definitive wave” (Hoeffel & Ginhoux, 2018).

Hematopoietic stem cell (HSC) dependent definitive hematopoiesis begins at approximately E9.5 in the mouse intra-embryonic Aorta-Gonad-Mesonephros region (Medvinsky & Dzierzak, 1996), as well as in the vitelline and umbilical arteries (Zovein et al., 2010). EMPs from the first two waves and HSCs both derive from the hemogenic endothelium (Gritz & Hirschi, 2016) but their development differs significantly from one another (Wu & Hirschi, 2020). HSC emerge in clusters budding from the endothelial lining of the aortic wall in the Aorta-Gonad-Mesonephros region, and then migrate into the developing fetal liver, where they undergo maturation and massive self-expansion. By E16.5, the HSCs migrate to and colonise the developing fetal bone marrow, where they remain throughout adulthood, and generate all

needed blood cell lineages (Dzierzak & Speck, 2008). EMP-derived macrophages are replaced by HSC-derived macrophages in most tissues early in the postnatal period. For example, during the weaning period in mice, EMPs of the intestinal mucosa are diluted by tissue-resident macrophages that were generated by HSC-derived monocytes (Bain et al., 2014). A similar process was also observed in skin, spleen and heart, in which fetal monocyte-derived macrophages are replaced by adult monocyte-derived macrophages progressively over time (Hoeffel et al., 2015; Molawi et al., 2014; Tamoutounour et al., 2013). Yolk sac- and HSC-derived macrophages can coexist in the same tissue and maintain a balance in a steady state, except under inflammatory conditions, when large numbers of HSC derived macrophages invade tissues, such as the heart and liver (Bleriot, Li, Kairi, Newell, & Ginhoux, 2020; Yap, Cabrera-Fuentes, Irei, Hausenloy, & Boisvert, 2019).

Tissue-resident macrophages are best known as immune sentinels that sense and respond to invading pathogens and challenging surroundings. They are also essential in tissue development, remodelling, and homeostasis (McGrath, Frame, & Palis, 2015). Tissue-resident macrophages are heterogeneous, because of their diverse origins and the influence of tissue-specific microenvironments, and exhibit tissue-specific functions during development and adulthood (Naito et al., 1989; Takahashi et al., 1989). Specifically microglia, the tissue resident macrophages of the CNS, are the only line of defence since the CNS is an isolated environment. Due to their impact on the development, homeostasis and presence in every CNS pathology, microglia have been at the center of attention for more than two decades.

Microglia

Microglia were first described by Spanish neuroscientist Rio-Hortega in 1919 as a separate glia cell type (Rio-Hortega, 1919). They are a long lived, self-renewing population, generated by EMPs in the yolk sac early during embryogenesis (Ginhoux et al., 2010; Hoeffel & Ginhoux, 2015; Q. Li & Barres, 2018; Perdiguero et al., 2015). Apart from their immune surveillance role, these cells contribute to the development of the brain by modulating neurogenesis and synaptic pruning (Cunningham, Martinez-Cerdeno, & Noctor, 2013; Q. Li & Barres, 2018; Paolicelli et al., 2011; Schafer et al., 2012).

Microglia Development

Ontogeny of microglia was intensively studied for decades. The scientific community believed that they are of neuroectodermal origin, as the other glia cells of the CNS. Lineage tracing analysis formally proved that microglia rise from EMPs during the primitive wave (Ginhoux & Guilliams, 2016). However, microglia are not replaced by HSCs like other tissue resident macrophages of the primitive wave. In mice, the first EMPs develop from c-Kit^{lo}CD41^{lo} progenitors at E7.25 in the yolk sac (**Figure 11**) (Ginhoux et al., 2010). This early ontogeny of microglia in the yolk sac is supported by data from other model organisms such as chicken and zebrafish (Alliot, Godin, & Pessac, 1999; Cuadros, Martin, Coltey, Almendros, & Navascues, 1993; Herbomel et al., 2001). Yolk sac derived microglia progenitors enter the embryo circulation from E8 to E10 where they colonise into the CNS. This process is terminated before the establishment of the BBB.

Microglia development is highly dependent on specific transcription factors and cytokines (**Figure 11**) (Wang & Stifani, 2017). Initially, EMPs are RUNX1 positive. These progenitors give rise to primitive macrophages that are PU.1 and Interferon Regulatory Factor 8 (IRF8) dependent. Furthermore, primitive yolk sac macrophages are dependent on Colony Stimulating Factor 1 Receptor (CSF1R) signalling. Studies showed that CSF1R deficient mice lack completely microglia, thus highlighting the importance of this cytokine during microglia

development and migration (Greter et al., 2012; Y. Wang et al., 2012). Finally, adult microglia can be distinguished from other macrophages by the expression of ionized calcium-binding adapter molecule 1 (Iba-1), CX3CR1 and Transmembrane Protein 119 (TMEM119) (Jurga et al., 2020).

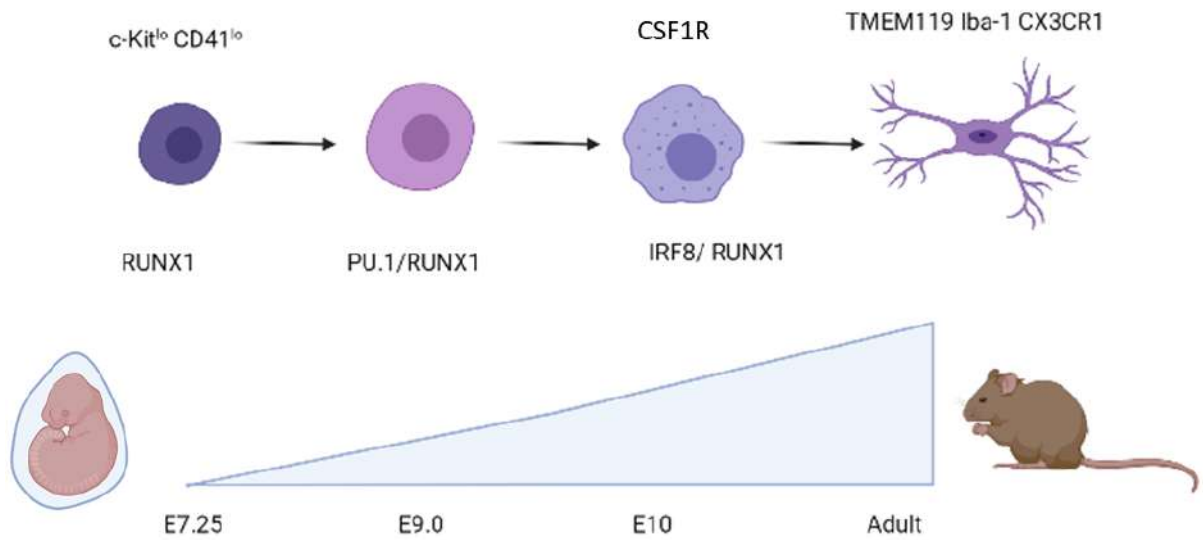


Figure 11. Microglia development with the main known transcription factors and markers. Early microglia express c-Kit and CD41 at low level and in the adult brain they are distinguished by the expression of CSF1R, TMEM119, Iba-1 and CX3CR1. Microglia development is highly dependent on the expression of RUNX1, PU.1 and IRF8.

Microglia functions during development and homeostasis

Microglia of the developing and early postnatal CNS and microglia of the adult CNS represent functionally different entities. These differences accrue from transcriptomic, functional, and morphological data, where different microglia stages also show different molecular signatures (**Figure 12**).

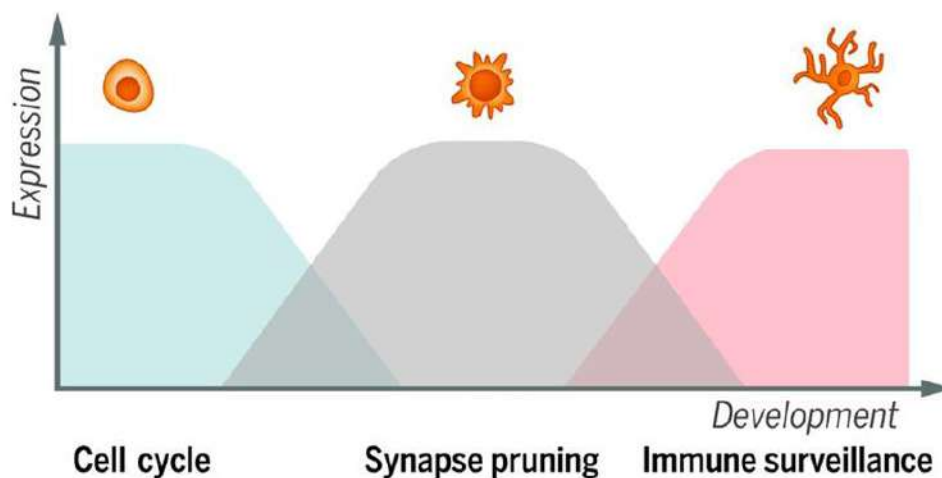


Figure 12. Microglia have different expression profiles that depend on the developmental stage. Early in development microglia primarily express cell cycle related genes that are important for their expansion. During development and early postnatal days microglia express genes that are associated with synapse pruning and finally in the adult brain microglia express genes related with immune surveillance (modified from Matcovitch-Natan et al., 2016)

In the developing brain, microglia are characterised by an amoeboid morphology without their characteristic ramifications. This amoeboid morphology indicates an activated state of microglia, which enables them to be more motile (Lawson, Perry, Dri, & Gordon, 1990). Furthermore, data concerning their expression profile confirm that in this state microglia contribute both to phagocytosis and to tissue remodelling (Matacovitch-Natan et al., 2016). In this study, they combined RNA-seq, ChIP-seq, ATAC-seq and single-cell RNA-seq data from early developing (E14), early postnatal (P14) and young adult microglia. The results showed three distinct signatures for each specific state. During CNS development microglia express

genes related to the cell cycle, while postnatal period microglia are responsible for synapse pruning (**Figure 12**). Finally, adult microglia express genes related to immunosurveillance.

Microglia during development and early post-natal stages assist in the CNS developing environment. They engulf cells of the CNS thus, contributing to the control of neuronal population by promoting apoptosis and performing phagocytosis of apoptotic or dying neuronal progenitors (**Figure 13**) (Ashwell, 1990; Mazaheri et al., 2014; Peri & Nusslein-Volhard, 2008). This process starts during embryonic development and remains up to the early postnatal period, where microglia also participate in the modelling of the neuronal circuits (Sierra et al., 2010). Furthermore, microglia also promote neurogenesis by supporting proliferation, survival and maturation of neuronal progenitors and neurons (Frost & Schafer, 2016). Studies have also shown that microglia support other types of CNS cells besides neurons. They are proven to participate during myelinogenesis and they can communicate with oligodendrocyte precursors during the early postnatal period (Hagemeyer et al., 2017). Finally, studies from mouse and zebrafish models suggest that microglia control neovascularization by promoting angiogenesis during development (Fantin et al., 2010).

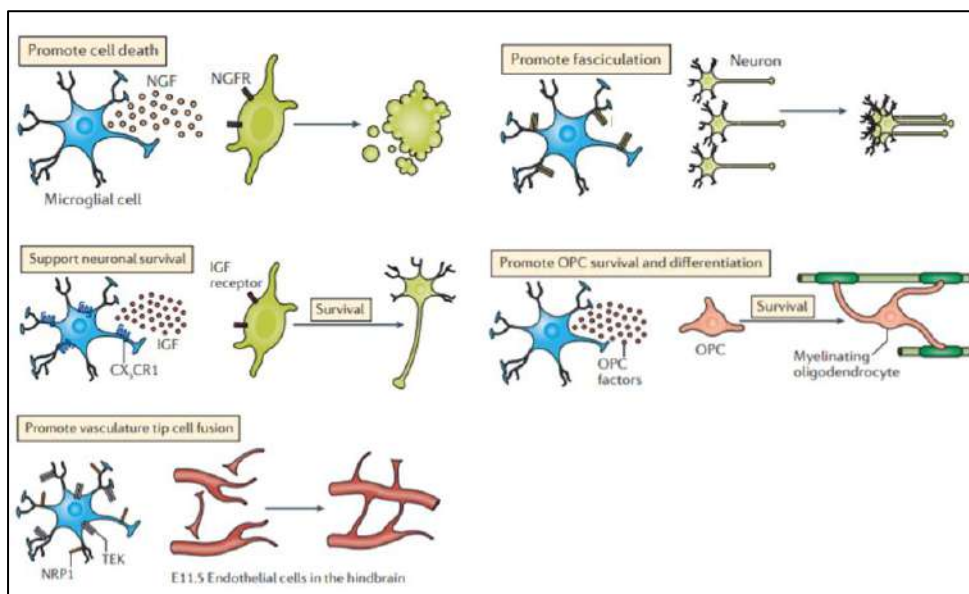


Figure 13. The main functions of microglia during development and early postnatal days. Microglia contribute to the control of CNS populations by promoting apoptosis or survival of neurons and oligodendrocytes (modified from Li and Barres 2018).

During adulthood, microglia constitute a crucial component for the maintenance of homeostasis (**Figure 14**). Based on time-lapse recording, it is estimated that microglia can scan the entire brain parenchyma within a few hours (Nimmerjahn, Kirchhoff, & Helmchen, 2005; Tremblay, Lowery, & Majewska, 2010; Wake, Moorhouse, Miyamoto, & Nabekura, 2013). During this scanning process they phagocytose dead, dying and sometimes healthy live cells in the developing and adult brain. Microglia also phagocytose myelin, which later in life can form insoluble protein aggregates in microglia lysosomes and compromise the cell function (Safaiyan et al., 2016). This might be a mechanism for controlling myelin turnover and a cause of aging. Furthermore, microglia control the size of the neuronal pool by engulfing neural precursor cells (NPCs) during adult neurogenesis (Cunningham et al., 2013; Sierra et al., 2010) and neuronal activity through ATP release (Y. Li, Du, Liu, Wen, & Du, 2012). Finally, microglia maintain the oligodendrocyte progenitor pool under homeostatic conditions (Hagemeyer et al., 2017). All these data show that microglia cells contribute more to the homeostasis of the CNS, rather than having just an immunosurveillance role.

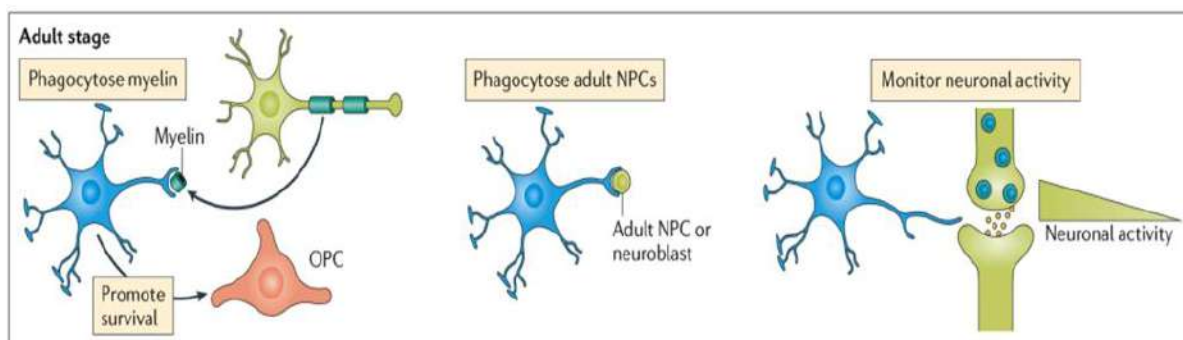


Figure 14. Main functions of microglia during adulthood. They are responsible for surveillance, phagocytosis and the survival of oligodendrocytes (OPC) (modified from Li and Barres 2018).

The CNS also participates in the general homeostasis and metabolism of the animal, with microglia being one of the key players. The first data came after the identification of the hypothalamus as a center of metabolic homeostasis. The theory that the CNS is a key player in the metabolic pathway arose from the observation that hypothalamic damage inflicted by either

tumours or by lesions (Brobeck, 1946; Hetherington, Altemus, Nelson, Bernat, & Gold, 1994), elicits voracious hunger (hyperphagia) and obesity. Since then, specific hypothalamic neuronal networks have emerged as key orchestrators of systemic metabolism, food intake, and body weight. Astrocytes and microglia, as well as neuronal–glia interactions, have recently been established as highly relevant for the control of systemic metabolism and could lead to improved pharmacological strategies to prevent and treat metabolic diseases (Rahman, Rao, & Khan, 2018). These data prompted research in immunometabolism, a ground-breaking field of investigation that studies the impact of chronic inflammation which leads to metabolic dysfunctions such as obesity and diabetes.

Direct data indicate that microglia have an important role during metabolic regulation since they control and regulate the hypothalamic microenvironment. For example, mouse models of diet-induced obesity (DIO) reported a rapid increase in expansion and activation of microglia populations, especially in the hypothalamus, even preceding weight gain (Milanski et al., 2009; L. Thaler et al., 2012). Microglia then respond by up-regulating pro-inflammatory molecules and ultimately mediating neuronal stress in the hypothalamic region (Valdearcos et al., 2014). Diet with saturated fatty acids, such as palmitic and stearic acids, can signal in microglia through Toll-like receptor 4 (TLR4) and its NF- κ B downstream pathway, thus resulting in the secretion of pro-inflammatory cytokines, Reactive Oxygen species (ROS) and Nitric Oxide (NO), thus confirming the notion that obesity is a chronic inflammatory disease (Z. Wang et al., 2012). For this reason, studies targeting microglia regulation show that preventing microglia proliferation in the CNS is sufficient to reduce diet-induced central and peripheral inflammation (Andre et al., 2017). Taken all these data into consideration I think that regulation of the microglia inflammation in the hypothalamus could have beneficial effects on people suffering from diabetes and obesity.

Microglia functions during an immune response

In the adult brain microglia have an immunosurveillance role and are characterised as resting microglia. This is reflected in both their morphology as well as their expression profile. Studies from CX3CR1^{GFP} animals reveal that even though their small somata are static, their ramified processes constantly survey their microenvironment (Davalos et al., 2005; Jung et al., 2000; Nimmerjahn et al., 2005). During homeostasis, microglia are mostly responsible for surveillance and phagocytosis. Phagocytosis of debris is part of all innate immune cells, and it is highly beneficial for the clearance of dying cells. This action prevents the spread of pro-inflammatory and neurotoxic molecules (Green et al., 2016; Wolf, Boddeke, & Kettenmann, 2017).

Microglia activation due to an inflammatory response causes changes in their gene expression, morphology, migration, motility, phagocytosis, proliferation, metabolism, and death. Activation of microglia can result into two different states. The first one is the classical activation of macrophages/microglia which are characterised as pro-inflammatory or M1 microglia. The second is the alternative activation that is known as anti-inflammatory or M2 microglia (**Figure 15**) (Stein, Keshav, Harris, & Gordon, 1992). An acute injury in the CNS causes injured cells to release pro-inflammatory cytokines such as tumour necrosis factor α (TNF- α) and interferon γ (INF γ). These cytokines along with debris activate microglia to start producing pro-inflammatory cytokines and molecules such as TNF α , IL1 β and IL12 as well as inducible NO species (iNOS) (Taylor et al., 2005; Villalta, Nguyen, Deng, Gotoh, & Tidball, 2009). IL1 β specifically is one of the most important mediators of the inflammatory response, and is involved in a variety of cellular activities, including cell proliferation, differentiation, and apoptosis (Y. Li et al., 2018). Then microglia migrate towards the site of the damage. During this migration, their processes are getting shorter, and they adopt an amoeboid form (Davalos et al., 2005; Jung et al., 2000; Nimmerjahn et al., 2005). Apart from release of

cytokines and morphological changes, microglia initiate proliferation. This mechanism is mediated by upregulating the CSF1R and the proliferation is controlled through autocrine signalling (Tay et al., 2017). Eventually, resolving of the inflammation causes microglia apoptosis in order to maintain their population.

Activated microglia also show altered gene expression. For example, resting microglia express Major Histocompatibility Complex Class II (MHC II) molecules at low levels that get upregulated along with adhesion molecules in response to CNS inflammation or injury (Aloisi, De Simone, Columba-Cabezas, Penna, & Adorini, 2000). These molecules are the leukocyte function-associated molecule1 (LFA1 or CD11a) and the intercellular adhesion molecule 1 (ICAM1 or CD54). These genes promote the antigen presenting ability of microglia which is reinforced by the expression of co-stimulatory molecules. This final step is crucial for the activation of the adaptive immunity.

Upon resolving the inflammation or the injury microglia also contribute to tissue regeneration and remodelling (M2 microglia) (**Figure 15**) (Deng, Wehling-Henricks, Villalta, Wang, & Tidball, 2012; Longbrake, Lai, Ankeny, & Popovich, 2007; Novak & Koh, 2013; Ruffell et al., 2009; Shechter & Schwartz, 2013a, 2013b). During this state microglia release anti-inflammatory cytokines and molecules such as IL4, IL10, TGF β and Arginase 1 (Arg-1) (Chhor et al., 2013; Fenn, Henry, Huang, Dugan, & Godbout, 2012; Freilich, Woodbury, & Ikezu, 2013; H. C. Liu et al., 2012). Their main role is to deactivate the pro-inflammatory cells such as M1 microglia/macrophages and initiate tissue repair (Ortega-Gomez, Perretti, & Soehnlein, 2013). For example, IL10 up-regulates the production of extracellular matrix proteins and promote wound repair by microglia phagocytosis of cell debris (Martinez, Helming, & Gordon, 2009).

For years many studies tried to understand whether the M2 microglia come from resting microglia or whether the M1 microglia could transition into the M2 phenotype. So far, most data suggest that indeed M1 microglia could transition into the M2 phenotype in order to promote tissue repair (Bolos, Perea, & Avila, 2017; Subramaniam & Federoff, 2017; Zheng et al., 2018). Thus, the study of the transition from M1 to M2 and the transcription factors that participate is of imperative importance as new insights of these mechanisms could lead to potential therapeutic targets for neuroinflammatory diseases such as multiple sclerosis and Parkinson’s disease.

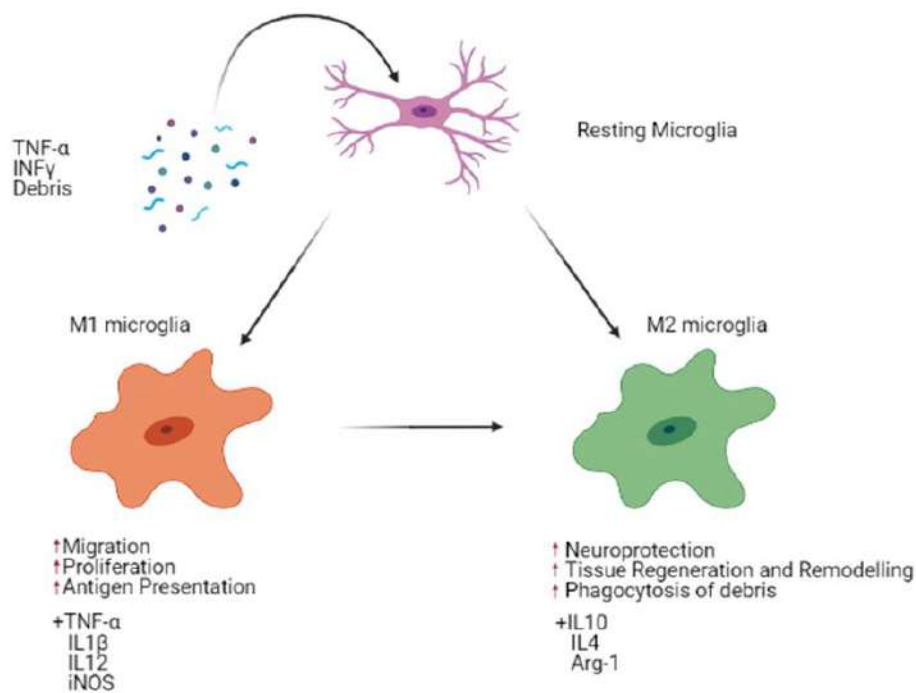


Figure 15. Classification of macrophages/microglia as M1 (pro-inflammatory) or M2 (anti-inflammatory).

Microglia during aging

Aging within the human brain is of considerable interest because age-related changes are frequently irreversible and can severely impair normal activity (Damoiseaux, 2017). However, our understanding of the cause of aging is limited. Neuronal survival and normal function may be affected by cell autonomous changes. However, neurons are highly dependent on glia for many reasons (York, Bernier, & MacVicar, 2018). Two different models could explain the effects of aging on microglia. Either microglia react to aging-related changes in their environment, or microglia may be directly affected by the aging process itself. Regarding the former, a primary function of microglia is surveillance of the CNS microenvironment, including the monitoring of extracellular chemical changes, debris accumulation, pathogen invasion, and altered neuronal signalling (Anderson, Hubbard, Coghil, & Slidders, 1983; Duffy, Huang, Rapport, & Graf, 1980; Sykova, Mazel, & Simonova, 1998; Terry, DeTeresa, & Hansen, 1987). It is also possible that these changes affect microglia secondarily. Just as aging related astrogliosis, which is an abnormal increase of the number of astrocytes due to the destruction of nearby neurons, has been interpreted as a secondary reactive glia cell response to neuronal changes, the microglia activation that reportedly occurs with aging may also be considered a secondary glia response (DiPatre & Gelman, 1997; Rogers & Rovigatti, 1988; Streit & Sparks, 1997).

Nonetheless, aged microglia have been characterised as senescent or dystrophic. But it is currently unclear whether the two terms describe one state or are actually two different states because senescence can imply different states. Originally derived from the study of cancer cells, cellular senescence implies a loss of the ability to divide (Campisi, 2013). On the other hand, dystrophic is a term derived from a morphological change as observed from the study of brain sections (Streit, Sammons, Kuhns, & Sparks, 2004). However, all studies confirm similar changes in aged microglia.

Aged microglia show similar morphological changes and expression of pro-inflammatory proteins as in the case of activation during an immune challenge (Streit et al., 2004). Aging microglia have also been found to have an altered surveillance phenotype with less dendritic branching and reduced process motility (**Figure 16**) (Angelova & Brown, 2019). Furthermore, when confronted with injury they exhibit lower migration rates and have a more sustained inflammatory response in reaction to damage (Damani et al., 2011). Concerning their function, aged microglia have been found to exhibit reduced phagocytosis and increased ROS production compared to young healthy microglia (Koellhoffer, McCullough, & Ritzel, 2017). Finally, a study observed increased expression of cytokine genes and that microglia have a reduced ability to migrate to sites of injury and stimulate inflammation in Alzheimer's disease (Orre et al., 2014). Overall, these data suggest that microglia during aging lose their capacity to initiate a strong and effective immune response upon challenge.

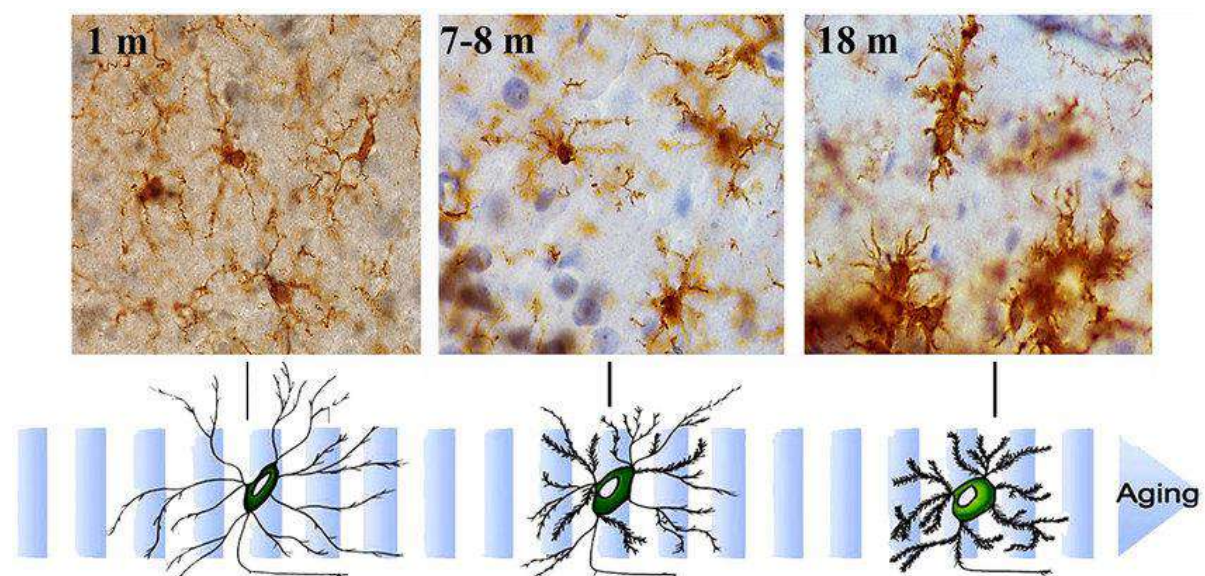


Figure 16. Aging-related morphological changes of microglia. Microglia cell morphology changes with aging. Immunohistochemistry for Iba-1 (a constitutive identity marker for monocyte-macrophage cells) and counterstaining with hematoxylin of hippocampal sections from animals of different ages (1- to 18-month old). Microglia obtained from young mice have a small cell body and very long and slender ramifications. As mice age, microglia gradually show bigger cell bodies and progressively shorter and thicker cell processes (from von Bernhardi et al., 2015).

The vast majority of studies of aging-related immune changes in microglia demonstrate a steady increase in the expression of markers usually found to be up-regulated on activated microglia after acute CNS injuries. These markers include MHC class II molecules, which have been reported in humans (Rogers et al., 1988; Streit et al., 1997; DiPatre et al., 1997), monkeys (Sheffield & Berman, 1998; Sloane, Hollander, Moss, Rosene, & Abraham, 1999), and rats (Ogura, Ogawa, & Yoshida, 1994; V. H. Perry, Matyszak, & Fearn, 1993). The increases in MHC II expression very likely represent immune-related changes in the existing microglia population (Long et al., 1998). In addition to MHC II antigens, molecules such as the ED1 macrophage antigen, the leukocyte common antigen (LCA), and the CD4 antigen are present with increasing frequency on microglia in the aging CNS of the rat (V. H. Perry et al., 1993).

Activated microglia have been found in association with disease markers such as plaques of β amyloid in Alzheimer's Disease (AD) (Mattiace, Davies, Yen, & Dickson, 1990). Aged microglia lose their ability to clear β -amyloid effectively from the extracellular space. In mouse models, aged microglia have reduced expression of β -amyloid degrading enzymes and reduced phagocytotic capacity (Hickman, Allison, & El Khoury, 2008). However, there has been recent discussion as to whether these microglia are activated or dystrophic, and which form is most likely to be causative in the relevant pathological changes (Navarro et al., 2018). Evidence suggests that both markers of M1 and M2 activation states are present in AD (Hopperton, Mohammad, Trepanier, Giuliano, & Bazinet, 2018). Other studies suggest both activation states are present but at different times (Tang & Le, 2016). Sc-RNA seq studies also suggest that there is a continuous, heterogeneous spectrum of states present in the brain of mouse models of AD (von Maydell & Jorfi, 2019). Unfortunately, most data from the normal aging process have not been extensively studied and more research should be conducted. During my PhD I characterised the role of mGcm2 in microglia during aging.

Microglia during autoimmune and neurodegenerative diseases

Microglia not only are responsible for the development and the homeostasis of the CNS but they have also been repeatedly implicated in neurodegenerative diseases, including Multiple Sclerosis, Alzheimer disease and Parkinson disease (Cai, Hussain, & Yan, 2014; Cooper-Knock et al., 2017; Lall & Baloh, 2017; Ransohoff, 2016; Sanchez-Guajardo, Tentillier, & Romero-Ramos, 2015).

Multiple Sclerosis (MS)

Multiple sclerosis (MS), the most prevalent neurological disability, is an autoimmune-mediated disorder that affects the CNS and often leads to severe physical or cognitive incapacitation and neurological problems (Compston & Coles, 2008). The primary causes of MS are myelin sheath destruction which creates multifocal zones (sclerotic plaques) of inflammation, T-lymphocytic and macrophage infiltrations as well as oligodendrocyte death (Loma & Heyman, 2011). These plaques are composed of inflammatory cells and their products, demyelinated and transected axons. The lesions lead to neuronal dysfunctions such as autonomic and sensorimotor defects, visual disturbances, ataxia, fatigue, difficulties in thinking, and emotional problems (Compston & Coles, 2008). The role of microglia in MS has been complex and controversial, with evidence suggesting that these cells play key roles in both active inflammation and remyelination.

The initial pool of phagocytic cells in an early MS lesions is comprised of roughly 40% microglia (TMEM119 positive cells) and the rest were infiltrated macrophages (Satoh et al., 2016; Zrzavy et al., 2017). Furthermore, active demyelination is usually associated with a pro-inflammatory microglia phenotype (positive for CD68, CD86, MHC II antigens) while anti-inflammatory markers (CD206, CD163, ferritin) peak in the inactive lesion center (**Figure 17**) (Zelinka, Scott, Volkov, & Fischer, 2012). In multiple animal models, internalization of myelin by microglia leads to a pro-regenerative phenotype expressing Arg-1, CD206, and insulin-like

growth factor-1 (IGF-1) which facilitates oligodendrocyte differentiation and is necessary for remyelination (Bogie, Stinissen, & Hendriks, 2014; Boven et al., 2006; W. W. Li, Setzu, Zhao, & Franklin, 2005; Lloyd, Davies, & Miron, 2017; Miron et al., 2013). Due to this high impact of microglia in MS many studies target them as potential therapeutic strategies.

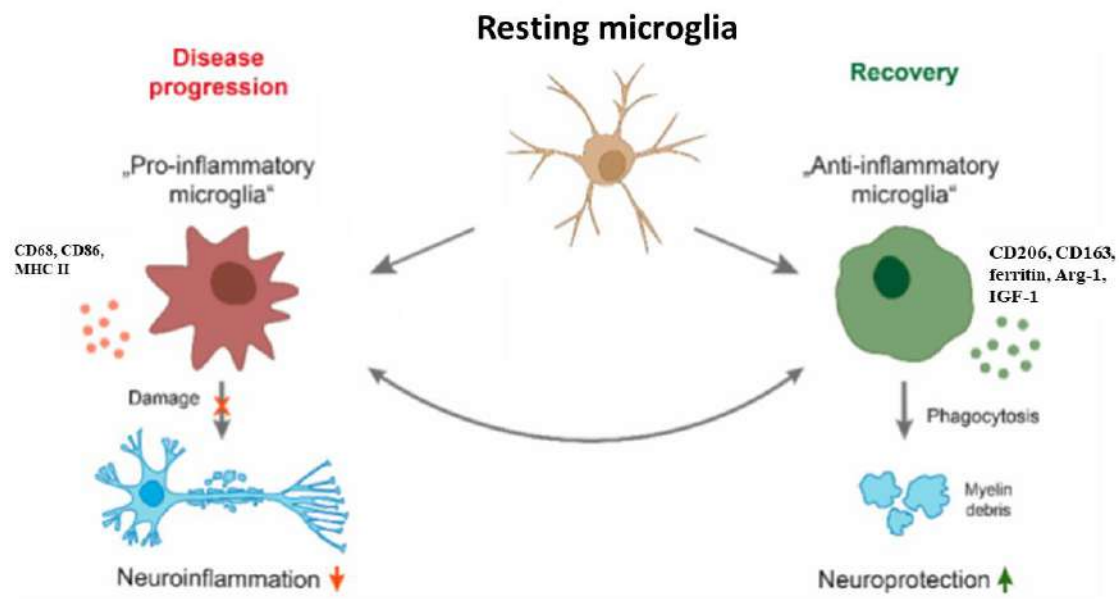


Figure 17. Schematic overview of microglia polarization in multiple sclerosis (MS). During disease progression, active microglia secrete cytokines and upregulate cell surface molecules. The phenotype triggers oligodendrocyte damage, resulting in demyelination, axonal damage, and neuronal loss. On the other side, microglia have important physiological functions in maintaining tissue homeostasis, including clearance of debris, resulting in neuroprotection. (modified from Geladaris et al., 2021).

Current disease modifying therapies (DMT), which are treatments that can reduce the activity and progression of MS, have been shown to affect microglia and are divided into indirect and direct effects (Giunti, Parodi, Cordano, Uccelli, & Kerlero de Rosbo, 2014; Healy, Michell-Robinson, & Antel, 2015). For example, interferon beta exerts an indirect effect by inducing a T helper type 2 cells (Th2) shift in lymphocyte profile thereby reducing the pro-inflammatory phenotype of microglia (Dasgupta, Jana, Liu, & Pahan, 2002; Kawanokuchi, Mizuno, Kato, Mitsuma, & Suzumura, 2004). So far, fingolimod probably has the most direct effect of any

DMT given that it can access the CNS and bind directly to microglia receptors, thus leading to downregulation of pro-inflammatory cytokines (Noda, Takeuchi, Mizuno, & Suzumura, 2013). There is also evidence that fingolimod may augment microglia related remyelination (Jackson, Giovannoni, & Baker, 2011). Similarly, many of the currently available DMTs have effects on microglia by decreasing inflammatory tone. Unfortunately, these mostly anti-inflammatory therapies have limited if any, effects on remyelination or the progression of the disease.

Emerging therapies targeting microglia directly are now being investigated in the experimental autoimmune encephalomyelitis (EAE) model with promising results. For example, PLX5622 is an oral CSF1R antagonist that inhibits its kinase activity and was shown to preferentially deplete microglia of the M1 phenotype, reduce demyelination, preserve mature oligodendrocytes, and improve mobility in EAE mice (Nissen, Thompson, West, & Tsirka, 2018). Moreover, another agent (ethyl pyruvate) was shown to reduce Iba1 positive microglia within the CNS and protect it against EAE (Djedovic et al., 2017). A peptide vaccine therapy (PADRE-Kv1.3) decreased numbers of infiltrating microglia, and promoted a shift in the phenotype of microglia from pro-inflammatory (expressing iNOs) to anti-inflammatory (expressing Arg-1) (Fan et al., 2018). These data show that both microglia and animal models such as the EAE could lead to new therapeutic strategies in order to discover a cure for one of the most prevalent autoimmune diseases of the CNS.

Alzheimer's disease

Alzheimer's disease (AD) classical hallmarks include brain atrophy, extracellular amyloid-beta (A β) deposits, intracellular aggregated phosphorylated tau, dystrophic neurites, synapses and neurons loss (Bedner et al., 2015). The presence of reactive glial cells within the AD plaques was first described by Alois Alzheimer and further studies identified both reactive astrocytes and microglia in the vicinity of the A β deposits (Graeber et al., 1997; Verkhratsky & Parpura, 2016). Human genetic studies identified over 25 genetic loci that robustly associate with AD risk (Hansen, Hanson, & Sheng, 2018; Verheijen & Sleegers, 2018). Among them, most of the common (ApoE, Sp11) or rare (Trem2, Cd33) genetic variants code for proteins that are preferentially or exclusively expressed in microglia. These findings strongly support an involvement of microglia cells in AD pathogenesis.

AD brains exhibit at least two very distinct morphological microglia phenotypes: cells associated to the amyloid plaques and those in the rest of the parenchyma have a homeostatic-like morphology (Krabbe et al., 2013). Microglia associated to plaques activate specific signalling pathways and functions. Using scRNA-seq of sorted AD mouse brain immune cells, Keren-Shaul et al. identified three distinct subtypes of microglia, including Disease Associated Microglia (DAM) (Keren-Shaul et al., 2017). DAM's relative abundance increases along with disease progression, and they are preferentially located around amyloid plaques. Deciphering, whether these subpopulations have beneficial, neutral or detrimental effects on brain cells, including neurons, will open the way for the design of innovative disease-modifying therapeutic strategies such in the case of MS.

Parkinson's disease (PD)

Parkinson's disease (PD) is the second most common neurodegenerative disorder. A hallmark of PD is the degeneration of dopaminergic neurons and it is responsible for the motor impairments of the disease (Moore, West, Dawson, & Dawson, 2005). Aging is a dominant risk factor for PD, with a sharp increase in incidence after age 60 years (de Lau & Breteler, 2006). After identifying the mutations responsible for the disease in the SNCA gene that encodes the α -Synuclein (α -Syn) protein (Polymeropoulos et al., 1997), many other pathogenic mutations associated with PD have been identified (Bandres-Ciga, Diez-Fairen, Kim, & Singleton, 2020; Klein & Westenberger, 2012; Trinh & Farrer, 2013). Genome-wide association studies (GWAS) also suggest that both adaptive and innate immunity may play a role in PD pathogenesis (Chang et al., 2017; Hamza et al., 2010; Holmans et al., 2013; Pierce & Coetzee, 2017). Recently, it was shown that many of the PD-related genes are expressed in glial cells as well as neurons (Booth, Hirst, & Wade-Martins, 2017), suggesting that mutated gene products in microglia and/or astrocytes could contribute to PD etiology.

The intraneuronal inclusions of α -Syn protein, commonly referred to as Lewy bodies (LB) or Lewy neurites (LN), are pathological hallmark of PD. These are caused by missense mutations and multiplications (duplications or triplications) of the α -Syn gene (Ibanez et al., 2004; Ibanez et al., 2009; Polymeropoulos et al., 1997; Singleton et al., 2003). Under physiological conditions, α -Syn regulates the trafficking of synaptic vesicles, but in pathologic states, α -Syn undergoes aggregation and fibrillization that leads to neurotoxicity in PD (Burre, Sharma, & Sudhof, 2014; Cookson, 2009; Jo et al., 2004). The microglia response to excess or mutant α -Syn species is the subject of ongoing investigations. So far it is known that extracellular α -Syn oligomers function as damage-associated molecular patterns, thus activating innate immune receptors on the surface of microglia (C. Kim et al., 2013). α -Syn is also reported to bind Fc gamma receptor IIB (Fc γ RIIB) on microglia surfaces and reduce microglia phagocytosis,

which could impair the clearance of aggregated species or other parenchymal debris (Choi et al., 2015). Thus, aggregated α -Syn induces pro-inflammatory microglia behaviours via both classic innate immune receptors and interactions with intracellular signalling cascades.

Due to the above data, many studies suggest that microglia could be an important target for treating PD. Interestingly, a recent study proposes that neuronal cell membrane (CM, i.e., MES23.5 cells) coated Cu_{2-x}Se -PVP-Qe biomimetic nanoparticles (abbreviated as CSPQ@CM) could target microglia and manipulate their polarization for improving the efficacy of PD therapy (H. Liu et al., 2020). These biomimetic nanoparticles have multienzyme-like activity for the effective elimination of ROS (i.e., H_2O_2 , $\cdot\text{OH}$, $\text{O}_2 \cdot^-$ radicals) in the microenvironment of the brain. More importantly, they could facilitate microglia polarization into the neuroprotective M2 phenotype, which can secrete anti-inflammatory cytokines and trophic factors thus promoting neuroprotection.

To summarise, microglia play an important role during all stages of the CNS from development to adulthood and aging. They also have an active role during autoimmune and neurodegenerative diseases. However, more information concerning their activation and regulation of their state are of immense importance. All actions of cells such as microglia are regulated by transcription factors that initiate the expression of proteins. Gcm has already been proven to have anti-inflammatory properties in different animal models such as the fly, the crayfish and the sea urchin. Furthermore, data from previous people from our lab showed that there is mGcm2 expression in microglia cells. Moreover, microglia resemble both the glia and the hemocytes of fly, the most famous Gcm animal model, which suggest that these cells could also depend on the Gcm cascade in order to regulate their immune response. For this reason, during my PhD I aimed to characterise the role of the transcription factor mGcm2 in the regulation of microglia activation.

During my PhD, I aimed to define the role of Gcm in the cells of the innate immune system that derive from the primitive wave. For this reason, I choose the microglia population which unlike the other tissue resident macrophages are not replaced by cells of the definitive wave.

More specifically my aims during my PhD were:

- Characterise the expression profile of mGcm2 (anti-mGcm2 Immunolabeling on whole mount embryos and sections from adult tissues)
- Analyse the requirement of mGcm2 in microglia by phenotyping a conditional knock out (cko) line (microglia proliferation, morphology, inflammatory marker expression and phenotypic analysis).
- Characterise the requirement of mGcm2 in microglia in vitro on primary cultures from cko neonatal mice (phagocytosis and migration assays).
- Characterise the expression of Gcm in *Drosophila* under neuroinflammatory conditions.

Finally, during my PhD I was extremely happy to participate in multiple group projects, one of which was to determine the heterogeneity of hemocytes in *Drosophila*. The results show that indeed those macrophage-like cells can be divided into different groups and the transcriptomic data show that as microglia they also participate in processes during development, homeostasis and immune challenge. From my work during this project, I discovered a novel marker (Shot) for lamellocytes that is also expressed in lower level in hemocytes as well. Further experiments revealed that Shot indeed participates during both homeostatic and challenged conditions in the function of hemocytes.

Materials and Methods

Mouse lines

All invasive procedures were reviewed and approved by the Comité d'Ethique en Expérimentation Animale IGBMC-ICS. Cx3cr1-Cre mice were obtained from TAAM Orléans and then bred to maintain them on the C57Bl/6J background. The mGcm2flox/flox line was created at the Institute Clinique de la Souris (ICS), in Strasbourg. Mutant mice with their littermate controls derived from Cx3cr1-Cre/+;mGcm2flox/+ crossed with mGcm2flox/flox. The mice were maintained on a normal diet in a 12-hour light/dark cycle. Approximately five to ten mice were used per group (per gender, age and genotype).

Genotyping

Tail, finger or ear clips were used for genotyping. Samples were incubated overnight at 56°C with 750 µl of extraction buffer and 40 µl of proteinase K. Then the samples were vortexed and mixed for 5 min. 250 µl of NaCl (5-6M) was added, the samples were vortex and centrifuged for 10 min at 13000 rpm. Then, 900 µl of the deeper phase supernatant were transferred into a new tube, avoiding the pellet. 600 µl of isopropanol was added and the samples were mixed for 1 min. Next, the samples were centrifuged at 13000 rpm for 10 min, the supernatant was discarded, the pellet was washed with 1ml of 70% ethanol and centrifuged for 10 min at 13000 rpm. Finally, the pellets were dried under a lamp and the DNA was resuspended in 30 µl of TE/H₂O and they were incubated at room temperature (RT) for 1 hour.

The extraction buffer was composed of 50ml Tris HCl pH8 at 1M, 200ml EDTA pH8 at 0.5M, 20ml NaCl at 5M, 50ml SDS, 1000 ml H₂O. The TE was composed of 10ml Tris pH8 at 1M, 2ml EDTA pH8at 0.5M and 1000 ml H₂O.

For the PCR 2 µl of sample were added in 0.5 µl of forward primer (100µM), 0.5 µl of reverse primer (100µM), 0.4 µl of dNTPs (Roche), 2 µl of Buffer (Roche), 0.2 µl of Taq polymerase

(Roche) and 14.4 µl of H₂O. The samples were incubated at 95°C for 4 min followed by 35 cycles of 94°C for 30 sec, 62°C for 30 sec and 72°C for 1min.

The amplified DNA was run in 1% agarose gel with TAE (Tris Acetate EDTA) and 1 drop of ethidium bromide at 150 volts for 45 min. The results were imaged under UV light.

Name	Forward primer	Reverse primer	Size
CX3Cr1cre	GTTCGCAAGAACCTGATG GACA	CTAGAGCCTGTTTTGCACGTT C	340
mGcm2flox	CAATAGGGAAGTGATCCC TAGAGTC	GGGAAACTTGTCTGTTCTTTC ACACAG	274
mGcm2WT	CAATAGGGAAGTGATCCC TAGAGTC	GGGAAACTTGTCTGTTCTTTC ACACAG	149

Weight measurements and body composition

In order to phenotype the mGcm2 cko line and the impact of the specific deletion in microglia cells I created two separate cohorts that were kept at the phenotyping area of the ICS with at least 5 animals per group. All groups were weighted weekly.

Furthermore, the second cohort was evaluated for their body composition by Quantitative Nuclear Magnetic Resonance (qNMR) using Minispec+ analyzer (Bruker BioSpin S.A.S., Wissembourg, France). The test gives precise analyses of the body composition with respect to fat content, lean tissues and free body fluids in a mouse. The qNMR uses protons which respond differently to disturbances according to the tissue. A magnet within the analyser is used to align the protons within a sample's tissues which are then hit with radio waves. This causes a temporary disturbance in the magnetic moments (spin states) of the protons. As the protons return to their original positions (relax), they produce peaks on a spectrum whose

positions and intensities (amplitudes) are measured and thus reflect their chemical environment (fat or lean). Fat produces greater peak amplitude and has a greater rate of relaxation than lean because its hydrogen (proton) density is greater (~40% more hydrogen per unit).

Metabolic cages

Mice of the second cohort were further evaluated by metabolic or calorimetry cages. Calorimetry cages allow the simultaneous measurement of energy expenditure, ambulatory activity as well as food and water intake. Energy expenditure was evaluated through indirect calorimetry by measuring oxygen consumption with an open flow respirometric system. The CO₂ production was also measured, thus the respiratory exchange ratio (RER) and the heat production were calculated. Infra-red frames integrated to the system measured the ambulatory activity. Finally, food intake monitoring system was integrated to allow measurement of feeding and drinking behaviours. The test was conducted at room temperature (25°C). The mice, at the age of 2 weeks, were left to settle in 12hours prior to the test. Then measurements concerning the energy expenditure, movement and water/food intake was recorded for 24hours.

P1 primary CNS cultures

For the *in vitro* studies, I used microglia from primary culture of the CNS. Postnatal day 1 (P1) mice were collected, decapitated and the heads were sterilized by quickly immersing them in ethanol. The ethanol was then removed by immersion in HBSS solution (Gibco) with 4-(2-hydroxyethyl)-1-piperazineethanesulfonic acid (Hepes) three times. For the dissection, the brain was removed, the hemispheres were separated, the meninges were removed, and the hemispheres were then cut into smaller pieces. For the disassociation, the brain pieces were transferred into a Falcon tube with 2ml of medium (DMEM with 1gr/L glucose, 10% Fetal Calf Serum (FCS, #95) and 1% Penicillin (1MU)/Streptomycin), and mechanically disassociated with a pipette. To ensure a single cell suspension the cells were passed through a filter (70µm)

to a new tube. The cells were finally counted and diluted to a concentration of 300.000 cells/ml. The cells were plated in Polyornithine (Sigma) covered wells or coverslips. The cultures were kept in the incubator at 37°C and 5%CO₂ for 14 days. The medium was changed at day 1 and day3. *In vitro* cultures were fixed with 4%PFA in 1xPBS and then proceed to the immunolabelling.

Tissue dissections

Mice were anesthetised by a solution of Ketamine (100 mg/ml) / Xylazine (Rompun, 20 mg/ml): 130mg/kg of ketamine + 13 mg/kg of xylazine, transcardially perfused with ice-cold PFA 4% in 1xPBS, and then the brains, the spinal cord, lungs, adipose tissue and spleen were dissected out. The tissues were fixed overnight with 4% PFA (Electron Microscopy Sciences) in 1xPBS and then the brains were cut into left and right hemisphere and the rest of the tissues were cut in half. Half of the samples were transferred into a 70% ethanol solution and they were used for paraffin sections. The tissue is dehydrated gently by immersion in increasing concentrations of a ethanol. This gradual change in hydrophobicity minimizes cell damage. The dehydrating agent is then cleared by incubation in xylene prior to paraffin embedding. Paraffin is heated to 60°C and then allowed to harden overnight. Finally, the tissue is sectioned using a microtome. Tissue sections are dried onto microscope slides, put at 37°C overnight and stored for extended periods at 4°C. The other half were incubated with 15% sucrose overnight, embedded into cryomatrix (Thermo Fischer) and used for cryosections. For the paraffin labelling 8µm thick sections are used while for cryosection 50µm thick sections are used.

Phagocytosis Assay

Phagocytosis assay was performed on *in vitro* primary cultures of the CNS to evaluate the phagocytic capacity of microglia. After 14 days in culture the medium was replaced by medium with latex fluorescent beads (0.5µm, Polysciences) at a concentration 1/500. The cultures were

incubated with beads for 0, 20 and 120 min. Then the cells were fixed with 4%PFA in 1xPBS and the samples were used for immunolabelling.

Migration Assay

Migration assay was performed on *in vitro* primary cultures of the CNS to evaluate the migratory capacity of microglia of the different genotypes. After 14 days in culture, the coverslips were scratched with the tip of 200 μ l pipette. Next, the samples were left in the incubator for 6, 12 and 24 hours. Finally, the samples were fixed with 4%PFA in 1xPBS and the samples were used for immunolabelling.

To study the healing process the scratch wound assay was performed at the screening facility of IGBMC. The nuclei of the cells were labelled with Hoechst 33342 to allow to live tracing. Then live images were acquired every 20 min for 24 hours. The healing process was assessed by counting the distance of the scratch at each time point.

Immunolabelling

Frozen sections were taken out, left to defreeze for 30 min. Then they were fixed with ice cold acetone for 10 min, rehydrated with 1xPBS for 10 min and the samples were used for immunolabelling. Paraffin sections were treated with 0.01M sodium citrate (WVR) pH6 as a demasking step. The samples were incubated in a bath of sodium citrate for 20 min at 96 $^{\circ}$ C and then the samples were used for immunolabelling.

For the immunolabelling samples were permeabilised with PTX (1xPBS, 0.1% Triton-X100) for 30 min and incubated with blocking buffer for 1h in RT. Samples from *in vitro* cultures and frozen sections were incubated in blocking buffer that contained 1xPBS, 4% BSA (MP Biomedicals) and 0.1% Triton-x. Paraffin sections were incubated with blocking buffer that contained 5% skim milk powder in 0.1% PTX. The samples were incubated with primary antibodies overnight at 4 $^{\circ}$ C, washed three times with PTX, incubated with the appropriate

secondaries and washed three times with PTX. Finally, the samples were incubated with 4',6-diamidino-2-phenylindole (DAPI (Sigma-Aldrich)) to label the nuclei and the samples were mounted with Aqua Poly/Mount (Polysciences).

Primary Antibodies:

Name	Host	Origin (ref)	Concentration
Arginase-1 (Arg-1)	Mouse	Santa Cruz Biotechnology (sc-271430)	1/200
CD11b	Rat	Bio-Rad (MCA 74G)	1/400
CD45	Rat	Invitrogen (MCD 4500)	1/50
CD68	Rat	Bio-Rad (MCA 1957)	1/400
F4/80	Rat	Bio-Rad (MCA 497)	1/100
Glia cells missing 1 (Gcm1)	Rabbit	Gift from B. Nait-Oumesmar	1/50
Glia cells missing 2 (Gcm2)	Rabbit	Abcam (ab201170)	1/200
Ionized calcium binding adaptor molecule 1 (Iba-1)	Rabbit	Wako Chemicals (019- 19741)	1/300
iNOS	Mouse	Abcam (ab210823)	1/100
Phosphohistone 3 (PH3)	Mouse	Millipore (05-806)	1/100
Myelin Basic Protein (MBP)	Chicken	Invitrogen (10008)	1/500

Secondary Antibodies:

Name	Host	Origin (ref)	Concentration
Anti- mouse Cy3	Donkey	Jackson (715-165-151)	1/500
Anti-rabbit Cy3	Donkey	Jackson (711-165-152)	1/500

Anti-rat Cy3	Goat	Jackson (112-165-167)	1/500
Anti-mouse Cy5	Goat	Jackson (115-605-166)	1/500
Anti-rabbit Cy5	Goat	Jackson (111-175-144)	1/500
Anti-rat Cy5	Goat	Jackson (112-175-144)	1/500
Anti-chicken FITC	Donkey	Molecular Probes (A11039)	1/500

Confocal Imaging

Leica Spinning Disk microscope equipped with 20,40 and 63X objectives was used to obtain confocal images. GFP/FITC was excited at 488nm; the emission filters 498-551 were used to collect the signal. Cy5 was excited at 642nm; emission signal was collected at 729-800nm and Cy3 was excited at 561nm; emission filter 648-701 were used to collect the signal. Finally, a step size of 0.2-1 μ m was used to obtain the Z-stack of images.

Image Analysis

Image analysis was done with Fiji image analysis program and Imaris. Fiji was mainly used to acquire fluorescent images with sum of Z-projections. In all images the signal was set to the same threshold in order to compare the different genotypes.

Imaris (version 9.5.1) was used to analyse the morphology of microglia cells in a semi-automatic protocol. To analyse the microglia morphology, I chose the filament module, then I set the soma diameter at 12 μ m, the seed points for the dendrite ending at 0.487 μ m, allowed the disconnected segments and smooth at 0.487 μ m. Finally, the absolute intensity and the local contrast threshold were set to automatic, and the detected spines options was disabled. For the

coverage area calculation, I used the convex hull tool. For the analysis of microglia morphology, I analysed 50 cells per sample. The p-values were estimated after comparing control to cko cells by ANOVA test and bilateral student test.

Fly strains

The *Drosophila* Gal4-UAS system was used to produce fly stocks and induce conditional expression of target genes (Brand & Perrimon, 1993). Similarly, I used the LexA system as a second independent transactivator (Yagi, Mayer, & Basler, 2010). All flies were raised on standard media at 25°C unless stated otherwise. The following list of fly stocks was used during my PhD.

Genotype	# B (BDSC catalogue number)
Oregon R	B#5
white1118	B#5905
y[1] v[1]; P{y[+7.7] v[+1.8]=TRiP.JF02971}attP2	B#28336
y[1] v[1]; P{y[+7.7] v[+1.8]=TRiP.HMJ23381}attP40	B#64041
w[1118]; P{w[+mC]=Hml-GAL4.Delta}3	B#30141
w[*]; P{w[+mC]=UAS-shot.L(C)-GFP}2	B#29042
w[*]; P{w[+mC]=UAS-shot.L(C)-GFP}3	B#29043
w[1118]; PBac{w[+mC]=IT.GAL4}shot[0146-G4]	B#62668
w[1118]; PBac{w[+mC]=IT.GAL4}shot[0241-G4]	B#62731
UAS-FLP:ubiFRT stop stinger III g-trace	B#28282
if/cyo; MKRS-Sb/ TM6 Tb	Gift
LexAop a-SynA3op Chr3	Gift from S.Birman
nSybLexA Chr2	B#52817
gcmGAL4.UASmcd8GFP.tubGAL80/CyOGFP	Home made (Soustelle and Giangrande, 2007)
w[1118];HmlΔGal4; pxnGal4.UASGFP	Home made

Hemocyte counting

Ten male 3rd instar larvae were washed in 1xPBS, then dried, and bled by opening the cuticle in a well containing 50µL of Schneider's Drosophila Medium (Gibco) complemented with 10% FCS, 0.5% penicillin, 0.5% streptomycin (PS), and few crystals of N-phenylthiourea ≥98% (PTU) (Sigma-Aldrich (P7629)) to prevent hemocyte melanization (Lerner & Fitzpatrick, 1950). The hemolymph was allowed to exit, and the total volume was transferred onto a haemocytometer, where the total number of cells were counted, multiplied by the original volume (50µL), and the average number of hemocytes per larva was calculated. Each counting was carried out in triplicates.

Hemocyte Immunolabelling

Ten male 3rd instar larvae were treated as stated above and bled in wells 200µL of Schneider medium. Hemocytes were collected as indicated above and transferred onto a slide using the Cyto-Tek®4325 Centrifuge (Miles Scientific). Slides were then surrounded by Dako Pen (Dako (Code S2002)) to introduce a hydrophobic medium around the transferred material, fixed for 10min in 4% PFA with 1xPBS at room temperature, incubated with blocking reagent (Roche) for 1hr at RT, incubated overnight at 4°C with primary antibodies diluted in blocking reagent, washed three times for 10min with PTX (PBS, 0.3% triton-x100), incubated for 2 hours with secondary antibodies (see the table above), washed two times for 10min with PTX, incubated for 20min with DAPI to label nuclei (diluted to 10g/Lin blocking reagent), and then mounted in Aqua Poly/Mount. The slides were analysed by confocal microscopy (see section above for confocal imaging).

Name	Host	Origin (ref)	Concentration
Shot	Mouse	DSHB mAbRod1	1/40
Actin	rabbit	Sigma	1/1000
Tubulin	Rat	Rat Ig2a #MAS 077	1/50
Cadherin DN	Mouse	DSHB	1/40
Cadherin DE	Mouse	DSHB	1/40
Hemese	Mouse	Gift from I. Ando	1/40
P1	Mouse	Gift from I. Ando	1/40

Integrin alpha	Mouse	DSHB	1/40
Integrin beta	Mouse	DSHB	1/40
Elav	Rat	DSHB	1/200
Repo	Mouse	DSHB	1//50
GFP	Chicken	Abcam (ab13970)	1/1000
Pxn	Rabbit	Gift from J. Shim	1/2000

Larval hemocyte RNA extraction and qPCR

Twenty male 3rd instar larvae were bled in wells containing 200µL of Schneider's medium to collect hemocytes as stated above. Cells were centrifuged at 3000rpm for 10 min at 4°C. RNA was then extracted using RNeasy kit (Qiagen) and Quantitative PCR (qPCR) assays (SyberGreen Fast start, Roche) were performed on a LightCycler LC480 with the primer pairs listed below. Each PCR was carried out in triplicates on at least three independent replicates. The p-values were estimated after comparing control to test cells using bilateral student test.

Gene	Forward	Reverse
Elav	GGAAGCTGACAACAGCCATT	TCTGCATTAGCTGTGCCTGT
Repo	CAGCTCCTGCAGCCAAAAAG	CCCGTGGTCACGGTCATAAA
Gapdh1	CCCAATGTCTCCGTTGTGGA	TGGGTGTCGCTGAAGAAGTC
Act5c	GCCAGCAGTCGTCTAATCCA	GACCATCACACCCTGGTGAC
upd2	ACCCTGGAGTACGGCAATCT	CTGATCCTTGCGGAACTTGT
upd3	CCACAGTGAGCACCAAGACT	CAGGTCCCAGTGCAACTTGA
Ptp61F	GAAACTGCCCCACGTCAAAC	CTTAAGGAATGCGTTCGGCG
Socs36E	GTGTCCAACACCAGCTACGA	GAGACCCGTATGTTGACCCC

Wasp survival and encapsulation assays

Wasp parasitisation by *Leptopilina boulardi* is commonly used to study the immune response of *Drosophila* larvae (Kari et al., 2016; Small, Paddibhatla, Rajwani, & Govind, 2012;

Vanha-Aho et al., 2015). For the wasp survival, 100 1st instar *Drosophila* larvae (24hours after egg laying) of the indicated genotypes were transferred into a fresh vial at 25°C. At 2nd instar stage (48hrs after egg laying), 10 couples of *L. boulandi* were added into the vial for infestation for 1 hour, and then the wasps were removed. Following this, the number of wasps hatching from each vial was counted to estimate the percentage of lethality (number of wasps/number of *Drosophila* larvae), which allows us to determine whether the larvae mounted an effective immune response against the wasp egg. This is represented by the number of wasp adults hatching.

For the encapsulation assay, *Drosophila* of the indicated genotypes were allowed to lay eggs for 4 hours at 25°C. The vials containing 100 1st instar larvae were then transferred to 25°C until 2nd instar stage. The *Drosophila* larvae were exposed to 10 couples of *L. boulandi* for 1hour at 25°C and after parasitisation the vials were incubated at 25°C for 24 hours. Early 3rd instar larvae were dissected to assess the level of encapsulation of the wasp larvae. The wasp embryos were dissected and labelled with phalloidin and DAPI. Images were acquired using the spinning disk and then treated with Imaris. For the encapsulation I calculated the area of lamellocytes covering the wasp egg using the surface tool. Then I calculated the surface of the wasp and created the ratio of lamellocyte area/wasp egg area.

Paraquat Assay

For the PQ assay fifty males of specified genotype were used, aged 3–5 days. Then they were starved for 6 hours followed by regimen with either 20mM PQ (Methyl viologen dichloride hydrate, Sigma-Aldrich) in 5% sucrose and 1.3% agarose (Sigma-Aldrich) or with sucrose and agarose only. Mortality was monitored daily for ten days.

Adult CNS dissection

Flies were anaesthetised with CO₂ and put on a silicone tray with 0.3% of PTX. The CNS was dissected out, fixed with 4% PFA 1xPBS overnight at 4°C, washed three times with PTX,

incubated with blocking reagent for 2 hours in RT, incubated overnight at 4°C with primary antibodies, washed three times for 10min with PTX, incubated for 2hrs with secondary antibodies, washed two times for 10min with PTX, incubated for 20min with DAPI and then mounted with Aqua Poly/Mount. The slides were analysed by confocal microscopy (see above).

Phagocytosis assay

Phagocytosis assay was performed on hemocytes to evaluate their phagocytic capacity. Five 3rd instar larvae per genotype were bled in a 96 glass-bottom wells (Greiner bio-one) containing 50µl of Schneider medium with PTU. The hemocytes were left to attach for 20 min in RT and then the medium was replaced by medium with latex FITC fluorescent beads (1/1000). The cells were incubated with the beads for 0,5,10 and 20 min. Then the cells were fixed with 4%PFA in 1xPBS and labelled with phalloidin (1/500) and DAPI. The samples were then processed at the Screening facility of the IGBMC, where the FITC intensity of the beads was counted for each cell.

Adhesion assay

Adhesion assay was performed on hemocytes to evaluate their adhesive capacity. Three 3rd instar larvae per genotype were bleed in a 8 well coverslips Teflon printed (Immuno-Cell Int.) containing 20µLof Schneider medium with PTU. The hemocytes were left to attach for 1 hour in RT and then the cells were fixed with 4%PFA in 1xPBS and procced for labelling with phalloidin (1/500) and DAPI. The samples were then imaged at the CBI (see confocal imaging above) and then the extensions or filopodia were counted for each cell.

Statistical analysis

Variance analysis using bilateral student tests for unpaired samples was used to estimate the p-values in hemocyte counting, hemocyte immunolabeling and qPCR assays, microglia ramifications and coverage area, iNOS and Arg-1 positive cells ; in each case, at least three

independent trials were performed. In all analyses, “ns” stands for not significant, for p-value >0.05 ; “*” for p-value < 0.05 ; “**” for p-value < 0.01 ; “***” for p-value < 0.001 .

Chapter I

Characterisation of the mGcm2 expression profile in mice

The first aim during my PhD was to characterise the expression pattern of the transcription factor mGcm2 in the immune cells of mice. My goal was to validate the transcriptomic data that previous people had conducted in our lab (**Figure 9**). These data showed a broad expression of mGcm2 in different organs. I labelled with an mGcm2 antibody at different stages and different tissues. Labelling from sections of embryos at different embryonic stages showed an early expression of mGcm2 in the yolk sac. Moreover, labelling of different adult tissues indicated that mGcm2 is expressed only in one population of cells from the innate immune system, the microglia. More specifically, mGcm2 expression is detected at specific time points, at 12 and 24 month old brains. Finally, mGcm1 is not expressed in microglia *in vitro* nor *in vivo*.

Introduction

Two paralogue genes are present in mammals, **GCM1** and **GCM2**. In the mouse, knock-out of **mGcm1** or **mGcm2** are lethal due to crucial roles in placenta (mGcm1) and in parathyroid development (mGcm2), two functions that are conserved in human GCM genes (Hashemolhosseini & Wegner, 2004). However, no role was detected in glial development and no study was performed in the immune system. The transcriptomic data suggest that mGcm2 is expressed in the thymus, the bone marrow and the brain at low levels. To see if these levels of expression lead to the production of detectable proteins, I characterised the expression profile of mGcm2 within the immune system. This gave me information about the spatial and temporal expression of mGcm2 and thus, I could connect it with specific functions during development and/or immune responses.

Results

Characterisation of the mGcm2 expression profile during development

Firstly, I characterised the mGcm2 expression during the embryonic development. I performed immunolabelling with mGcm2 and CD45 on sections of embryos from stages E7.5 to E16.5. CD45 is a transmembrane protein abundantly expressed on mature cells of hematopoietic origin (Thomas, Reasor, & Wierda, 1989). The results revealed that mGcm2 is expressed during E7.5 in the yolk sac, which is the site of the first hematopoietic wave (**Figure 18A**). Furthermore, the mGcm2 positive cells are CD45^{low}. Thus, the cells that show expression of mGcm2 could be non-hematopoietic cells or immature progenitors. Labelling at other embryonic stages showed no mGcm2 expression in the yolk sac past E7.5 (**Figure 18 B and C**).

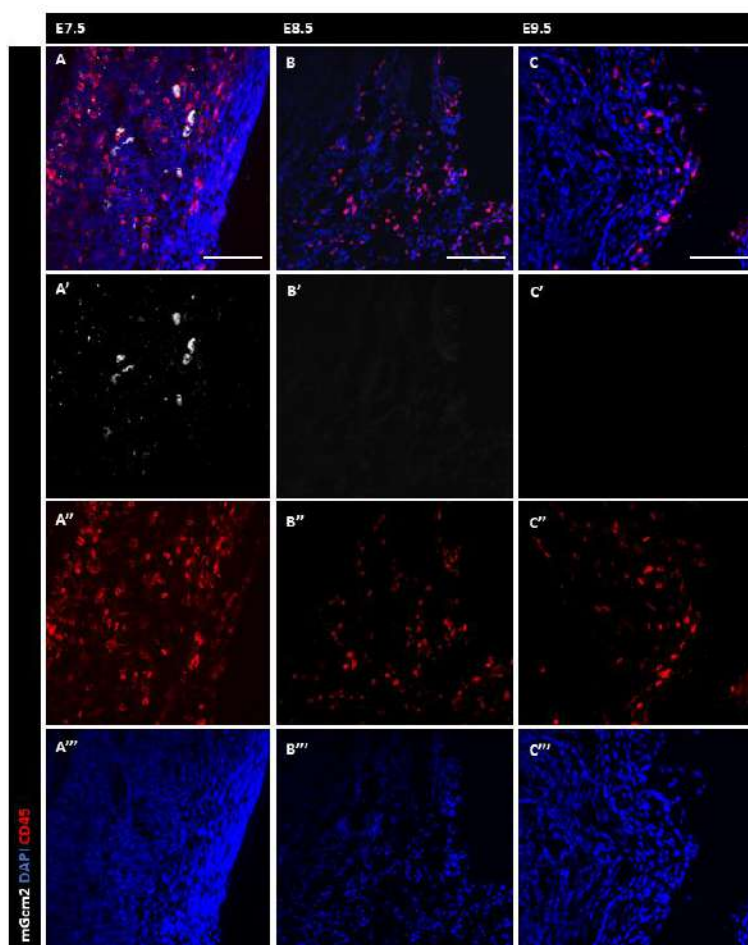


Figure 18. Confocal images from mouse embryo sections immunolabelled with mGcm2 at different embryonic stages from E7.5(A) to E8.5 (B) and E9.5(C). mGcm2 is specifically present in the yolk sac at E7.5. mGcm2 in grey (A',B',C'), CD45 in red indicates mature hematopoietic cells (A'',B'',C'') and DAPI in blue indicates the nuclei (A''',B''',C'''). N=3, scale bar 100um

The expression of mGcm2 was also evaluated in different tissues that contain resident macrophages, such as the CNS (**Figure 19**), liver and lungs. Nevertheless, no mGcm2 expression is detected in microglia or any other tissue resident macrophage population. Thus, mGcm2 is specifically expressed at the E7.5 in the yolk sac during embryogenesis.

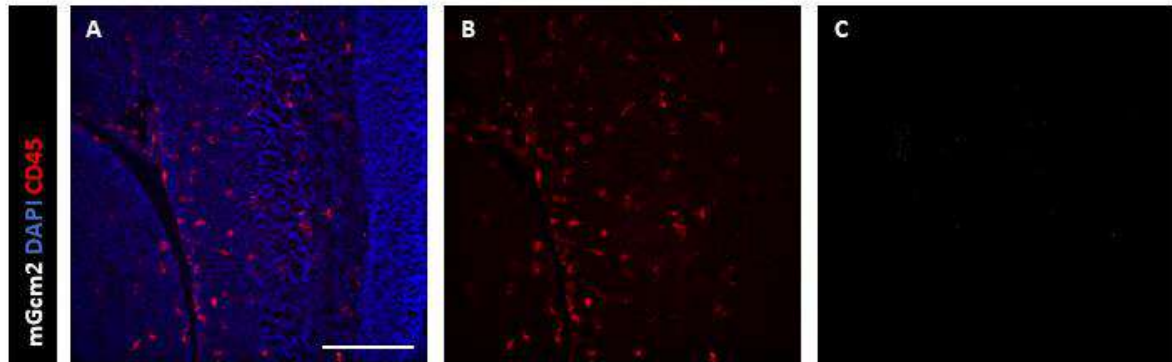


Figure 19. Confocal images from mouse brain sections immunolabelled with mGcm2 at E16.5 in the CNS(A), (B) CD45 in red, (C) mGcm2 in grey and DAPI in blue indicates the nuclei. N=3, scale bar 100um

Characterisation of the mGcm2 expression profile during life span

Upon assessing the expression of mGcm2 in development, I then continued with cells of the innate immune system in adults. Brain, spinal cord, adipose tissue, spleen and lung were collected from different ages from postnatal day 0 and 14 (P0 and P14) as well as from adults at 2, 12 and 24 months. CD45 was used for the different tissue resident macrophages while, for microglia, I used the microglia specific cocktail (CD11c, CD68, F4/80) in order to distinguish microglia from the meningeal macrophages and because microglia in homeostatic conditions display CD45^{low} expression (Rangaraju et al., 2018). All the analysis focus on microglia from the cortex. mGcm2 is expressed in microglia at 12 and 24 months but not in 2 month old animals (**Figure 20 A-C**). This expression is in different areas of the brain including the cortex, the cerebellum and the thalamus, while the number of positive mGcm2 cortex microglia progressively increases (**Figure 20D**). Animals at 12 months have 25% mGcm2 positive

microglia while 24month old animals have almost double the mGcm2 positive microglia (48%). These results indicate that mGcm2 is expressed in microglia of aged mice.

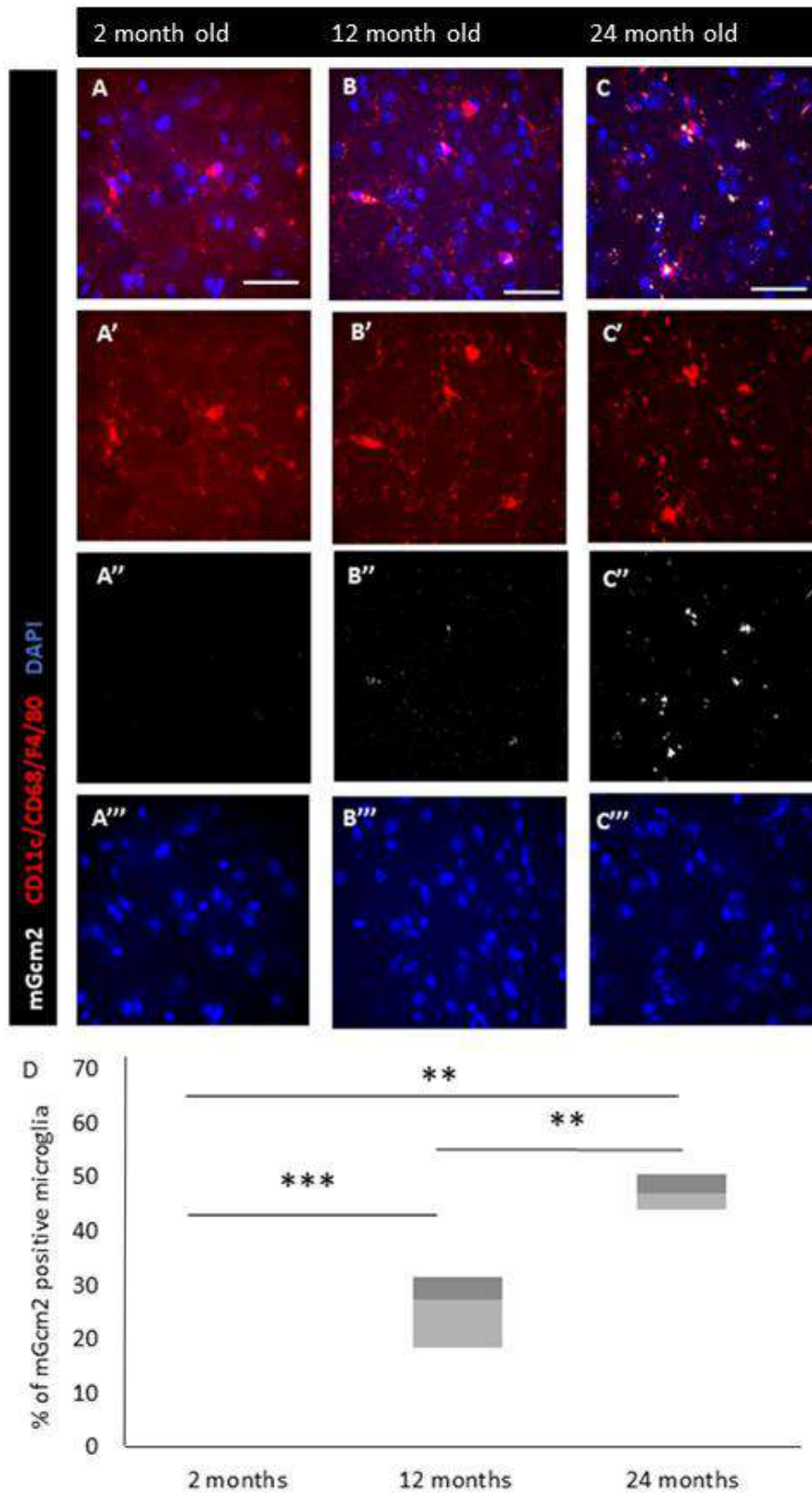


Figure 20. Confocal images from mouse brain sections immunolabelled with mGcm2 (A-C). mGcm2 is expressed in 12 and 24month old animals. mGcm2 is in grey (A',B',C'), microglia (CD68, CD11b and F4/80) are in red (A'',B'',C'') and DAPI in blue (A''',B''',C'''). N=6-13 animals per genotype, scale bar 50um (D) Quantification of mGcm2 positive microglia quantification in the cortex at different age points. (ANOVA p-value 1.64336E-07, p-value between 2 and 12 months 3.60372E-06, between 12 and 24 months 0.005 and between 2 and 24 months is 0.002).

In order to study the mGcm2 expression in other tissue resident macrophages, I performed immunolabelling in lung and adipose tissue. Tissues were dissected from 2, 12 and 24 month old animals and cryosections were labelled for CD45 and mGcm2. However, the results revealed no mGcm2 labelling in those resident macrophages (**Figure 21**). From all the tissues that I labelled I found that mGcm2 is expressed only in microglia cells. These interesting results indicate that mGcm2 is expressed in innate immune cells of the primitive hematopoietic wave (microglia) as it is the case for *Drosophila*.

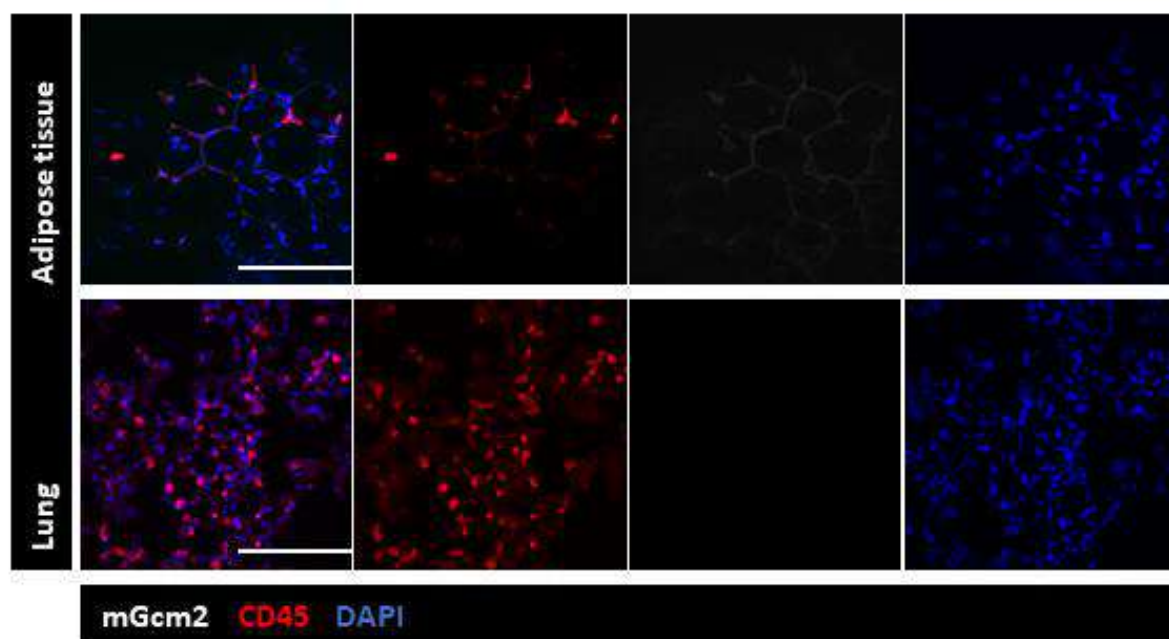


Figure 21. Confocal images from mouse brain sections immunolabelled with mGcm2(white) with CD45 (red). Upper panel shows tissue resident macrophages in lung and lower panel shows tissue resident macrophages in the adipose tissue. N=3, scale bar 100um

Characterisation of the mGcm1 and mGcm2 expression in CNS cultures

In parallel, I characterised the expression pattern of mGcm1 and mGcm2 in *in vitro* cultures of the CNS with previously published antibodies (Nait-Oumesmar et al., 2000; Peissig, Condie, & Manley, 2018) (**Figure 22**). The animals used for the P1 CNS cultures were WT (C57BL/6J) neonatal mice. As a marker for microglia, I labelled with CD45 since there are no other innate immune cells present in the co-cultures (Denes et al., 2015). The results revealed that mGcm2

is expressed *in vitro* in microglia unlike mGcm1 (**Figure 22A and B**). The next step was to evaluate and quantify the mGcm2 expression in microglia. *In vitro* microglia adopt one of the three morphologies: ramified microglia with small soma and long ramifications, round cells with a small cell body and no ramifications and amoeboid microglia with big cell body and no ramifications (Bohatschek, Kloss, Kalla, & Raivich, 2001; Thored et al., 2009). Round cells from primary cultures are considered as active microglia, the other two as resting cells (Ovanesov et al., 2006). The immunolabelling showed the expression of mGcm2 in a microglia subpopulation (**Figure 22A**). More specifically, only the round microglia express mGcm2, and of those only 30% are mGcm2 positive. Thus, mGcm2 is also expressed *in vitro* in microglia apart from 12 and 24 month old animals. This suggests that microglia can up-regulate mGcm2 expression independently of age. Interestingly, no other data suggest that mGcm2 is expressed in neonatal mice *in vivo*. This expression could be explained by the fact that even though microglia cultures were essential for the discovery of different pathways and key molecules, recent RNA transcriptome comparisons of *ex vivo* microglia with *in vitro* microglia revealed major differences (Butovsky et al., 2014). A recent publication also described that at least part of this difference can be attributed to culturing in the presence of serum (Bohlen et al., 2017). Thus, the mGcm2 expression on *in vitro* cultures do not represent the normal environment but under certain conditions microglia are able to express this transcription factor.

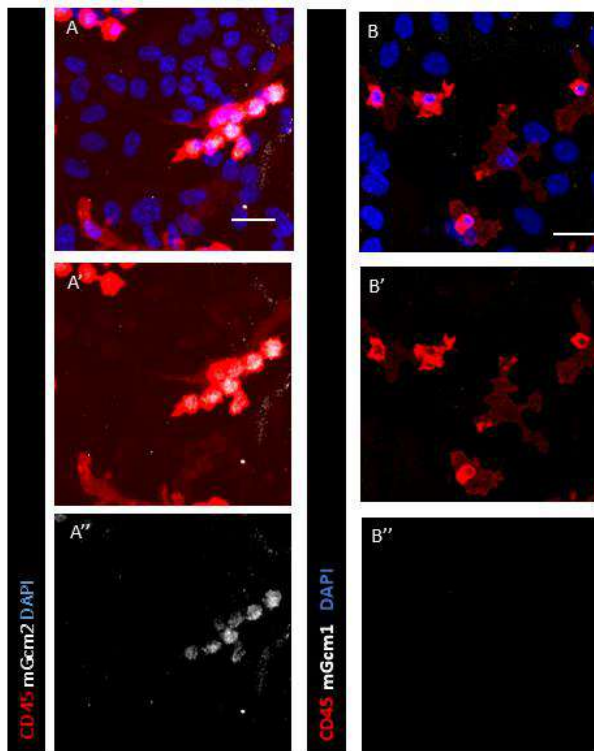


Figure 22. Confocal images from mouse *in vitro* CNS cultures immunolabelled with mGcm2 in primary CNS *in vitro* cultures (A,B). Microglia are labelled with CD45 (red) (A',B'), Dapi in blue and mGcm1 or mGcm2 is in grey (A'',B''). N=3 Scale bar 10 μ m

I decided to continue with a microglia specific mGcm2 knock out mouse model by using the Cre/Lox system. As microglia specific Cre I utilised the CX3CR1 receptor. CX3CR1 is a specific high-affinity and functional receptor for the chemokine CX3CL1 in mice and humans (Combadiere et al., 1995; Combadiere et al., 1998). This chemokine is the sole member of the CX3C chemokine subfamily and was identified in human cells as Fractalkine and in mouse as neurotactin (Bazan et al., 1997; Pan et al., 1997). In 2000, a transgenic mouse strain was generated, where the CX3CR1 gene was replaced with the gene encoding the enhanced green fluorescent protein (EGFP) (Jung et al., 2000). This approach allowed the examination of the CX3CR1 expression pattern that normally express this receptor. The CX3CL1 receptor was absent in tissue resident macrophages (hepatic Kupffer cells, splenic, and peritoneal macrophages), astrocytes, oligodendrocytes, neutrophils, eosinophils, B lymphocytes and resting T cells. Since then, CX3CR1 is a selective marker for microglia in the CNS (Wieghofer & Prinz, 2016).

Conditional knock out (cko) mice CX3CR1-Cre/+; mGcm2^{flox/+} males were crossed with mGcm2^{flox/flox} females. The mGcm2^{flox/flox} line was produced in the ICS at Strasbourg by introducing two LoxP sites upstream and downstream of the Gcm exons 2,3 and 4, respectively (**Figure 23A**). As control I used the double heterozygous animals CX3CR1-Cre/+; mGcm2^{flox/+}. Labelling of cko microglia showed no positive signal, thus, proving the efficiency of my model (**Figure 23C**). During this labelling I also assessed multiple mGcm2 antibodies, including two commercials, one gift from B. Nait-Oumesmar and one that I produced at the IGBMC. The best results were obtained with the commercial ones, and these were the ones I used for the rest of the studies.

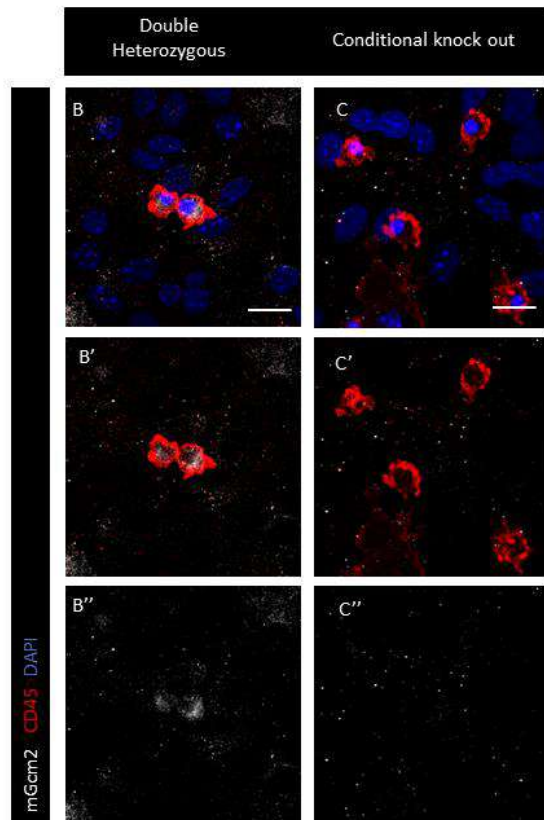
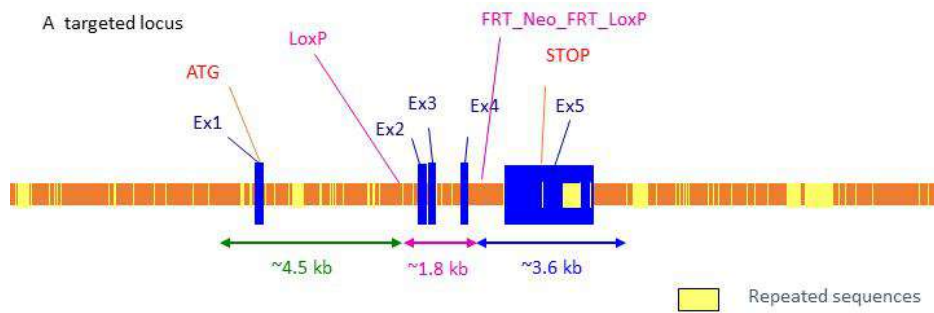


Figure 23. (A) $mGcm2^{fllox/fllox}$ line locus. (B,C) Confocal images from mouse *in vitro* CNS cultures immunolabelled with $mGcm2$. Microglia are labelled with CD45 (red) (B',C'), Dapi in blue and $mGcm2$ is in grey (B'',C''). As a control I used the double heterozygous, $CX3CR1-cre/+; mGcm2^{fllox/+}$ (B) and for the conditional knock out is $CX3CR1-cre/+; mGcm2^{fllox/fllox}$ (C). Scale bar 10 μm

Discussion

The labelling of whole mount embryos as well as tissues from different stages in the life span revealed the expression pattern of $mGcm2$. $mGcm2$ is expressed early during the primitive hematopoietic wave in the innate immune cells that originate from this wave. These cells are the microglia population that reside in the CNS. Finally, I found no expression of $mGcm1$ in *in vitro* cultures.

mGcm2 is expressed during the primitive hematopoietic wave

Hematopoiesis is observed in mouse embryos as early as embryonic day 7.5 (E7.5) in the extra-embryonic mesodermic layer of the yolk sac. Hematopoietic cells are cell aggregates (blood islands) until yolk sac vasculature is firmly formed. Primitive macrophages constitute the main cell lineage produced in the blood islands, and the yolk sac is the exclusive site of primitive erythropoiesis (Yamane, 2018). Expression of mGcm2 during the early stages of primitive hematopoiesis resembles the expression pattern during the same stage in *Drosophila melanogaster*. In the fly, Gcm triggers the expression of plasmacyte markers thus leading to the differentiation of prohemocytes into mature hemocytes. During this stage other transcription factors, such as the GATA family transcription factor *serpent* (*srp*), actively participate in the development of the innate immune system. In mammals, GATA transcription factors start to be expressed as early as E1.5 until E10.5 and participate in the development of the immune cells (Cantor & Orkin, 2005; Chlon & Crispino, 2012; Molkenin, 2000; Zaytouni, Efimenko, & Tevosian, 2011). Analysis of the Gcm binding sites revealed conserved Gcm binding sites within GATA3, GATA4, and GATA6 (Cattenoz et al., 2016). All three genes contain several GBSs in their promoters, and expression of both GATA3 and GATA6 is induced by mGcm2 in HeLa cells. These results suggest a potential role of Gcm in the regulation of the GATA factors. However, more experiments should be done and it would be extremely interesting to follow up those preliminary findings.

mGcm2 is expressed again during aging in the microglia

My data show that mGcm2 is expressed in microglia of aged animals, which are known to develop an inflammatory phenotype (Angelova and Brown 2019). Aged brains indeed show increased levels of pro-inflammatory cytokines and receptors on microglia (Norden & Godbout, 2013). Thus, aging studies may provide important information on the molecular pathways involved in the inflammatory response. For this reason, during my PhD I

concentrated on the cortex microglia and whether lack of mGcm2 led to phenotypic changes. However, it would be interesting to assess microglia from different parts of the CNS as well.

Chapter II

Characterisation of the mGcm2 conditional knock out in CX3CR1-cre expressing microglia

My data have shown that mGcm2 is expressed during the embryonic development of microglia and in aged microglia. My next step was to evaluate the role of mGcm2 in microglia development and function. I evaluated life span, metabolism, and microglia state of mGcm2 cko animals in homeostatic conditions at different stages. My results show that cko animals have increased weight compared to the control under normal diet. Similar preliminary data indicate a tendency of hyperphagia in the cko animals. The phenotype has already been linked with dysfunction of the CNS with microglia playing a pivotal role in controlling the brain region responsible for food consumption. Additionally, cko animals have an increased number of microglia in young adults. Finally, cko microglia present a pro-inflammatory status manifested in their morphology, increased expression of pro-inflammatory markers (iNOS) and decreased anti-inflammatory markers (Arg-1). Thus, these results suggest that mGcm2 has an anti-inflammatory function, similarly to its orthologue in *Drosophila*.

Introduction

My previous chapter showed that mGcm2 is specifically expressed in microglia cells in the aged brain. mGcm2 is expressed after 12 months and the percentage doubles by 24 months. The main question that I addressed was whether lack of mGcm2 is going to affect the microglia homeostasis. In order to characterise the role of mGcm2 in microglia, I used the microglia conditional knock out line CX3CR1-Cre/+; mGcm^{flox/flox}.

Microglia regulate the CNS environment during both homeostasis and inflammation. During homeostasis, their main role is to survey the environment for possible inflammatory cues.

Recent studies demonstrate a secondary role of microglia regulating metabolic pathways (Mendes, Kim, Velloso, & Araujo, 2018). Microglia are known to respond to high fat diet by secreting pro-inflammatory molecules and ultimately inducing neuronal stress in the hypothalamic region that leads to hyperphagia and obesity (Valdearcos et al., 2014). In order to fully characterise the role of mGcm2 in microglia, I performed a life span test, weight measurements, body composition test, metabolic cages, quantification of the microglia population, analysis of their morphology and expression of inflammatory markers at different ages.

Results

mGcm2 cko mice show increased weight compared to the controls

First, I characterised the cko line by creating a cohort of mutant mice (CX3CR1-Cre/+; mGcm2^{flox/flox}) and controls (CX3CR1-Cre/+; mGcm2^{flox/+}, double heterozygous). This cohort was comprised of 5-6 animals per group and per sex, since it is known that microglia show dimorphic states according to the sex (Guillot-Sestier et al., 2021). Both groups managed to reach 24 months of age, thus this transcription factor is not linked with the lifespan of mice.

These animals were also monitored weekly for their weight. Surprisingly, both cko males and females had a significantly increased weight compared to the controls (**Figure 24A**). Firstly, white adipose tissue was analysed as studies have shown that in case of obese phenotypes the adipocyte size increases (Kraakman, Murphy, Jandeleit-Dahm, & Kammoun, 2014). For the assay I used animals at 24 months where I had the highest difference in weight and for the tissue labelling I employed Oil Red O (**Figure 24B**). This labelling is widely used for staining lipids (Kraus et al., 2016). I then quantified the area of the adipocytes with the Fiji imaging analysis software (**Figure 24C**). The results showed no difference between the two genotypes.

Thus, mGcm2 cko animals have increased weight but this does not seem to affect the size of the adipocytes.

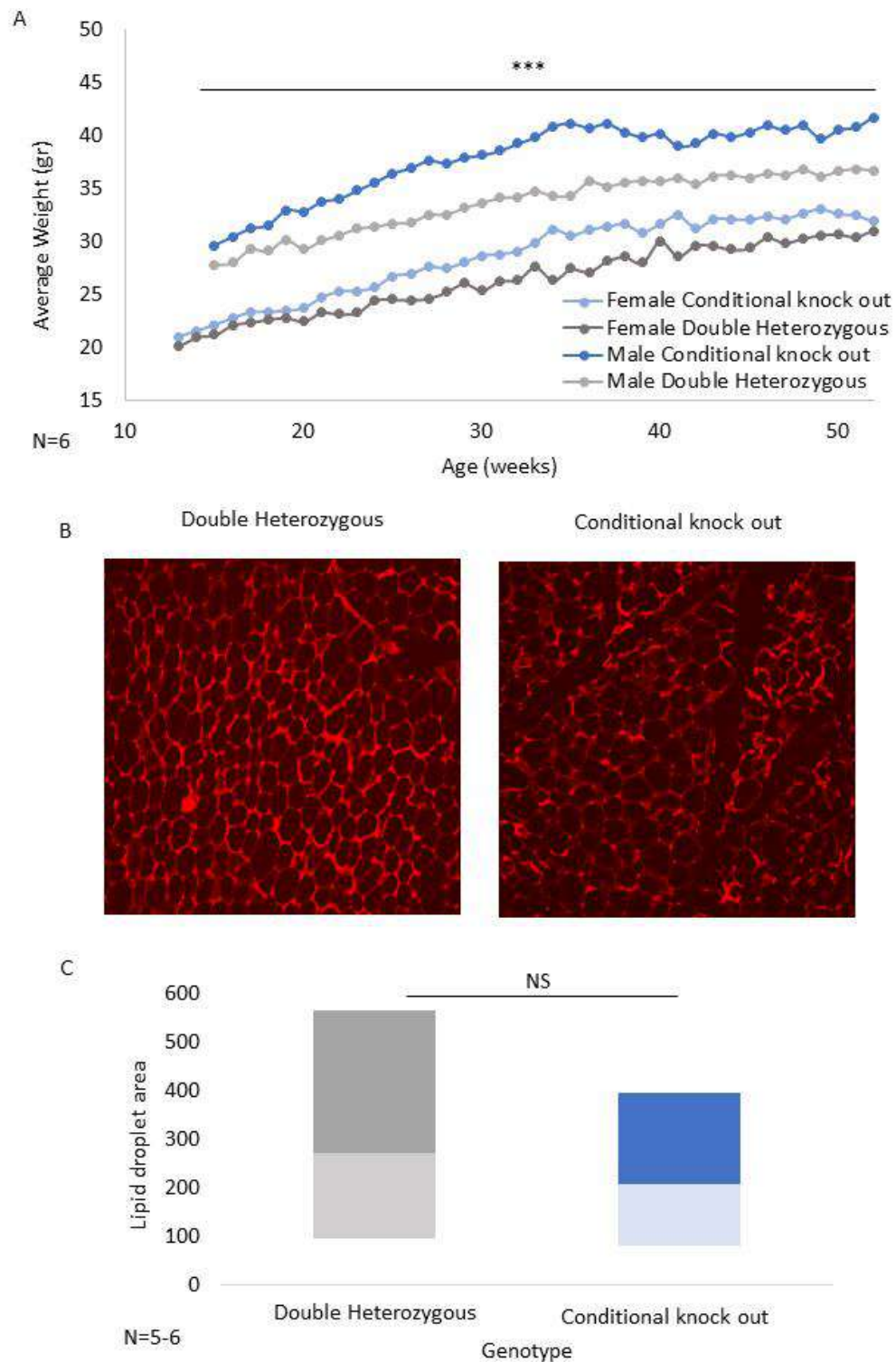


Figure 24. mGcm2 cko animals display increased weight compared to the controls. (A) Weekly weight measurement of the animals, n=5-6 animals per genotype and sex. (B) Oil Red O labelling of adipose tissue. (C) Quantification of the adipocyte size. P-value: * <0.05 , ** <0.01 , *** <0.001 and NS not significant. N=5-6 males, 5 fields per animal

I then created a second cohort in order to replicate the results of the first cohort and further study how lack of mGcm2 in microglia impairs the metabolism. To assess their body composition, I performed a quantitative Nuclear Magnetic Resonance (qNMR) test, which calculates the fat and lean muscle percentage for each animal (J. G. Jones, Garcia, Barosa, Delgado, & Diogo, 2009). Chronic disturbances of energy balance constitute a major cause of lifestyle diseases, and therefore it is of great interest to measure energy balance during intervention studies either as a confounder or as the target parameter. Because the accurate assessment of energy intake and total energy expenditure over longer periods is impractical and expensive, accurate measurement of changes in body composition assuming constants for energy equivalents of fat and lean masses is an attractive alternative (Bosy-Westphal & Muller, 2015). The lean mass is calculated by subtracting body fat weight from total body weight, and the free bodily fluids (FBF) is the remaining percentage. Furthermore, the animals were put in metabolic cages, monitoring for 24 hours to evaluate their activity, food/water intake and metabolic processes (n=10 males per genotype). Females were excluded from the metabolic experiments because they are more variable than males and they must be tested across the estrous cycle or have a synchronised cycle. During the COVID-19 pandemic, we had to reduce the number of experiments, which led me to restrict the analysis to males.

The results confirmed that cko animals show increased weight compared to the control, which was starting to show at 25 weeks (**Figure 25A**). qNMR analysis performed at 25 weeks, provided quantitative measurement of their body composition in regards of fat tissue (**Figure 25B**), lean mass (**Figure 25C**), FBF (**Figure 25D**) and their percentages that derived from the sum of the lean, fat and FBF (**Figure 25E, F, G** respectively). The results show a tendency for increased fat tissue, from 8.5gr (23%) in the control to 10 gr (26.6%) in the cko animals. However, the difference is not significant (**Figure 25H**). The animals from both groups have a similar composition regarding their lean mass, 24.7gr (69%) for the control and 24.6gr (65.5%)

in cko mice. Similarly, no difference was detected for the FBF, 2gr (5.5%) for the control and 2.1 gr (5.7%) for the cko mice. These results together suggest that, even though the cko animals have increased weight, there is no difference in the body composition at 25 weeks. It also raises new questions as to whether the differences that result in increased body weight (**Figure 24A and 25A**) are the consequence of an inflammatory condition in the hypothalamic region of the CNS since the only variable is lack of mGcm2 in microglia.

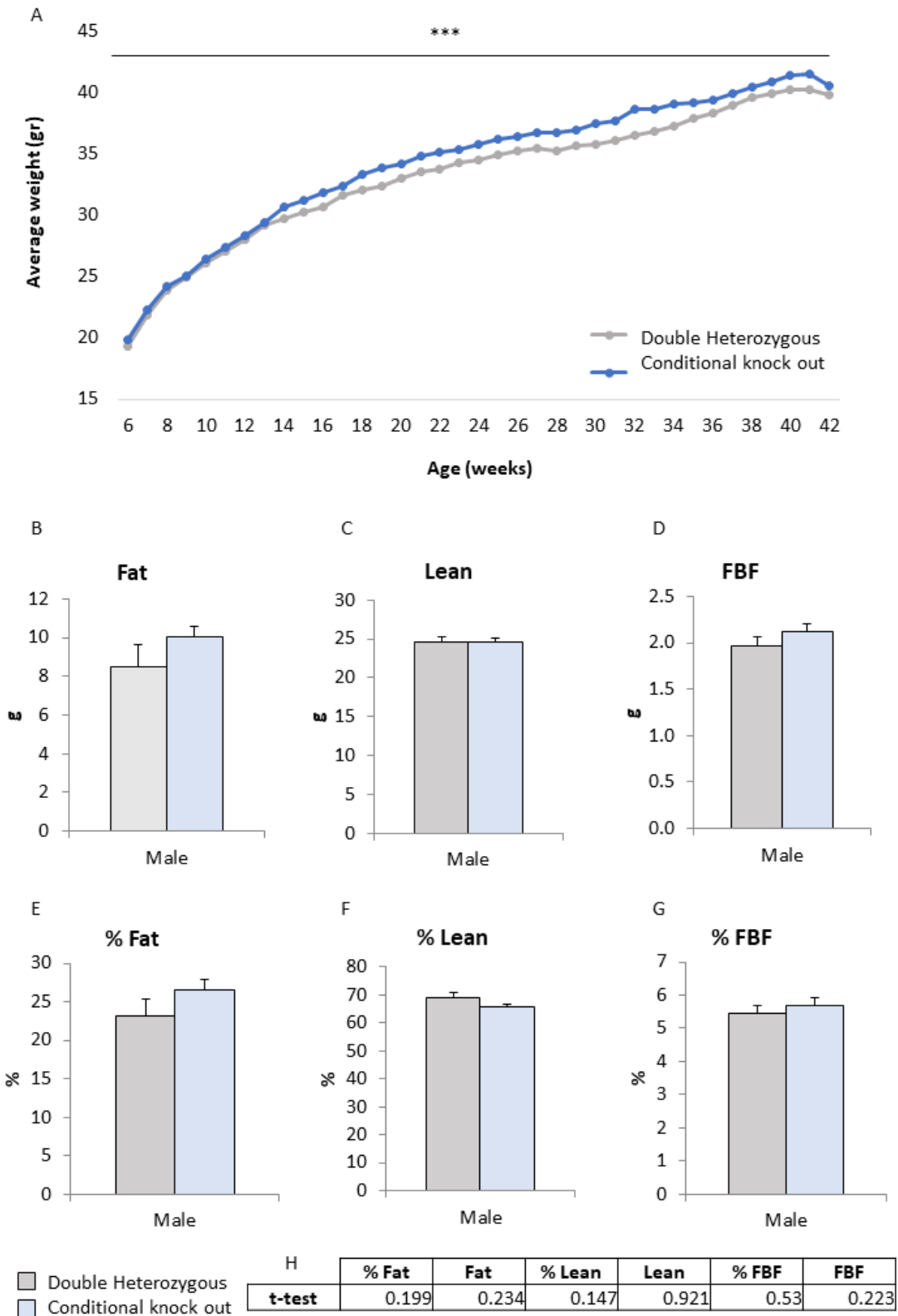


Figure 25. mGcm2 kco animals have increased weight compared to the controls but show no differences in their body composition. (A) Weekly measurements of the animals, n=10 males per genotype. qNMR results for their (B) fat tissue (C) lean tissue and (D) free bodily fluids (FBF). (E) fat tissue percentage, (F) lean tissue percentage, (G) FBF percentage. (H) Table with the p-values from the qNMR test. p-value: *<0.05, **<0.01, ***<0.001 and NS not significant. N=10 males per genotype

Finally, I evaluated the oxygen consumption, the respiratory exchange ratio (RER), the heat production, the activity and the food/water intake at 25 weeks. The RER represents the ratio between the amount of carbon dioxide (CO₂) produced in metabolism and oxygen (O₂) used. The ratio is determined by comparing exhaled gases to room air. Measuring this ratio can be used for estimating the respiratory quotient (RQ), an indicator of which fuel (e.g. carbohydrate or fat) is being metabolized to supply the body with energy (Farinatti, Castinheiras Neto, & Amorim, 2016). Consequently, these values suggest whether the body is fuelled by fat or not and thus whether there is a difference in the metabolic processes. These data were given from the TSE metabolic cages. The 10 male mice per genotype spent 12 hours in the cages to adjust to the new environment and then recordings for the above values were observed for 24 hours.

The results revealed no difference in oxygen consumption nor RER (**Figure 26A-F**). More specifically, the oxygen consumption value is 89 ml/h/animal during the day and 99 ml/h/animal during the night for the control (**Figure 26A-C**). For the cko, the oxygen consumption value is 86 ml/h/animal during the day and 99 ml/h/animal during the night. Concerning the RER, control mice show a ratio of 0.98 during the day and 1.02 during night (**Figure 26D-F**). Similarly, the cko mice have an RER ratio of 0.99 during the day and 1.03 during the night. Furthermore, the cages offer the opportunity to measure the heat production, which is a way to measure energy expenditure of the animals, The results showed no difference between the two genotypes (**Figure 26G-I**). More specifically, control mice had 0.45 Kcal/h/animal heat production during the day and 0.5 Kcal/h/animal during the night. Likewise, cko animals had a heat production of 0.43 Kcal/h/animal during the day and 0.5 Kcal/h/animal during the night.

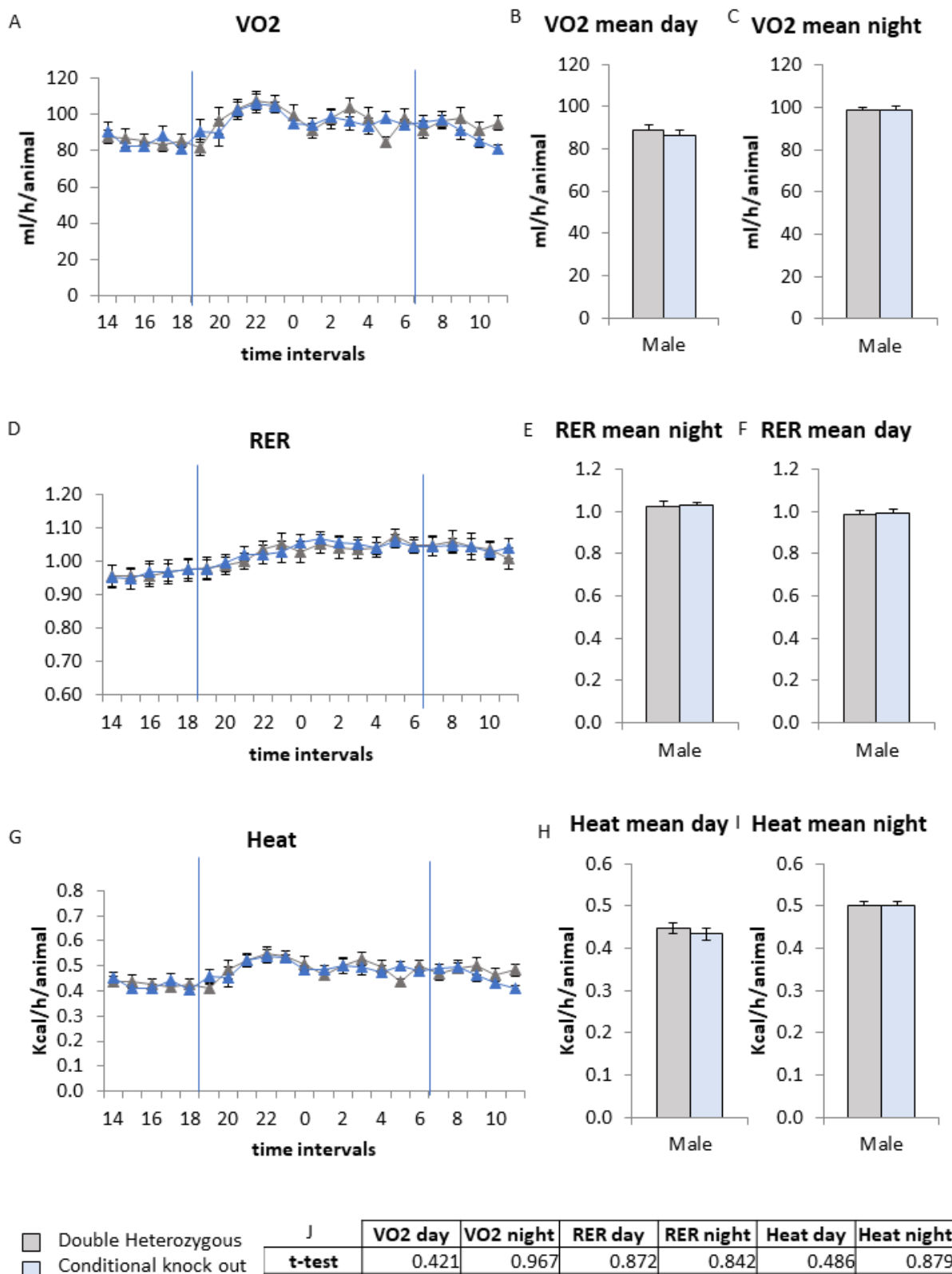


Figure 26. Calorimetry results from the TSE metabolic cages. (A) Average oxygen consumption per hour for 24 hours (B) Average oxygen consumption during the day (C) Average oxygen consumption during the night (D) Average RER per hour for 24 hours (E) Average RER during the day (F) Average RER during the night (G) Average heat production per hour for 24 hours (H) Average heat production during the day (I) Average heat production during the night (J) Table with the p-values from the qNMR test. P-value: * <0.05 , ** <0.01 , *** <0.001 and NS not significant. N=10 males per genotype

Finally, the metabolic cages evaluated the activity and the consumption of food and water, which represent the energy intake. Activity measurements, which represents the energy expenditure, was recorded via sensor frames and a passive wheel. The sensors frames were configured to measure locomotor activity in the x, y, and z plane. The software documented the number of beam interruptions caused by the animal's movement. The total number of beam breaks recorded was a sum of the ambulatory and fine movements. A passive wheel allowed measurement of spontaneous activity by the animal. Drinking and feeding behaviour for each animal in each cage were recorded via the sensors attached to the drinking and feeding stations.

The results revealed a tendency of the cko animals of increased food intake (**Figure 27A-C**) and a significant decrease in water consumption during the day (**Figure 27D-F**) compared to the controls. More specifically, control mice ate 1.62 gr of food during the day and 2.97 gr during the night (4.59 gr of total consumption). The cko animal ate 1.7gr of food during the day and 3.32gr during the night (5.02 gr of total consumption). Concerning water consumption, control animals drunk 1.76 ml of water during the day and 1.68 ml during night (total of 3.44 ml of water). The cko animals consumed 1.44 ml of water during the day and 1.31 ml during the night (total of 2.74 ml of water). Finally, the cko animals showed a statistically significant decreased ambulatory movement (**Figure 27G-I**), especially on the X-axis (XTOT). The control animals did 7760 beam counts during the day and 14540 beam counts during the night. The cko animals did 5684 counts during the day and 13516 counts during the night.

All the data together show that the cko animals do not show dramatic differences compared to the control animals. Thus, indicating that the energy intake and expenditure of the cko mice is not affected by the deletion of the mGcm2 in microglia under standard diet. However, all those tendencies suggest that a stimulation, such as a high fat diet, could increase the difference in body fat and food consumption.

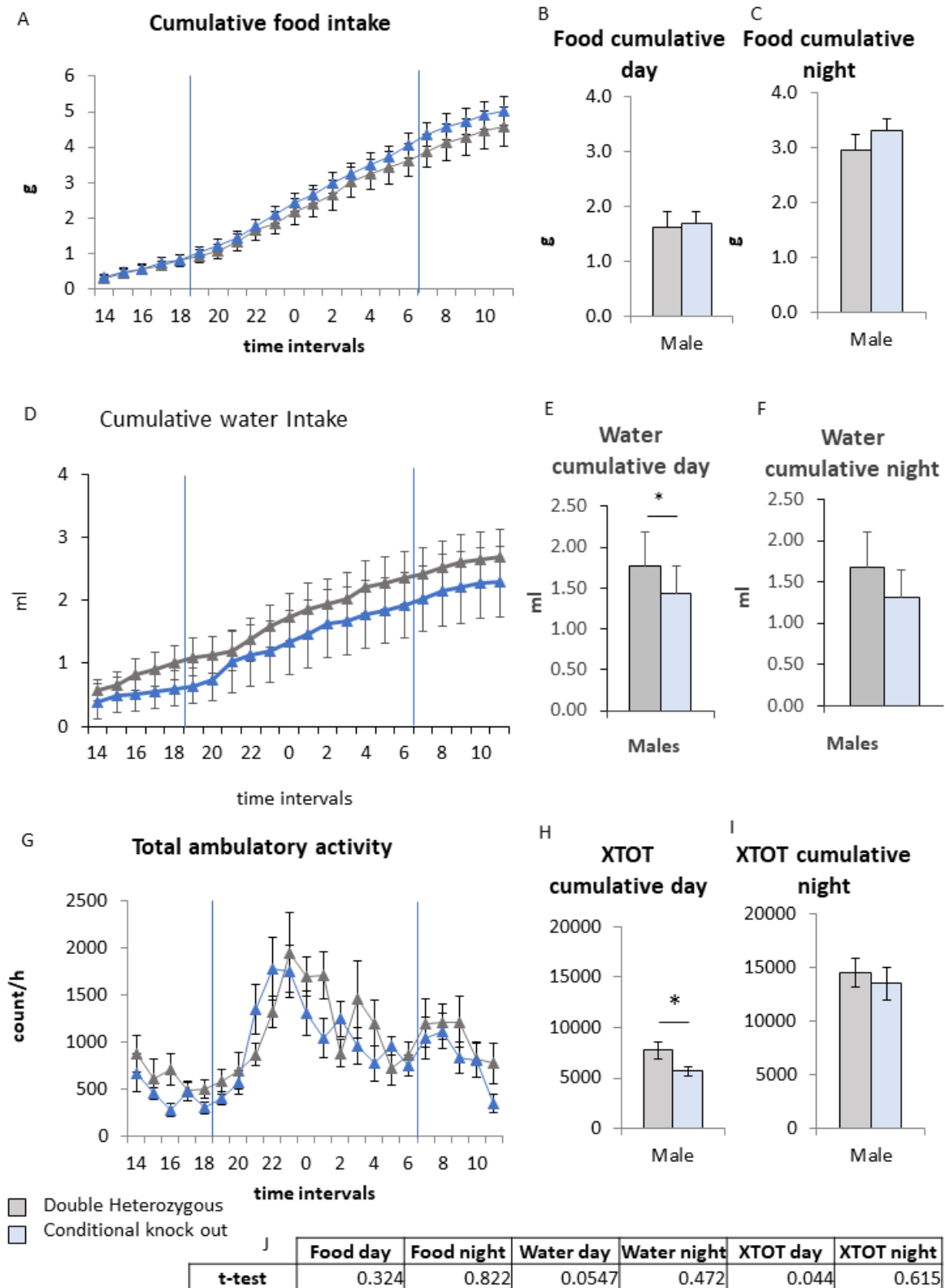


Figure 27. Movement and food/water intake results from the TSE metabolic cages. (A) Average food intake per hour for 24 hours (B) Average food intake during the day (C) Average food intake during the night (D) Average water intake per hour for 24 hours (E) Average water intake during the day (F) Average water intake during the night (G) Average ambulatory activity per hour for 24 hours (H) Average ambulatory activity on the X-axis during the day (I) Average ambulatory activity on the X-axis during the night (J) Table with the p-values from the qNMR test. P-value: * <0.05 , ** <0.01 , *** <0.001 and NS not significant.

Neonatal and young adults mGcm2 cko mice have increased number of microglia

Primitive haematopoiesis occurs from E7.0 to E9.5 in the yolk sac, giving rise to primitive macrophages and erythrocytes, including a subset of erythromyeloid progenitors (EMPs) (Bertrand et al., 2005; Ginhoux et al., 2010). From E10.5, EMPs migrate from the yolk sac into the CNS where they differentiate into microglia. During the postnatal period, the number of microglia increase 2.2-fold, peaking at postnatal day 14 (P14) (Nikodemova et al., 2015). By 6 weeks of age, the microglia number decreases and reaches the density that is maintained throughout adulthood (10-15% of the cells in the CNS) (Askew et al., 2017; Nikodemova et al., 2015). During neuroinflammation, activated microglia migrate to the area of the inflammation and proliferate (Tay et al., 2017).

To analyse the effect of mGcm2 on the microglia population, the number of microglia was quantified in different parts of the CNS in neonates P1, P14 and adults from 6 and 24 month old cko and control mice (n=4 males per genotype and age) (collaboration with Dr. Katrin Kierdorf, University of Freiburg for labelling and quantification). Control and cko mice have the same microglia number at P1, 14 cells per mm² for the control and 16 cells for the cko. By P14, cko mice have a higher number of microglia (182 cells per mm²) than controls (147 cells per mm²) (**Figure 28**). This increase is also detected in 6 month old animals, in specific areas of the brain: the thalamus and the cerebellum, associated with sensory signals and movement, respectively (**Figure 29**). More specifically, control mice have 12 cells per mm², while cko mice have 21 cells in the cerebellum. In the thalamus control mice have 24 cells per mm² and cko mice have 32 cells per mm². Finally, 24 month old cko animals do not show any difference in the number of microglia.

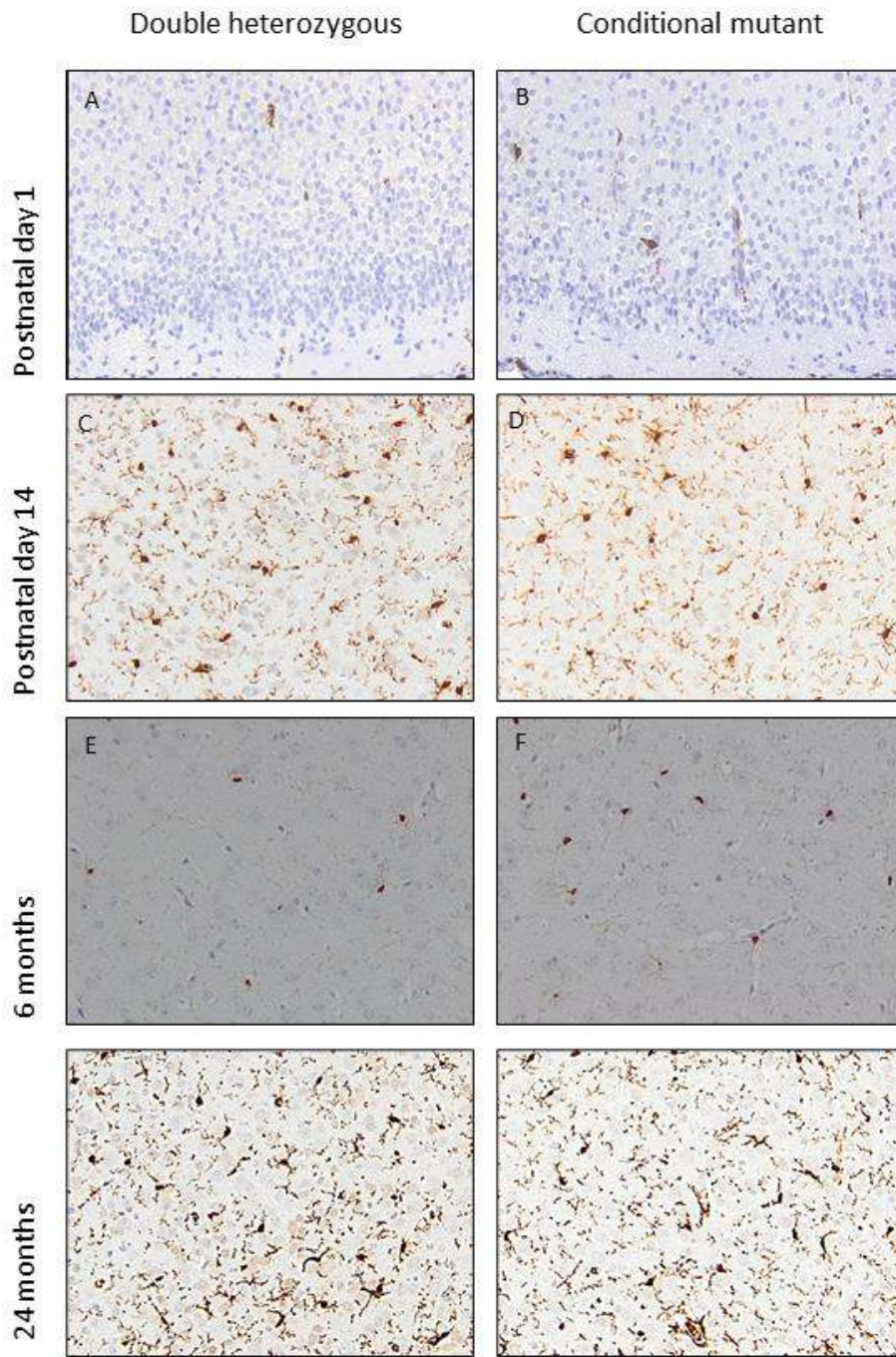


Figure 28. Images showing Iba-1(brown) labelling of microglia at different ages in the cortex area.

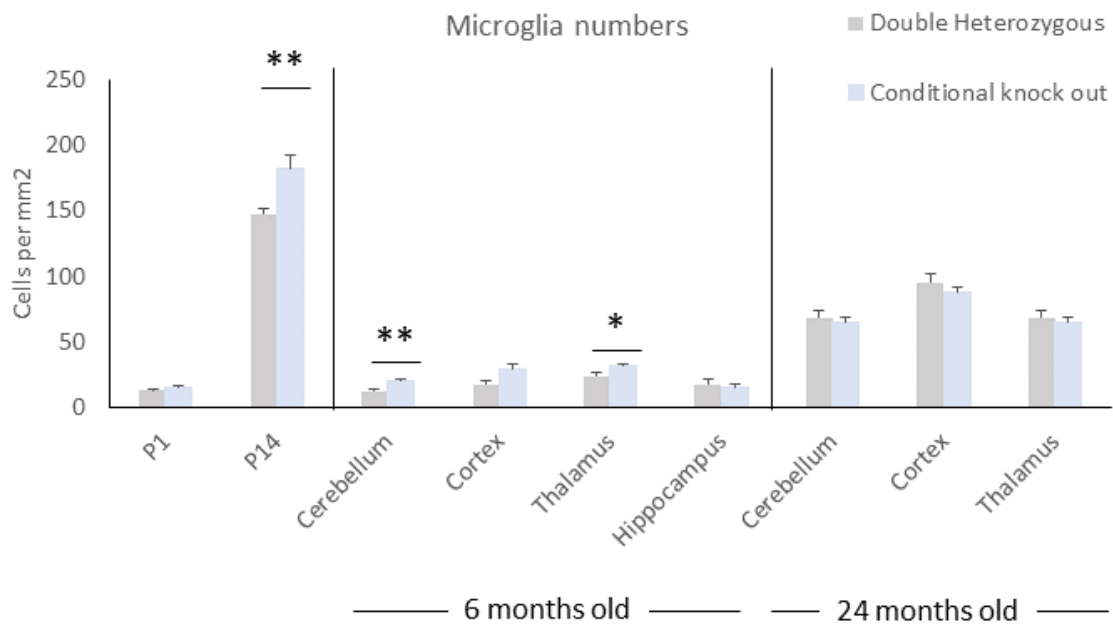


Figure 29. Quantification of microglia at different stages (P1, P14, 6 and 24 month old animals). N=4 males per group. p-value: * <0.05 , ** <0.01 and *** <0.001

Microglia of mGcm2 cko mice have an activated morphology under basal conditions Previous data show mGcm2 expression in microglia at 12 and 24 months. To explore further the role of mGcm2 in microglia *in vivo* I characterised the microglia morphology which is highly linked with their activated state (Heindl et al., 2018). Resting microglia have long ramifications while activated microglia have shorter ramifications. Sections of brains from different age groups of adult mice were labelled with Iba-1 (**Figure 30A-F**). Then the microglia morphology was evaluated with the filament tracing by Imaris software a powerful tool that has been extensively used for microglia morphology studies (Althammer et al., 2020; Cengiz et al., 2019). My criteria for the morphological analysis included the number of ramifications and the coverage area of the cell which is the area where microglia extend their ramifications.

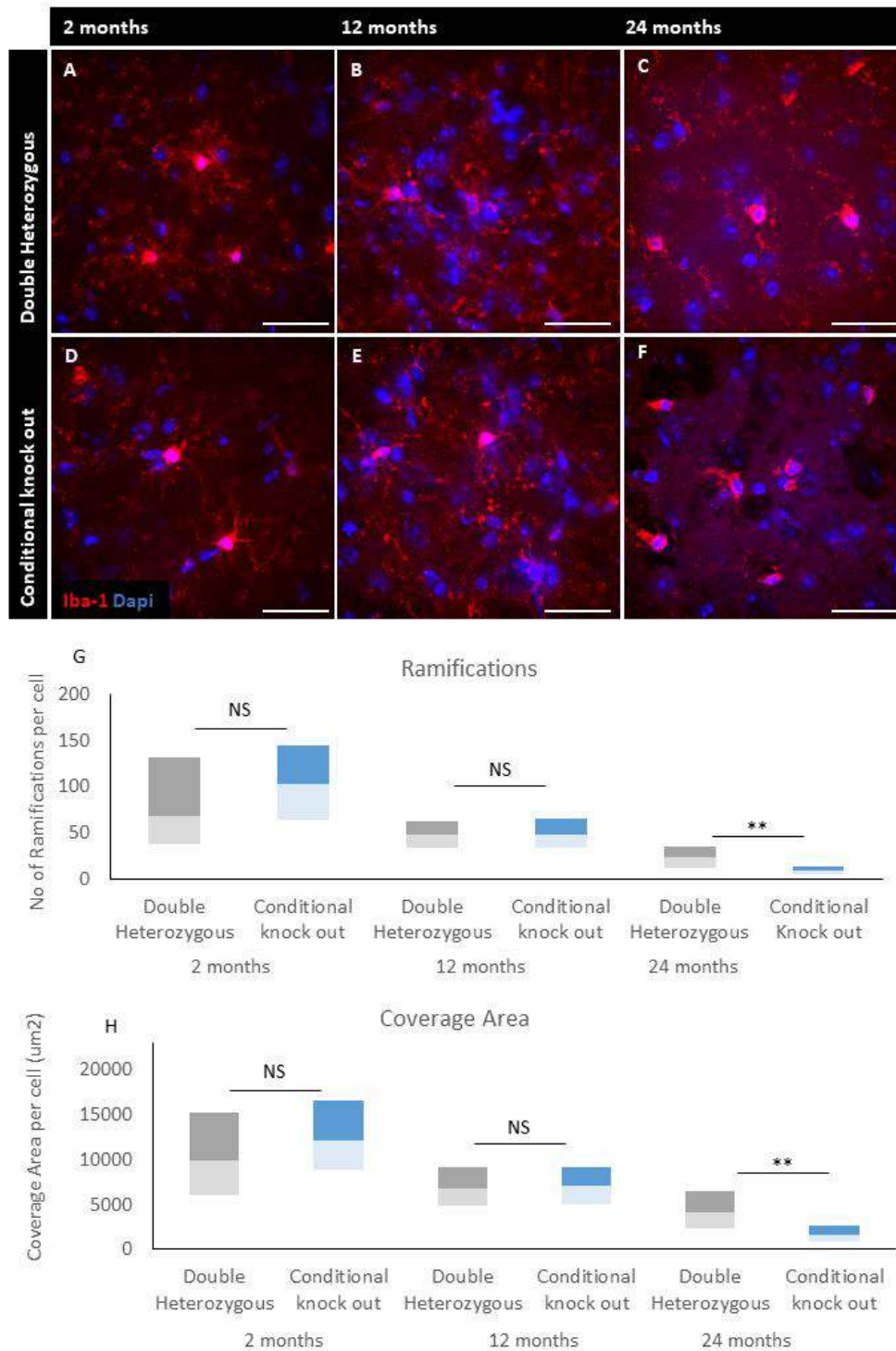


Figure 30. Immunolabelling with microglia anti-Iba-1 (red) at 2 (A,D) 12 (B,E) and 24 months (C,F). The first row is from double heterozygous animals (A-B), the second row is for cko animals (D-F). Analysis of microglia morphology at 2, 12 and 24 month old animals between the different genotypes. (G) Number of Ramifications results coming from image analysis with Imaris. At 2 and 12 months there is no difference in the ramification number of microglia. At 24 months, cko mice show significant decrease in the ramifications compared to the control mice. ANOVA p-value 3.2366E-09, p-value at 24 months 0.006 (H) Coverage area (µm²) results from image analysis with Imaris. At 2 and 12 months, there is no difference in the coverage area of microglia, however, at 24 months, cko mice show a significant decrease of coverage area compared to the control mice, ANOVA p-value 7.83E-11, p-value at 24 months 0.009. p-value: *<0.05, **<0.01 and ***<0.001 N=5-13, scale bar 50µm

The results show that microglia morphology changes through the life span (**Figure 30G, H**). More specifically, the number of ramifications significantly decreases over time in both genotypes (**Figure 31A, B**). In control animals, the number of ramifications decreases from 87 per cell in 2 month old animals, to 50 and 26 ramifications per cell in 12 and 24 month old mice, respectively. Similarly, in cko animals the number of microglia ramifications decreases from 114 at 2 months, to 52 and 10 ramifications per cell at 12 and 24 months. Comparison of the different genotypes at the same time point reveals that there is a statistically significant decrease in ramifications in microglia in the cko compared to the control animals (**Figure 31A**).

The same trend is also visible for the coverage area (**Figure 31C, D**). More specifically, the coverage area of the cells significantly decreases over time in both genotypes. Coverage area in control animals decreases from 11290 μm^2 per cell in 2 month old animals, to 7067 and 4656 μm^2 per cell at 12 and 24 month old mice, respectively. Similarly, the microglia coverage area of cko animals decreases from 12979 μm^2 at 2 months to 7331 and 1979 μm^2 per cell at 12 and 24 months respectively. Comparison of the different genotypes at the same time point reveals a statistically significant decrease in the coverage area of microglia in the cko compared to the control animals (**Figure 30B**). These results for the first time reveal that lack of mGcm2 has an impact on their morphology. Cko microglia, at 24 months, have less ramifications and coverage area that shows a more pro-inflammatory morphology compared to the control.

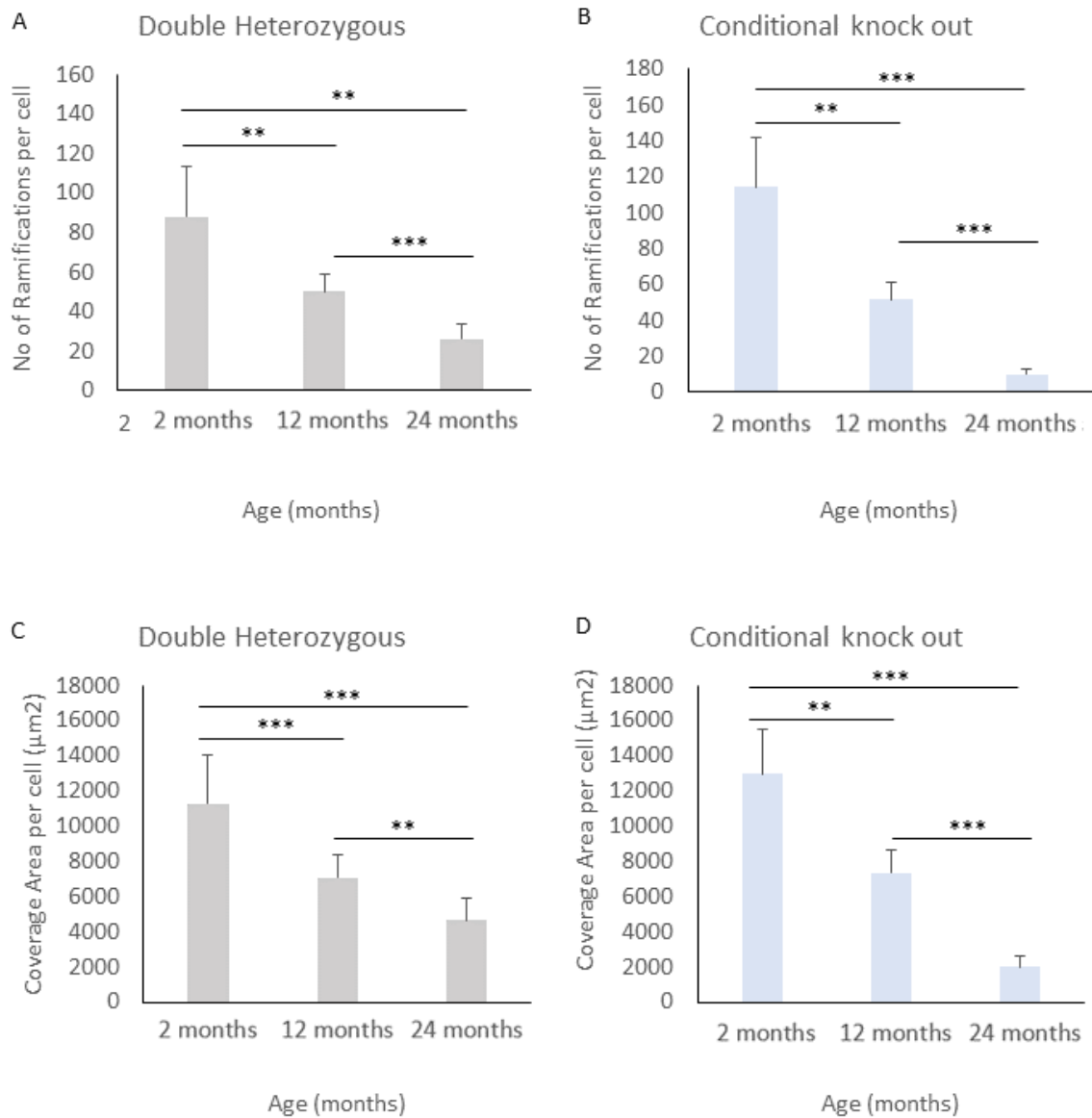


Figure 31. Analysis of microglia morphology in 2, 12 and 24 month old animals between the different age groups of the same genotype. (A) Number of terminal filament point (Ramifications) results of double heterozygous animals (control) coming from image analysis with Imaris. There is a significant decrease of ramification number between the different age groups, p-value between 2 and 12 months 0.002, between 12 and 24 months 0.0003 and between 2 and 24 months 0.004 (B) Number of terminal filament point (Ramifications) results of cko animals coming from image analysis with Imaris. There is a significant decrease of ramification number between the different age groups, p-value between 2 and 12 months 0.003, between 12 and 24 months 1.77E-06 and between 2 and 24 7.18637E-05 (C) Coverage area (µm²) results in double heterozygous animals (control) from image analysis with Imaris. There is a significant decrease of ramification number between the different age groups, p-value between 2 and 12 months 0.0007, between 12 and 24 months 0.007 and between 2 and 24 0.001 (D) Coverage area (µm²) results in cko animals from image analysis with Imaris. There is a significant decrease of ramification number between the different age groups, p-value between 2 and 12 months 0.002, between 12 and 24 months 1.11E-05 and between 2 and 24 0.0001, p-value: *<0.05, **<0.01 and ***<0.001 N=5-13

mGcm2 cko animals have a pro-inflammatory profile

The data above suggest a pro-inflammatory phenotype in the old cko animals. To further support these data, I labelled 2, 12 and 24 month old animals with pro- and anti-inflammatory markers. Microglia/macrophage activation states are classified as pro-inflammatory (or M1) state or anti-inflammatory (or M2) state. I chose the marker iNOS for the M1 and Arginase-1 (Arg-1) for the M2 state which have already been used to characterise the state of microglia *in vivo* (Lisi et al., 2017). Both markers were quantified in microglia co-labelled with Iba1.

First, I evaluated the expression of the M1, pro-inflammatory marker, iNOS. Labelling from different age groups shows that iNOS is present mostly in 12 and 24 month old animals (**Figure 32**). The expression is increased in both groups as they age. Next, I quantified the iNOS positive microglia via Fiji software (**Figure 32 A-F**). 2 month old control animals have less than 1% iNOS positive microglia (**Figure 32G**). By 12 months, the percentage of iNOS positive microglia increases (17%) and remains stable by 24 months (14%). Similarly, cko animals initially have a very low number of iNOS positive microglia (0.6%), which progressively increases up to 16% and 26% by 12 and 24 months, respectively (**Figure 32H**). Finally, I compared the two different genotypes of the same age group. The results revealed that 2 and 12 months old animals show no difference. In contrast, by 24 months the cko animals have a statistically significant increased number of iNOS positive microglia compared to the control animals (**Figure 32I**). Thus, these data confirm that the pro-inflammatory morphology is accompanied by increased expression of pro-inflammatory markers such as iNOS.

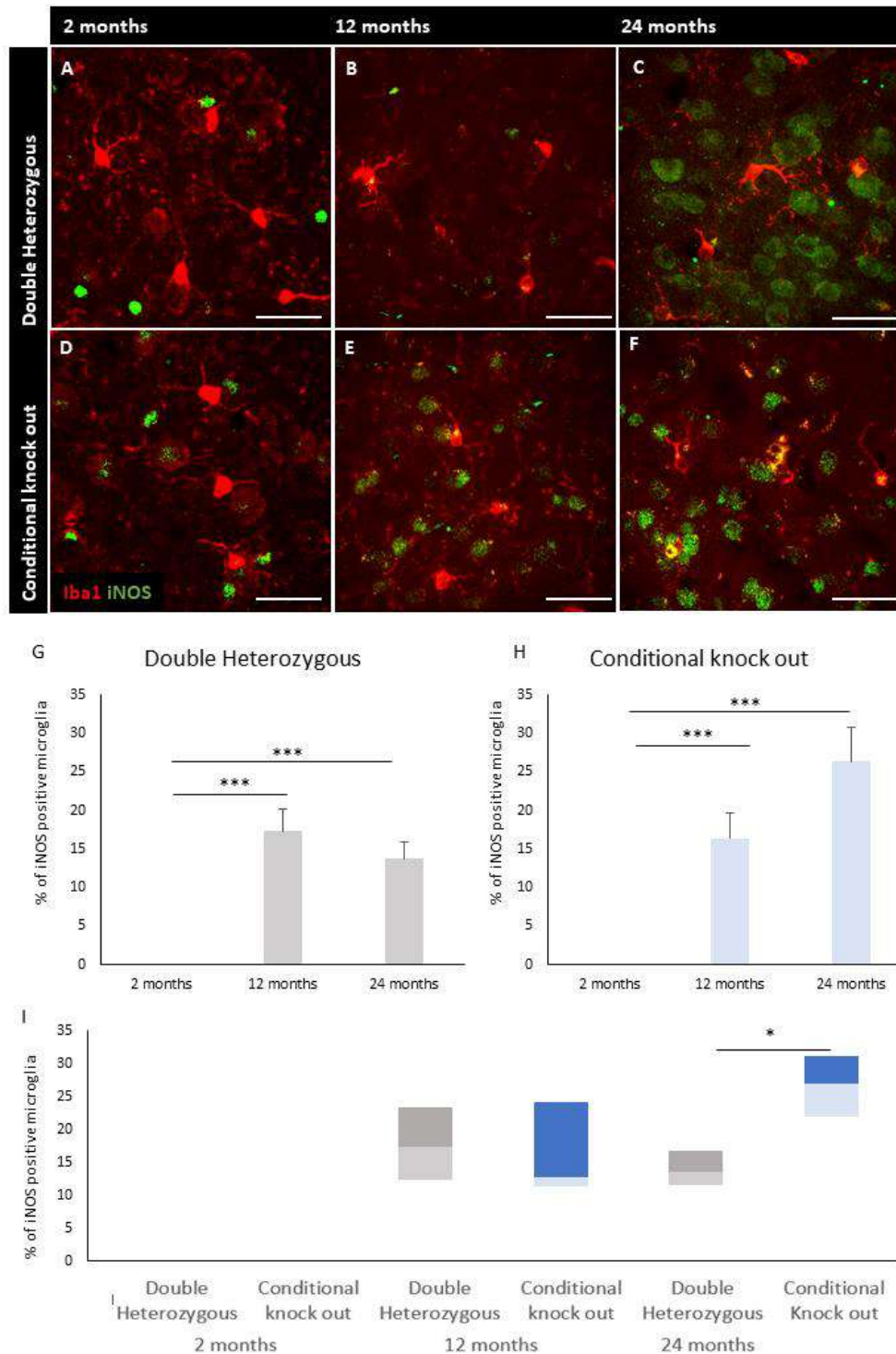


Figure 32. Immunolabelling of the CNS with the pro-inflammatory marker iNOS (green). The upper panel (A-C) shows control animals (double heterozygous) and the lower panel (D-E) shows cko animals. The first row shows 2 month old CNS, the second 12month old CNS and the third 24 month old CNS. Microglia cells are labelled with Iba-1 (red). Quantification of iNOS positive microglia at 2, 12 and 24 month old animals. (G) iNOS positive microglia of double heterozygous animals coming from image analysis with Imaris. , p-value between 2 and 12 months 0.0005 and between 2 and 24 0.00007 (H) iNOS positive microglia of cko animals coming from image analysis with Imaris. , p-value between 2 and 12 months 0.001 and between 2 and 24 0.00001 (I) Comparison of iNOS positive microglia between different genotypes at the same age group. , ANOVA p-value 1.80826E-06, p-value between cko and double heterozygous animals at 24 months 0.04. p-value: *<0.05, **<0.01 and ***<0.001 N=5-13, scale bar 50um

My next goal was to evaluate the expression of Arg-1 in the different age groups and genotypes. Since the morphology and the high number of iNOS positive microglia show a pro-inflammatory profile, Arg-1 should be decreased in cko animals compared to the controls. For this I labelled brain sections with Iba-1 and Arg-1 (**Figure 33A-F**). Arg-1 labelling decreases over time in both genotypes. Comparison between controls of the same group shows that 2 month old animals have a higher number of Arg-1 positive microglia compared to 12 and 24 month old animals, from 85% to 43% and 34 %, for each age group respectively (**Figure 32G**). Likewise, cko animals show a significant decrease in the number of Arg-1 positive microglia, from 2 (74%) to 12 month old animals (47%) (**Figure 32H**). Importantly, the percentage of Arg-1 expressing microglia further decreases from 12 to 24 months, resulting in a statistically significant decline (from 47% to 15%). Although there is a tendency of decreased Arg-1 microglia at 24 month old cko animals compared to the control, comparison of the Arg-1 positive microglia between the two genotypes of the same age group show no difference between the two groups (**Figure 32I**). These data confirm my initial hypothesis that Arg-1 would be impacted from the loss of mGcm2.

In conclusion, all the data from both the morphology and the expression of inflammatory markers show for the first time that mGcm2 has an anti-inflammatory role in microglia. Microglia of cko animals at 24 months show less ramification and coverage area. Furthermore, they show a statistically significant increase of the pro-inflammatory marker iNOS. At the same time, these animals show a significant decrease of the anti-inflammatory marker Arg-1 when I compared the 12 and the 24 month old cko animals, while the controls showed a stable level of Arg-1. This anti-inflammatory role is in agreement with the other species where the Gcm cascade is important during immune challenges (*Drosophila*, sea urchin).

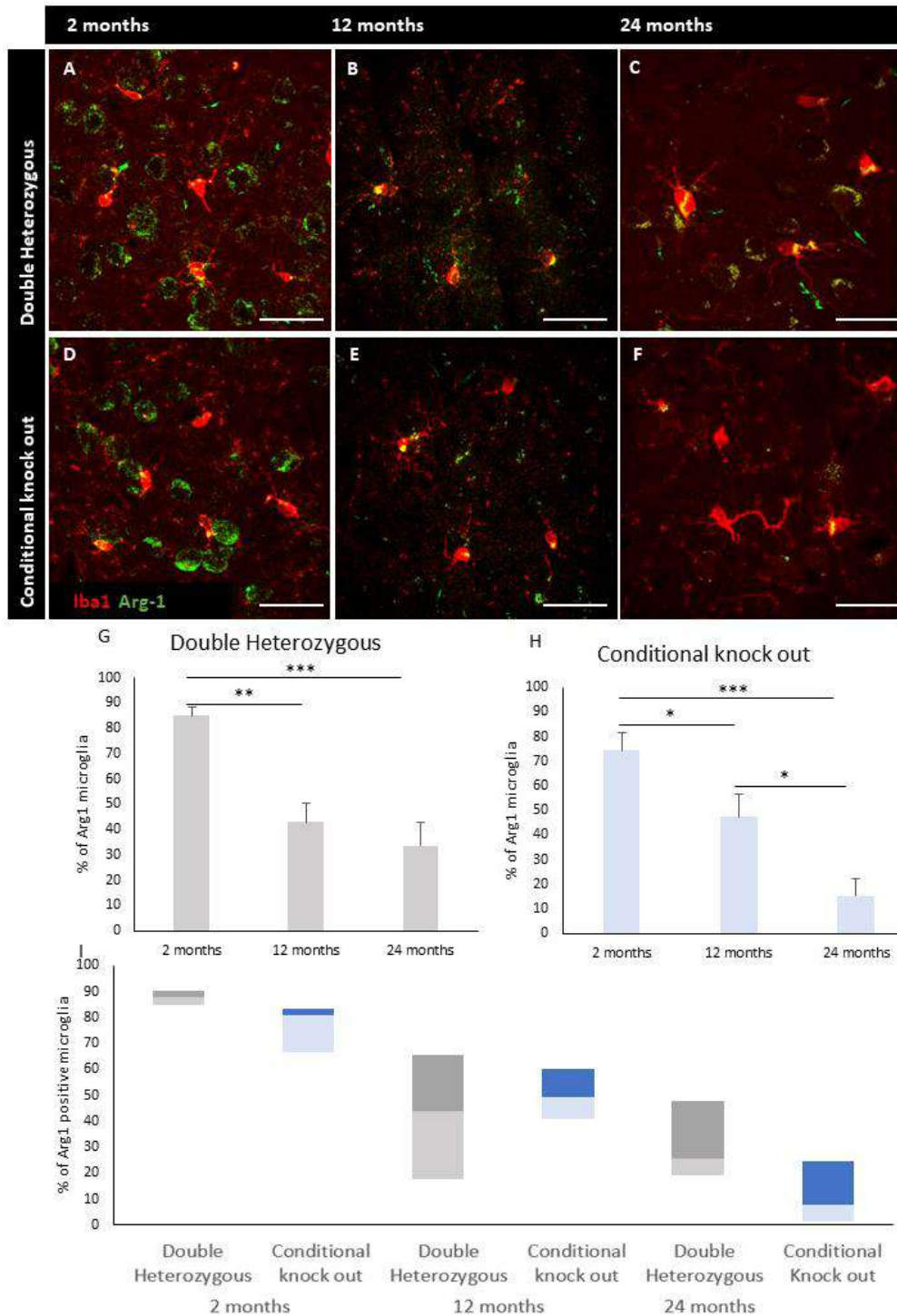


Figure 33. Immunolabelling of the CNS with the anti-inflammatory marker Arginase 1 (green). The upper panel (A-C) shows control animals (double heterozygous) and the lower panel (D-E) shows cko animals. The first row shows 2 month old CNS, the second 12 month old CNS and the third 24 month old CNS. Microglia cells are labelled with Iba-1 (red). Quantification of Arg-1 positive microglia at 2, 12 and 24month old animals. (G) Arg-1 positive microglia of double heterozygous animals coming from image analysis with Imaris., p-value between 2 and 12 months 0.002 and between 2 and 24 months 0.003 (H) Arg-1 positive microglia of cko animals coming from image analysis with Imaris. p-value between 2 and 12 months 0.04 and between 2 and 24 months 0.00009 and between 12 and 24 months 0.01 (I) Comparison of Arg-1 positive microglia between different genotypes at the same age group. ANOVA p-value 1.4949E-05. p-value: *<0.05, **<0.01 and ***<0.001, N=5-13, scale bar 50um

Discussion

mGcm2 profiling in mouse tissues revealed its presence in microglia of the CNS of aged animals. In this chapter I characterised the phenotype of microglia from mGcm2 cko animals. The results showed that cko animals have a pro-inflammatory phenotype. This is manifested with increased weight and higher number of microglia cells in young adults. Furthermore, aged microglia at 24 months have a pro-inflammatory morphology with less ramifications and coverage area. Finally, I showed that cko animals present a higher expression of the pro-inflammatory marker iNOS and decreased expression of the anti-inflammatory marker Arg-1.

[mGcm2 cko animals show an increased weight compared to the controls](#)

Obesity is one of the most common chronic inflammatory diseases as increased weight is linked with observations of altered levels of cytokines (Cox, Moscovis, Blackwell, & Scott, 2014; de Heredia, Gomez-Martinez, & Marcos, 2012; Krela-Kazmierczak et al., 2021). Even though many studies have focused on the inflammatory state of the adipose tissue, new studies demonstrated that the CNS plays a pivotal role in the maintenance and regulation of the metabolism.

The CNS senses and controls the energy status of the organism (Myers & Olson, 2012), and the hypothalamus in particular has emerged as an integrating, superordinate master regulator of whole-body energy homeostasis. As an early event in obesity development and even within a few days of ingesting a HFD, an increased amount of saturated fatty acids from the periphery crosses the BBB and induces an inflammatory response in hypothalamic neurons (L. Thaler et al., 2012). This involves activation of microglia thus, promoting endoplasmic reticulum (ER) stress in hypothalamic neurons. ER stress ultimately leads to insulin resistance (Kleinridders et al., 2009; Pimentel, Ganeshan, & Carvalheira, 2014). In two rodent models where obesity was induced by the consumption of a HFD, hypothalamic inflammation occurred within 1-3 days of the HFD start, before changes in body weight ensued (J. P. Thaler et al., 2012). This

could suggest that inflammation in the hypothalamus is sufficient to initiate weight gain and/or hyperphagia. Furthermore, within the first week of HFD there was evidence of microglia activation.

My findings show that lack of mGcm2 in microglia leads to increased weight, and a tendency for hyperphagia and higher fat content. However, the metabolic cages did not reveal any significant changes in energy expenditure. This phenotype could be linked with the role of microglia in the hypothalamus, which can trigger hyperphagia and result in increased weight that was observed in the cko animals. In order to confirm this hypothesis, it would be extremely interesting to study the hypothalamic region of cko mice that are under HFD in order to increase any phenotypes. If my hypothesis is correct, then the triggering of the diet will increase the expression of mGcm2 in the controls that acts as an anti-inflammatory mediator. Furthermore, HFD in cko animals should show increased weight accompanied by higher fat percentage and food consumption compared to the control animals.

[mGcm2 cko animals have increased microglia populations](#)

The microglia population in the adult brain is highly heterogeneous, accounting for between 5% and 12% of the total population of glial cells in the healthy murine CNS (Lawson et al., 1990). My results showed that cko animals have a significantly increased number of microglia at P14 and young adults compared to the control. These results indicate that there is an increased expansion in the population during the first two weeks of the animal's life. Furthermore, the increased numbers during the young adult stages could indicate that either more cells remained after the postnatal expansion or that the cko microglia have a higher self-renewal capacity.

Although microglia cells have critical roles in the maintenance of brain homeostasis, the impact of altering the population in the absence of pathology is not well understood. Given the diverse array of microglia functions in the healthy and diseased CNS, changes to population dynamics

may be implicated in the development of neurological and neurodegenerative conditions. Few studies have reported the impact of increased microglia numbers in the non-diseased CNS. For example, overexpression of CSF1 promotes microglia proliferation and thus results in a 2-fold increase in cell numbers in the parenchyma (De et al., 2014). To further explore changes in microglia proliferation, it would be interesting to study the expression of genes related to the CSF1R-driven proliferative response (Gomez-Nicola, Fransen, Suzzi, & Perry, 2013). These genes include the PU.1 and IRF8 (Askew et al., 2017). This simple labelling will give more information about the role of mGcm2 during microglia proliferation.

mGcm2 cko animals show a more pro-inflammatory profile in the aged brain compared to the controls

Aging results in gradual loss of normal function. Changes at the cellular level are believed to contribute to this process (Lopez-Otin, Blasco, Partridge, Serrano, & Kroemer, 2013). Understanding how the molecular processes in neurons and glia cells change as we age and how the interactions of these cells are affected by such changes could lead to new breakthroughs in therapeutic targets of age-related neurodegenerative diseases. My data suggest that during aging cko animals show significant pro-inflammatory changes compared to the control animals. These data suggest that mGcm2 acts as a regulator of the activation state in microglia. Loss of its expression leads to an uncontrolled stimulation and thus a higher pro-inflammatory profile even under basal conditions. Future studies should focus on additional markers for the two inflammatory states that are specific to microglia, such as MHC II.

Microglia exhibit an exaggerated pro-inflammatory response during aging, a phenomenon referred to as microglia priming (Michell-Robinson et al., 2015; J. R. Perry et al., 2014). Morphologically, aged microglia have enlarged processes, cytoplasmic hypertrophy, and a less ramified appearance (Damani et al., 2011; Tremblay, Zettel, Ison, Allen, & Majewska, 2012).

They also express higher levels of activation markers such as MHC II (Conde & Streit, 2006). All these changes lead to impaired remyelination and are associated with decreased M2 microglia (Miron et al., 2013). On the other hand, rejuvenation of remyelination in aged mice correlates with increased M2 microglia. These data suggest that targeting anti-inflammatory (M2) regulators of microglia, such as mGcm2, could potentially lead to new therapeutic targets not only for aging but also other neuroinflammatory diseases. With my study I proved that mGcm2 could be one of those anti-inflammatory targets, although more studies are important to further dissect the mGcm2 cascade in microglia.

Chapter III

Functional characterisation of mGcm2 *in vitro*

My data showed that mGcm2 is expressed in microglia of aged animals and the lack of mGcm2 leads to an increased inflammatory state in microglia. My next goal was to evaluate the main functions of microglia, phagocytosis and migration. Since the use of animals was not feasible due to the pandemic, I used *in vitro* CNS cultures which also show mGcm2 expression in microglia. The phagocytosis assay showed that exposure to latex beads leads to the inhibition of mGcm2 in microglia after 20 min of exposition. The levels of mGcm2 are restored by 120 min. For further validation of the mGcm2 role on phagocytosis I used the cko animals for CNS cultures and repeated the experiment. However, cko cultures do not show any difference concerning their phagocytic capacity compared to the control, thus concluding that mGcm2 expression is indeed affected by the bead exposure but it does not regulate phagocytosis. Finally, I performed scratch wound migration assays with cko and control cultures. The results did not show any differences in the migratory capacity of the cko cultures. Thus, results did not reveal any direct functional role during the phagocytosis nor the migration of microglia *in vitro*.

Introduction

Microglia are highly active cells that constantly survey their environment. During this process microglia are highly dependent on phagocytosis and migration. Phagocytosis is one of their main tasks as they continuously scan the environment for pathogens and damage associated cues (Paolicelli et al., 2011). Furthermore, microglia also regulate apoptosis, synaptogenesis, synapse survival and neuronal maturation through phagocytosis during development (Reemst, Noctor, Lucassen, & Hol, 2016). Apart from phagocytosis, microglia rely on their migratory capacity during development, homeostasis as well as an immune response (Davalos et al.,

2005). Furthermore, in *Drosophila* migration of glia cells involves the expression of Gcm (Gupta et al., 2016). More specifically, Gcm induces the expression of the netrin receptor *Frazzled* in a dose-dependent manner. Then, *Frazzled* triggers the initiation of glia migration in the developing fly wing, thus proving critical data on the glial determinant that also regulates the efficiency of collective migration.

The *in vivo* assays show that mGcm2 is expressed very early in embryogenesis and later in microglia cells of aged animals. Moreover, I proved that old mGcm2 cko animals (24 months) show increased expression of the pro-inflammatory marker iNOS and decreased expression of the anti-inflammatory marker Arg-1. Even though those results were extremely interesting I wanted to further evaluate the mGcm2 expression in microglia and see if Gcm has multiple roles such as the initiation of migration in *Drosophila*.

Due to the complexity of *in vivo* evaluation of phagocytosis and migration, I choose to work on the CNS cultures *in vitro*. Furthermore, previous data already show that mGcm2 is expressed in microglia cells *in vitro*, while the *in vivo* models required at least one year old animals because this is when the mGcm2 protein is present. Moreover, most information available on microglia phagocytosis and migration originates from *in vitro* studies using primary rodent microglia thus giving me established protocols to work with (Milner, 2009; Milner & Campbell, 2002, 2003; Welser-Alves, Boroujerdi, Tigges, & Milner, 2011).

Results

mGcm2 is decreased upon bead exposure but it does not control their phagocytosis. In order to evaluate the impact of mGcm2 in microglia cultures I used P1 primary cultures. First, I evaluated the mGcm2 expression upon phagocytosis in WT (C57BL/6) cultures. For the assay, I used fluorescent latex beads (Lian, Roy, & Zheng, 2016; X. Liu, Xu, & Zhang, 2013; Lucin et al., 2013). I exposed the cultures to the beads for different times (0, 20, 120 min) (**Figure 34A-C**) and measured the intensity of the fluorescence inside the cells (**Figure 34D**). The results revealed that, as time progresses only microglia phagocytose more and more beads. Interestingly, round microglia phagocytose most of the beads, while ramified and amoeboid microglia phagocytose much less. These findings agree with similar phagocytosis assays of microglia since round microglia are considered as active *in vitro*, thus they can phagocytose quicker than the resting microglia (He et al., 2016). Finally, I semi-quantified the mGcm2 expression by measuring the antibody intensity inside the cells at different time points (0, 20, 120 min of bead exposure). The results show that mGcm2 expression statistically decreases in the first 20 min of bead exposure, from 5700000 to 4200000 units (**Figure 34E**). Then the mGcm2 expression returns to the basal levels after 120 min of exposure (7500000 units). These results show that mGcm2 is influenced by the bead exposure and its expression is decreased. In order to see whether mGcm2 actively participates in phagocytosis I repeated the assay with cko cultures.

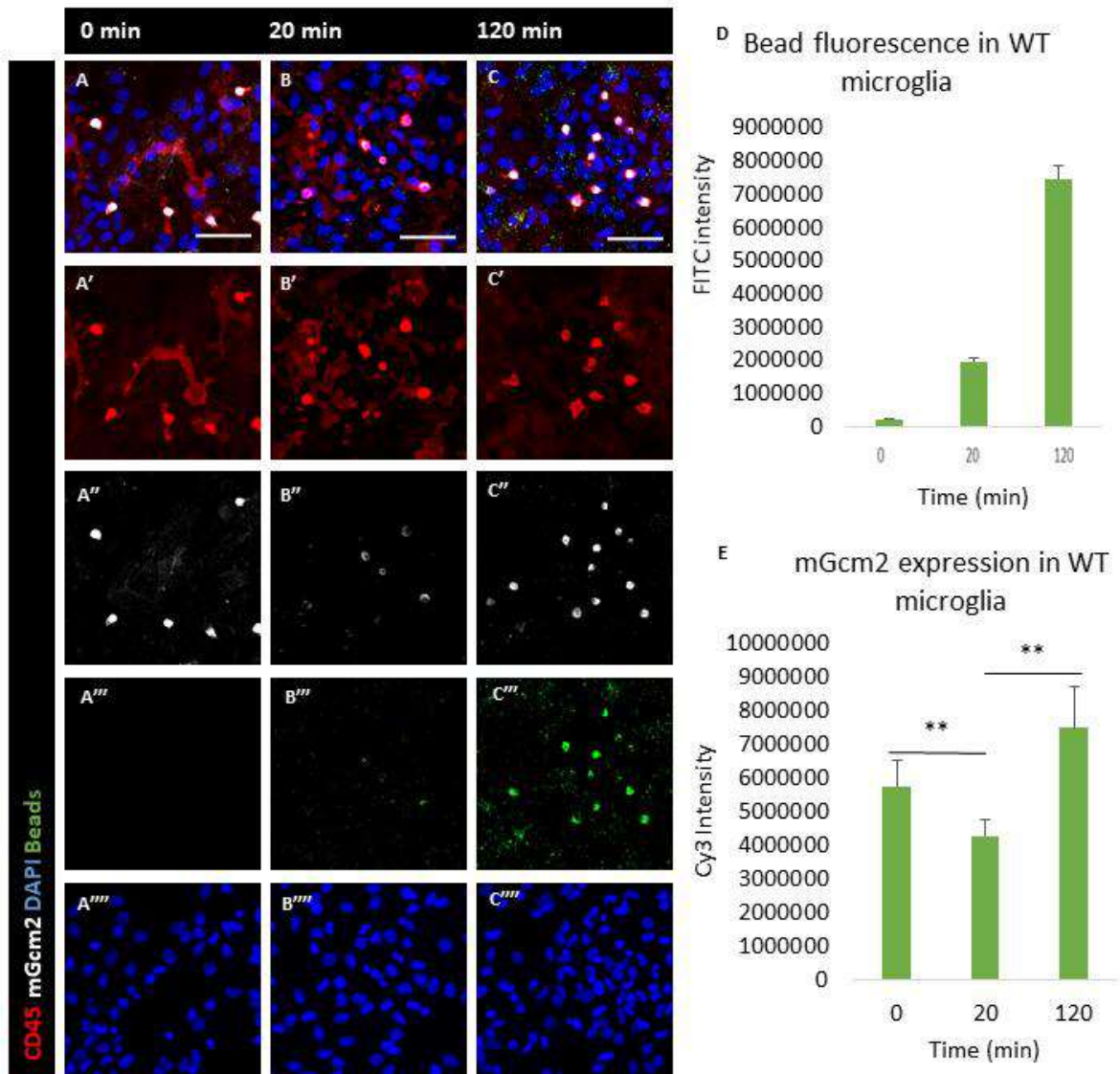


Figure 34. Expression of mGcm2 in wild type microglia of P1 cultures upon bead exposure for 20 and 120 min (A-C). CD45 in red indicate microglia, mGcm2 in grey, beads are green and Dapi in blue indicates the nuclei. (D) Bead fluorescence in microglia and (E) mGcm2 protein expression measured by the fluorescence of the secondary antibody. ANOVA p-value 0.042, p-value between 0 and 20 min 0.005, between 20 and 120 0.007. p-value: * <0.05 , ** <0.01 and *** <0.001 N=18, scale bar 50um

Microglia cells from both genotypes phagocytose beads, and the fluorescence of the beads inside the cells increases over time, thus even the cko has phagocytic activity (**Figure 35A-F**). In order to detect differences in the phagocytic capacity of the cells, I quantified the fluorescence of the beads inside microglia (**Figure 35G**). This provided an indirect way to measure the quantity of the beads in the cells, as more beads means higher intensity. The results did not show any difference between the two genotypes. Consequently, mGcm2 does not

actively participates during phagocytosis but its expression is influenced by an external stimulation.

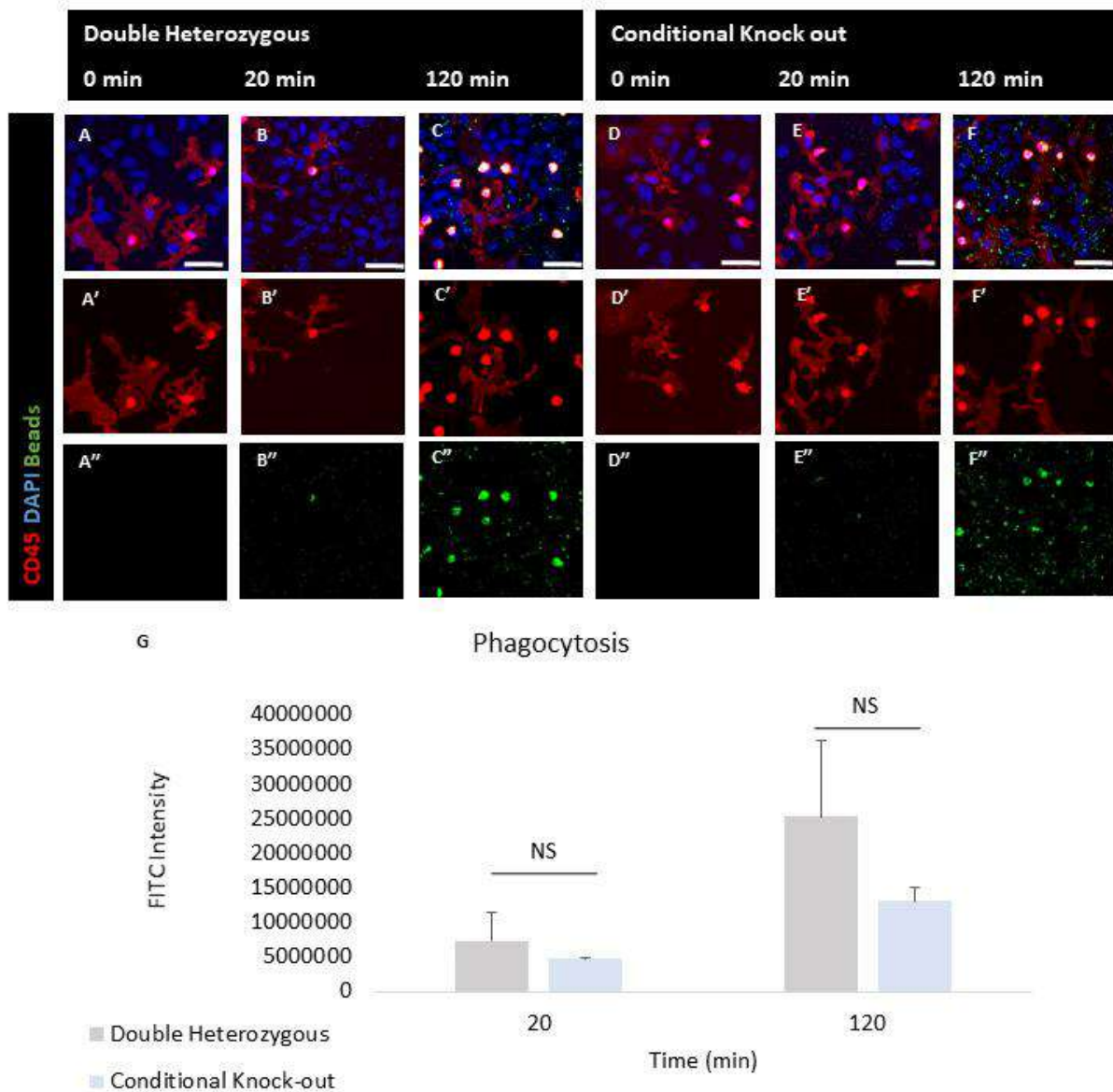


Figure 35. Phagocytosis assay in double heterozygous and cko microglia of P1 cultures upon bead exposure for 20 and 120 min (A-F). CD45 in red indicate microglia, beads are green and Dapi in blue indicate the nuclei. (G) Beads fluorescence in microglia. p-value: $* < 0.05$, $** < 0.01$ and $*** < 0.001$ ns=not significant N=6 per genotype more than a 100 cells per sample, scale bar 50um

mGcm2 is not implicated in the migration of microglia *in vitro*

Next, I performed a migratory assay. This assay was inspired by the fact that Gcm is participating in glia migration of flies, thus I wanted to study if this mechanism is evolutionary conserved. For this, I used the screening facility of IGBMC that has a well-established protocol for automated scratch wound and live tracking of the cells (Liang, Park, & Guan, 2007; Lively & Schlichter, 2013; Pinheiro, Linden, & Mariante, 2015). After the scratch was done, pictures from different time points were collected for up to 24 hours (**Figure 36**). I then counted the number of cells in the scratch area. My results show no difference in the number of cells migrating into the scratch wound area between the two groups. More specifically, for the control cultures, there is an average of 47 cells migrating to the area after 24 hours, and for the cko, approximately 53 cells migrate into the area.

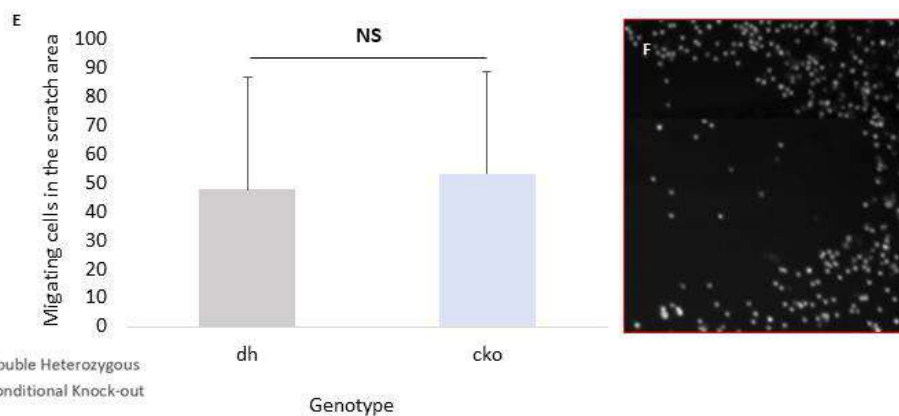
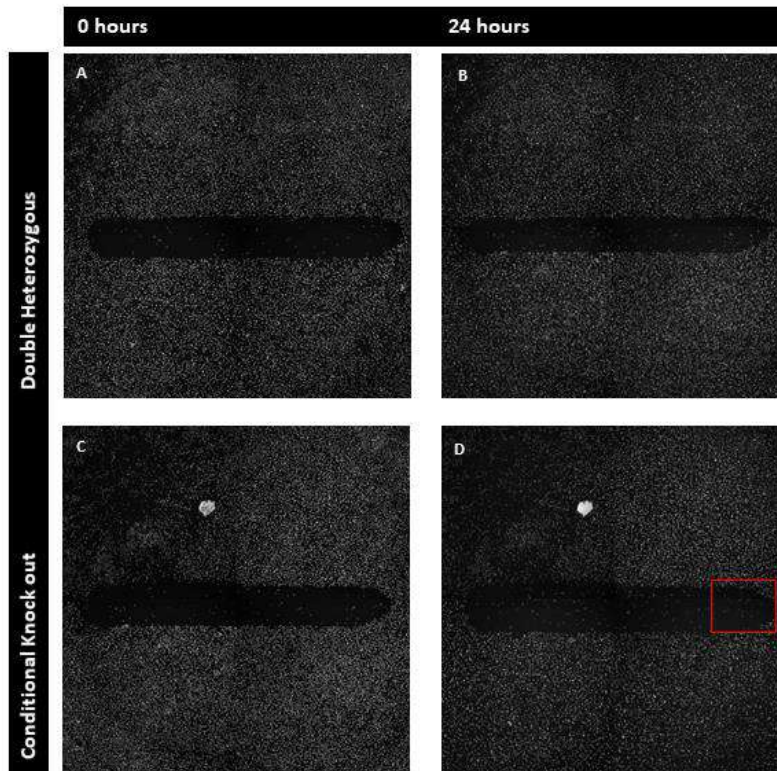


Figure 36. Migration assay in double heterozygous and cko microglia of P1 cultures for 24hours (A-D). Hoercest in grey indicates the nuclei. (E) Migating cells in the scratch area. p-value: * <0.05 , ** <0.01 and *** <0.001 ns=not significant N=3 per genotype

Finally, in order to investigate whether the cells that migrate into the scratch were microglia I performed the migration assay and then label with CD45 and mGcm2 to see whether the migrating cells express the protein. At t=0 there are cells expressing mGcm2 (**Figure 37A**). Furthermore, most of the cells migrating to the scratch area are microglia since they are CD45 positive (**Figure 37**) but do not express mGcm2. These data indicate that mGcm2 does not participate in the migration of microglia *in vitro*.

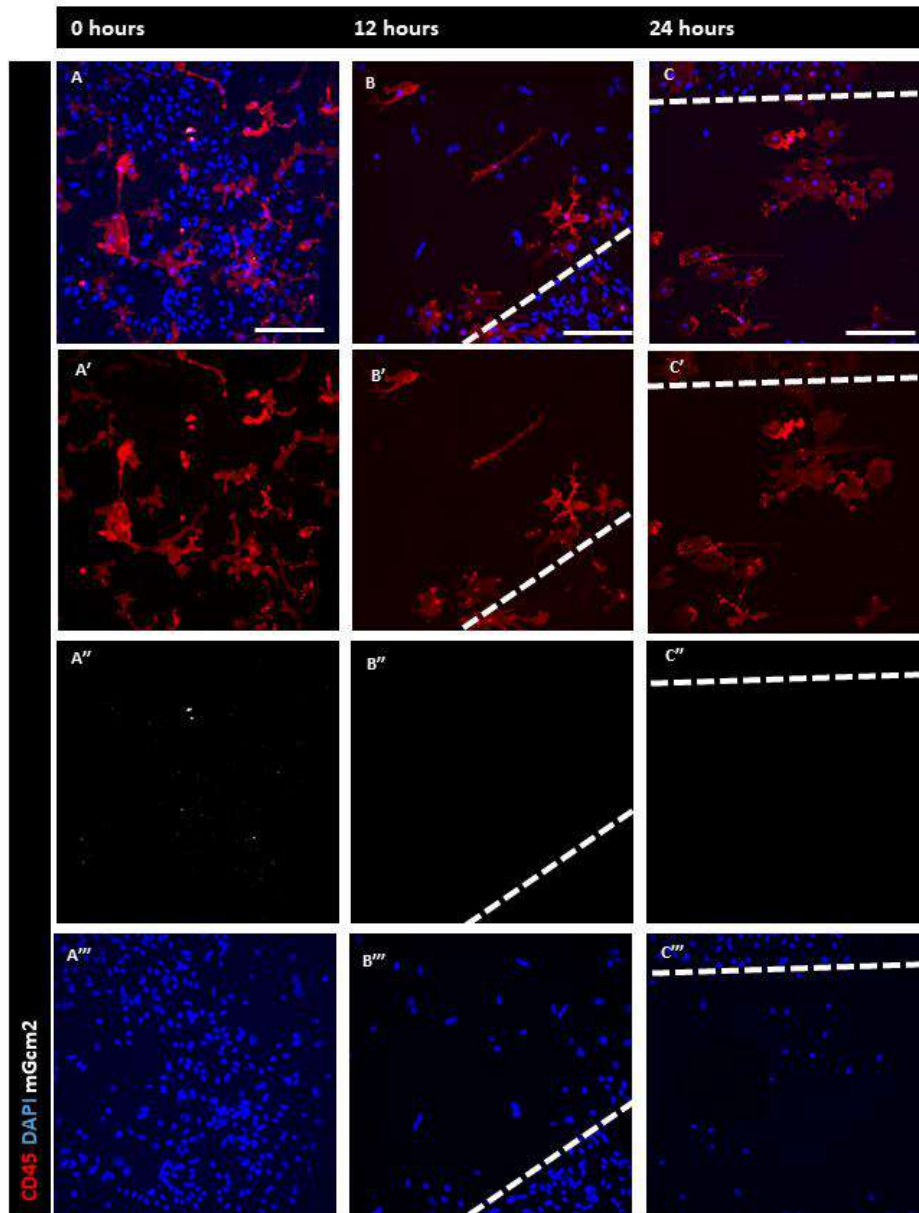


Figure 37. Confocal images acquired upon migration assay in wild type microglia of P1 cultures for up to 24 hours (A-C). CD45 in red indicates microglia (A'-C'), mGcm2 is in grey (A''-C''), and Dapi indicates the nuclei (A'''-C''').

Discussion

I characterised the mGcm2 expression profile during phagocytosis and migration and found that mGcm2 expression decreases during the first 20 min upon bead exposure and then it returns to basal levels. Similarly, phagocytosis of apoptotic neurons by microglia was associated with enhanced pro-inflammatory and dampened anti-inflammatory profile in microglia (Siddiqui, Lively, & Schlichter, 2016). However, the phagocytosis assay in cko

cultures did not reveal any difference compared to the controls. Consequently, mGcm2 does not directly control phagocytosis of latex beads. Nevertheless, exposure to the beads influences microglia thus suggesting that mGcm2 expression is linked to the presence of foreign bodies. So, it would be interesting to evaluate the phagocytic capacity of microglia with other molecules that exist *in vivo*, such as myelin particles. Maybe a more specific stimulation can highlight variations in the cko model.

Finally, I performed a migration assay to evaluate the migratory capacity of the cko microglia. As mentioned above migration is a pivotal function of microglia and *gcm* has been shown to promote the migration of glia cells in *Drosophila* (Gupta et al., 2016). However, the results showed no difference in the migration of the cko microglia compared to the control animals. Thus, mGcm2 does not control migration of microglia cells in this experimental set up.

These experiments show that mGcm2 does not have a direct connection with phagocytosis nor migration *in vitro*. However, *in vitro* approaches are not ideal as they lack the complexity of *in vivo* experiments. One major challenge is that *in vitro* cultures do not reflect the effect of aging which is where I found the most striking phenotype (Timmerman, Burm, & Bajramovic, 2018). However, aged microglia are very close to other immune challenges *in vivo*, thus I am currently collaborating with Dr B. Nait-Oumesmar from the ICM in Paris who is interested in acute neuroinflammatory conditions and has previously worked on the Gcm factors. Together, we are going to use cko lines to introduce acute and chronic demyelinating diseases and then study the effect of mGcm2 in those animals. Our experiments already gave the first preliminary data confirming the anti-inflammatory role of mGcm2 in LPC acute lesions in the spinal cord. The next aim is to use the cko lines to study the effect of mGcm2 in chronic demyelinating disease models such as the EAE, which is the equivalent of MS. These experiments will help us understand better the role of the mGcm2 immune cascade in microglia.

Chapter IV

Study of Gcm expression during neuroinflammation in *Drosophila melanogaster*

During my PhD, I have studied the role of mGcm2 in microglia. The results proved that this transcription factor has an anti-inflammatory role. In the last year of my PhD, I explored the possible evolutionary conserved role of Gcm in neuroinflammatory conditions in *Drosophila*. Firstly, I evaluated whether there is Gcm expression in glia of the aged brain of the fly. In homeostatic conditions Gcm is expressed only in specific neurons of the adult fly CNS in two clusters (dorsolateral and medial) per central brain hemisphere (Soustelle & Giangrande, 2007). Next, I characterised whether Gcm is present in the brain of flies with Parkinson's like syndrome using two different models: expression of α -Syn and exposure to neurotoxic paraquat (PQ). The α -Syn expression model revealed some Gcm positive cells, which seem to express hemocyte markers. In parallel, the PQ model suggested that hemocytes enter in the fly CNS after exposure. Next steps should aim to determine whether under PQ treatment Gcm is expressed in hemocytes. Establishing that Gcm is also expressed during a CNS related challenge in *Drosophila* as it is in mammals, could lead to new potential targets of Gcm that could be easily characterised in the fly model.

Introduction

The fly CNS is isolated from the rest of the body and is protected from the potassium-rich hemolymph by the BBB, warranting optimal neuronal function (Featherstone, 2011; Hindle & Bainton, 2014; Limmer, Weiler, Volkenhoff, Babatz, & Klambt, 2014). The mechanisms of neural development are conserved from flies to mammals and neurodegeneration and human neurodegenerative diseases can be effectively modelled in the fly (Lessing & Bonini, 2009). Studies on fly models of axonal injury suggested the use of *Drosophila* as an attractive model to investigate innate immunity within the CNS (Doherty, Logan, Tasdemir, & Freeman, 2009; Kounatidis & Chtarbanova, 2018; MacDonald et al., 2006; Petersen & Wassarman, 2012).

Studies in flies gave new insights into neurodegenerative diseases such as the PD pathology. Epidemiological studies have identified the herbicide, paraquat (PQ), as a potential environmental risk factor in the onset of PD (Di Monte, Lavasani, & Manning-Bog, 2002; Liou et al., 1997; Uversky, 2004). Exposure of adult flies to low doses of PQ (3–20 mM) results in a recapitulation of parkinsonism movement disorders, including tremors, loss of balance and slowed locomotion, accompanied by loss of dopaminergic neurons, with regionally specific differences in neuron susceptibility (Chaudhuri et al., 2007; Inamdar, Chaudhuri, & O'Donnell, 2012). More specifically, PQ exposure correlates with glutamate excitotoxicity in the *Drosophila* CNS, thus resembling the loss of dopaminergic neurons during PD (Cassar et al., 2015; Hajji et al., 2019; Rival et al., 2006).

Another model of neuroinflammation in *Drosophila* is the expression of α -synuclein (α -Syn), a major component of protein inclusions known as Lewy bodies (LB), which are hallmarks of synucleinopathies such as PD. Feany and Bender first developed transgenic *Drosophila* models expressing either wild-type or familial PD-linked mutants (A53T and A30P) of human α -Syn (Feany & Bender, 2000). The α -Syn expressing flies replicate several features of human PD, including locomotor dysfunction, LB-like inclusion body formation, and age-dependent loss of

dopaminergic neurons. They are widely used for studying the molecular pathogenesis of α -Syn-induced neurodegeneration in not only PD but also synucleinopathies in general. Studies of α -Syn in *Drosophila* helped unravel mechanisms underlying the misfolding and aggregation of this protein, including the protective role of molecular chaperones such as HSP70 and HSP90, protein degradation and post-translational modifications (Auluck & Bonini, 2002; Auluck, Chan, Trojanowski, Lee, & Bonini, 2002; Chen & Feany, 2005; Chen et al., 2009; Du et al., 2010; Karpinar et al., 2009; Lee et al., 2009).

Most of the studies done in flies did not explore the potential role of the innate immune cells during neuroinflammation. A recent transcriptomic analysis showed that upon PQ treatment there is an upregulation of hemocyte specific genes (Maitra, Scaglione, Chtarbanova, & O'Donnell, 2019). These hemocytes markers include *hemese* (*he*), *hemolectin* (*hml*), two *nimrod* genes, (*nimB5* and *nimC4*), three *turandot* genes (*totA*, *totM*, and *totX*), and scavenger receptor C1 (*sr-C1*), thus suggesting the involvement of the *Drosophila* immune response in PQ-induced neurodegeneration. These data give new insights into the potential role of hemocytes during an inflammatory response in the fly CNS. My main question was whether there is Gcm expression in glia or hemocytes during a CNS related immune challenge in flies.

For my studies I used the two common systems for induced gene expression, Gal4/UAS and LexA/LexAop (**Figure 38**). The Gal4/UAS system is a binary expression system consisting of two main components: the yeast Gal4 transcriptional activator expressed in a specific pattern and a transgene under the control of a UAS promoter that is largely silent in the absence of Gal4 (Brand and Perrimon, 1993). The Gal4/UAS system can be used for cell- or tissue-specific genetic mutant rescue, gene overexpression, RNA interference screens and many other applications, and has been extensively used for developmental studies in tissues such as the CNS, retina and muscle (del Valle Rodriguez, Didiano, & Desplan, 2011). Additionally, the Gal4/UAS system is repressible by the Gal80 protein (Lue, Chasman, Buchman, & Kornberg,

1987). The Gal80 represses activation of Gal4 by acting specifically through the Gal4 activation domain (**Figure 38A**). It can be used to restrict transgene expression both spatially and temporally. For temporal control, one can use the temperature sensitive mutant Gal80, which is active at 18 °C but does not repress Gal4 at 29 °C or higher temperatures. The utility of the Gal4/UAS system spawned the generation of a second independent binary expression system for *Drosophila*, the LexA/LexAop system (Lai & Lee, 2006). The LexA (transcription factor) binds to and activates the LexA operator (LexAop, promoter) thus allowing the target gene expression (**Figure 38C**).

Gcm expression was traced by cell lineage analysis. Cell lineage analysis within tissues has contributed significantly to our understanding of the morphogenetic events that occur during the development of *Drosophila*. A vast repertoire of powerful genetic tools has been created for and utilized in such developmental analyses (Brand & Perrimon, 1993; Harrison & Perrimon, 1993; Kanca, Caussinus, Denes, Percival-Smith, & Affolter, 2014; Pignoni & Zipursky, 1997; Struhl & Basler, 1993; Worley, Setiawan, & Hariharan, 2013). One such tool is the g-trace system that allows gathering of spatial, temporal and genetic information about the origins of individual cells in *Drosophila melanogaster* (**Figure 38D**) (Evans et al., 2009).

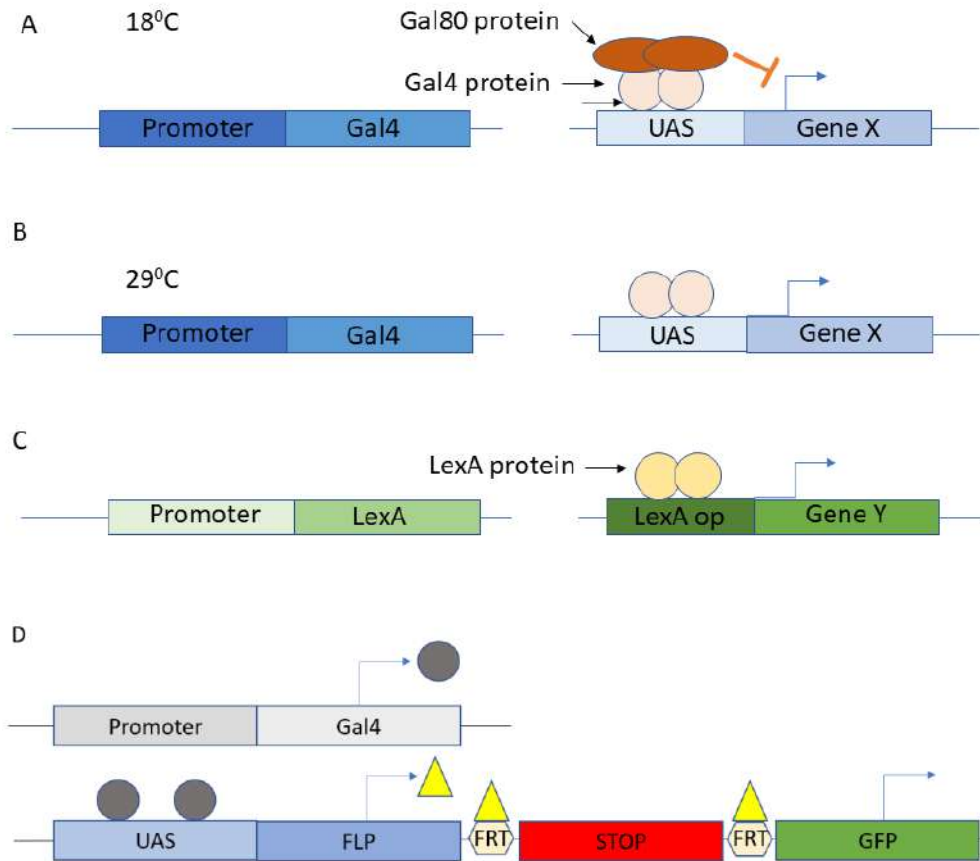


Figure 38. Combined UAS--Gal4 system. (A) The Gal80 protein blocks the Gal4 function at 18 °C and UAS-dependent gene transcription. (B) At 29 °C the Gal80 is unstable, and the Gal4-dependent transcription can occur. (C) The LexA op system allows a second independent binary expression system for *Drosophila*, (D) g-trace system for lineage tracing in *Drosophila*, Flippase (FLP) Flippase Recognition Target (FRT).

My main question was whether under different CNS related immune responses Gcm was going to be expressed in either glia or hemocytes in similar fashion to what was observed in the murine microglia. For this reason, I used not only the aging process as I did with mice, but also assays that result in PD like syndromes, such as α -Syn expression or PQ treatment.

Results

Gcm is not re-expressed in the aged brain of *Drosophila*

In mice mGcm2 is expressed in microglia cells starting by 12 months and the number of mGcm2 positive microglia increases overtime. In order to evaluate whether this is a conserved

mechanism, I labelled brains of flies at different time points (one, two and three weeks). Due to lack of *Drosophila* anti-Gcm antibodies as well as the short half-life of the protein, I used the Gal4/UAS system along with the g-trace. This combination allows to constantly have GFP expression in cells that expressed *Gcm* at any point. *Gcm* is expressed in primitive hemocytes and glia, so the g-trace would label all those cells as well. To overcome this obstacle, I used the temperature sensitive Gal80 protein. I crossed *gcmGal4,UASmcD8GFP,tubGal80* line with a g-trace and the crosses were kept at 18°C until the offspring were transferred to 29°C in order to silence the Gal80.

In homeostatic conditions, *Gcm* is expressed only in specific neurons of the adult fly CNS (**Figure 39**) in two clusters (dorsolateral and medial) per central brain hemisphere (Soustelle et al, 2007). I then labelled *Drosophila* CNS at different time points and used glia and neuron specific markers, Repo and Elav, respectively. The results showed that *Gcm* is only traced at the specific neuronal clusters that were already known. These data suggest that there is no expression of *Gcm* in the adult CNS of the fly under basal conditions.

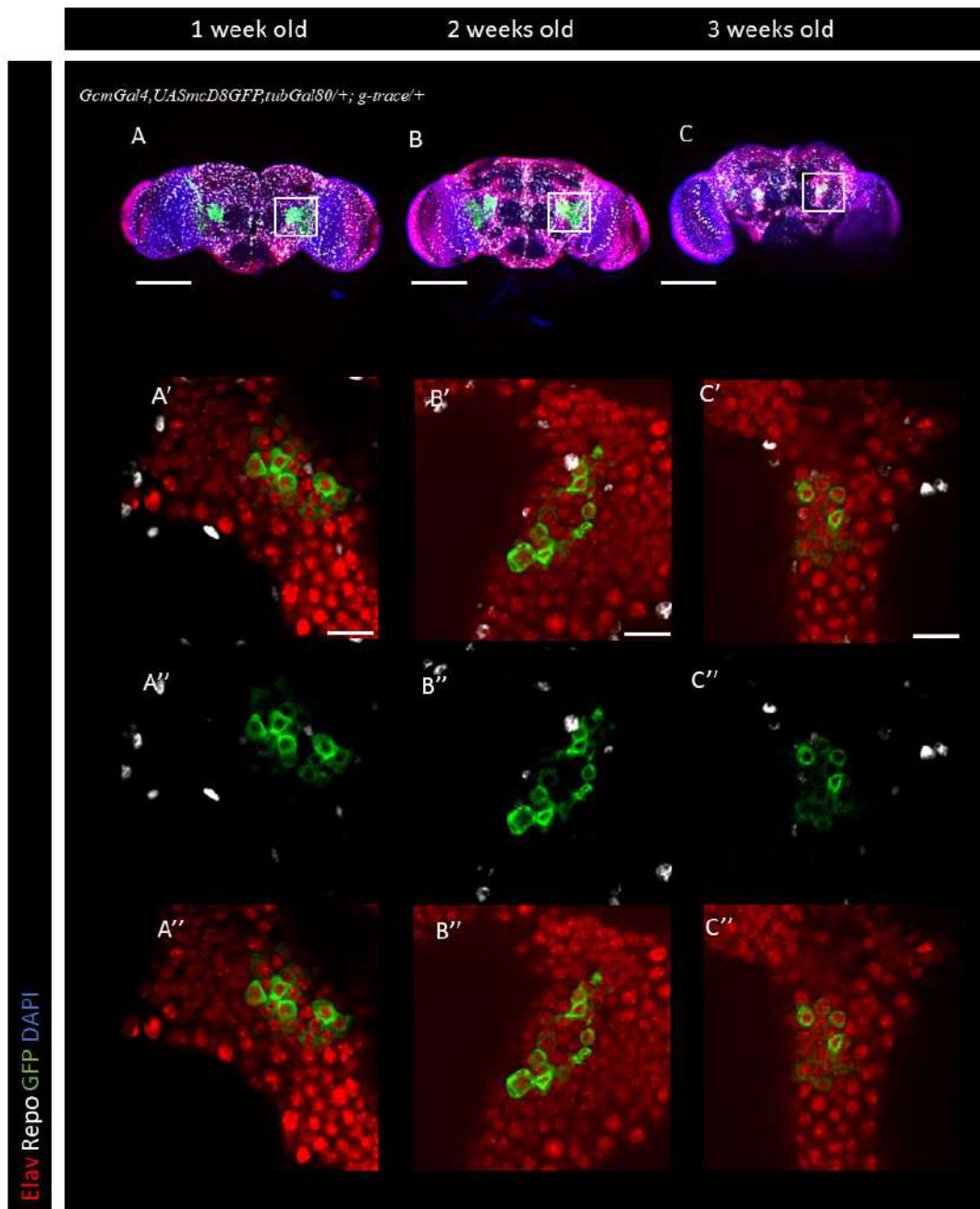


Figure 39. *Gcm* expression at different time points in the adult CNS of *Drosophila*. *Elav* in red indicates the neurons, *repo* in grey indicates the glia, GFP marks the cells that expressed *gcm* at some point during the adult stages. First pane (A,B,C): whole CNS brain at different time points, scale bar (100 μ m). Lower panels (A',B',C'): single section of the GFP positive areas, scale bar (10 μ m), N=3

Gcm is re-expressed in hemocytes upon α -Syn overexpression

Aging in *Drosophila* and mammals do not follow the same processes (Sun et al., 2013). I thought that an induced neuroinflammation assay could give more information. For this reason, I used the same line as before (*gcmGal4,UASmcD8GFP,tubGal80/+; g-trace/+*), combined with the LexA/LexAop system to induce α -Syn in neurons. This allowed me to express the LexAop- α -SynA30P, which is the mutant isoform of a-Syn, in all neurons upon using the nSyb LexA transgenic line (Sethi & Wang, 2017). The flies were kept at 18°C from embryos until pupae and then moved to 29°C for adult stages. Thus, the CNS were dissected at 10 and 20 days after enclosure and labelled with Repo and Elav (**Figure 40A, b and C**). In these conditions there are cells that express GFP and that are negative for both neuronal and glia markers. My next hypothesis was that these cells may be hemocytes since they are the innate immune cells of the fly, thus I labelled with a hemocyte marker (*peroxidasin, pxn*). The results showed that indeed the cells that express the GFP are also Pxn positive (**Figure 40D,E and F**). In contrast, control CNS from flies that do not express α -Syn do not show any GFP expression in hemocytes or other cells in the CNS, apart from the known neuronal clusters (**Figure 40 A and D**). These new data show the possible role of hemocytes during a PD like syndrome model in flies.

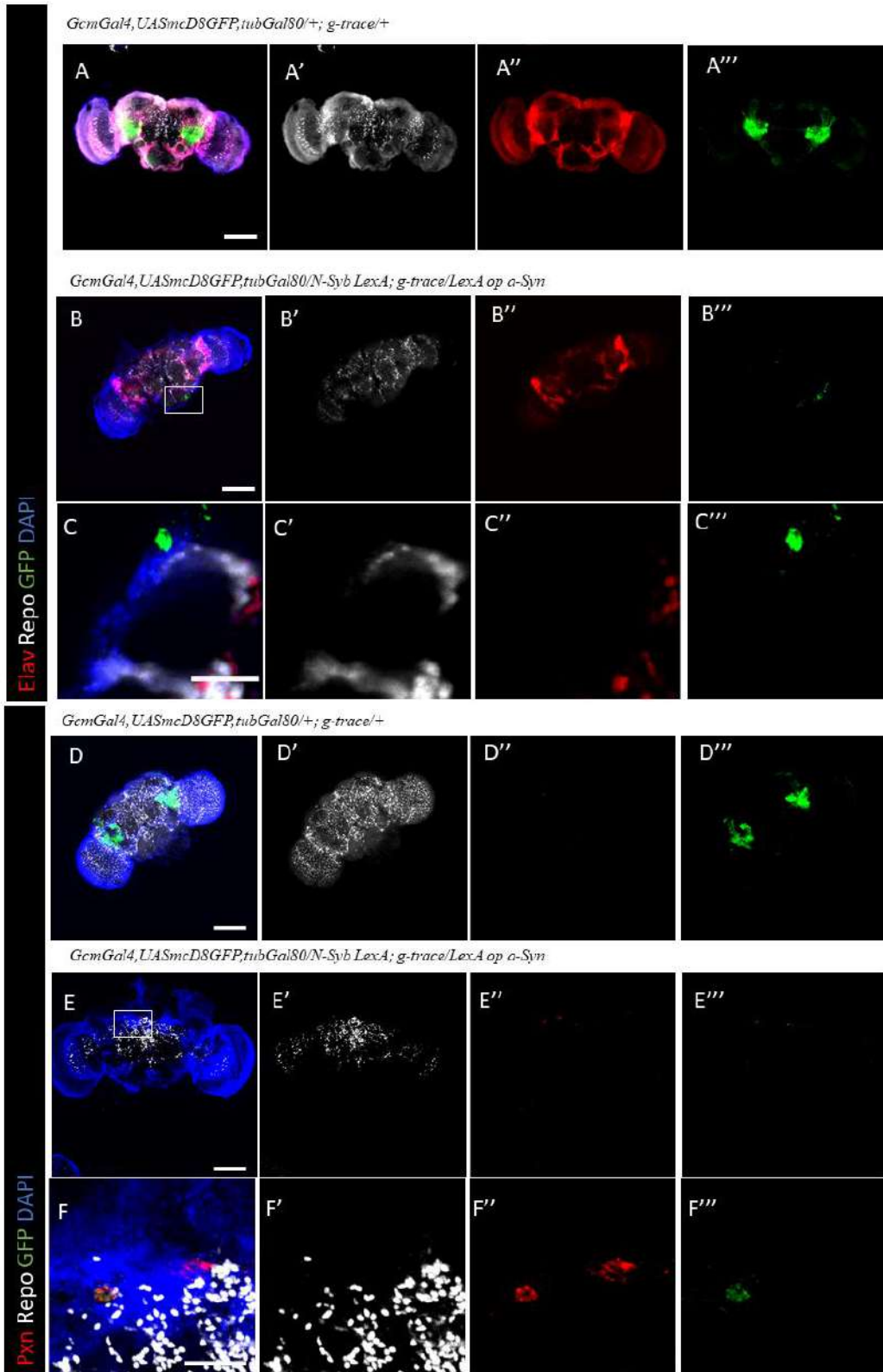


Figure 40. Gcm expression at different time points in adult CNS of *Drosophila* upon α -Syn expression. Repo in grey indicates the glia (A',B',C',D',E',F'), Elav in red indicates the neurons (A'',B'',C''), GFP marks the cells that expressed Gcm at some point during the adult stages (A''',B''',C''', D''',E''',F'''). (D'',E'',F'') Pxn in red indicates the hemocytes, repo in grey indicates the glia, GFP marks the cells that expressed Gcm at some point during the adult stages. Scale bar for full brain 100 μ m and for magnification 10 μ m, N=3

Hemocytes enter the *Drosophila* CNS upon paraquat exposure

Even though α -Syn expression showed very promising data, the penetration of the assay is not 100% effective since approximately 50% of the brains had hemocytes associated with the CNS. For this reason, I chose to explore stronger assays that could validate the above results. PQ is an easy and acute assay that has been extensively used to produce a PD model in *Drosophila* (Maitra et al. 2019). PQ assays have multiple advantages compared to the α -Syn. First of all, I did not need to build strains which is time consuming. Furthermore, it takes 10 or 20 days to see hemocytes associated with the brain upon α -Syn expression while with PQ this takes less time (approximately 24 to 36 hours).

WT (Oregon R) adult males at 4 days after enclosure were starved for 3 hours, and then exposed to 20mM of PQ for 12h. Brains from 12, 24 and 36 hours after exposure were labelled with hemocyte markers (P1/Hemese) (**Figure 41A**). The results showed that there are hemocytes associated with the brain after 12 hours of PQ exposure (**Figure 41B**). By 36 hours, the hemocytes have penetrated the BBB and they are inside the brain (**Figure 41C**). These results suggest that the hemocytes participate in the response due to the PQ.

The next step will be to combine this assay along with the Gcm g-trace in order to see if in these conditions the expression of the Gcm transcription factor is induced with the PQ treatment. Finally, in contrast to the α -Syn assay, PQ exposure has more homogeneous effects, as all the brains at 36 hours have at least a few hemocytes that had penetrated the CNS, thus proving the robustness of the PQ assay compares to the α -Syn expression.

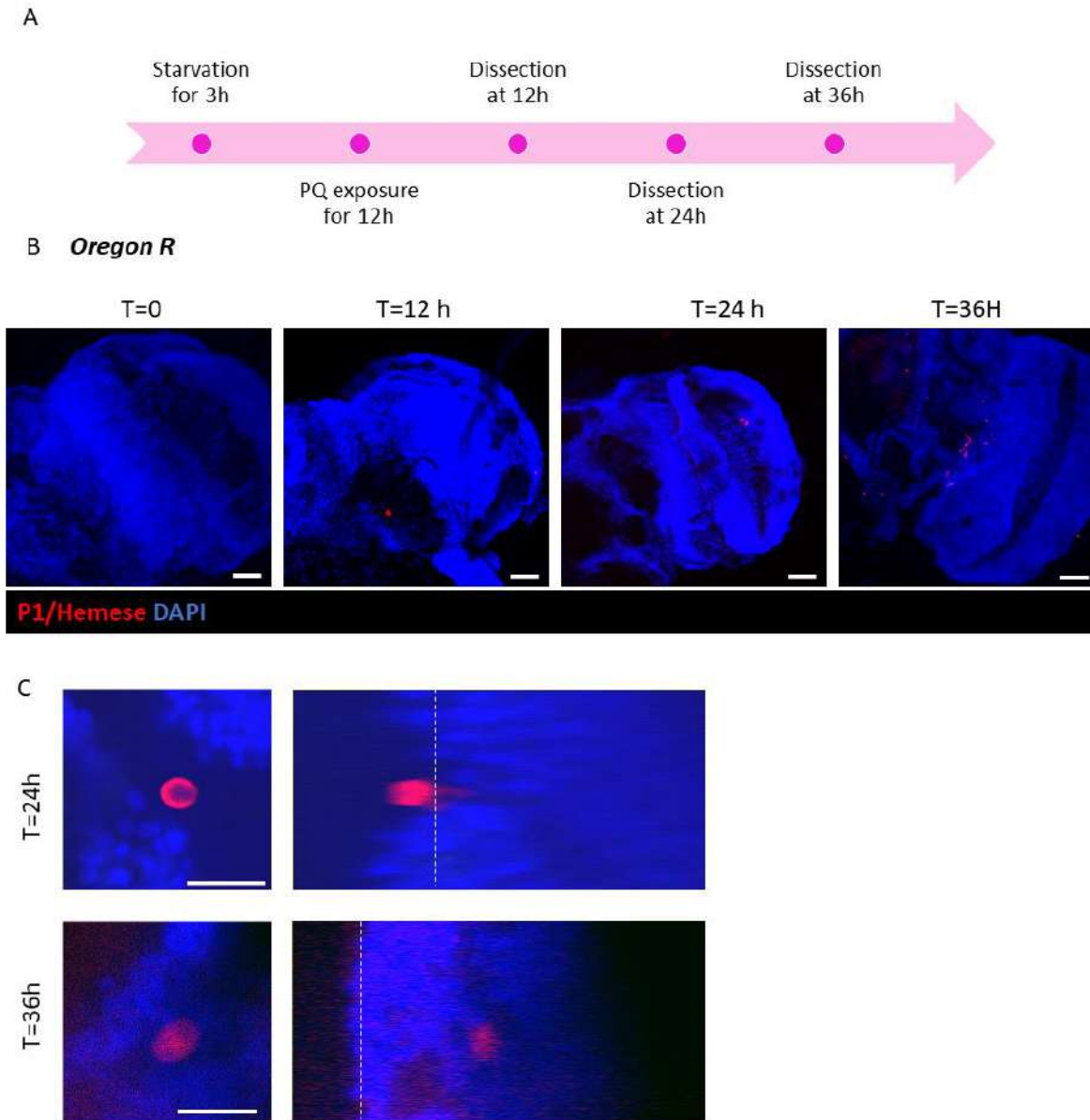


Figure 41. PQ treatment in *Drosophila* adults. (A) PQ treatment stages and dissection points (B) Brain of adult flies at different stages after the PQ treatment, P1/Hemese in red indicate the hemocytes. Scale bar 30 μ m. (C) Orthogonal view of hemocytes associated with the CNS at different time points (24 and 36 hours). Dotted lines indicate the brain surface. Scale bar 20 μ m N=3

Discussion

My results so far showed that mGcm2 in microglia modulates neuroinflammation caused by aging. My next goal was to transpose this model in flies thus, providing new data for an evolutionary conserved cascade. I studied the expression profile of Gcm in the fly CNS during aging. The results showed no Gcm positive cells apart from the known Gcm positive neurons. *Drosophila melanogaster* is a widely used model organism that has distinct advantages in aging research. But most aging studies in flies concentrate in basic metabolic and reproductive outputs rather than CNS related changes (Sun et al., 2013). Normal aging in flies is not the same as in mammals as the short life span of this model may not result in the same biological processes. This may be why I did not find any Gcm expression in the aged brain of the *Drosophila* CNS.

Consequently, I tried to induce inflammation in the CNS of flies with two different models. First, I expressed α -Syn in the neurons of *Drosophila* which has proven to simulate PD like symptoms. Then, I studied whether there is Gcm expression during the course of the disease. Surprisingly, the results showed that not only there is expression of Gcm but also that this expression is found in hemocytes that are closely associated with the brain. Although neuroinflammation in fly has been extensively studied, the role of hemocytes has not been explored at all. With the advances of technology such as scRNA seq we now have the possibility to characterise all the cell types. For example, a recent single cell RNA seq study showed that upon PQ treatment hemocyte specific genes are upregulated in the CNS (Maitra et al. 2019). This led me to establish a PQ assay. This assay showed that indeed there are hemocytes associated with the brain after 24h of exposure and that they can penetrate the BBB and enter the CNS after 36h. In the future, I am going to validate whether Gcm is expressed upon PQ treatment, as in the case of α -Syn.

Chapter V

Characterisation of Shot in the immune cells of *Drosophila melanogaster*

During my thesis, I also contributed to a team effort aiming at discovering the heterogeneity of hemocytes by single cell RNA seq (Cattenoz et al., 2020). This project highlighted the *short stop* gene (*shot*) as being expressed in a specific subtype of immune cells in *Drosophila*. Shot is a member of the spectraplakins family of large cytoskeletal linker molecules. It binds both actin and microtubules, as well as scaffold proteins, certain signalling factors and calcium. It plays developmental and maintenance roles in multiple tissues. Our data show that Shot is expressed in hemocytes, and its expression is increased upon wasp infestation in lamellocytes. Since Shot binds to the cytoskeleton, I hypothesised that this protein is important for the adhesion and the formation of cell-cell junctions upon wasp infestation that will allow the wasp egg encapsulation. My aim was to characterise the role of Shot in hemocytes during both normal and infested conditions. The results revealed that Shot plays an important role in the adhesion of hemocytes under normal conditions *in vitro*. Furthermore, Shot mutants have reduced expression of other cytoskeleton related proteins (DN-Cadherin) and, upon infestation shot KD hemocytes present impaired encapsulation properties *in vivo*. Thus, my work showed for the first time the role of Shot in hemocytes of *Drosophila*.

Introduction

A recent study from our lab characterised the different hemocyte populations by scRNA seq in basal and challenged conditions (Cattenoz et al., 2020). Infestation was done by the parasitic wasp *Leptopilina bouvardi*, one of the most studied pathways linked to cellular immunity. The wasp lays eggs in the *Drosophila* larva and triggers hemocyte proliferation as well as lamellocyte differentiation (Honti et al., 2009), with subsequent encapsulation of the wasp egg and its death through the increased levels of ROS (Anderl et al., 2016). The results revealed that Shot is expressed in the cells of the immune system (**Figure 42**). However, upon infestation its expression is increased. The role of this project was to evaluate the possible role of Shot in hemocytes under normal and challenged conditions.

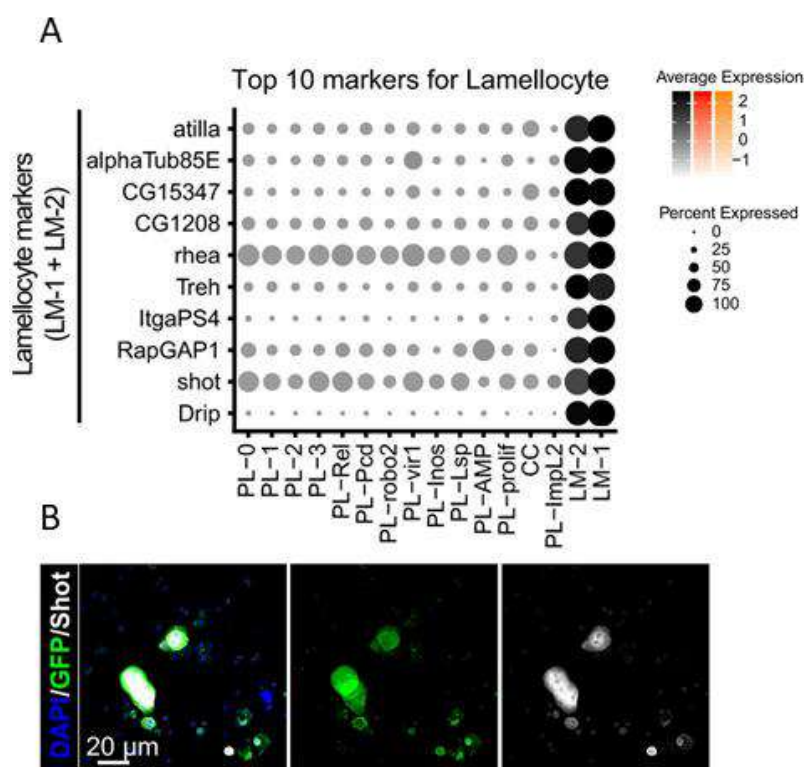


Figure 42. (A) Dotplot from single cell RNA seq. The x-axis shows the clusters of hemocytes and the y-axis the expression of lamellocyte associated genes. Expression levels (gradient of colour) and the percentage of cells (size of the dots) for the top 10 markers of lamellocytes. (B) Hemocytes from WL OregonR infested by wasp, Shot (in gray, lower panels). Phalloidin-FITC (in green) labels the actin filament particularly abundant in lamellocytes (Tokusumi et al, 2009), and the nuclei were marked with DAPI (blue) (processed from Cattenoz et al., 2020).

The cytoskeleton is comprised of actin, intermediate filaments and microtubules and is essential for most cellular processes. These include cell division, shape, dynamics, intracellular transport, membrane dynamics, organelle function and adhesion (Voelzmann et al., 2017). Spectraplakins are one of the most complex protein families of cytoskeletal regulators that are conserved throughout evolution from VAB-10 in the worm *Caenorhabditis* and Short Stop (Shot) or Kakapo in *Drosophila* to Dystonin and Microtubule-Actin Crosslinking Factor 1 (MACF1) in vertebrates.

Spectraplakins encode seven functional domains that can interact with other cytoskeletal molecules (**Figure 43**). The domains include an actin-binding domain (ABD), a plakin domain (PD), a plakin repeat region (PRR), a spectrin repeat rod (SRR), two EF-hand motifs (EFH), a Gas-related domain (GRD) and a C-tail (Hahn, Ronshaugen, Sanchez-Soriano, & Prokop, 2016). Through this interaction they can establish numerous structural or regulatory links between cytoskeleton components, or cytoskeleton-molecules or cytoskeleton- cell compartments (Roper, Gregory, & Brown, 2002). Spectraplakins are divided into three different categories: the plakins, the spectrins and the Gas2-like proteins. The plakins are mostly cytoskeleton- associated scaffold proteins that maintain tissues under mechanical stress primarily at cell junctions (Sonnenberg & Liem, 2007). The spectrins are responsible for link formation between proteins of the cell cortex and the Gas2-like proteins are responsible for the link formation of microtubules, F-actin and end binding proteins (EB) during cell division and development (Broderick & Winder, 2005; Gamper et al., 2016; Machnicka et al., 2014; Sharaby et al., 2014; Stroud, Banerjee, Veevers, & Chen, 2014).

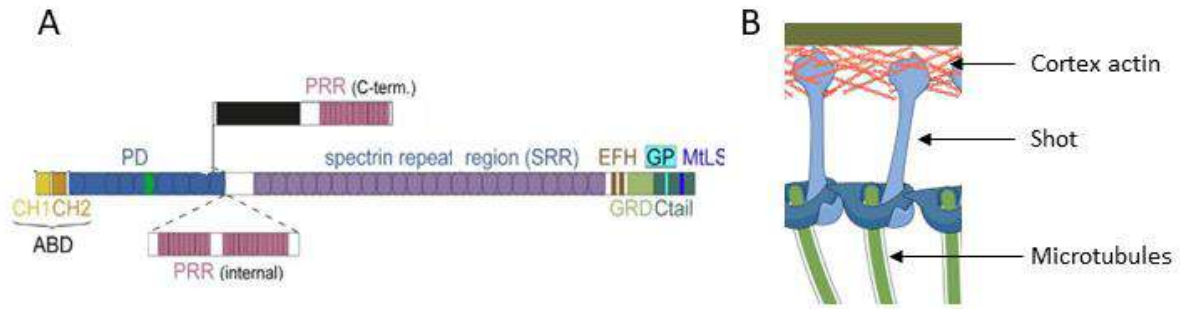


Figure 43. (A) Functional domains of spectraplakins. Actin-binding domain (ABD), a plakin domain (PD), a plakin repeat region (PRR), a spectrin repeat rod (SRR), EF-hand motifs (EFH), a Gas-related domain (GRD) and a C-tail (modified from Voelzmann et al., 2017). (B) Representation of Shot connecting cortex actin with microtubules (modified from (Nashchekin, Fernandes, & St Johnston, 2016))

Since spectraplakins are essential for fundamental functions of the cell, they have been linked to a variety of disorders and conditions. In humans, they have been implicated with Parkinson's disease, neuro-developmental disorders, skin blistering and different forms of cancer (Aumailley, Has, Tunggal, & Bruckner-Tuderman, 2006; Elliott, Kim, Gorissen, Halliday, & Kwok, 2012; Giorda et al., 2004; Groves et al., 2010; Kunzli, Favre, Chofflon, & Borradori, 2016; L. Liu et al., 2012; Shimbo et al., 2010; J. B. Vincent et al., 2008). Furthermore, mice lacking Dystonin functions show glia, Schwann cell and neuromuscular junction defects (Bernier, De Repentigny, Mathieu, David, & Kothary, 1998; Boyer, Bernstein, & Boudreau-Lariviere, 2010; Dalpe et al., 1999; Laffitte et al., 2005; Saulnier, De Repentigny, Yong, & Kothary, 2002).

Due to the complexity of the functions behind the spectraplakins proteins, simple model organisms such as *Drosophila* consist ideal models to dissect their basic mechanism. This invertebrate model organism has a long and important history of pioneering fundamental concepts and delivering understanding of molecular and biological functions, which can then be used as facilitating or instructive paradigms for related studies in higher organisms including humans.

The S2 cell line is believed to be derived from blood cells that contain acentrosomal microtubule (MT) arrays and actin-rich lamellipodia, but they display poor integrin expression accompanied by lack of focal adhesion and stress fibres, weak extracellular matrix adhesion and low motility in the culture dish (Lammel et al., 2014; Nye, Buster, & Rogers, 2014). Shot functions in S2 cells favour its localisation to the MT plus end, mediated by binding of the Ctail's MtLS motifs to the EB1protein (Applewhite, Grode, Duncan, & Rogers, 2013; Applewhite et al., 2010; Slep et al., 2005). This localisation is made possible through an auto-inhibitory "closed conformation" so that Shot becomes an actin-MT linker that can regulate MT behaviours at the cell edge. Thus, Shot already provides a useful paradigm for the mechanisms involving EB1-dependent MT guidance along actin networks, but its full potential to provide insights into spectraplakin functions during adhesion has by far not been reached; its studies can be easily extended to powerful *in vivo* models (e.g. hemocyte adhesion) (Montell, 2003; Wood & Jacinto, 2007). The aim of my project was to determine the role of Shot in hemocytes during both homeostatic and challenged conditions.

Results

Evaluation of the transgenic lines of Shot

I first evaluated the efficiency of my strains for both the *UASShotGFP* Gain of Function (GOF) or the *UASShotRNAi* Loss of Function (LOF). I used the hemocyte specific driver *HmlΔGal4* that I crossed with either the Shot GOF or the Shot LOF strains. Then, 3rd phase wandering larvae (WL3) were evaluated for the expression of Shot and other immune related genes in basal conditions in order to confirm that none of the conditions would initiate an immune response (**Figure 44A**). Among the genes tested by qPCR, I evaluated the levels of the cytokines *upd2* and *upd3*, the suppressor of cytokine signalling (SOCS) and protein-tyrosine phosphatase (*ptp*). The qPCR also confirmed that the Shot GOF leads to increased mRNA levels of Shot, while the Shot LOF leads to decreased expression compared to the *UASshotRNAi/+* control (**Figure 44A**). Furthermore, I used hemocytes from the same stage in order to label for Shot and thus evaluate protein expression (**Figure 44D**). The Shot GOF cells have an increased level of the protein while the Shot LOF cells have decreased expression (**Figure 44E**). Other than that, the hemocytes did not present any difference concerning their population number (**Figure 44B and C**). Interestingly, the Shot LOF cells present a different cytoplasm compartmentalisation when I used a double hemocyte driver with an endogenous GFP (*w*; *HmlΔGal4*; *pxnGal4UASGFP*) (**Figure 44F and G**). This driver combines to different hemocyte markers, the Hml and the Pxn. Our sc-RNA seq data showed that 75% of hemocytes express Hml and the other 25% is Pxn positive. Thus, the double driver provides a stronger system.

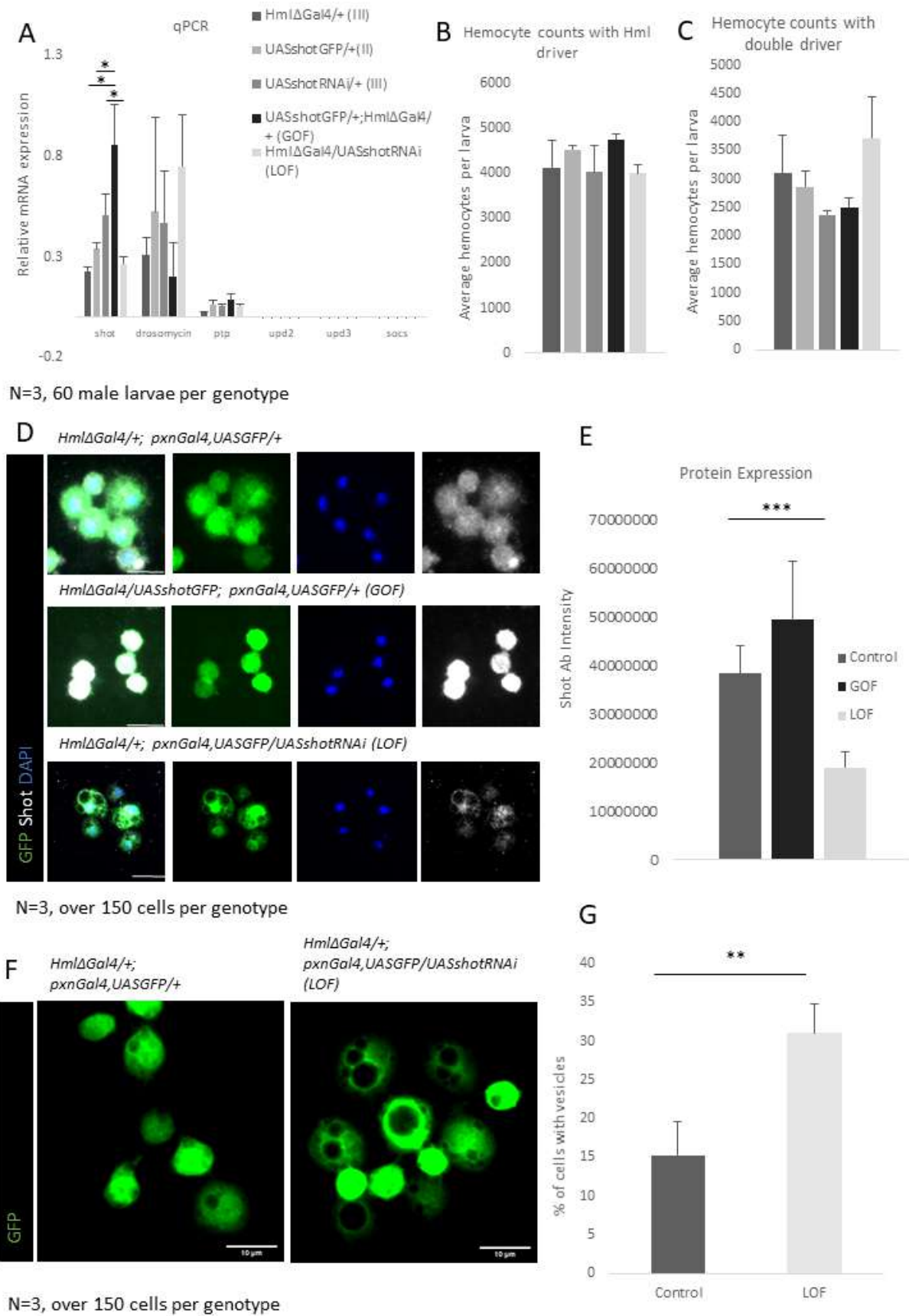
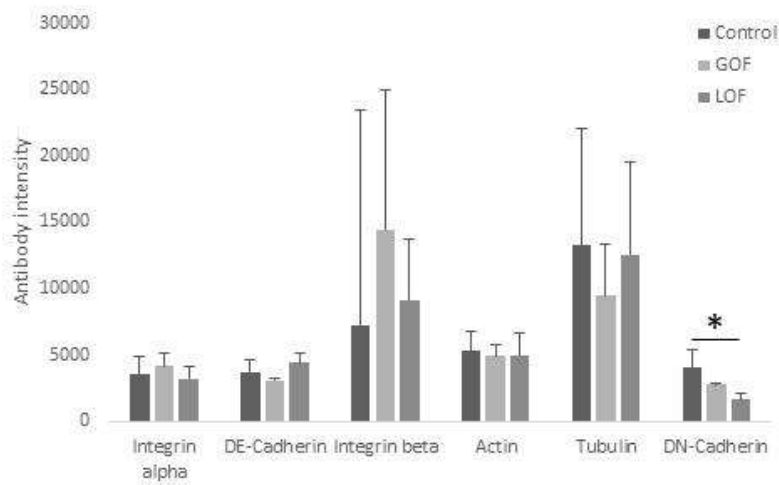
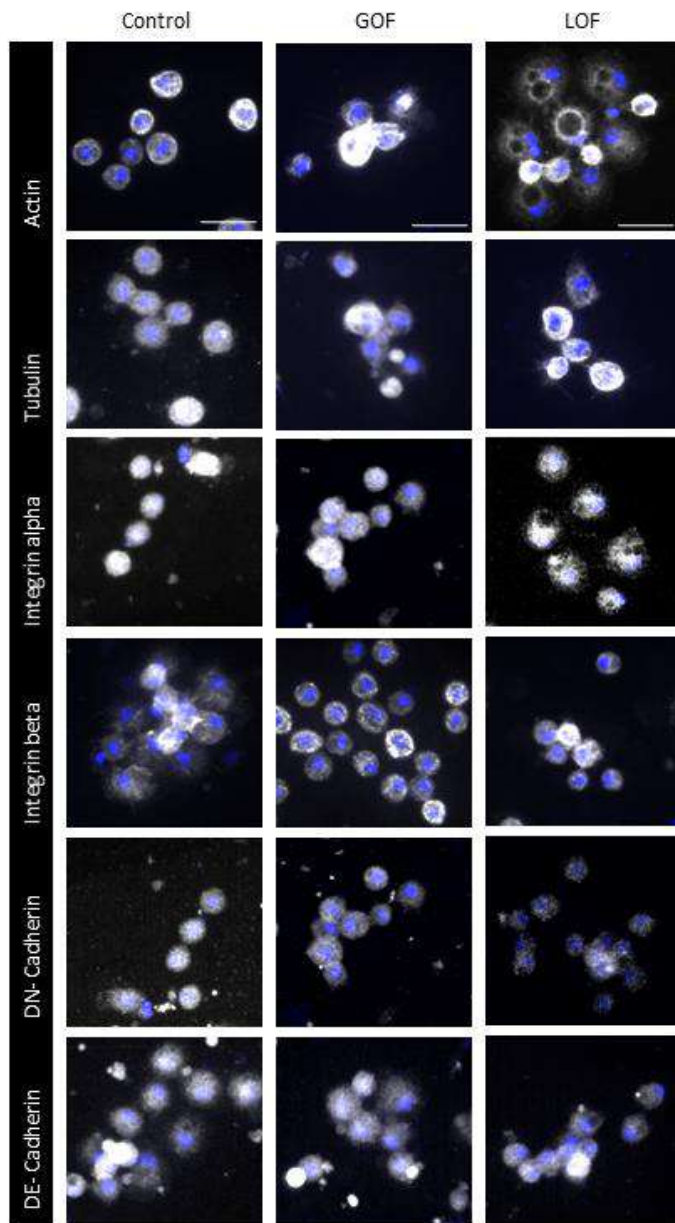


Figure 44. (A) qPCR results from L3 hemocytes in homeostatic conditions. p-value between *HmlΔGal4/+* and *HmlΔGal4/+;UASshotGFP* (GOF) is 0.029 and between *UASshotGFP/+* and *HmlΔGal4/+;UASshotGFP* (GOF)

is 0.041. Hemocyte counting in Shot GOF and Shot LOF animals using the (B) *HmlΔGal4* driver or (C) the *HmlΔGal4/+;pxnGal4UASGFP*, double driver. (D) Protein expression in Shot GOF and Shot LOF animals, scale bar 10um. (E) Quantification of Shot protein expression in Shot GOF and Shot LOF. (F) Cytoplasm compartmentalisation difference in LOF hemocytes and (G) Quantification of the percentage of vesicles in the hemocytes.

Shot is one of the major cytoskeleton proteins and interacts with other similar proteins. In order to study whether the differential expression of Shot would result in differences in other cytoskeleton proteins, I evaluated actin, tubulin, integrin alpha and beta, DN- and DE- cadherin protein expression by immunolabelling. The results revealed that the levels of DN- cadherin are decreased in Shot LOF hemocytes compared to the control (**Figure 45**). However, the protein expression levels of the Shot GOF are not statistically increased compared to the control (**Figure 44E**). This could mean that the Shot GOF strain is not as potent as it should be. Other than that, no other protein seems to be differentially expressed. Notably, the cytoplasm organisation with the large vesicles is visible with actin and integrin alpha but not with the others (**Figure 45A and C**). This means that these vesicles are not empty space, but some proteins are differently organised inside the hemocytes.



10um.

Figure 45. Labelling of control, GOF and LOF Shot hemocytes for the cytoskeletal markers actin, tubulin, integrin alpha or beta, and DN- or DE- Cadherin. (B) Quantification of the fluorescence intensity of the cytoskeletal markers. p-value for DN-Cadherin between control and LOF 0.039 N=3, 50 cells per trial scale bar

Even though Shot GOF or Shot LOF hemocytes do not show any differences, I decided to study the effects of the strains during functional assays. This assay was inspired mostly from the mammalian orthologue of Shot, Dystonin. Dystonin is required for myoblast and keratinocyte migration through mechanisms that are unclear but seem to involve adhesion control (Hamill, Hopkinson, DeBiase, & Jones, 2009; Michael et al., 2014; Poliakova et al., 2014). Hence, I evaluated the adhesion capacity of the hemocytes in both Shot LOF and Shot GOF *in vitro* based on already known protocols (Moreira, Jacinto, & Prag, 2013). For this I used hemocytes from WL3 that were left to attach for 1 hour on coverslips (**Figure 46**). Then I counted the number of cytoplasmic extensions per cell. The more cytoplasmic extensions the greater the adhesive capacity of the cells is. Interestingly, the results revealed that all controls had approximately 2 extensions per cell. In contrast, the Shot GOF hemocytes have an average of 5 extensions per cell and the Shot LOF have 1 extension only. Thus, Shot has an important role in the adhesion of hemocytes *in vitro*.

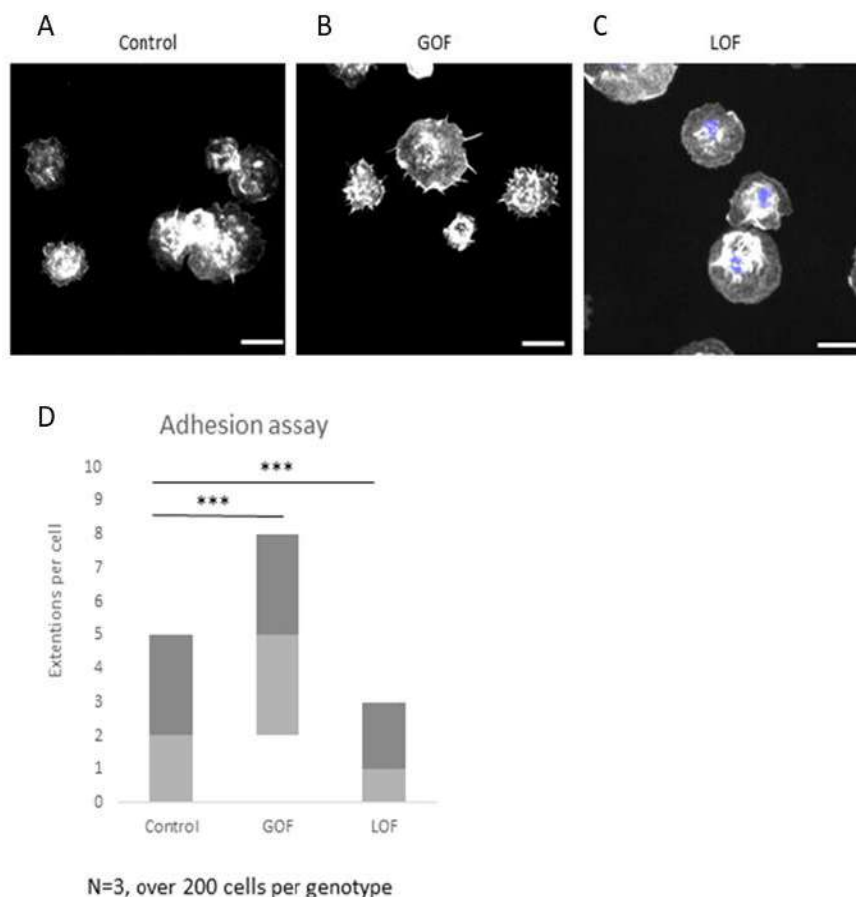


Figure 46. Adhesion assay for LOF and GOF of Shot in hemocytes (A,B,C). The hemocytes were labelled with phalloidin (grey) and the extensions were counted for each cells. (D) Extension quantification. ANOVA p-value 6.36E-34, the p-value between control and GOF is 2.12E-12 and between control and LOF is 0.00066, N=3, 50 cells per trial scale bar 10um.

Shot actively participates during the encapsulation of wasp eggs

Finally, I evaluated the role of hemocytes upon challenge. For these experiments, I used wasps to infest L2 larvae and then I assessed the rate of fly survival. Infestation was done with the parasitic wasp *Leptopilina boulardi*. The wasp lays eggs in the *Drosophila* larva and triggers an immune response (Markus et al., 2009), which ultimately leads to the wasp egg encapsulation. Being much larger than the plasmatocytes, the wasp egg cannot be phagocytosed. Instead, hemocytes (plasmatocytes, crystal cells and lamellocytes) cooperate and physically surround and encapsulate the egg. This encapsulation reaction involves hemocyte division and differentiation. This reaction is relatively slow, and capsules are not observed until 1–2 days after infection. I monitored wasp eggs after 24 hours of infestation before the melanisation of the egg, which alters the efficiency of the immunolabelling (**Figure 47**). I then assessed the area of lamellocytes surrounding the egg with the Imaris image analysis software. For the encapsulation, I calculated the area of lamellocytes covering the wasp egg using the surface tool. Then I calculated the surface of the wasp (Dapi) and created the ratio of lamellocyte area/wasp egg area. The results showed that Shot LOF animals display statistically significant reduced encapsulation ratio compared to the control animals. However, there was no statistically significant difference between the Shot GOF and the control. Thus, Shot participates in the encapsulation process of the wasp egg.

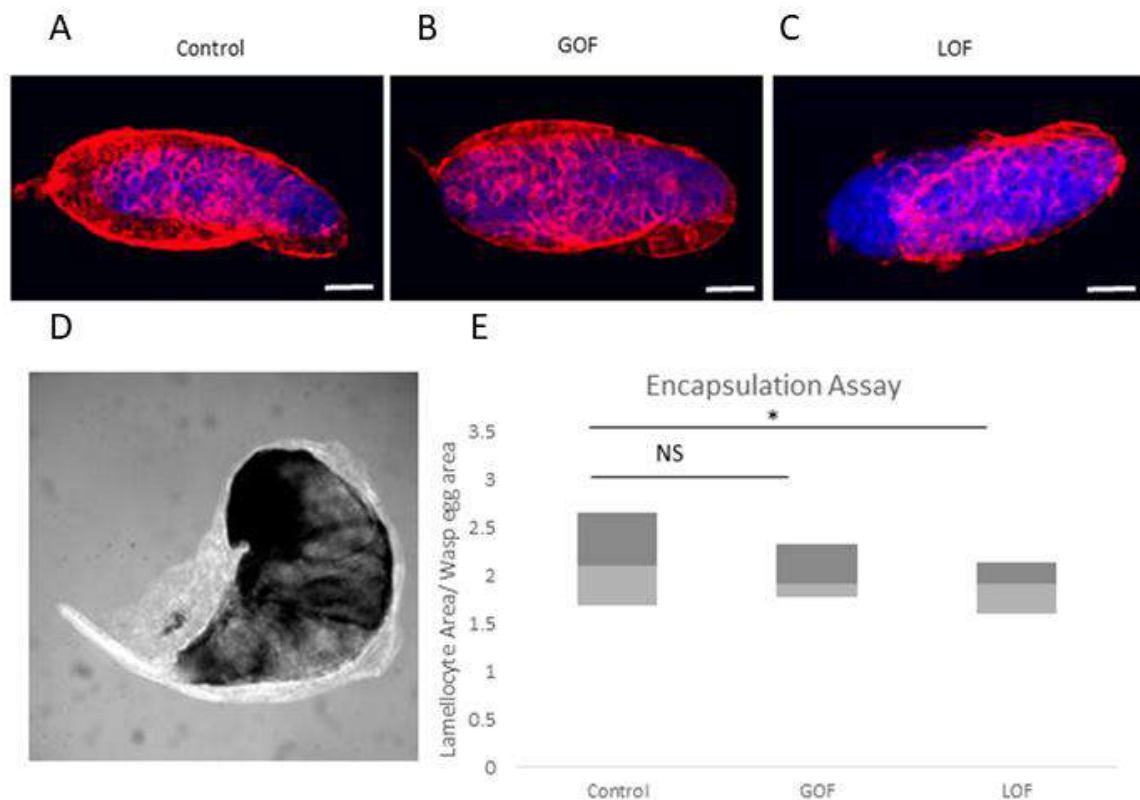


Figure 47. (A,B,C) Encapsulation assay for Shot LOF and Shot GOF of Shot in hemocytes. The hemocytes were labelled with phalloidin (red) and Dapi. (D) Brightfield image of a wasp egg melanised by lamellocytes (E) Quantification of the encapsulation rate. ANOVA p-value 0.117, the p-value between control and LOF is 0.021, N=3, more than 20 eggs per genotype, scale bar 50um.

Discussion

Shot is a cytoskeletal protein that has been extensively studied in *Drosophila* as it participates in major functions during both development and homeostasis. Recent data from our lab showed that Shot is expressed in hemocytes and that its expression increased in lamellocytes upon wasp infestation. My aim was to characterise the role of Shot in hemocytes both during basal and infested conditions.

I found that in basal conditions Shot participates in the adhesion of the hemocytes. Shot actively participates in the formation of the cytoplasmic extensions in hemocytes. Studies have already shown that Shot acts along with EB-1, where the former acts as an actin-MT linker that

regulates MT behaviours at the cell edge (Applewhite et al., 2013; Applewhite et al., 2010). Nevertheless, more experiments are required in order to study the effect of Shot *in vivo*. For example, expression of either the RNAi or overexpression of Shot along with an endogenous hemocyte marker could reveal differences in the homing of hemocytes where adhesion plays a pivotal role. Hemocytes in larva that reside in the sessile pockets are characterised as resident hemocytes. Homing assays disturb the sessile pockets with gentle brushing, thus making the hemocytes enter the circulation. Upon that, the time that it takes for the hemocytes to enter the circulation is counted. Since Shot participates in the formation of the extension *in vitro*, I hypothesise that the time to reform the sessile pockets will be increased in the Shot LOF and decreased in the Shot GOF. To test this hypothesis, I will use the double driver Shot LOF and Shot GOF. This strain expresses GFP fluorescence in hemocytes, thus allowing live tracing of hemocytes *in vivo*. This simple but very informative assay will let me know whether the phenotype that I observed *in vitro* of less adhesive hemocytes in the case of the Shot LOF is also going to be observed *in vivo*.

Finally, I characterised the role of Shot upon wasp infestation. Shot has been shown to participate in the formation of cell junctions. In the absence of Shot, the formation and anchorage of the basal MT arrays is defective, so that tendon cells fail to resist muscle contractions and their basal junctions get torn away (Alves-Silva et al., 2008; Bottenberg et al., 2009; Prokop, Martin-Bermudo, Bate, & Brown, 1998; Subramanian et al., 2003). Cell junctions are important for the formation of the capsule during infestation in order to insure the encapsulation of the wasp embryo. The results showed that Shot LOF has a decreased encapsulation 24 hours after infestation. Since, the LOF did not impact the survival of the larvae it seems that one or more cytoskeletal proteins are participating in the process. For example, during our scRNA seq analysis we also found that Talin is also increased in lamellocytes. Talin or Rhea is a large adaptor protein that is essential for all adhesive functions

of integrins. Thus, multiple mutations of different genes could present a stronger phenotype. It would be extremely interesting to combine Shot and Talin mutants and observe whether there is an additive effect on the adhesion of hemocytes and lamellocytes in homeostatic and challenged conditions respectively.

Discussion and Perspectives

Microglia, the innate immune cells of the CNS, play pivotal roles during development, homeostasis and inflammation (Ginhoux et al., 2010; Hoeffel & Ginhoux, 2015; Q. Li & Barres, 2018; Perdiguero et al., 2015). These cells derive directly from the first hematopoietic wave and colonise the brain during the early stages of the embryogenesis (Ginhoux et al., 2010). Microglia are not replaced by other monocyte derived macrophages as they are a self-renewing population, and they are linked with all known pathologies of the CNS such as MS. Thus, it is important to better understand the role of these cells during homeostatic and challenged conditions. Reprogramming microglia in order to influence the course of the disease has already been implemented with microglia cells during PD (H. Liu et al., 2020), indicating that this represents a new option to design more specific therapeutical targets.

One possible way to reprogram these cells is through the regulation of the transcription factors expressed in microglia because these factors can regulate the expression of multiple genes at the same time. Gcm is a transcription factor that has been extensively studied in *Drosophila melanogaster* (Vincent et al., 1996; Bazzi et al., 2018). More specifically, in the fly Gcm is expressed in the macrophages from the first hematopoietic wave where it has an anti-inflammatory role. During my PhD I, studied the expression profile of the murine orthologue, mGcm2, in macrophages of the primitive wave, and more specifically microglia.

Here are my main findings on the evolutionary conservation of the Gcm pathway in the immune system:

- mGcm2 is expressed at different stages during the murine life, both during development and in adults.
- Lack of mGcm2 from microglia cells leads to an increased pro-inflammatory state during aging.
- This mechanism is conserved throughout evolution in a PD-like model in flies.

During my PhD, I also contributed to two studies of our group that led me to start my own project concerning the role the spectraplakins protein *Shot* in the hemocytes of *Drosophila* under normal and challenged conditions.

mGcm2 is expressed in microglia and regulates their activated state

My data showed that mGcm2 is expressed in different stages during the murine life. mGcm2 is first expressed at E7.5 in the yolk sac, in cells that express CD45 at low levels. This could suggest a regulation of mGcm2 in the development of primitive macrophages that resembles the development of hemocytes at early developmental stages in *Drosophila*. It will be interesting to perform immunolabelling with additional markers in order to define those cells and whether or not they are microglia progenitors with CSF1R, one of the first microglia markers at E7.5 (Ginhoux & Guilliams, 2016; Hoeffel et al., 2015; Hoeffel & Ginhoux, 2015). Another interesting marker would be c-Kit1, that labels EMPs and can show whether or not these cells are hematopoietic progenitors (Kierdorf et al., 2013). The results will indicate if these mGcm2 positive cells are microglia progenitors or if they represent other hematopoietic progenitors. Hence, these experiments could lead to a new perspectives into the molecular mechanisms of cell differentiation of the primitive hematopoietic wave.

Next, I showed that the absence of mGcm2 leads to a characteristic pro-inflammatory morphology and an increased number of iNOs positive microglia in cko 24 month old mice compared to controls. To further evaluate the inflammatory state of microglia in both genotypes, I will use microglia specific markers for inflammation. TREM2, ApoE, P2RY12, TMEM119, and MHC II could be potential candidates. TREM2 controls the phagocytosis of apoptotic neurons (Piccio et al., 2007; Takahashi, Prinz, Stagi, Chechneva, & Neumann, 2007; Yuan et al., 2016). ApoE potently induces phenotypic changes in disease-associated microglia and is upregulated during inflammation (Krasemann et al., 2017). Another large study utilizing single-cell RNA-seq to identify unique microglia subpopulations found increased ApoE and TREM2 expression in disease-associated microglia. At the same time, the same microglia subpopulations exhibited decreased expression of homeostatic gene P2RY12 (Keren-Shaul et al., 2017). Furthermore, both TMEM119 and P2RY12 labelling is reduced in active white matter lesions (WMLs) of MS patients compared to normal-appearing white matter. This indicates either a decrease in microglia presence in the WML or regulation of the microglia markers by the local inflammatory environment (Beaino et al., 2017; Zrzavy et al., 2017). So, homeostatic microglia have high TMEM119 and P2RY12 expression, while reactive microglia should have high expression of ApoE and TREM2. Finally, TREM2 and TMEM119 have also been found to have the same expression pattern during aging (Bonham, Sirkis, & Yokoyama, 2019; Norden, Muccigrosso, & Godbout, 2015; Ruan et al., 2020). The vast majority of studies of aging-related immunophenotypic changes in microglia have demonstrated a steady increase in the expression of markers usually found to be upregulated on activated microglia after acute CNS injuries. Most notable is an aging-related increase in microglia expression of MHC II antigens (Norden and Godbout 2014). Because expression of MHC II antigens seems to steadily increase on existing microglia cells as the brain ages, one should therefore consider the possibility that MHC II expression is a marker of cell maturation or cell senescence in

addition to being an activation marker. These experiments will validate the anti-inflammatory properties of mGcm2, as cko microglia should have increased microglia specific pro-inflammatory markers such as MHC II.

Characterisation of astrocytes, oligodendrocytes and neurons in the cko and control animals

My PhD focused on the effect of mGcm2 in microglia. However, microglia communicate and respond to other cell types in the CNS, three major ones being astrocytes and oligodendrocytes. All these cell types are responsible for maintaining homeostasis and actively participate to inflammation.

Similar to microglia, astrocytes can adopt pro- or anti-inflammatory states, named A1 or A2 state respectively. Neuroinflammatory diseases, such as MS, include activation of both microglia and astrocytes, as these two cell types become reactive in concert. Furthermore, microglia can potentially activate the pro-inflammatory A1 state of astrocytes (Liddelow & Barres, 2017). In response, A1 astrocytes upregulate Glia fibrillary acidic protein (GFAP) production, which is a widely used marker for activated astrocytes. Oligodendrocytes are important for ensheathing axons with their myelin sheath, which is destroyed in neuroinflammatory diseases such as MS. Mature Oligodendroglia cells express (NG2 and PDGFR) at the oligodendrocyte progenitor (OPC) stage and CC1 at the differentiated oligodendrocyte stage, while Olig2, a transcription factor necessary for the development of oligodendrocytes, is expressed at all stages of this cell lineage. Thus, it would be interesting to assess whether lack of mGcm2 from microglia will lead to defects on those other glia types by immunolabelling with the above characteristic markers.

Study the role of mGcm2 in microglia in demyelinated lesions of the spinal cord

To decipher the function of mGcm2 in microglia activation state, I started collaborating with the lab of B. Nait-Oumesmar and we recently generated a conditional mouse line for inducible Cre-mediated deletion of mGcm2, specifically in microglia. In order to determine the impact of mGcm2 ablation in microglia activation state, we performed LPC-induced demyelinated lesions of the spinal cord of mGcm2 cko (Cx3Cr1::CreER/+;mGcm2^{flox/flox}) and controls (Cx3Cr1::CreER/+;mGcm2^{flox/+} and mGcm2^{flox/flox}) mice. Morphological analyses of microglia on spinal cord sections, labelled with CD11b/F4/80/CD68, using the Visiopharm's image analysis software, revealed a pro-inflammatory state of the mutant microglia. This was manifested with decreased number of ramifications at 14 days post injection in the cko compared to the controls. Interestingly, the expression levels of iNOS and TLR2 (M1 pro-inflammatory markers) are increased significantly in LPC lesions in the mGcm2 cko compared to control groups, while the Arg-1 expression levels tended to decrease. Altogether, our data strongly suggest that the mGcm2 transcription factor is associated with an anti-inflammatory state of microglia during neuroinflammation. Therefore, determining the role of mGcm2 in neuroinflammation could be valuable in understanding its implication in similar human diseases such as MS.

To decipher the role of Gcm2 in inflammatory demyelination in the CNS, we will use the MOG-EAE model in the mGcm2 cko and control mice. MOG-induced EAE mimics important pathological hallmarks of MS lesions, with inflammatory lesions occurring mainly in the spinal cord and resulting in chronic demyelination. In this EAE model, the onset of clinical symptoms is strongly correlated with the occurrence of inflammatory white matter lesions, which extend with disease progression. The classical picture of acute EAE lesions are characterised by the

presence of patchy perivascular inflammatory infiltrates, composed of T lymphocytes, B cells and microglia/macrophages. According to our previous experience in WT (C57BL/6) mice, inflammation and demyelination take place from day 11 to day 40 post-immunization, while axonal loss becomes a major feature only during the chronic stages of the disease. MOG-induced EAE model is already well established in the Nait Oumesmar lab (Blanchard et al., 2013). For these experiments, mGcm2 cKO (Cx3Cr1::CreER/+;mGcm2flox/flox) and controls (Cx3Cr1::CreER/+;mGcm2flox/+ and mGcm2flox/flox) mice, have already been generated by Nait Oumesmar's lab. This will be the first time that mGcm2 will be tested for its role in neuroinflammation *in vivo* in mammals.

Gcm expression in *Drosophila melanogaster* in neuroinflammation

Upon induction of PD like disease in the fly CNS triggered by α -Syn neuronal expression, I showed that there is *de novo* expression of Gcm and that it is not coming from glia cells but rather hemocytes. I complemented this work by using another model of CNS inflammation by PQ treatment. So far, I proved that also in this model there are hemocytes associated with the CNS, which likely enter into the brain. The next goal will be to assess whether Gcm is *de novo* expressed in hemocytes upon the PQ treatment as well. Nowadays, new data have surfaced that show increase of hemocyte related genes in flies treated with PQ (Maitra et al., 2019).

To dissect the Gcm pathway using the *Drosophila* model it would be very exciting to use Gcm mutants in hemocytes and then assess the survival and the phenotype of the flies upon PQ treatment. The latter could be achieved with a climbing assay. This test is widely used to evaluate the mobility of adult flies from each treatment group as flies with PD like syndrome present lower climbing potential. Generally, the mobility is recorded using a negative geotaxis where ten flies per treatment group are placed in an empty plastic vial and gently tapped to the

bottom. The percentage of flies that cross a line 5 cm from the bottom of the vial in 20 sec is finally calculated (Maitra et al., 2019). Next, it will be interesting to perform an RNA seq on fly brains and hemocytes from both the knock down and the control. The RNA seq analysis will reveal all the differentially expressed genes, thus, revealing the pathway that is important during neuroinflammation in flies since the targets of Gcm in fly are already known. These findings will finally enable to propose specific targets in mice that are under the regulation of mGcm2 in similar conditions, such as PD models.

Conclusive remarks

Given the known impact of microglia in the development, homeostasis and inflammation of the CNS, future studies will better characterise the role of Gcm in neuroinflammation. Furthermore, focusing on Gcm orthologues in flies will provide additional evidence of conserved function in immunity. Given the evolutionary conservation of the basic biological process, I believe that my work will shed light on the immune response in humans as well. In the long term, this may help in understanding the physio-pathological mechanisms underlying human diseases of the CNS such as MS and PD, which represent a heavy burden on our societies.

References

- Akiyama-Oda, Y., Hosoya, T., & Hotta, Y. (1998). Alteration of cell fate by ectopic expression of *Drosophila* glial cells missing in non-neural cells. *Dev Genes Evol*, *208*(10), 578-585. doi:10.1007/s004270050217
- Akiyama, Y., Hosoya, T., Poole, A. M., & Hotta, Y. (1996). The *gcm*-motif: a novel DNA-binding motif conserved in *Drosophila* and mammals. *Proc Natl Acad Sci U S A*, *93*(25), 14912-14916. doi:10.1073/pnas.93.25.14912
- Alfonso, T. B., & Jones, B. W. (2002). *gcm2* promotes glial cell differentiation and is required with glial cells missing for macrophage development in *Drosophila*. *Dev Biol*, *248*(2), 369-383. doi:10.1006/dbio.2002.0740
- Alliot, F., Godin, I., & Pessac, B. (1999). Microglia derive from progenitors, originating from the yolk sac, and which proliferate in the brain. *Brain Res Dev Brain Res*, *117*(2), 145-152. doi:10.1016/s0165-3806(99)00113-3
- Aloisi, F., De Simone, R., Columba-Cabezas, S., Penna, G., & Adorini, L. (2000). Functional maturation of adult mouse resting microglia into an APC is promoted by granulocyte-macrophage colony-stimulating factor and interaction with Th1 cells. *Journal of immunology*, *164*(4), 1705-1712. doi:10.4049/jimmunol.164.4.1705
- Althammer, F., Ferreira-Neto, H. C., Rubaharan, M., Roy, R. K., Patel, A. A., Murphy, A., . . . Stern, J. E. (2020). Three-dimensional morphometric analysis reveals time-dependent structural changes in microglia and astrocytes in the central amygdala and hypothalamic paraventricular nucleus of heart failure rats. *J Neuroinflammation*, *17*(1), 221. doi:10.1186/s12974-020-01892-4
- Alves-Silva, J., Hahn, I., Huber, O., Mende, M., Reissaus, A., & Prokop, A. (2008). Prominent actin fiber arrays in *Drosophila* tendon cells represent architectural elements different from stress fibers. *Mol Biol Cell*, *19*(10), 4287-4297. doi:10.1091/mbc.E08-02-0182
- Anderl, I., Vesala, L., Ihalainen, T. O., Vanha-Aho, L. M., Ando, I., Ramet, M., & Hultmark, D. (2016). Transdifferentiation and Proliferation in Two Distinct Hemocyte Lineages in *Drosophila melanogaster* Larvae after Wasp Infection. *PLoS Pathog*, *12*(7), e1005746. doi:10.1371/journal.ppat.1005746
- Anderson, J. M., Hubbard, B. M., Coghill, G. R., & Slidders, W. (1983). The effect of advanced old age on the neurone content of the cerebral cortex. Observations with an automatic image analyser point counting method. *J Neurol Sci*, *58*(2), 235-246. doi:10.1016/0022-510x(83)90220-4
- Andre, C., Guzman-Quevedo, O., Rey, C., Remus-Borel, J., Clark, S., Castellanos-Jankiewicz, A., . . . Cota, D. (2017). Inhibiting Microglia Expansion Prevents Diet-Induced Hypothalamic and Peripheral Inflammation. *Diabetes*, *66*(4), 908-919. doi:10.2337/db16-0586
- Angelova, D. M., & Brown, D. R. (2019). Microglia and the aging brain: are senescent microglia the key to neurodegeneration? *J Neurochem*, *151*(6), 676-688. doi:10.1111/jnc.14860
- Anson-Cartwright, L., Dawson, K., Holmyard, D., Fisher, S. J., Lazzarini, R. A., & Cross, J. C. (2000). The glial cells missing-1 protein is essential for branching morphogenesis in the chorioallantoic placenta. *Nat Genet*, *25*(3), 311-314. doi:10.1038/77076
- Applewhite, D. A., Grode, K. D., Duncan, M. C., & Rogers, S. L. (2013). The actin-microtubule cross-linking activity of *Drosophila* Short stop is regulated by intramolecular inhibition. *Mol Biol Cell*, *24*(18), 2885-2893. doi:10.1091/mbc.E12-11-0798
- Applewhite, D. A., Grode, K. D., Keller, D., Zadeh, A. D., Slep, K. C., & Rogers, S. L. (2010). The spectraplakins Short stop is an actin-microtubule cross-linker that contributes to organization of the microtubule network. *Mol Biol Cell*, *21*(10), 1714-1724. doi:10.1091/mbc.E10-01-0011
- Ashwell, K. (1990). Microglia and cell death in the developing mouse cerebellum. *Brain Res Dev Brain Res*, *55*(2), 219-230. doi:10.1016/0165-3806(90)90203-b

- Askew, K., Li, K., Olmos-Alonso, A., Garcia-Moreno, F., Liang, Y., Richardson, P., . . . Gomez-Nicola, D. (2017). Coupled Proliferation and Apoptosis Maintain the Rapid Turnover of Microglia in the Adult Brain. *Cell reports*, *18*(2), 391-405. doi:10.1016/j.celrep.2016.12.041
- Auluck, P. K., & Bonini, N. M. (2002). Pharmacological prevention of Parkinson disease in *Drosophila*. *Nat Med*, *8*(11), 1185-1186. doi:10.1038/nm1102-1185
- Auluck, P. K., Chan, H. Y., Trojanowski, J. Q., Lee, V. M., & Bonini, N. M. (2002). Chaperone suppression of alpha-synuclein toxicity in a *Drosophila* model for Parkinson's disease. *Science*, *295*(5556), 865-868. doi:10.1126/science.1067389
- Aumailley, M., Has, C., Tunggal, L., & Bruckner-Tuderman, L. (2006). Molecular basis of inherited skin-blistering disorders, and therapeutic implications. *Expert Rev Mol Med*, *8*(24), 1-21. doi:10.1017/S1462399406000123
- Avet-Rochex, A., Boyer, K., Polesello, C., Gobert, V., Osman, D., Roch, F., . . . Waltzer, L. (2010). An in vivo RNA interference screen identifies gene networks controlling *Drosophila melanogaster* blood cell homeostasis. *BMC Dev Biol*, *10*, 65. doi:10.1186/1471-213X-10-65
- Bain, C. C., Bravo-Blas, A., Scott, C. L., Perdiguero, E. G., Geissmann, F., Henri, S., . . . Mowat, A. M. (2014). Constant replenishment from circulating monocytes maintains the macrophage pool in the intestine of adult mice. *Nat Immunol*, *15*(10), 929-937. doi:10.1038/ni.2967
- Bandres-Ciga, S., Diez-Fairen, M., Kim, J. J., & Singleton, A. B. (2020). Genetics of Parkinson's disease: An introspection of its journey towards precision medicine. *Neurobiol Dis*, *137*, 104782. doi:10.1016/j.nbd.2020.104782
- Basyuk, E., Cross, J. C., Corbin, J., Nakayama, H., Hunter, P., Nait-Oumesmar, B., & Lazzarini, R. A. (1999). Murine *Gcm1* gene is expressed in a subset of placental trophoblast cells. *Dev Dyn*, *214*(4), 303-311. doi:10.1002/(SICI)1097-0177(199904)214:4<303::AID-AJA3>3.0.CO;2-B
- Bazan, J. F., Bacon, K. B., Hardiman, G., Wang, W., Soo, K., Rossi, D., . . . Schall, T. J. (1997). A new class of membrane-bound chemokine with a CX3C motif. *Nature*, *385*(6617), 640-644. doi:10.1038/385640a0
- Bazzi, W., Cattenoz, P. B., Delaporte, C., Dasari, V., Sakr, R., Yuasa, Y., & Giangrande, A. (2018). Embryonic hematopoiesis modulates the inflammatory response and larval hematopoiesis in *Drosophila*. *eLife*, *7*. doi:10.7554/eLife.34890
- Beaino, W., Janssen, B., Kooij, G., van der Pol, S. M. A., van Het Hof, B., van Horsen, J., . . . de Vries, H. E. (2017). Purinergic receptors P2Y12R and P2X7R: potential targets for PET imaging of microglia phenotypes in multiple sclerosis. *J Neuroinflammation*, *14*(1), 259. doi:10.1186/s12974-017-1034-z
- Bedner, P., Dupper, A., Huttman, K., Muller, J., Herde, M. K., Dublin, P., . . . Steinhäuser, C. (2015). Astrocyte uncoupling as a cause of human temporal lobe epilepsy. *Brain*, *138*(Pt 5), 1208-1222. doi:10.1093/brain/awv067
- Bernardoni, R., Miller, A. A., & Giangrande, A. (1998). Glial differentiation does not require a neural ground state. *Development*, *125*(16), 3189-3200.
- Bernardoni, R., Vivancos, V., & Giangrande, A. (1997). *glide/gcm* is expressed and required in the scavenger cell lineage. *Dev Biol*, *191*(1), 118-130. doi:10.1006/dbio.1997.8702
- Bernier, G., De Repentigny, Y., Mathieu, M., David, S., & Kothary, R. (1998). Dystonin is an essential component of the Schwann cell cytoskeleton at the time of myelination. *Development*, *125*(11), 2135-2148.
- Bertrand, J. Y., Jalil, A., Klaine, M., Jung, S., Cumano, A., & Godin, I. (2005). Three pathways to mature macrophages in the early mouse yolk sac. *Blood*, *106*(9), 3004-3011. doi:10.1182/blood-2005-02-0461
- Bleriot, C., Li, S., Kairi, M., Newell, E., & Ginhoux, F. (2020). Kupffer Cell Characterization by Mass Cytometry. *Methods Mol Biol*, *2164*, 87-99. doi:10.1007/978-1-0716-0704-6_10
- Bogie, J. F., Stinissen, P., & Hendriks, J. J. (2014). Macrophage subsets and microglia in multiple sclerosis. *Acta Neuropathol*, *128*(2), 191-213. doi:10.1007/s00401-014-1310-2

- Bohatschek, M., Kloss, C. U., Kalla, R., & Raivich, G. (2001). In vitro model of microglial deramification: ramified microglia transform into amoeboid phagocytes following addition of brain cell membranes to microglia-astrocyte cocultures. *J Neurosci Res*, *64*(5), 508-522. doi:10.1002/jnr.1103
- Bohlen, C. J., Bennett, F. C., Tucker, A. F., Collins, H. Y., Mulinyawe, S. B., & Barres, B. A. (2017). Diverse Requirements for Microglial Survival, Specification, and Function Revealed by Defined-Medium Cultures. *Neuron*, *94*(4), 759-773 e758. doi:10.1016/j.neuron.2017.04.043
- Bolos, M., Perea, J. R., & Avila, J. (2017). Alzheimer's disease as an inflammatory disease. *Biomol Concepts*, *8*(1), 37-43. doi:10.1515/bmc-2016-0029
- Bonham, L. W., Sirkis, D. W., & Yokoyama, J. S. (2019). The Transcriptional Landscape of Microglial Genes in Aging and Neurodegenerative Disease. *Front Immunol*, *10*, 1170. doi:10.3389/fimmu.2019.01170
- Booth, H. D. E., Hirst, W. D., & Wade-Martins, R. (2017). The Role of Astrocyte Dysfunction in Parkinson's Disease Pathogenesis. *Trends Neurosci*, *40*(6), 358-370. doi:10.1016/j.tins.2017.04.001
- Bossing, T., Udolph, G., Doe, C. Q., & Technau, G. M. (1996). The embryonic central nervous system lineages of *Drosophila melanogaster*. I. Neuroblast lineages derived from the ventral half of the neuroectoderm. *Dev Biol*, *179*(1), 41-64. doi:10.1006/dbio.1996.0240
- Bosy-Westphal, A., & Muller, M. J. (2015). Identification of skeletal muscle mass depletion across age and BMI groups in health and disease--there is need for a unified definition. *Int J Obes (Lond)*, *39*(3), 379-386. doi:10.1038/ijo.2014.161
- Bottenberg, W., Sanchez-Soriano, N., Alves-Silva, J., Hahn, I., Mende, M., & Prokop, A. (2009). Context-specific requirements of functional domains of the Spectraplakins Short stop in vivo. *Mechanisms of development*, *126*(7), 489-502. doi:10.1016/j.mod.2009.04.004
- Boven, L. A., Van Meurs, M., Van Zwam, M., Wierenga-Wolf, A., Hintzen, R. Q., Boot, R. G., . . . Laman, J. D. (2006). Myelin-laden macrophages are anti-inflammatory, consistent with foam cells in multiple sclerosis. *Brain*, *129*(Pt 2), 517-526. doi:10.1093/brain/awh707
- Boyer, J. G., Bernstein, M. A., & Boudreau-Lariviere, C. (2010). Plakins in striated muscle. *Muscle Nerve*, *41*(3), 299-308. doi:10.1002/mus.21472
- Brand, A. H., & Perrimon, N. (1993). Targeted gene expression as a means of altering cell fates and generating dominant phenotypes. *Development*, *118*(2), 401-415.
- Brobeck, J. R. (1946). Mechanism of the development of obesity in animals with hypothalamic lesions. *Physiol Rev*, *26*(4), 541-559. doi:10.1152/physrev.1946.26.4.541
- Broderick, M. J., & Winder, S. J. (2005). Spectrin, alpha-actinin, and dystrophin. *Adv Protein Chem*, *70*, 203-246. doi:10.1016/S0065-3233(05)70007-3
- Burre, J., Sharma, M., & Sudhof, T. C. (2014). alpha-Synuclein assembles into higher-order multimers upon membrane binding to promote SNARE complex formation. *Proc Natl Acad Sci U S A*, *111*(40), E4274-4283. doi:10.1073/pnas.1416598111
- Butovsky, O., Jedrychowski, M. P., Moore, C. S., Cialic, R., Lanser, A. J., Gabriely, G., . . . Weiner, H. L. (2014). Identification of a unique TGF-beta-dependent molecular and functional signature in microglia. *Nature neuroscience*, *17*(1), 131-143. doi:10.1038/nn.3599
- Cai, Z., Hussain, M. D., & Yan, L. J. (2014). Microglia, neuroinflammation, and beta-amyloid protein in Alzheimer's disease. *Int J Neurosci*, *124*(5), 307-321. doi:10.3109/00207454.2013.833510
- Campisi, J. (2013). Aging, cellular senescence, and cancer. *Annu Rev Physiol*, *75*, 685-705. doi:10.1146/annurev-physiol-030212-183653
- Cantor, A. B., & Orkin, S. H. (2005). Coregulation of GATA factors by the Friend of GATA (FOG) family of multitype zinc finger proteins. *Semin Cell Dev Biol*, *16*(1), 117-128. doi:10.1016/j.semcdb.2004.10.006
- Cassar, M., Issa, A. R., Riemensperger, T., Petitgas, C., Rival, T., Coulom, H., . . . Birman, S. (2015). A dopamine receptor contributes to paraquat-induced neurotoxicity in *Drosophila*. *Hum Mol Genet*, *24*(1), 197-212. doi:10.1093/hmg/ddu430

- Cattenoz, P. B., & Giangrande, A. (2013). Lineage specification in the fly nervous system and evolutionary implications. *Cell cycle*, *12*(17), 2753-2759. doi:10.4161/cc.25918
- Cattenoz, P. B., & Giangrande, A. (2015). New insights in the clockwork mechanism regulating lineage specification: Lessons from the Drosophila nervous system. *Dev Dyn*, *244*(3), 332-341. doi:10.1002/dvdy.24228
- Cattenoz, P. B., Popkova, A., Southall, T. D., Aiello, G., Brand, A. H., & Giangrande, A. (2016). Functional Conservation of the Glide/Gcm Regulatory Network Controlling Glia, Hemocyte, and Tendon Cell Differentiation in Drosophila. *Genetics*, *202*(1), 191-219. doi:10.1534/genetics.115.182154
- Cattenoz, P. B., Sakr, R., Pavlidaki, A., Delaporte, C., Riba, A., Molina, N., . . . Giangrande, A. (2020). Temporal specificity and heterogeneity of Drosophila immune cells. *Embo j*, *39*(12), e104486. doi:10.15252/embj.2020104486
- Cengiz, P., Zafer, D., Chandrashekhar, J. H., Chanana, V., Bogost, J., Waldman, A., . . . Ferrazzano, P. A. (2019). Developmental differences in microglia morphology and gene expression during normal brain development and in response to hypoxia-ischemia. *Neurochem Int*, *127*, 137-147. doi:10.1016/j.neuint.2018.12.016
- Chang, D., Nalls, M. A., Hallgrimsdottir, I. B., Hunkapiller, J., van der Brug, M., Cai, F., . . . Graham, R. R. (2017). A meta-analysis of genome-wide association studies identifies 17 new Parkinson's disease risk loci. *Nat Genet*, *49*(10), 1511-1516. doi:10.1038/ng.3955
- Chaudhuri, A., Bowling, K., Funderburk, C., Lawal, H., Inamdar, A., Wang, Z., & O'Donnell, J. M. (2007). Interaction of genetic and environmental factors in a Drosophila parkinsonism model. *The Journal of neuroscience : the official journal of the Society for Neuroscience*, *27*(10), 2457-2467. doi:10.1523/JNEUROSCI.4239-06.2007
- Chen, L., & Feany, M. B. (2005). Alpha-synuclein phosphorylation controls neurotoxicity and inclusion formation in a Drosophila model of Parkinson disease. *Nature neuroscience*, *8*(5), 657-663. doi:10.1038/nn1443
- Chen, L., Periquet, M., Wang, X., Negro, A., McLean, P. J., Hyman, B. T., & Feany, M. B. (2009). Tyrosine and serine phosphorylation of alpha-synuclein have opposing effects on neurotoxicity and soluble oligomer formation. *J Clin Invest*, *119*(11), 3257-3265. doi:10.1172/JCI39088
- Chhor, V., Le Charpentier, T., Lebon, S., Ore, M. V., Celador, I. L., Josserand, J., . . . Fleiss, B. (2013). Characterization of phenotype markers and neuronotoxic potential of polarised primary microglia in vitro. *Brain Behav Immun*, *32*, 70-85. doi:10.1016/j.bbi.2013.02.005
- Chinen, J., & Shearer, W. T. (2010). Secondary immunodeficiencies, including HIV infection. *J Allergy Clin Immunol*, *125*(2 Suppl 2), S195-203. doi:10.1016/j.jaci.2009.08.040
- Chlon, T. M., & Crispino, J. D. (2012). Combinatorial regulation of tissue specification by GATA and FOG factors. *Development*, *139*(21), 3905-3916. doi:10.1242/dev.080440
- Choi, Y. R., Kang, S. J., Kim, J. M., Lee, S. J., Jou, I., Joe, E. H., & Park, S. M. (2015). FcgammaRIIB mediates the inhibitory effect of aggregated alpha-synuclein on microglial phagocytosis. *Neurobiol Dis*, *83*, 90-99. doi:10.1016/j.nbd.2015.08.025
- Cohen, S. X., Moulin, M., Schilling, O., Meyer-Klaucke, W., Schreiber, J., Wegner, M., & Muller, C. W. (2002). The GCM domain is a Zn-coordinating DNA-binding domain. *FEBS Lett*, *528*(1-3), 95-100. doi:10.1016/s0014-5793(02)03257-x
- Combadiere, C., Ahuja, S. K., Van Damme, J., Tiffany, H. L., Gao, J. L., & Murphy, P. M. (1995). Monocyte chemoattractant protein-3 is a functional ligand for CC chemokine receptors 1 and 2B. *Journal of Biological Chemistry*, *270*(50), 29671-29675. doi:10.1074/jbc.270.50.29671
- Combadiere, C., Salzwedel, K., Smith, E. D., Tiffany, H. L., Berger, E. A., & Murphy, P. M. (1998). Identification of CX3CR1. A chemotactic receptor for the human CX3C chemokine fractalkine and a fusion coreceptor for HIV-1. *Journal of Biological Chemistry*, *273*(37), 23799-23804. doi:10.1074/jbc.273.37.23799

- Compston, A., & Coles, A. (2008). Multiple sclerosis. *Lancet*, 372(9648), 1502-1517. doi:10.1016/S0140-6736(08)61620-7
- Conde, J. R., & Streit, W. J. (2006). Microglia in the aging brain. *J Neuropathol Exp Neurol*, 65(3), 199-203. doi:10.1097/01.jnen.0000202887.22082.63
- Cookson, M. R. (2009). alpha-Synuclein and neuronal cell death. *Mol Neurodegener*, 4, 9. doi:10.1186/1750-1326-4-9
- Cooper-Knock, J., Green, C., Altschuler, G., Wei, W., Bury, J. J., Heath, P. R., . . . Hide, W. (2017). A data-driven approach links microglia to pathology and prognosis in amyotrophic lateral sclerosis. *Acta Neuropathol Commun*, 5(1), 23. doi:10.1186/s40478-017-0424-x
- Cooper, M. D. (2010). A life of adventure in immunobiology. *Annu Rev Immunol*, 28, 1-19. doi:10.1146/annurev-immunol-030409-101248
- Cox, A. J., Moscovis, S. M., Blackwell, C. C., & Scott, R. J. (2014). Cytokine gene polymorphism among Indigenous Australians. *Innate Immun*, 20(4), 431-439. doi:10.1177/1753425913498911
- Cuadros, M. A., Martin, C., Coltey, P., Almendros, A., & Navascues, J. (1993). First appearance, distribution, and origin of macrophages in the early development of the avian central nervous system. *J Comp Neurol*, 330(1), 113-129. doi:10.1002/cne.903300110
- Cunningham, C. L., Martinez-Cerdeno, V., & Noctor, S. C. (2013). Microglia regulate the number of neural precursor cells in the developing cerebral cortex. *The Journal of neuroscience : the official journal of the Society for Neuroscience*, 33(10), 4216-4233. doi:10.1523/JNEUROSCI.3441-12.2013
- Dalpe, G., Mathieu, M., Comtois, A., Zhu, E., Wasiak, S., De Repentigny, Y., . . . Kothary, R. (1999). Dystonin-deficient mice exhibit an intrinsic muscle weakness and an instability of skeletal muscle cytoarchitecture. *Dev Biol*, 210(2), 367-380. doi:10.1006/dbio.1999.9263
- Damani, M. R., Zhao, L., Fontainhas, A. M., Amaral, J., Fariss, R. N., & Wong, W. T. (2011). Age-related alterations in the dynamic behavior of microglia. *Aging Cell*, 10(2), 263-276. doi:10.1111/j.1474-9726.2010.00660.x
- Damoiseaux, J. S. (2017). Effects of aging on functional and structural brain connectivity. *Neuroimage*, 160, 32-40. doi:10.1016/j.neuroimage.2017.01.077
- Dasgupta, S., Jana, M., Liu, X., & Pahan, K. (2002). Myelin basic protein-primed T cells induce nitric oxide synthase in microglial cells. Implications for multiple sclerosis. *Journal of Biological Chemistry*, 277(42), 39327-39333. doi:10.1074/jbc.M111841200
- Davalos, D., Grutzendler, J., Yang, G., Kim, J. V., Zuo, Y., Jung, S., . . . Gan, W. B. (2005). ATP mediates rapid microglial response to local brain injury in vivo. *Nature neuroscience*, 8(6), 752-758. doi:10.1038/nn1472
- Davidson, A. J., & Zon, L. I. (2004). The 'definitive' (and 'primitive') guide to zebrafish hematopoiesis. *Oncogene*, 23(43), 7233-7246. doi:10.1038/sj.onc.1207943
- Davidson, E. H., Rast, J. P., Oliveri, P., Ransick, A., Caestani, C., Yuh, C. H., . . . Bolouri, H. (2002). A genomic regulatory network for development. *Science*, 295(5560), 1669-1678. doi:10.1126/science.1069883
- Davies, L. C., Jenkins, S. J., Allen, J. E., & Taylor, P. R. (2013). Tissue-resident macrophages. *Nat Immunol*, 14(10), 986-995. doi:10.1038/ni.2705
- de Heredia, F. P., Gomez-Martinez, S., & Marcos, A. (2012). Obesity, inflammation and the immune system. *Proc Nutr Soc*, 71(2), 332-338. doi:10.1017/S0029665112000092
- De, I., Nikodemova, M., Steffen, M. D., Sokn, E., Maklakova, V. I., Watters, J. J., & Collier, L. S. (2014). CSF1 overexpression has pleiotropic effects on microglia in vivo. *Glia*, 62(12), 1955-1967. doi:10.1002/glia.22717
- de Lau, L. M., & Breteler, M. M. (2006). Epidemiology of Parkinson's disease. *Lancet Neurology*, 5(6), 525-535. doi:10.1016/S1474-4422(06)70471-9
- del Valle Rodriguez, A., Didiano, D., & Desplan, C. (2011). Power tools for gene expression and clonal analysis in *Drosophila*. *Nat Methods*, 9(1), 47-55. doi:10.1038/nmeth.1800

- Denes, A., Coutts, G., Lenart, N., Cruickshank, S. M., Pelegrin, P., Skinner, J., . . . Brough, D. (2015). AIM2 and NLRC4 inflammasomes contribute with ASC to acute brain injury independently of NLRP3. *Proc Natl Acad Sci U S A*, *112*(13), 4050-4055. doi:10.1073/pnas.1419090112
- Deng, B., Wehling-Henricks, M., Villalta, S. A., Wang, Y., & Tidball, J. G. (2012). IL-10 triggers changes in macrophage phenotype that promote muscle growth and regeneration. *Journal of immunology*, *189*(7), 3669-3680. doi:10.4049/jimmunol.1103180
- Desjardins, S. F., Berchiche, Y. A., Haddad, E., & Heveker, N. (2007). [Multiple talents of the chemokine receptor-CXCR4]. *Med Sci (Paris)*, *23*(11), 980-984. doi:10.1051/medsci/20072311980
- Di Monte, D. A., Lavasani, M., & Manning-Bog, A. B. (2002). Environmental factors in Parkinson's disease. *Neurotoxicology*, *23*(4-5), 487-502. doi:10.1016/s0161-813x(02)00099-2
- DiPatre, P. L., & Gelman, B. B. (1997). Microglial cell activation in aging and Alzheimer disease: partial linkage with neurofibrillary tangle burden in the hippocampus. *J Neuropathol Exp Neurol*, *56*(2), 143-149. doi:10.1097/00005072-199702000-00004
- Djedovic, N., Stanisavljevic, S., Jevtic, B., Momcilovic, M., Lavrnja, I., & Miljkovic, D. (2017). Anti-encephalitogenic effects of ethyl pyruvate are reflected in the central nervous system and the gut. *Biomed Pharmacother*, *96*, 78-85. doi:10.1016/j.biopha.2017.09.110
- Doherty, J., Logan, M. A., Tasdemir, O. E., & Freeman, M. R. (2009). Ensheathing glia function as phagocytes in the adult Drosophila brain. *The Journal of neuroscience : the official journal of the Society for Neuroscience*, *29*(15), 4768-4781. doi:10.1523/JNEUROSCI.5951-08.2009
- Du, G., Liu, X., Chen, X., Song, M., Yan, Y., Jiao, R., & Wang, C. C. (2010). Drosophila histone deacetylase 6 protects dopaminergic neurons against {alpha}-synuclein toxicity by promoting inclusion formation. *Mol Biol Cell*, *21*(13), 2128-2137. doi:10.1091/mbc.E10-03-0200
- Duffy, P. E., Huang, Y. Y., Rapport, M. M., & Graf, L. (1980). Glial fibrillary acidic protein in giant cell tumors of brain and other gliomas. A possible relationship to malignancy, differentiation, and pleomorphism of glia. *Acta Neuropathol*, *52*(1), 51-57. doi:10.1007/BF00687228
- Dunin-Horkawicz, S., Kopec, K. O., & Lupas, A. N. (2014). Prokaryotic ancestry of eukaryotic protein networks mediating innate immunity and apoptosis. *J Mol Biol*, *426*(7), 1568-1582. doi:10.1016/j.jmb.2013.11.030
- Dzierzak, E., & Speck, N. A. (2008). Of lineage and legacy: the development of mammalian hematopoietic stem cells. *Nat Immunol*, *9*(2), 129-136. doi:10.1038/ni1560
- Elliott, D. A., Kim, W. S., Gorissen, S., Halliday, G. M., & Kwok, J. B. (2012). Leucine-rich repeat kinase 2 and alternative splicing in Parkinson's disease. *Mov Disord*, *27*(8), 1004-1011. doi:10.1002/mds.25005
- Evans, C. J., Hartenstein, V., & Banerjee, U. (2003). Thicker than blood: conserved mechanisms in Drosophila and vertebrate hematopoiesis. *Dev Cell*, *5*(5), 673-690. doi:10.1016/s1534-5807(03)00335-6
- Evans, C. J., Olson, J. M., Ngo, K. T., Kim, E., Lee, N. E., Kuoy, E., . . . Banerjee, U. (2009). G-TRACE: rapid Gal4-based cell lineage analysis in Drosophila. *Nat Methods*, *6*(8), 603-605. doi:10.1038/nmeth.1356
- Fan, C., Long, R., You, Y., Wang, J., Yang, X., Huang, S., . . . Liu, K. (2018). A novel PADRE-Kv1.3 vaccine effectively induces therapeutic antibodies and ameliorates experimental autoimmune encephalomyelitis in rats. *Clinical immunology (Orlando, Fla.)*, *193*, 98-109. doi:10.1016/j.clim.2018.02.012
- Fantin, A., Vieira, J. M., Gestri, G., Denti, L., Schwarz, Q., Prykhodzhiy, S., . . . Ruhrberg, C. (2010). Tissue macrophages act as cellular chaperones for vascular anastomosis downstream of VEGF-mediated endothelial tip cell induction. *Blood*, *116*(5), 829-840. doi:10.1182/blood-2009-12-257832

- Farinatti, P., Castinheiras Neto, A. G., & Amorim, P. R. (2016). Oxygen Consumption and Substrate Utilization During and After Resistance Exercises Performed with Different Muscle Mass. *Int J Exerc Sci*, 9(1), 77-88.
- Feany, M. B., & Bender, W. W. (2000). A Drosophila model of Parkinson's disease. *Nature*, 404(6776), 394-398. doi:10.1038/35006074
- Featherstone, D. E. (2011). Glial solute carrier transporters in Drosophila and mice. *Glia*, 59(9), 1351-1363. doi:10.1002/glia.21085
- Fenn, A. M., Henry, C. J., Huang, Y., Dugan, A., & Godbout, J. P. (2012). Lipopolysaccharide-induced interleukin (IL)-4 receptor-alpha expression and corresponding sensitivity to the M2 promoting effects of IL-4 are impaired in microglia of aged mice. *Brain Behav Immun*, 26(5), 766-777. doi:10.1016/j.bbi.2011.10.003
- Fischer, A., Hacein-Bey Abina, S., Touzot, F., & Cavazzana, M. (2015). Gene therapy for primary immunodeficiencies. *Clin Genet*, 88(6), 507-515. doi:10.1111/cge.12576
- Fossett, N., & Schulz, R. A. (2001). Conserved cardiogenic functions of the multitype zinc-finger proteins: U-shaped and FOG-2. *Trends Cardiovasc Med*, 11(5), 185-190. doi:10.1016/s1050-1738(01)00092-5
- Fossett, N., Tevosian, S. G., Gajewski, K., Zhang, Q., Orkin, S. H., & Schulz, R. A. (2001). The Friend of GATA proteins U-shaped, FOG-1, and FOG-2 function as negative regulators of blood, heart, and eye development in Drosophila. *Proc Natl Acad Sci U S A*, 98(13), 7342-7347. doi:10.1073/pnas.131215798
- Freeman, M. R. (2015). Drosophila Central Nervous System Glia. *Cold Spring Harb Perspect Biol*, 7(11). doi:10.1101/cshperspect.a020552
- Freilich, R. W., Woodbury, M. E., & Ikezu, T. (2013). Integrated expression profiles of mRNA and miRNA in polarized primary murine microglia. *PLOS ONE*, 8(11), e79416. doi:10.1371/journal.pone.0079416
- Frost, J. L., & Schafer, D. P. (2016). Microglia: Architects of the Developing Nervous System. *Trends Cell Biol*, 26(8), 587-597. doi:10.1016/j.tcb.2016.02.006
- Gamper, I., Fleck, D., Barlin, M., Spehr, M., El Sayad, S., Kleine, H., . . . Sechi, A. (2016). GAR22beta regulates cell migration, sperm motility, and axoneme structure. *Mol Biol Cell*, 27(2), 277-294. doi:10.1091/mbc.E15-06-0426
- Ginhoux, F., Greter, M., Leboeuf, M., Nandi, S., See, P., Gokhan, S., . . . Merad, M. (2010). Fate mapping analysis reveals that adult microglia derive from primitive macrophages. *Science*, 330(6005), 841-845. doi:10.1126/science.1194637
- Ginhoux, F., & Guilliams, M. (2016). Tissue-Resident Macrophage Ontogeny and Homeostasis. *Immunity*, 44(3), 439-449. doi:10.1016/j.immuni.2016.02.024
- Giorda, R., Cerritello, A., Bonaglia, M. C., Bova, S., Lanzi, G., Repetti, E., . . . Zuffardi, O. (2004). Selective disruption of muscle and brain-specific BPAG1 isoforms in a girl with a 6;15 translocation, cognitive and motor delay, and tracheo-oesophageal atresia. *J Med Genet*, 41(6), e71. doi:10.1136/jmg.2003.012260
- Giunti, D., Parodi, B., Cordano, C., Uccelli, A., & Kerlero de Rosbo, N. (2014). Can we switch microglia's phenotype to foster neuroprotection? Focus on multiple sclerosis. *Immunology*, 141(3), 328-339. doi:10.1111/imm.12177
- Gomez-Nicola, D., Fransen, N. L., Suzzi, S., & Perry, V. H. (2013). Regulation of microglial proliferation during chronic neurodegeneration. *The Journal of neuroscience : the official journal of the Society for Neuroscience*, 33(6), 2481-2493. doi:10.1523/JNEUROSCI.4440-12.2013
- Gordon, J., Bennett, A. R., Blackburn, C. C., & Manley, N. R. (2001). Gcm2 and Foxn1 mark early parathyroid- and thymus-specific domains in the developing third pharyngeal pouch. *Mechanisms of development*, 103(1-2), 141-143. doi:10.1016/s0925-4773(01)00333-1
- Govind, S. (2008). Innate immunity in Drosophila: Pathogens and pathways. *Insect Sci*, 15(1), 29-43. doi:10.1111/j.1744-7917.2008.00185.x

- Graeber, M. B., Kosel, S., Egensperger, R., Banati, R. B., Muller, U., Bise, K., . . . Mehraein, P. (1997). Rediscovery of the case described by Alois Alzheimer in 1911: historical, histological and molecular genetic analysis. *Neurogenetics*, *1*(1), 73-80. doi:10.1007/s100480050011
- Green, F., Samaranch, L., Zhang, H. S., Manning-Bog, A., Meyer, K., Forsayeth, J., & Bankiewicz, K. S. (2016). Axonal transport of AAV9 in nonhuman primate brain. *Gene Ther*, *23*(6), 520-526. doi:10.1038/gt.2016.24
- Greter, M., Lelios, I., Pelczar, P., Hoeffel, G., Price, J., Leboeuf, M., . . . Becher, B. (2012). Stroma-derived interleukin-34 controls the development and maintenance of langerhans cells and the maintenance of microglia. *Immunity*, *37*(6), 1050-1060. doi:10.1016/j.immuni.2012.11.001
- Grigorian, M., Mandal, L., & Hartenstein, V. (2011). Hematopoiesis at the onset of metamorphosis: terminal differentiation and dissociation of the Drosophila lymph gland. *Dev Genes Evol*, *221*(3), 121-131. doi:10.1007/s00427-011-0364-6
- Gritz, E., & Hirschi, K. K. (2016). Specification and function of hemogenic endothelium during embryogenesis. *Cell Mol Life Sci*, *73*(8), 1547-1567. doi:10.1007/s00018-016-2134-0
- Groves, R. W., Liu, L., Dopping-Hepenstal, P. J., Markus, H. S., Lovell, P. A., Ozoemena, L., . . . McGrath, J. A. (2010). A homozygous nonsense mutation within the dystonin gene coding for the coiled-coil domain of the epithelial isoform of BPAG1 underlies a new subtype of autosomal recessive epidermolysis bullosa simplex. *J Invest Dermatol*, *130*(6), 1551-1557. doi:10.1038/jid.2010.19
- Guillot-Sestier, M. V., Araiz, A. R., Mela, V., Gaban, A. S., O'Neill, E., Joshi, L., . . . Lynch, M. A. (2021). Microglial metabolism is a pivotal factor in sexual dimorphism in Alzheimer's disease. *Commun Biol*, *4*(1), 711. doi:10.1038/s42003-021-02259-y
- Gunther, T., Chen, Z. F., Kim, J., Priemel, M., Rueger, J. M., Amling, M., . . . Karsenty, G. (2000). Genetic ablation of parathyroid glands reveals another source of parathyroid hormone. *Nature*, *406*(6792), 199-203. doi:10.1038/35018111
- Gupta, T., Kumar, A., Cattenoz, P. B., VijayRaghavan, K., & Giangrande, A. (2016). The Glide/Gcm fate determinant controls initiation of collective cell migration by regulating Frazzled. *eLife*, *5*. doi:10.7554/eLife.15983
- Hagemeyer, N., Hanft, K. M., Akriditou, M. A., Unger, N., Park, E. S., Stanley, E. R., . . . Prinz, M. (2017). Microglia contribute to normal myelinogenesis and to oligodendrocyte progenitor maintenance during adulthood. *Acta Neuropathol*, *134*(3), 441-458. doi:10.1007/s00401-017-1747-1
- Hahn, I., Ronshaugen, M., Sanchez-Soriano, N., & Prokop, A. (2016). Functional and Genetic Analysis of Spectraplakins in Drosophila. *Methods Enzymol*, *569*, 373-405. doi:10.1016/bs.mie.2015.06.022
- Hajji, K., Mteyrek, A., Sun, J., Cassar, M., Mezghani, S., Leprince, J., . . . Birman, S. (2019). Neuroprotective effects of PACAP against paraquat-induced oxidative stress in the Drosophila central nervous system. *Hum Mol Genet*, *28*(11), 1905-1918. doi:10.1093/hmg/ddz031
- Hamill, K. J., Hopkinson, S. B., DeBiase, P., & Jones, J. C. (2009). BPAG1e maintains keratinocyte polarity through beta4 integrin-mediated modulation of Rac1 and cofilin activities. *Mol Biol Cell*, *20*(12), 2954-2962. doi:10.1091/mbc.E09-01-0051
- Hamza, T. H., Zabetian, C. P., Tenesa, A., Laederach, A., Montimurro, J., Yearout, D., . . . Payami, H. (2010). Common genetic variation in the HLA region is associated with late-onset sporadic Parkinson's disease. *Nat Genet*, *42*(9), 781-785. doi:10.1038/ng.642
- Hansen, D. V., Hanson, J. E., & Sheng, M. (2018). Microglia in Alzheimer's disease. *Journal of Cell Biology*, *217*(2), 459-472. doi:10.1083/jcb.201709069
- Harrison, D. A., & Perrimon, N. (1993). Simple and efficient generation of marked clones in Drosophila. *Curr Biol*, *3*(7), 424-433. doi:10.1016/0960-9822(93)90349-s
- Hartline, D. K. (2011). The evolutionary origins of glia. *Glia*, *59*(9), 1215-1236. doi:10.1002/glia.21149

- Hashemolhosseini, S., Schmidt, K., Kilian, K., Rodriguez, E., & Wegner, M. (2004). Conservation and variation of structure and function in a newly identified GCM homolog from chicken. *J Mol Biol*, 336(2), 441-451. doi:10.1016/j.jmb.2003.12.029
- Hashemolhosseini, S., & Wegner, M. (2004). Impacts of a new transcription factor family: mammalian GCM proteins in health and disease. *Journal of Cell Biology*, 166(6), 765-768. doi:10.1083/jcb.200406097
- He, G. L., Luo, Z., Shen, T. T., Li, P., Yang, J., Luo, X., . . . Yang, X. S. (2016). Inhibition of STAT3- and MAPK-dependent PGE2 synthesis ameliorates phagocytosis of fibrillar beta-amyloid peptide (1-42) via EP2 receptor in EMF-stimulated N9 microglial cells. *J Neuroinflammation*, 13(1), 296. doi:10.1186/s12974-016-0762-9
- Healy, L. M., Michell-Robinson, M. A., & Antel, J. P. (2015). Regulation of human glia by multiple sclerosis disease modifying therapies. *Semin Immunopathol*, 37(6), 639-649. doi:10.1007/s00281-015-0514-4
- Heindl, S., Gesierich, B., Benakis, C., Llovera, G., Duering, M., & Liesz, A. (2018). Automated Morphological Analysis of Microglia After Stroke. *Frontiers in cellular neuroscience*, 12, 106. doi:10.3389/fncel.2018.00106
- Herbomel, P. (1999). Spinning nuclei in the brain of the zebrafish embryo. *Curr Biol*, 9(17), R627-628. doi:10.1016/s0960-9822(99)80407-2
- Herbomel, P., Thisse, B., & Thisse, C. (2001). Zebrafish early macrophages colonize cephalic mesenchyme and developing brain, retina, and epidermis through a M-CSF receptor-dependent invasive process. *Dev Biol*, 238(2), 274-288. doi:10.1006/dbio.2001.0393
- Hetherington, M. M., Altemus, M., Nelson, M. L., Bernat, A. S., & Gold, P. W. (1994). Eating behavior in bulimia nervosa: multiple meal analyses. *Am J Clin Nutr*, 60(6), 864-873. doi:10.1093/ajcn/60.6.864
- Hickman, S. E., Allison, E. K., & El Khoury, J. (2008). Microglial dysfunction and defective beta-amyloid clearance pathways in aging Alzheimer's disease mice. *The Journal of neuroscience : the official journal of the Society for Neuroscience*, 28(33), 8354-8360. doi:10.1523/JNEUROSCI.0616-08.2008
- Hindle, S. J., & Bainton, R. J. (2014). Barrier mechanisms in the Drosophila blood-brain barrier. *Front Neurosci*, 8, 414. doi:10.3389/fnins.2014.00414
- Hitoshi, S., Ishino, Y., Kumar, A., Jasmine, S., Tanaka, K. F., Kondo, T., . . . Ikenaka, K. (2011). Mammalian Gcm genes induce Hes5 expression by active DNA demethylation and induce neural stem cells. *Nature neuroscience*, 14(8), 957-964. doi:10.1038/nn.2875
- Hoeffel, G., Chen, J., Lavin, Y., Low, D., Almeida, F. F., See, P., . . . Ginhoux, F. (2015). C-Myb(+) erythro-myeloid progenitor-derived fetal monocytes give rise to adult tissue-resident macrophages. *Immunity*, 42(4), 665-678. doi:10.1016/j.immuni.2015.03.011
- Hoeffel, G., & Ginhoux, F. (2015). Ontogeny of Tissue-Resident Macrophages. *Front Immunol*, 6, 486. doi:10.3389/fimmu.2015.00486
- Hoeffel, G., & Ginhoux, F. (2018). Fetal monocytes and the origins of tissue-resident macrophages. *Cell Immunol*, 330, 5-15. doi:10.1016/j.cellimm.2018.01.001
- Hoffmann, J. A. (2003). The immune response of Drosophila. *Nature*, 426(6962), 33-38. doi:10.1038/nature02021
- Holmans, P., Moskva, V., Jones, L., Sharma, M., International Parkinson's Disease Genomics, C., Vedernikov, A., . . . Williams, N. M. (2013). A pathway-based analysis provides additional support for an immune-related genetic susceptibility to Parkinson's disease. *Hum Mol Genet*, 22(5), 1039-1049. doi:10.1093/hmg/ddt492
- Honti, V., Kurucz, E., Csordas, G., Laurinyecz, B., Markus, R., & Ando, I. (2009). In vivo detection of lamellocytes in Drosophila melanogaster. *Immunol Lett*, 126(1-2), 83-84. doi:10.1016/j.imlet.2009.08.004

- Hopperton, K. E., Mohammad, D., Trepanier, M. O., Giuliano, V., & Bazinet, R. P. (2018). Markers of microglia in post-mortem brain samples from patients with Alzheimer's disease: a systematic review. *Mol Psychiatry*, *23*(2), 177-198. doi:10.1038/mp.2017.246
- Hosoya, T., Takizawa, K., Nitta, K., & Hotta, Y. (1995). glial cells missing: a binary switch between neuronal and glial determination in *Drosophila*. *Cell*, *82*(6), 1025-1036. doi:10.1016/0092-8674(95)90281-3
- Hultmark, D. (2003). *Drosophila* immunity: paths and patterns. *Curr Opin Immunol*, *15*(1), 12-19. doi:10.1016/s0952-7915(02)00005-5
- Hultmark, D., & Ekengren, S. (2003). A cytokine in the *Drosophila* stress response. *Dev Cell*, *5*(3), 360-361. doi:10.1016/s1534-5807(03)00268-5
- Ibanez, P., Bonnet, A. M., Debarges, B., Lohmann, E., Tison, F., Pollak, P., . . . Brice, A. (2004). Causal relation between alpha-synuclein gene duplication and familial Parkinson's disease. *Lancet*, *364*(9440), 1169-1171. doi:10.1016/S0140-6736(04)17104-3
- Ibanez, P., Lesage, S., Janin, S., Lohmann, E., Durif, F., Destee, A., . . . French Parkinson's Disease Genetics Study, G. (2009). Alpha-synuclein gene rearrangements in dominantly inherited parkinsonism: frequency, phenotype, and mechanisms. *Arch Neurol*, *66*(1), 102-108. doi:10.1001/archneurol.2008.555
- Inamdar, A. A., Chaudhuri, A., & O'Donnell, J. (2012). The Protective Effect of Minocycline in a Paraquat-Induced Parkinson's Disease Model in *Drosophila* is Modified in Altered Genetic Backgrounds. *Parkinsons Dis*, *2012*, 938528. doi:10.1155/2012/938528
- Jackson, S. J., Giovannoni, G., & Baker, D. (2011). Fingolimod modulates microglial activation to augment markers of remyelination. *J Neuroinflammation*, *8*, 76. doi:10.1186/1742-2094-8-76
- Jacques, C., Soustelle, L., Nagy, I., Diebold, C., & Giangrande, A. (2009). A novel role of the glial fate determinant glial cells missing in hematopoiesis. *Int J Dev Biol*, *53*(7), 1013-1022. doi:10.1387/ijdb.082726cj
- Jo, E., Darabie, A. A., Han, K., Tandon, A., Fraser, P. E., & McLaurin, J. (2004). alpha-Synuclein-synaptosomal membrane interactions: implications for fibrillogenesis. *Eur J Biochem*, *271*(15), 3180-3189. doi:10.1111/j.1432-1033.2004.04250.x
- Jones, B. W., Fetter, R. D., Tear, G., & Goodman, C. S. (1995). glial cells missing: a genetic switch that controls glial versus neuronal fate. *Cell*, *82*(6), 1013-1023. doi:10.1016/0092-8674(95)90280-5
- Jones, J. G., Garcia, P., Barosa, C., Delgado, T. C., & Diogo, L. (2009). Hepatic anaplerotic outflow fluxes are redirected from gluconeogenesis to lactate synthesis in patients with Type 1a glycogen storage disease. *Metab Eng*, *11*(3), 155-162. doi:10.1016/j.ymben.2009.01.003
- Jung, S., Aliberti, J., Graemmel, P., Sunshine, M. J., Kreutzberg, G. W., Sher, A., & Littman, D. R. (2000). Analysis of fractalkine receptor CX(3)CR1 function by targeted deletion and green fluorescent protein reporter gene insertion. *Mol Cell Biol*, *20*(11), 4106-4114. doi:10.1128/MCB.20.11.4106-4114.2000
- Junkunlo, K., Soderhall, K., & Soderhall, I. (2020). A transcription factor glial cell missing (*Gcm*) in the freshwater crayfish *Pacifastacus leniusculus*. *Dev Comp Immunol*, *113*, 103782. doi:10.1016/j.dci.2020.103782
- Jurga, A. M., Paleczna, M., & Kuter, K. Z. (2020). Overview of General and Discriminating Markers of Differential Microglia Phenotypes. *Frontiers in cellular neuroscience*, *14*, 198. doi:10.3389/fncel.2020.00198
- Kammerer, M., & Giangrande, A. (2001). *Glide2*, a second glial promoting factor in *Drosophila melanogaster*. *Embo j*, *20*(17), 4664-4673. doi:10.1093/emboj/20.17.4664
- Kanca, O., Caussinus, E., Denes, A. S., Percival-Smith, A., & Affolter, M. (2014). *Raepli*: a whole-tissue labeling tool for live imaging of *Drosophila* development. *Development*, *141*(2), 472-480. doi:10.1242/dev.102913

- Kari, B., Csordas, G., Honti, V., Cinege, G., Williams, M. J., Ando, I., & Kurucz, E. (2016). The raspberry Gene Is Involved in the Regulation of the Cellular Immune Response in *Drosophila melanogaster*. *PLOS ONE*, *11*(3), e0150910. doi:10.1371/journal.pone.0150910
- Karpinar, D. P., Balijs, M. B., Kugler, S., Opazo, F., Rezaei-Ghaleh, N., Wender, N., . . . Zweckstetter, M. (2009). Pre-fibrillar alpha-synuclein variants with impaired beta-structure increase neurotoxicity in Parkinson's disease models. *Embo j*, *28*(20), 3256-3268. doi:10.1038/emboj.2009.257
- Kasahara, M., Suzuki, T., & Pasquier, L. D. (2004). On the origins of the adaptive immune system: novel insights from invertebrates and cold-blooded vertebrates. *Trends Immunol*, *25*(2), 105-111. doi:10.1016/j.it.2003.11.005
- Kawanokuchi, J., Mizuno, T., Kato, H., Mitsuma, N., & Suzumura, A. (2004). Effects of interferon-beta on microglial functions as inflammatory and antigen presenting cells in the central nervous system. *Neuropharmacology*, *46*(5), 734-742. doi:10.1016/j.neuropharm.2003.11.007
- Keren-Shaul, H., Spinrad, A., Weiner, A., Matcovitch-Natan, O., Dvir-Szternfeld, R., Ulland, T. K., . . . Amit, I. (2017). A Unique Microglia Type Associated with Restricting Development of Alzheimer's Disease. *Cell*, *169*(7), 1276-1290 e1217. doi:10.1016/j.cell.2017.05.018
- Kierdorf, K., Erny, D., Goldmann, T., Sander, V., Schulz, C., Perdiguero, E. G., . . . Prinz, M. (2013). Microglia emerge from erythromyeloid precursors via Pu.1- and Irf8-dependent pathways. *Nature neuroscience*, *16*(3), 273-280. doi:10.1038/nn.3318
- Kim, C., Ho, D. H., Suk, J. E., You, S., Michael, S., Kang, J., . . . Lee, S. J. (2013). Neuron-released oligomeric alpha-synuclein is an endogenous agonist of TLR2 for paracrine activation of microglia. *Nature communications*, *4*, 1562. doi:10.1038/ncomms2534
- Kim, J., Jones, B. W., Zock, C., Chen, Z., Wang, H., Goodman, C. S., & Anderson, D. J. (1998). Isolation and characterization of mammalian homologs of the *Drosophila* gene *glial cells missing*. *Proc Natl Acad Sci U S A*, *95*(21), 12364-12369. doi:10.1073/pnas.95.21.12364
- Klein, C., & Westenberger, A. (2012). Genetics of Parkinson's disease. *Cold Spring Harb Perspect Med*, *2*(1), a008888. doi:10.1101/cshperspect.a008888
- Kleinridders, A., Schenten, D., Konner, A. C., Belgardt, B. F., Mauer, J., Okamura, T., . . . Bruning, J. C. (2009). MyD88 signaling in the CNS is required for development of fatty acid-induced leptin resistance and diet-induced obesity. *Cell Metab*, *10*(4), 249-259. doi:10.1016/j.cmet.2009.08.013
- Koellhoffer, E. C., McCullough, L. D., & Ritzel, R. M. (2017). Old Maids: Aging and Its Impact on Microglia Function. *Int J Mol Sci*, *18*(4). doi:10.3390/ijms18040769
- Kounatidis, I., & Chtarbanova, S. (2018). Role of Glial Immunity in Lifespan Determination: A *Drosophila* Perspective. *Front Immunol*, *9*, 1362. doi:10.3389/fimmu.2018.01362
- Kraakman, M. J., Murphy, A. J., Jandeleit-Dahm, K., & Kammoun, H. L. (2014). Macrophage polarization in obesity and type 2 diabetes: weighing down our understanding of macrophage function? *Front Immunol*, *5*, 470. doi:10.3389/fimmu.2014.00470
- Krabbe, G., Halle, A., Matyash, V., Rinnenthal, J. L., Eom, G. D., Bernhardt, U., . . . Heppner, F. L. (2013). Functional impairment of microglia coincides with Beta-amyloid deposition in mice with Alzheimer-like pathology. *PLOS ONE*, *8*(4), e60921. doi:10.1371/journal.pone.0060921
- Krasemann, S., Madore, C., Cialic, R., Baufeld, C., Calcagno, N., El Fatimy, R., . . . Butovsky, O. (2017). The TREM2-APOE Pathway Drives the Transcriptional Phenotype of Dysfunctional Microglia in Neurodegenerative Diseases. *Immunity*, *47*(3), 566-581 e569. doi:10.1016/j.immuni.2017.08.008
- Kraus, N. A., Ehebauer, F., Zapp, B., Rudolphi, B., Kraus, B. J., & Kraus, D. (2016). Quantitative assessment of adipocyte differentiation in cell culture. *Adipocyte*, *5*(4), 351-358. doi:10.1080/21623945.2016.1240137
- Krela-Kazmierczak, I., Szymczak-Tomczak, A., Tomczak, M., Lykowska-Szuber, L., Eder, P., Kucharski, M. A., . . . Dobrowolska, A. (2021). Is there a relation between vitamin D, interleukin-17, and

- bone mineral density in patients with inflammatory bowel disease? *Archives of medical science : AMS*, 17(3), 662-674. doi:10.5114/aoms.2018.78009
- Kunzli, K., Favre, B., Chofflon, M., & Borradori, L. (2016). One gene but different proteins and diseases: the complexity of dystonin and bullous pemphigoid antigen 1. *Exp Dermatol*, 25(1), 10-16. doi:10.1111/exd.12877
- Laffitte, E., Burkhard, P. R., Fontao, L., Jaunin, F., Saurat, J. H., Chofflon, M., & Borradori, L. (2005). Bullous pemphigoid antigen 1 isoforms: potential new target autoantigens in multiple sclerosis? *Br J Dermatol*, 152(3), 537-540. doi:10.1111/j.1365-2133.2004.06338.x
- Lai, S. L., & Lee, T. (2006). Genetic mosaic with dual binary transcriptional systems in *Drosophila*. *Nature neuroscience*, 9(5), 703-709. doi:10.1038/nn1681
- Lall, D., & Baloh, R. H. (2017). Microglia and C9orf72 in neuroinflammation and ALS and frontotemporal dementia. *J Clin Invest*, 127(9), 3250-3258. doi:10.1172/JCI90607
- Lammel, U., Bechtold, M., Risse, B., Berh, D., Fleige, A., Bunse, I., . . . Bogdan, S. (2014). The *Drosophila* FHOD1-like formin Knittrig acts through Rok to promote stress fiber formation and directed macrophage migration during the cellular immune response. *Development*, 141(6), 1366-1380. doi:10.1242/dev.101352
- Lawson, L. J., Perry, V. H., Dri, P., & Gordon, S. (1990). Heterogeneity in the distribution and morphology of microglia in the normal adult mouse brain. *Neuroscience*, 39(1), 151-170. doi:10.1016/0306-4522(90)90229-w
- Lebestky, T., Chang, T., Hartenstein, V., & Banerjee, U. (2000). Specification of *Drosophila* hematopoietic lineage by conserved transcription factors. *Science*, 288(5463), 146-149. doi:10.1126/science.288.5463.146
- Lebestky, T., Jung, S. H., & Banerjee, U. (2003). A Serrate-expressing signaling center controls *Drosophila* hematopoiesis. *Genes Dev*, 17(3), 348-353. doi:10.1101/gad.1052803
- Lee, F. K., Wong, A. K., Lee, Y. W., Wan, O. W., Chan, H. Y., & Chung, K. K. (2009). The role of ubiquitin linkages on alpha-synuclein induced-toxicity in a *Drosophila* model of Parkinson's disease. *J Neurochem*, 110(1), 208-219. doi:10.1111/j.1471-4159.2009.06124.x
- Lemaitre, B., & Hoffmann, J. (2007). The host defense of *Drosophila melanogaster*. *Annu Rev Immunol*, 25, 697-743. doi:10.1146/annurev.immunol.25.022106.141615
- Lerner, A. B., & Fitzpatrick, T. B. (1950). Biochemistry of melanin formation. *Physiol Rev*, 30(1), 91-126. doi:10.1152/physrev.1950.30.1.91
- Lessing, D., & Bonini, N. M. (2009). Maintaining the brain: insight into human neurodegeneration from *Drosophila melanogaster* mutants. *Nat Rev Genet*, 10(6), 359-370. doi:10.1038/nrg2563
- Li, Q., & Barres, B. A. (2018). Microglia and macrophages in brain homeostasis and disease. *Nature Reviews Immunology*, 18(4), 225-242. doi:10.1038/nri.2017.125
- Li, W. W., Setzu, A., Zhao, C., & Franklin, R. J. (2005). Minocycline-mediated inhibition of microglia activation impairs oligodendrocyte progenitor cell responses and remyelination in a non-immune model of demyelination. *J Neuroimmunol*, 158(1-2), 58-66. doi:10.1016/j.jneuroim.2004.08.011
- Li, Y., Du, X. F., Liu, C. S., Wen, Z. L., & Du, J. L. (2012). Reciprocal regulation between resting microglial dynamics and neuronal activity in vivo. *Dev Cell*, 23(6), 1189-1202. doi:10.1016/j.devcel.2012.10.027
- Li, Y., Han, L., Huang, C., Dai, W., Tian, G., Huang, F., . . . Zhou, Z. (2018). New Contributions to Asarum Powder on Immunology Related Toxicity Effects in Lung. *Evid Based Complement Alternat Med*, 2018, 1054032. doi:10.1155/2018/1054032
- Lian, H., Roy, E., & Zheng, H. (2016). Microglial Phagocytosis Assay. *Bio Protoc*, 6(21). doi:10.21769/BioProtoc.1988
- Liang, C. C., Park, A. Y., & Guan, J. L. (2007). In vitro scratch assay: a convenient and inexpensive method for analysis of cell migration in vitro. *Nat Protoc*, 2(2), 329-333. doi:10.1038/nprot.2007.30

- Liddelw, S. A., & Barres, B. A. (2017). Reactive Astrocytes: Production, Function, and Therapeutic Potential. *Immunity*, *46*(6), 957-967. doi:10.1016/j.immuni.2017.06.006
- Limmer, S., Weiler, A., Volkenhoff, A., Babatz, F., & Klambt, C. (2014). The Drosophila blood-brain barrier: development and function of a glial endothelium. *Front Neurosci*, *8*, 365. doi:10.3389/fnins.2014.00365
- Liongue, C., O'Sullivan, L. A., Trengove, M. C., & Ward, A. C. (2012). Evolution of JAK-STAT pathway components: mechanisms and role in immune system development. *PLOS ONE*, *7*(3), e32777. doi:10.1371/journal.pone.0032777
- Liou, H. H., Tsai, M. C., Chen, C. J., Jeng, J. S., Chang, Y. C., Chen, S. Y., & Chen, R. C. (1997). Environmental risk factors and Parkinson's disease: a case-control study in Taiwan. *Neurology*, *48*(6), 1583-1588. doi:10.1212/wnl.48.6.1583
- Lisi, L., Ciotti, G. M., Braun, D., Kalinin, S., Curro, D., Dello Russo, C., . . . Navarra, P. (2017). Expression of iNOS, CD163 and ARG-1 taken as M1 and M2 markers of microglial polarization in human glioblastoma and the surrounding normal parenchyma. *Neurosci Lett*, *645*, 106-112. doi:10.1016/j.neulet.2017.02.076
- Liu, H., Han, Y., Wang, T., Zhang, H., Xu, Q., Yuan, J., & Li, Z. (2020). Targeting Microglia for Therapy of Parkinson's Disease by Using Biomimetic Ultrasmall Nanoparticles. *J Am Chem Soc*, *142*(52), 21730-21742. doi:10.1021/jacs.0c09390
- Liu, H. C., Zheng, M. H., Du, Y. L., Wang, L., Kuang, F., Qin, H. Y., . . . Han, H. (2012). N9 microglial cells polarized by LPS and IL4 show differential responses to secondary environmental stimuli. *Cell Immunol*, *278*(1-2), 84-90. doi:10.1016/j.cellimm.2012.06.001
- Liu, L., Dopping-Hepenstal, P. J., Lovell, P. A., Michael, M., Horn, H., Fong, K., . . . McGrath, J. A. (2012). Autosomal recessive epidermolysis bullosa simplex due to loss of BPAG1-e expression. *J Invest Dermatol*, *132*(3 Pt 1), 742-744. doi:10.1038/jid.2011.379
- Liu, X., Xu, N., & Zhang, S. (2013). Calreticulin is a microbial-binding molecule with phagocytosis-enhancing capacity. *Fish Shellfish Immunol*, *35*(3), 776-784. doi:10.1016/j.fsi.2013.06.013
- Liu, Z., Yu, S., & Manley, N. R. (2007). Gcm2 is required for the differentiation and survival of parathyroid precursor cells in the parathyroid/thymus primordia. *Dev Biol*, *305*(1), 333-346. doi:10.1016/j.ydbio.2007.02.014
- Lively, S., & Schlichter, L. C. (2013). The microglial activation state regulates migration and roles of matrix-dissolving enzymes for invasion. *J Neuroinflammation*, *10*, 75. doi:10.1186/1742-2094-10-75
- Lloyd, A. F., Davies, C. L., & Miron, V. E. (2017). Microglia: origins, homeostasis, and roles in myelin repair. *Curr Opin Neurobiol*, *47*, 113-120. doi:10.1016/j.conb.2017.10.001
- Loma, I., & Heyman, R. (2011). Multiple sclerosis: pathogenesis and treatment. *Curr Neuropharmacol*, *9*(3), 409-416. doi:10.2174/157015911796557911
- Long, J. M., Kalehua, A. N., Muth, N. J., Hengemihle, J. M., Jucker, M., Calhoun, M. E., . . . Mouton, P. R. (1998). Stereological estimation of total microglia number in mouse hippocampus. *J Neurosci Methods*, *84*(1-2), 101-108. doi:10.1016/s0165-0270(98)00100-9
- Longbrake, E. E., Lai, W., Ankeny, D. P., & Popovich, P. G. (2007). Characterization and modeling of monocyte-derived macrophages after spinal cord injury. *J Neurochem*, *102*(4), 1083-1094. doi:10.1111/j.1471-4159.2007.04617.x
- Lopez-Otin, C., Blasco, M. A., Partridge, L., Serrano, M., & Kroemer, G. (2013). The hallmarks of aging. *Cell*, *153*(6), 1194-1217. doi:10.1016/j.cell.2013.05.039
- Loureiro, A., & da Silva, G. J. (2019). CRISPR-Cas: Converting A Bacterial Defence Mechanism into A State-of-the-Art Genetic Manipulation Tool. *Antibiotics (Basel)*, *8*(1). doi:10.3390/antibiotics8010018
- Lucin, K. M., O'Brien, C. E., Bieri, G., Czirr, E., Mosher, K. I., Abbey, R. J., . . . Wyss-Coray, T. (2013). Microglial beclin 1 regulates retromer trafficking and phagocytosis and is impaired in Alzheimer's disease. *Neuron*, *79*(5), 873-886. doi:10.1016/j.neuron.2013.06.046

- Lue, N. F., Chasman, D. I., Buchman, A. R., & Kornberg, R. D. (1987). Interaction of GAL4 and GAL80 gene regulatory proteins in vitro. *Mol Cell Biol*, *7*(10), 3446-3451. doi:10.1128/mcb.7.10.3446-3451.1987
- MacDonald, J. M., Beach, M. G., Porpiglia, E., Sheehan, A. E., Watts, R. J., & Freeman, M. R. (2006). The Drosophila cell corpse engulfment receptor Draper mediates glial clearance of severed axons. *Neuron*, *50*(6), 869-881. doi:10.1016/j.neuron.2006.04.028
- Machnicka, B., Czogalla, A., Hryniewicz-Jankowska, A., Boguslawska, D. M., Grochowalska, R., Heger, E., & Sikorski, A. F. (2014). Spectrins: a structural platform for stabilization and activation of membrane channels, receptors and transporters. *Biochim Biophys Acta*, *1838*(2), 620-634. doi:10.1016/j.bbamem.2013.05.002
- Maitra, U., Scaglione, M. N., Chtarbanova, S., & O'Donnell, J. M. (2019). Innate immune responses to paraquat exposure in a Drosophila model of Parkinson's disease. *Sci Rep*, *9*(1), 12714. doi:10.1038/s41598-019-48977-6
- Manfruelli, P., Reichhart, J. M., Steward, R., Hoffmann, J. A., & Lemaitre, B. (1999). A mosaic analysis in Drosophila fat body cells of the control of antimicrobial peptide genes by the Rel proteins Dorsal and DIF. *Embo j*, *18*(12), 3380-3391. doi:10.1093/emboj/18.12.3380
- Markus, R., Laurinyecz, B., Kurucz, E., Honti, V., Bajusz, I., Sipos, B., . . . Ando, I. (2009). Sessile hemocytes as a hematopoietic compartment in Drosophila melanogaster. *Proc Natl Acad Sci U S A*, *106*(12), 4805-4809. doi:10.1073/pnas.0801766106
- Martinek, N., Shahab, J., Saathoff, M., & Ringuette, M. (2008). Haemocyte-derived SPARC is required for collagen-IV-dependent stability of basal laminae in Drosophila embryos. *J Cell Sci*, *121*(Pt 10), 1671-1680. doi:10.1242/jcs.021931
- Martinelli, C., & Reichhart, J. M. (2005). Evolution and integration of innate immune systems from fruit flies to man: lessons and questions. *J Endotoxin Res*, *11*(4), 243-248. doi:10.1179/096805105X37411
- Martinez, F. O., Helming, L., & Gordon, S. (2009). Alternative activation of macrophages: an immunologic functional perspective. *Annu Rev Immunol*, *27*, 451-483. doi:10.1146/annurev.immunol.021908.132532
- Matcovitch-Natan, O., Winter, D. R., Giladi, A., Vargas Aguilar, S., Spinrad, A., Sarrazin, S., . . . Amit, I. (2016). Microglia development follows a stepwise program to regulate brain homeostasis. *Science*, *353*(6301), aad8670. doi:10.1126/science.aad8670
- Mattiace, L. A., Davies, P., Yen, S. H., & Dickson, D. W. (1990). Microglia in cerebellar plaques in Alzheimer's disease. *Acta Neuropathol*, *80*(5), 493-498. doi:10.1007/BF00294609
- Mazaheri, F., Breus, O., Durdu, S., Haas, P., Wittbrodt, J., Gilmour, D., & Peri, F. (2014). Distinct roles for BAI1 and TIM-4 in the engulfment of dying neurons by microglia. *Nature communications*, *5*, 4046. doi:10.1038/ncomms5046
- McGrath, K. E., Frame, J. M., Fegan, K. H., Bowen, J. R., Conway, S. J., Catherman, S. C., . . . Palis, J. (2015). Distinct Sources of Hematopoietic Progenitors Emerge before HSCs and Provide Functional Blood Cells in the Mammalian Embryo. *Cell reports*, *11*(12), 1892-1904. doi:10.1016/j.celrep.2015.05.036
- McGrath, K. E., Frame, J. M., & Palis, J. (2015). Early hematopoiesis and macrophage development. *Seminars in immunology*, *27*(6), 379-387. doi:10.1016/j.smim.2016.03.013
- Medvinsky, A., & Dzierzak, E. (1996). Definitive hematopoiesis is autonomously initiated by the AGM region. *Cell*, *86*(6), 897-906. doi:10.1016/s0092-8674(00)80165-8
- Mendes, N. F., Kim, Y. B., Velloso, L. A., & Araujo, E. P. (2018). Hypothalamic Microglial Activation in Obesity: A Mini-Review. *Front Neurosci*, *12*, 846. doi:10.3389/fnins.2018.00846
- Michael, M., Begum, R., Fong, K., Pourreyrone, C., South, A. P., McGrath, J. A., & Parsons, M. (2014). BPAG1-e restricts keratinocyte migration through control of adhesion stability. *J Invest Dermatol*, *134*(3), 773-782. doi:10.1038/jid.2013.382

- Michell-Robinson, M. A., Touil, H., Healy, L. M., Owen, D. R., Durafourt, B. A., Bar-Or, A., . . . Moore, C. S. (2015). Roles of microglia in brain development, tissue maintenance and repair. *Brain*, *138*(Pt 5), 1138-1159. doi:10.1093/brain/awv066
- Milanski, M., Degasperi, G., Coope, A., Morari, J., Denis, R., Cintra, D. E., . . . Velloso, L. A. (2009). Saturated fatty acids produce an inflammatory response predominantly through the activation of TLR4 signaling in hypothalamus: implications for the pathogenesis of obesity. *The Journal of neuroscience : the official journal of the Society for Neuroscience*, *29*(2), 359-370. doi:10.1523/JNEUROSCI.2760-08.2009
- Miller, A. A., Bernardoni, R., & Giangrande, A. (1998). Positive autoregulation of the glial promoting factor glide/gcm. *Embo j*, *17*(21), 6316-6326. doi:10.1093/emboj/17.21.6316
- Milner, R. (2009). Microglial expression of alphavbeta3 and alphavbeta5 integrins is regulated by cytokines and the extracellular matrix: beta5 integrin null microglia show no defects in adhesion or MMP-9 expression on vitronectin. *Glia*, *57*(7), 714-723. doi:10.1002/glia.20799
- Milner, R., & Campbell, I. L. (2002). Cytokines regulate microglial adhesion to laminin and astrocyte extracellular matrix via protein kinase C-dependent activation of the alpha6beta1 integrin. *The Journal of neuroscience : the official journal of the Society for Neuroscience*, *22*(5), 1562-1572.
- Milner, R., & Campbell, I. L. (2003). The extracellular matrix and cytokines regulate microglial integrin expression and activation. *Journal of immunology*, *170*(7), 3850-3858. doi:10.4049/jimmunol.170.7.3850
- Miron, V. E., Boyd, A., Zhao, J. W., Yuen, T. J., Ruckh, J. M., Shadrach, J. L., . . . Ffrench-Constant, C. (2013). M2 microglia and macrophages drive oligodendrocyte differentiation during CNS remyelination. *Nature neuroscience*, *16*(9), 1211-1218. doi:10.1038/nn.3469
- Molawi, K., Wolf, Y., Kandalla, P. K., Favret, J., Hagemeyer, N., Frenzel, K., . . . Sieweke, M. H. (2014). Progressive replacement of embryo-derived cardiac macrophages with age. *J Exp Med*, *211*(11), 2151-2158. doi:10.1084/jem.20140639
- Molkentin, J. D. (2000). The zinc finger-containing transcription factors GATA-4, -5, and -6. Ubiquitously expressed regulators of tissue-specific gene expression. *Journal of Biological Chemistry*, *275*(50), 38949-38952. doi:10.1074/jbc.R000029200
- Montell, D. J. (2003). Border-cell migration: the race is on. *Nat Rev Mol Cell Biol*, *4*(1), 13-24. doi:10.1038/nrm1006
- Moore, D. J., West, A. B., Dawson, V. L., & Dawson, T. M. (2005). Molecular pathophysiology of Parkinson's disease. *Annu Rev Neurosci*, *28*, 57-87. doi:10.1146/annurev.neuro.28.061604.135718
- Moreira, C. G., Jacinto, A., & Prag, S. (2013). Drosophila integrin adhesion complexes are essential for hemocyte migration in vivo. *Biol Open*, *2*(8), 795-801. doi:10.1242/bio.20134564
- Myers, M. G., Jr., & Olson, D. P. (2012). Central nervous system control of metabolism. *Nature*, *491*(7424), 357-363. doi:10.1038/nature11705
- Myllymaki, H., & Ramet, M. (2014). JAK/STAT pathway in Drosophila immunity. *Scand J Immunol*, *79*(6), 377-385. doi:10.1111/sji.12170
- Nait-Oumesmar, B., Copperman, A. B., & Lazzarini, R. A. (2000). Placental expression and chromosomal localization of the human Gcm 1 gene. *J Histochem Cytochem*, *48*(7), 915-922. doi:10.1177/002215540004800704
- Naito, M., Yamamura, F., Nishikawa, S., & Takahashi, K. (1989). Development, differentiation, and maturation of fetal mouse yolk sac macrophages in cultures. *J Leukoc Biol*, *46*(1), 1-10. doi:10.1002/jlb.46.1.1
- Nashchekin, D., Fernandes, A. R., & St Johnston, D. (2016). Patronin/Shot Cortical Foci Assemble the Noncentrosomal Microtubule Array that Specifies the Drosophila Anterior-Posterior Axis. *Dev Cell*, *38*(1), 61-72. doi:10.1016/j.devcel.2016.06.010

- Navarro, V., Sanchez-Mejias, E., Jimenez, S., Munoz-Castro, C., Sanchez-Varo, R., Davila, J. C., . . . Vitorica, J. (2018). Microglia in Alzheimer's Disease: Activated, Dysfunctional or Degenerative. *Front Aging Neurosci*, *10*, 140. doi:10.3389/fnagi.2018.00140
- Nikodemova, M., Kimyon, R. S., De, I., Small, A. L., Collier, L. S., & Watters, J. J. (2015). Microglial numbers attain adult levels after undergoing a rapid decrease in cell number in the third postnatal week. *J Neuroimmunol*, *278*, 280-288. doi:10.1016/j.jneuroim.2014.11.018
- Nimmerjahn, A., Kirchhoff, F., & Helmchen, F. (2005). Resting microglial cells are highly dynamic surveillants of brain parenchyma in vivo. *Science*, *308*(5726), 1314-1318. doi:10.1126/science.1110647
- Nissen, J. C., Thompson, K. K., West, B. L., & Tsirka, S. E. (2018). Csf1R inhibition attenuates experimental autoimmune encephalomyelitis and promotes recovery. *Exp Neurol*, *307*, 24-36. doi:10.1016/j.expneurol.2018.05.021
- Noda, H., Takeuchi, H., Mizuno, T., & Suzumura, A. (2013). Fingolimod phosphate promotes the neuroprotective effects of microglia. *J Neuroimmunol*, *256*(1-2), 13-18. doi:10.1016/j.jneuroim.2012.12.005
- Norden, D. M., & Godbout, J. P. (2013). Review: microglia of the aged brain: primed to be activated and resistant to regulation. *Neuropathol Appl Neurobiol*, *39*(1), 19-34. doi:10.1111/j.1365-2990.2012.01306.x
- Norden, D. M., Muccigrosso, M. M., & Godbout, J. P. (2015). Microglial priming and enhanced reactivity to secondary insult in aging, and traumatic CNS injury, and neurodegenerative disease. *Neuropharmacology*, *96*(Pt A), 29-41. doi:10.1016/j.neuropharm.2014.10.028
- Novak, M. L., & Koh, T. J. (2013). Macrophage phenotypes during tissue repair. *J Leukoc Biol*, *93*(6), 875-881. doi:10.1189/jlb.1012512
- Nye, J., Buster, D. W., & Rogers, G. C. (2014). The use of cultured Drosophila cells for studying the microtubule cytoskeleton. *Methods Mol Biol*, *1136*, 81-101. doi:10.1007/978-1-4939-0329-0_6
- Ogura, K., Ogawa, M., & Yoshida, M. (1994). Effects of ageing on microglia in the normal rat brain: immunohistochemical observations. *Neuroreport*, *5*(10), 1224-1226. doi:10.1097/00001756-199406020-00016
- Orre, M., Kamphuis, W., Osborn, L. M., Melief, J., Kooijman, L., Huitinga, I., . . . Hol, E. M. (2014). Acute isolation and transcriptome characterization of cortical astrocytes and microglia from young and aged mice. *Neurobiol Aging*, *35*(1), 1-14. doi:10.1016/j.neurobiolaging.2013.07.008
- Ortega-Gomez, A., Perretti, M., & Soehnlein, O. (2013). Resolution of inflammation: an integrated view. *EMBO Mol Med*, *5*(5), 661-674. doi:10.1002/emmm.201202382
- Ovanesov, M. V., Sauder, C., Rubin, S. A., Richt, J., Nath, A., Carbone, K. M., & Pletnikov, M. V. (2006). Activation of microglia by borna disease virus infection: in vitro study. *J Virol*, *80*(24), 12141-12148. doi:10.1128/JVI.01648-06
- Palis, J. (2016). Interaction of the Macrophage and Primitive Erythroid Lineages in the Mammalian Embryo. *Front Immunol*, *7*, 669. doi:10.3389/fimmu.2016.00669
- Palis, J., Robertson, S., Kennedy, M., Wall, C., & Keller, G. (1999). Development of erythroid and myeloid progenitors in the yolk sac and embryo proper of the mouse. *Development*, *126*(22), 5073-5084.
- Palis, J., & Yoder, M. C. (2001). Yolk-sac hematopoiesis: the first blood cells of mouse and man. *Exp Hematol*, *29*(8), 927-936. doi:10.1016/s0301-472x(01)00669-5
- Pan, Y., Lloyd, C., Zhou, H., Dolich, S., Deeds, J., Gonzalo, J. A., . . . Gearing, D. (1997). Neurotactin, a membrane-anchored chemokine upregulated in brain inflammation. *Nature*, *387*(6633), 611-617. doi:10.1038/42491
- Paolicelli, R. C., Bolasco, G., Pagani, F., Maggi, L., Scianni, M., Panzanelli, P., . . . Gross, C. T. (2011). Synaptic pruning by microglia is necessary for normal brain development. *Science*, *333*(6048), 1456-1458. doi:10.1126/science.1202529

- Peissig, K., Condie, B. G., & Manley, N. R. (2018). Embryology of the Parathyroid Glands. *Endocrinol Metab Clin North Am*, 47(4), 733-742. doi:10.1016/j.ecl.2018.07.002
- Perdiguero, E. G., Klapproth, K., Schulz, C., Busch, K., de Bruijn, M., Rodewald, H. R., & Geissmann, F. (2015). The Origin of Tissue-Resident Macrophages: When an Erythro-myeloid Progenitor Is an Erythro-myeloid Progenitor. *Immunity*, 43(6), 1023-1024. doi:10.1016/j.immuni.2015.11.022
- Peri, F., & Nusslein-Volhard, C. (2008). Live imaging of neuronal degradation by microglia reveals a role for v0-ATPase a1 in phagosomal fusion in vivo. *Cell*, 133(5), 916-927. doi:10.1016/j.cell.2008.04.037
- Perry, J. R., Hsu, Y. H., Chasman, D. I., Johnson, A. D., Elks, C., Albrecht, E., . . . Murray, A. (2014). DNA mismatch repair gene MSH6 implicated in determining age at natural menopause. *Hum Mol Genet*, 23(9), 2490-2497. doi:10.1093/hmg/ddt620
- Perry, V. H., Matyszak, M. K., & Fearn, S. (1993). Altered antigen expression of microglia in the aged rodent CNS. *Glia*, 7(1), 60-67. doi:10.1002/glia.440070111
- Petersen, A. J., & Wassarman, D. A. (2012). Drosophila innate immune response pathways moonlight in neurodegeneration. *Fly (Austin)*, 6(3), 169-172. doi:10.4161/fly.20999
- Piccio, L., Buonsanti, C., Mariani, M., Cella, M., Gilfillan, S., Cross, A. H., . . . Panina-Bordignon, P. (2007). Blockade of TREM-2 exacerbates experimental autoimmune encephalomyelitis. *Eur J Immunol*, 37(5), 1290-1301. doi:10.1002/eji.200636837
- Pierce, S., & Coetzee, G. A. (2017). Parkinson's disease-associated genetic variation is linked to quantitative expression of inflammatory genes. *PLOS ONE*, 12(4), e0175882. doi:10.1371/journal.pone.0175882
- Pignoni, F., & Zipursky, S. L. (1997). Induction of Drosophila eye development by decapentaplegic. *Development*, 124(2), 271-278.
- Pimentel, G. D., Ganeshan, K., & Carnevali, J. B. (2014). Hypothalamic inflammation and the central nervous system control of energy homeostasis. *Mol Cell Endocrinol*, 397(1-2), 15-22. doi:10.1016/j.mce.2014.06.005
- Pinheiro, L. P., Linden, R., & Mariante, R. M. (2015). Activation and function of murine primary microglia in the absence of the prion protein. *J Neuroimmunol*, 286, 25-32. doi:10.1016/j.jneuroim.2015.07.002
- Poliakova, K., Adebola, A., Leung, C. L., Favre, B., Liem, R. K., Schepens, I., & Borradori, L. (2014). BPAG1a and b associate with EB1 and EB3 and modulate vesicular transport, Golgi apparatus structure, and cell migration in C2.7 myoblasts. *PLOS ONE*, 9(9), e107535. doi:10.1371/journal.pone.0107535
- Polymeropoulos, M. H., Lavedan, C., Leroy, E., Ide, S. E., Dehejia, A., Dutra, A., . . . Nussbaum, R. L. (1997). Mutation in the alpha-synuclein gene identified in families with Parkinson's disease. *Science*, 276(5321), 2045-2047. doi:10.1126/science.276.5321.2045
- Prokop, A., Martin-Bermudo, M. D., Bate, M., & Brown, N. H. (1998). Absence of PS integrins or laminin A affects extracellular adhesion, but not intracellular assembly, of hemiadherens and neuromuscular junctions in Drosophila embryos. *Dev Biol*, 196(1), 58-76. doi:10.1006/dbio.1997.8830
- Ragone, G., Van De Bor, V., Sorrentino, S., Kammerer, M., Galy, A., Schenck, A., . . . Giangrande, A. (2003). Transcriptional regulation of glial cell specification. *Dev Biol*, 255(1), 138-150. doi:10.1016/s0012-1606(02)00081-7
- Rahman, A., Rao, M. S., & Khan, K. M. (2018). Intraventricular infusion of quinolinic acid impairs spatial learning and memory in young rats: a novel mechanism of lead-induced neurotoxicity. *J Neuroinflammation*, 15(1), 263. doi:10.1186/s12974-018-1306-2
- Rangaraju, S., Raza, S. A., Li, N. X., Betarbet, R., Dammer, E. B., Duong, D., . . . Levey, A. I. (2018). Differential Phagocytic Properties of CD45(low) Microglia and CD45(high) Brain Mononuclear Phagocytes-Activation and Age-Related Effects. *Front Immunol*, 9, 405. doi:10.3389/fimmu.2018.00405

- Ransick, A., & Davidson, E. H. (2006). cis-regulatory processing of Notch signaling input to the sea urchin glial cells missing gene during mesoderm specification. *Dev Biol*, *297*(2), 587-602. doi:10.1016/j.ydbio.2006.05.037
- Ransick, A., & Davidson, E. H. (2012). Cis-regulatory logic driving glial cells missing: self-sustaining circuitry in later embryogenesis. *Dev Biol*, *364*(2), 259-267. doi:10.1016/j.ydbio.2012.02.003
- Ransohoff, R. M. (2016). A polarizing question: do M1 and M2 microglia exist? *Nature neuroscience*, *19*(8), 987-991. doi:10.1038/nn.4338
- Rast, J. P., Smith, L. C., Loza-Coll, M., Hibino, T., & Litman, G. W. (2006). Genomic insights into the immune system of the sea urchin. *Science*, *314*(5801), 952-956. doi:10.1126/science.1134301
- Reemst, K., Noctor, S. C., Lucassen, P. J., & Hol, E. M. (2016). The Indispensable Roles of Microglia and Astrocytes during Brain Development. *Front Hum Neurosci*, *10*, 566. doi:10.3389/fnhum.2016.00566
- Reichert, H. (2011). Drosophila neural stem cells: cell cycle control of self-renewal, differentiation, and termination in brain development. *Results Probl Cell Differ*, *53*, 529-546. doi:10.1007/978-3-642-19065-0_21
- Reifegerste, R., Schreiber, J., Gulland, S., Ludemann, A., & Wegner, M. (1999). mGCMa is a murine transcription factor that overrides cell fate decisions in Drosophila. *Mechanisms of development*, *82*(1-2), 141-150. doi:10.1016/s0925-4773(99)00027-1
- Rival, T., Soustelle, L., Cattaert, D., Strambi, C., Iche, M., & Birman, S. (2006). Physiological requirement for the glutamate transporter dEAAT1 at the adult Drosophila neuromuscular junction. *J Neurobiol*, *66*(10), 1061-1074. doi:10.1002/neu.20270
- Rizki, T. M., & Rizki, R. M. (1978). Larval adipose tissue of homoecotic bithorax mutants of Drosophila. *Dev Biol*, *65*(2), 476-482. doi:10.1016/0012-1606(78)90042-8
- Rogers, J., & Rovigatti, U. (1988). Immunologic and tissue culture approaches to the neurobiology of aging. *Neurobiol Aging*, *9*(5-6), 759-762. doi:10.1016/s0197-4580(88)80143-x
- Roper, K., Gregory, S. L., & Brown, N. H. (2002). The 'spectraplakins': cytoskeletal giants with characteristics of both spectrin and plakin families. *J Cell Sci*, *115*(Pt 22), 4215-4225. doi:10.1242/jcs.00157
- Ruan, C., Sun, L., Kroshilina, A., Beckers, L., De Jager, P., Bradshaw, E. M., . . . Elyaman, W. (2020). A novel Tmem119-tdTomato reporter mouse model for studying microglia in the central nervous system. *Brain Behav Immun*, *83*, 180-191. doi:10.1016/j.bbi.2019.10.009
- Ruffell, D., Mourkioti, F., Gambardella, A., Kirstetter, P., Lopez, R. G., Rosenthal, N., & Nerlov, C. (2009). A CREB-C/EBPbeta cascade induces M2 macrophage-specific gene expression and promotes muscle injury repair. *Proc Natl Acad Sci U S A*, *106*(41), 17475-17480. doi:10.1073/pnas.0908641106
- Safaiyan, S., Kannaiyan, N., Snaidero, N., Brioschi, S., Biber, K., Yona, S., . . . Simons, M. (2016). Age-related myelin degradation burdens the clearance function of microglia during aging. *Nature neuroscience*, *19*(8), 995-998. doi:10.1038/nn.4325
- Sanchez-Guajardo, V., Tentillier, N., & Romero-Ramos, M. (2015). The relation between alpha-synuclein and microglia in Parkinson's disease: Recent developments. *Neuroscience*, *302*, 47-58. doi:10.1016/j.neuroscience.2015.02.008
- Satoh, J., Kino, Y., Asahina, N., Takitani, M., Miyoshi, J., Ishida, T., & Saito, Y. (2016). TMEM119 marks a subset of microglia in the human brain. *Neuropathology*, *36*(1), 39-49. doi:10.1111/neup.12235
- Saulnier, R., De Repentigny, Y., Yong, V. W., & Kothary, R. (2002). Alterations in myelination in the central nervous system of dystonia musculorum mice. *J Neurosci Res*, *69*(2), 233-242. doi:10.1002/jnr.10289
- Schafer, D. P., Lehrman, E. K., Kautzman, A. G., Koyama, R., Mardinly, A. R., Yamasaki, R., . . . Stevens, B. (2012). Microglia sculpt postnatal neural circuits in an activity and complement-dependent manner. *Neuron*, *74*(4), 691-705. doi:10.1016/j.neuron.2012.03.026

- Schreiber, J., Riethmacher-Sonnenberg, E., Riethmacher, D., Tuerk, E. E., Enderich, J., Bosl, M. R., & Wegner, M. (2000). Placental failure in mice lacking the mammalian homolog of glial cells missing, GCMa. *Mol Cell Biol*, *20*(7), 2466-2474. doi:10.1128/MCB.20.7.2466-2474.2000
- Schreiber, J., Sock, E., & Wegner, M. (1997). The regulator of early gliogenesis glial cells missing is a transcription factor with a novel type of DNA-binding domain. *Proc Natl Acad Sci U S A*, *94*(9), 4739-4744. doi:10.1073/pnas.94.9.4739
- Schulz, C., Gomez Perdiguero, E., Chorro, L., Szabo-Rogers, H., Cagnard, N., Kierdorf, K., . . . Geissmann, F. (2012). A lineage of myeloid cells independent of Myb and hematopoietic stem cells. *Science*, *336*(6077), 86-90. doi:10.1126/science.1219179
- Sethi, S., & Wang, J. W. (2017). A versatile genetic tool for post-translational control of gene expression in *Drosophila melanogaster*. *eLife*, *6*. doi:10.7554/eLife.30327
- Sharaby, Y., Lahmi, R., Amar, O., Elbaz, I., Lerer-Goldshtein, T., Weiss, A. M., . . . Tzur, A. (2014). Gas2l3 is essential for brain morphogenesis and development. *Dev Biol*, *394*(2), 305-313. doi:10.1016/j.ydbio.2014.08.006
- Shechter, R., & Schwartz, M. (2013a). CNS sterile injury: just another wound healing? *Trends Mol Med*, *19*(3), 135-143. doi:10.1016/j.molmed.2012.11.007
- Shechter, R., & Schwartz, M. (2013b). Harnessing monocyte-derived macrophages to control central nervous system pathologies: no longer 'if' but 'how'. *J Pathol*, *229*(2), 332-346. doi:10.1002/path.4106
- Sheffield, L. G., & Berman, N. E. (1998). Microglial expression of MHC class II increases in normal aging of nonhuman primates. *Neurobiol Aging*, *19*(1), 47-55. doi:10.1016/s0197-4580(97)00168-1
- Shimbo, T., Tanemura, A., Yamazaki, T., Tamai, K., Katayama, I., & Kaneda, Y. (2010). Serum anti-BPAG1 auto-antibody is a novel marker for human melanoma. *PLOS ONE*, *5*(5), e10566. doi:10.1371/journal.pone.0010566
- Siddiqui, T. A., Lively, S., & Schlichter, L. C. (2016). Complex molecular and functional outcomes of single versus sequential cytokine stimulation of rat microglia. *J Neuroinflammation*, *13*(1), 66. doi:10.1186/s12974-016-0531-9
- Sierra, A., Encinas, J. M., Deudero, J. J., Chancey, J. H., Enikolopov, G., Overstreet-Wadiche, L. S., . . . Maletic-Savatic, M. (2010). Microglia shape adult hippocampal neurogenesis through apoptosis-coupled phagocytosis. *Cell Stem Cell*, *7*(4), 483-495. doi:10.1016/j.stem.2010.08.014
- Singleton, A. B., Farrer, M., Johnson, J., Singleton, A., Hague, S., Kachergus, J., . . . Gwinn-Hardy, K. (2003). alpha-Synuclein locus triplication causes Parkinson's disease. *Science*, *302*(5646), 841. doi:10.1126/science.1090278
- Slep, K. C., Rogers, S. L., Elliott, S. L., Ohkura, H., Kolodziej, P. A., & Vale, R. D. (2005). Structural determinants for EB1-mediated recruitment of APC and spectraplakins to the microtubule plus end. *Journal of Cell Biology*, *168*(4), 587-598. doi:10.1083/jcb.200410114
- Sloane, J. A., Hollander, W., Moss, M. B., Rosene, D. L., & Abraham, C. R. (1999). Increased microglial activation and protein nitration in white matter of the aging monkey. *Neurobiol Aging*, *20*(4), 395-405. doi:10.1016/s0197-4580(99)00066-4
- Small, C., Paddibhatla, I., Rajwani, R., & Govind, S. (2012). An introduction to parasitic wasps of *Drosophila* and the antiparasite immune response. *J Vis Exp*(63), e3347. doi:10.3791/3347
- Song, X., Jin, P., Qin, S., Chen, L., & Ma, F. (2012). The evolution and origin of animal Toll-like receptor signaling pathway revealed by network-level molecular evolutionary analyses. *PLOS ONE*, *7*(12), e51657. doi:10.1371/journal.pone.0051657
- Sonnenberg, A., & Liem, R. K. (2007). Plakins in development and disease. *Exp Cell Res*, *313*(10), 2189-2203. doi:10.1016/j.yexcr.2007.03.039
- Soustelle, L., & Giangrande, A. (2007). Novel gcm-dependent lineages in the postembryonic nervous system of *Drosophila melanogaster*. *Dev Dyn*, *236*(8), 2101-2108. doi:10.1002/dvdy.21232




- Stecca, B., Nait-Oumesmar, B., Kelley, K. A., Voss, A. K., Thomas, T., & Lazzarini, R. A. (2002). Gcm1 expression defines three stages of chorio-allantoic interaction during placental development. *Mechanisms of development*, 115(1-2), 27-34. doi:10.1016/s0925-4773(02)00095-3
- Stein, M., Keshav, S., Harris, N., & Gordon, S. (1992). Interleukin 4 potently enhances murine macrophage mannose receptor activity: a marker of alternative immunologic macrophage activation. *J Exp Med*, 176(1), 287-292. doi:10.1084/jem.176.1.287
- Streit, W. J., Sammons, N. W., Kuhns, A. J., & Sparks, D. L. (2004). Dystrophic microglia in the aging human brain. *Glia*, 45(2), 208-212. doi:10.1002/glia.10319
- Streit, W. J., & Sparks, D. L. (1997). Activation of microglia in the brains of humans with heart disease and hypercholesterolemic rabbits. *J Mol Med (Berl)*, 75(2), 130-138. doi:10.1007/s001090050097
- Stroud, M. J., Banerjee, I., Veevers, J., & Chen, J. (2014). Linker of nucleoskeleton and cytoskeleton complex proteins in cardiac structure, function, and disease. *Circ Res*, 114(3), 538-548. doi:10.1161/CIRCRESAHA.114.301236
- Struhl, G., & Basler, K. (1993). Organizing activity of wingless protein in *Drosophila*. *Cell*, 72(4), 527-540. doi:10.1016/0092-8674(93)90072-x
- Subramaniam, S. R., & Federoff, H. J. (2017). Targeting Microglial Activation States as a Therapeutic Avenue in Parkinson's Disease. *Front Aging Neurosci*, 9, 176. doi:10.3389/fnagi.2017.00176
- Subramanian, A., Prokop, A., Yamamoto, M., Sugimura, K., Uemura, T., Betschinger, J., . . . Volk, T. (2003). Shortstop recruits EB1/APC1 and promotes microtubule assembly at the muscle-tendon junction. *Curr Biol*, 13(13), 1086-1095. doi:10.1016/s0960-9822(03)00416-0
- Sullivan, J. C., Sher, D., Eisenstein, M., Shigesada, K., Reitzel, A. M., Marlow, H., . . . Gat, U. (2008). The evolutionary origin of the Runx/CBFbeta transcription factors--studies of the most basal metazoans. *BMC Evol Biol*, 8, 228. doi:10.1186/1471-2148-8-228
- Sun, Y., Yolitz, J., Wang, C., Spangler, E., Zhan, M., & Zou, S. (2013). Aging studies in *Drosophila melanogaster*. *Methods Mol Biol*, 1048, 77-93. doi:10.1007/978-1-62703-556-9_7
- Sykova, E., Mazel, T., & Simonova, Z. (1998). Diffusion constraints and neuron-glia interaction during aging. *Exp Gerontol*, 33(7-8), 837-851. doi:10.1016/s0531-5565(98)00038-2
- Takahashi, K., Prinz, M., Stagi, M., Chechneva, O., & Neumann, H. (2007). TREM2-transduced myeloid precursors mediate nervous tissue debris clearance and facilitate recovery in an animal model of multiple sclerosis. *PLoS Med*, 4(4), e124. doi:10.1371/journal.pmed.0040124
- Takahashi, K., Yamamura, F., & Naito, M. (1989). Differentiation, maturation, and proliferation of macrophages in the mouse yolk sac: a light-microscopic, enzyme-cytochemical, immunohistochemical, and ultrastructural study. *J Leukoc Biol*, 45(2), 87-96. doi:10.1002/jlb.45.2.87
- Tamoutounour, S., Guillemins, M., Montanana Sanchis, F., Liu, H., Terhorst, D., Malosse, C., . . . Henri, S. (2013). Origins and functional specialization of macrophages and of conventional and monocyte-derived dendritic cells in mouse skin. *Immunity*, 39(5), 925-938. doi:10.1016/j.immuni.2013.10.004
- Tang, Y., & Le, W. (2016). Differential Roles of M1 and M2 Microglia in Neurodegenerative Diseases. *Mol Neurobiol*, 53(2), 1181-1194. doi:10.1007/s12035-014-9070-5
- Tanji, T., & Ip, Y. T. (2005). Regulators of the Toll and Imd pathways in the *Drosophila* innate immune response. *Trends Immunol*, 26(4), 193-198. doi:10.1016/j.it.2005.02.006
- Tay, T. L., Mai, D., Dautzenberg, J., Fernandez-Klett, F., Lin, G., Sagar, . . . Prinz, M. (2017). A new fate mapping system reveals context-dependent random or clonal expansion of microglia. *Nature neuroscience*, 20(6), 793-803. doi:10.1038/nn.4547
- Taylor, P. R., Reid, D. M., Heinsbroek, S. E., Brown, G. D., Gordon, S., & Wong, S. Y. (2005). Dectin-2 is predominantly myeloid restricted and exhibits unique activation-dependent expression on

- maturing inflammatory monocytes elicited in vivo. *Eur J Immunol*, 35(7), 2163-2174. doi:10.1002/eji.200425785
- Tepass, U., Fessler, L. I., Aziz, A., & Hartenstein, V. (1994). Embryonic origin of hemocytes and their relationship to cell death in *Drosophila*. *Development*, 120(7), 1829-1837.
- Terry, R. D., DeTeresa, R., & Hansen, L. A. (1987). Neocortical cell counts in normal human adult aging. *Annals of Neurology*, 21(6), 530-539. doi:10.1002/ana.410210603
- Thaler, J. P., Yi, C. X., Schur, E. A., Guyenet, S. J., Hwang, B. H., Dietrich, M. O., . . . Schwartz, M. W. (2012). Obesity is associated with hypothalamic injury in rodents and humans. *J Clin Invest*, 122(1), 153-162. doi:10.1172/JCI59660
- Thaler, L., Groleau, P., Badawi, G., Sycz, L., Zeramdini, N., Too, A., . . . Steiger, H. (2012). Epistatic interactions implicating dopaminergic genes in bulimia nervosa (BN): relationships to eating- and personality-related psychopathology. *Prog Neuropsychopharmacol Biol Psychiatry*, 39(1), 120-128. doi:10.1016/j.pnpbp.2012.05.019
- Thomas, D. J., Reasor, M. J., & Wierda, D. (1989). Macrophage regulation of myelopoiesis is altered by exposure to the benzene metabolite hydroquinone. *Toxicol Appl Pharmacol*, 97(3), 440-453. doi:10.1016/0041-008x(89)90249-4
- Thored, P., Heldmann, U., Gomes-Leal, W., Gisler, R., Darsalia, V., Taneera, J., . . . Lindvall, O. (2009). Long-term accumulation of microglia with proneurogenic phenotype concomitant with persistent neurogenesis in adult subventricular zone after stroke. *Glia*, 57(8), 835-849. doi:10.1002/glia.20810
- Timmerman, R., Burm, S. M., & Bajramovic, J. J. (2018). An Overview of in vitro Methods to Study Microglia. *Frontiers in cellular neuroscience*, 12, 242. doi:10.3389/fncel.2018.00242
- Tremblay, M. E., Lowery, R. L., & Majewska, A. K. (2010). Microglial interactions with synapses are modulated by visual experience. *PLoS Biol*, 8(11), e1000527. doi:10.1371/journal.pbio.1000527
- Tremblay, M. E., Zettel, M. L., Ison, J. R., Allen, P. D., & Majewska, A. K. (2012). Effects of aging and sensory loss on glial cells in mouse visual and auditory cortices. *Glia*, 60(4), 541-558. doi:10.1002/glia.22287
- Trinh, J., & Farrer, M. (2013). Advances in the genetics of Parkinson disease. *Nat Rev Neurol*, 9(8), 445-454. doi:10.1038/nrneurol.2013.132
- Udolph, G., Prokop, A., Bossing, T., & Technau, G. M. (1993). A common precursor for glia and neurons in the embryonic CNS of *Drosophila* gives rise to segment-specific lineage variants. *Development*, 118(3), 765-775.
- Uversky, V. N. (2004). Neurotoxicant-induced animal models of Parkinson's disease: understanding the role of rotenone, maneb and paraquat in neurodegeneration. *Cell Tissue Res*, 318(1), 225-241. doi:10.1007/s00441-004-0937-z
- Valdearcos, M., Robblee, M. M., Benjamin, D. I., Nomura, D. K., Xu, A. W., & Koliwad, S. K. (2014). Microglia dictate the impact of saturated fat consumption on hypothalamic inflammation and neuronal function. *Cell reports*, 9(6), 2124-2138. doi:10.1016/j.celrep.2014.11.018
- Vanha-Aho, L. M., Anderl, I., Vesala, L., Hultmark, D., Valanne, S., & Ramet, M. (2015). Edin Expression in the Fat Body Is Required in the Defense Against Parasitic Wasps in *Drosophila melanogaster*. *PLoS Pathog*, 11(5), e1004895. doi:10.1371/journal.ppat.1004895
- Verheijen, J., & Sleegers, K. (2018). Understanding Alzheimer Disease at the Interface between Genetics and Transcriptomics. *Trends Genet*, 34(6), 434-447. doi:10.1016/j.tig.2018.02.007
- Verkhatsky, A., & Parpura, V. (2016). Astroglial pathology in neurological, neurodevelopmental and psychiatric disorders. *Neurobiol Dis*, 85, 254-261. doi:10.1016/j.nbd.2015.03.025
- Villalta, S. A., Nguyen, H. X., Deng, B., Gotoh, T., & Tidball, J. G. (2009). Shifts in macrophage phenotypes and macrophage competition for arginine metabolism affect the severity of muscle pathology in muscular dystrophy. *Hum Mol Genet*, 18(3), 482-496. doi:10.1093/hmg/ddn376

- Vincent, J. B., Choufani, S., Horike, S., Stachowiak, B., Li, M., Dill, F. J., . . . Scherer, S. W. (2008). A translocation t(6;7)(p11-p12;q22) associated with autism and mental retardation: localization and identification of candidate genes at the breakpoints. *Psychiatr Genet*, *18*(3), 101-109. doi:10.1097/YPG.0b013e3282f97df7
- Vincent, S., Vonesch, J. L., & Giangrande, A. (1996). Glide directs glial fate commitment and cell fate switch between neurones and glia. *Development*, *122*(1), 131-139.
- Voelzmann, A., Liew, Y. T., Qu, Y., Hahn, I., Melero, C., Sanchez-Soriano, N., & Prokop, A. (2017). Drosophila Short stop as a paradigm for the role and regulation of spectraplakins. *Semin Cell Dev Biol*, *69*, 40-57. doi:10.1016/j.semcdb.2017.05.019
- von Maydell, D., & Jorfi, M. (2019). The interplay between microglial states and major risk factors in Alzheimer's disease through the eyes of single-cell RNA-sequencing: beyond black and white. *J Neurophysiol*, *122*(4), 1291-1296. doi:10.1152/jn.00395.2019
- Wake, H., Moorhouse, A. J., Miyamoto, A., & Nabekura, J. (2013). Microglia: actively surveying and shaping neuronal circuit structure and function. *Trends Neurosci*, *36*(4), 209-217. doi:10.1016/j.tins.2012.11.007
- Wang, J. W., & Stifani, S. (2017). Roles of Runx Genes in Nervous System Development. *Adv Exp Med Biol*, *962*, 103-116. doi:10.1007/978-981-10-3233-2_8
- Wang, Y., Szretter, K. J., Vermi, W., Gilfillan, S., Rossini, C., Cella, M., . . . Colonna, M. (2012). IL-34 is a tissue-restricted ligand of CSF1R required for the development of Langerhans cells and microglia. *Nat Immunol*, *13*(8), 753-760. doi:10.1038/ni.2360
- Wang, Z., Liu, D., Wang, F., Liu, S., Zhao, S., Ling, E. A., & Hao, A. (2012). Saturated fatty acids activate microglia via Toll-like receptor 4/NF-kappaB signalling. *Br J Nutr*, *107*(2), 229-241. doi:10.1017/S0007114511002868
- Welser-Alves, J. V., Boroujerdi, A., Tigges, U., & Milner, R. (2011). Microglia use multiple mechanisms to mediate interactions with vitronectin; non-essential roles for the highly-expressed alphavbeta3 and alphavbeta5 integrins. *J Neuroinflammation*, *8*, 157. doi:10.1186/1742-2094-8-157
- Wessel, G. M., Kiyomoto, M., Shen, T. L., & Yajima, M. (2020). Genetic manipulation of the pigment pathway in a sea urchin reveals distinct lineage commitment prior to metamorphosis in the bilateral to radial body plan transition. *Sci Rep*, *10*(1), 1973. doi:10.1038/s41598-020-58584-5
- Wieghofer, P., & Prinz, M. (2016). Genetic manipulation of microglia during brain development and disease. *Biochim Biophys Acta*, *1862*(3), 299-309. doi:10.1016/j.bbadis.2015.09.019
- Wolf, S. A., Boddeke, H. W., & Kettenmann, H. (2017). Microglia in Physiology and Disease. *Annu Rev Physiol*, *79*, 619-643. doi:10.1146/annurev-physiol-022516-034406
- Wood, W., & Jacinto, A. (2007). Drosophila melanogaster embryonic haemocytes: masters of multitasking. *Nat Rev Mol Cell Biol*, *8*(7), 542-551. doi:10.1038/nrm2202
- Worley, M. I., Setiawan, L., & Hariharan, I. K. (2013). TIE-DYE: a combinatorial marking system to visualize and genetically manipulate clones during development in Drosophila melanogaster. *Development*, *140*(15), 3275-3284. doi:10.1242/dev.096057
- Wu, Y., & Hirschi, K. K. (2020). Tissue-Resident Macrophage Development and Function. *Front Cell Dev Biol*, *8*, 617879. doi:10.3389/fcell.2020.617879
- Yagi, R., Mayer, F., & Basler, K. (2010). Refined LexA transactivators and their use in combination with the Drosophila Gal4 system. *Proc Natl Acad Sci U S A*, *107*(37), 16166-16171. doi:10.1073/pnas.1005957107
- Yamane, T. (2018). Mouse Yolk Sac Hematopoiesis. *Front Cell Dev Biol*, *6*, 80. doi:10.3389/fcell.2018.00080
- Yap, J., Cabrera-Fuentes, H. A., Irei, J., Hausenloy, D. J., & Boisvert, W. A. (2019). Role of Macrophages in Cardioprotection. *Int J Mol Sci*, *20*(10). doi:10.3390/ijms20102474
- York, E. M., Bernier, L. P., & MacVicar, B. A. (2018). Microglial modulation of neuronal activity in the healthy brain. *Dev Neurobiol*, *78*(6), 593-603. doi:10.1002/dneu.22571

- Yuan, P., Condello, C., Keene, C. D., Wang, Y., Bird, T. D., Paul, S. M., . . . Grutzendler, J. (2016). TREM2 Haplodeficiency in Mice and Humans Impairs the Microglia Barrier Function Leading to Decreased Amyloid Compaction and Severe Axonal Dystrophy. *Neuron*, *90*(4), 724-739. doi:10.1016/j.neuron.2016.05.003
- Zaytouni, T., Efimenko, E. E., & Tevosian, S. G. (2011). GATA transcription factors in the developing reproductive system. *Adv Genet*, *76*, 93-134. doi:10.1016/B978-0-12-386481-9.00004-3
- Zelinka, C. P., Scott, M. A., Volkov, L., & Fischer, A. J. (2012). The reactivity, distribution and abundance of Non-astrocytic Inner Retinal Glial (NIRG) cells are regulated by microglia, acute damage, and IGF1. *PLOS ONE*, *7*(9), e44477. doi:10.1371/journal.pone.0044477
- Zheng, W., Li, Q., Zhao, C., Da, Y., Zhang, H. L., & Chen, Z. (2018). Differentiation of Glial Cells From hiPSCs: Potential Applications in Neurological Diseases and Cell Replacement Therapy. *Frontiers in cellular neuroscience*, *12*, 239. doi:10.3389/fncel.2018.00239
- Zovein, A. C., Turlo, K. A., Ponc, R. M., Lynch, M. R., Chen, K. C., Hofmann, J. J., . . . Iruela-Arispe, M. L. (2010). Vascular remodeling of the vitelline artery initiates extravascular emergence of hematopoietic clusters. *Blood*, *116*(18), 3435-3444. doi:10.1182/blood-2010-04-279497
- Zrzavy, T., Hametner, S., Wimmer, I., Butovsky, O., Weiner, H. L., & Lassmann, H. (2017). Loss of 'homeostatic' microglia and patterns of their activation in active multiple sclerosis. *Brain*, *140*(7), 1900-1913. doi:10.1093/brain/awx113

Temporal specificity and heterogeneity of *Drosophila* immune cells

Pierre B Cattenoz^{1,2,3,4,*} , Rosy Sakr^{1,2,3,4,†}, Alexia Pavlidaki^{1,2,3,4,†}, Claude Delaporte^{1,2,3,4}, Andrea Riba^{1,2,3,4}, Nacho Molina^{1,2,3,4} , Nivedita Hariharan^{5,6}, Tina Mukherjee⁵ & Angela Giangrande^{1,2,3,4,**} 

Abstract

Immune cells provide defense against non-self and have recently been shown to also play key roles in diverse processes such as development, metabolism, and tumor progression. The heterogeneity of *Drosophila* immune cells (hemocytes) remains an open question. Using bulk RNA sequencing, we find that the hemocytes display distinct features in the embryo, a closed and rapidly developing system, compared to the larva, which is exposed to environmental and metabolic challenges. Through single-cell RNA sequencing, we identify fourteen hemocyte clusters present in unchallenged larvae and associated with distinct processes, e.g., proliferation, phagocytosis, metabolic homeostasis, and humoral response. Finally, we characterize the changes occurring in the hemocyte clusters upon wasp infestation, which triggers the differentiation of a novel hemocyte type, the lamellocyte. This first molecular atlas of hemocytes provides insights and paves the way to study the biology of the *Drosophila* immune cells in physiological and pathological conditions.

Keywords *Drosophila melanogaster*; immune cells; single-cell RNA-seq; wasp infestation

Subject Categories Immunology; Methods & Resources

DOI 10.15252/embj.2020104486 | Received 15 January 2020 | Revised 18 February 2020 | Accepted 21 February 2020 | Published online 12 March 2020
The EMBO Journal (2020) 39: e104486

See also: **V Hartenstein** (June 2020)

Introduction

The innate immune response has been the object of intense investigation in *Drosophila melanogaster*, as this model shows mechanisms that are conserved throughout evolution, from pattern recognition molecules to immune molecular cascades

(Akira *et al.*, 2006; Kleino & Silverman, 2014). Given the importance of innate immunity in a variety of physiological and pathological processes including tumor progression (Ratheesh *et al.*, 2015), the current challenge is to characterize immune cell heterogeneity and identify specific hemocyte populations. This is the aim of the present work.

Three classes of hemocytes have so far been identified as follows: the plasmatocytes, the crystal cells, and the lamellocytes (Honti *et al.*, 2014). The plasmatocytes are the most abundant cell type and are responsible for the main functions of the hemocytes: phagocytosis, secretion of extracellular matrix proteins (ECM), signaling molecules, and antimicrobial peptides (AMPs; Yasothornsrikul *et al.*, 1997; Basset *et al.*, 2000; Sears *et al.*, 2003; Ferrandon *et al.*, 2004; Baer *et al.*, 2010; Gold & Bruckner, 2015). The crystal cells account for less than 5% of the total hemocyte population, with distinctive crystals inside them that are composed of prophe-noloxidases (PPO; Rizki & Rizki, 1959). These enzymes are released in large quantity upon wounding and constitute a key component for the melanization process (Rizki & Rizki, 1959). The lamellocytes are flat and large cells that only appear upon challenge. They are considered activated immune cells (Gold & Bruckner, 2015) that arise through plasmatocyte trans-differentiation or from a mitotic-dedicated precursor (Anderl *et al.*, 2016).

In the embryo, the hemocytes contribute to the clearance of apoptotic cells and the deposition of ECM-related molecules including Peroxidase (Pxn) and Viking (Vkg; Nelson *et al.*, 1994; Yasothornsrikul *et al.*, 1997). By the larval stage, the organism interacts with the external environment and responds to metabolic and oxidative stress as well as to infection- or injury-related stimuli. The hemocytes must therefore adapt to these new, highly demanding, settings. In addition, while during embryogenesis, the hemocytes are highly motile and patrol the whole organism, during the larval life a large fraction of them, called resident hemocytes, colonize segmentally repeated epidermal-muscular pockets in which cell proliferation is enhanced (Makhijani *et al.*, 2011). Upon wounding, septic infection, or infestation by parasitic wasps, the resident

1 Institut de Génétique et de Biologie Moléculaire et Cellulaire, Illkirch, France

2 Centre National de la Recherche Scientifique, UMR7104, Illkirch, France

3 Institut National de la Santé et de la Recherche Médicale, U1258, Illkirch, France

4 Université de Strasbourg, Illkirch, France

5 Institute for Stem Cell Science and Regenerative Medicine (inStem), Bangalore, India

6 The University of Trans-disciplinary Health Sciences and Technology, Bangalore, India

*Corresponding author. Tel: +33 388653376; E-mail: cattenoz@igbmc.fr

**Corresponding author. Tel: +33 388653381; E-mail: angela@igbmc.fr

†These authors contributed equally to this work

hemocytes are mobilized and enter in circulation to reach the site of the immune challenge (Owusu-Ansah & Banerjee, 2009; Dragojlovic-Munther & Martinez-Agosto, 2012). Thus, hemocyte localization adapts to homeostatic and challenged conditions.

We here characterize the transcriptional changes occurring during development and the different types of hemocytes present in the larva. Comparing the bulk RNA sequencing data allows us to define stage-specific features: In the embryo, hemocytes contribute to the shaping of the tissues and are glycolytic, whereas in the larva, hemocytes show a strong phagocytic potential and a metabolic switch toward internalization of glucose and lipid and toward beta oxidation. The single-cell RNA sequencing (scRNA-seq) assay allows us to identify fourteen clusters of larval plasmatocytes and to assign specific molecular and cellular features, including nutrient storage, proliferative potential, antimicrobial peptide production, and phagocytosis.

Finally, as a first characterization of the immune response at the single-cell level, we assess the transcriptional changes induced by infestation by the parasitic wasp *Leptopilina boulardi*, one of the most studied pathways linked to cellular immunity. The wasp lays eggs in the *Drosophila* larva and triggers hemocyte proliferation as well as lamellocyte differentiation (Markus *et al*, 2009), with subsequent encapsulation of the wasp egg and its death through the increased levels of reactive oxygen species (ROS). The scRNA-seq assay identifies two lamellocyte populations, a mature one with a strong glycolytic signature, and a population that expresses both lamellocyte and plasmatocyte features, likely originating through trans-differentiation (Anderl *et al*, 2016).

The response to wasp infestation involves the embryonic hemocytes that differentiate from the procephalic mesoderm (1st wave of hematopoiesis; Tepass *et al*, 1994), as well as the hemocytes that originate from the lymph gland, the site of the 2nd hematopoietic wave. While in not-infested (NI) conditions, the lymph gland histolyses and releases hemocytes in circulation during the pupal life, upon wasp infestation (WI), it undergoes precocious histolysis so that both lymph gland and embryonic-derived hemocytes populate the larva (Letourneau *et al*, 2016; Bazzi *et al*, 2018; Banerjee *et al*, 2019). Our single-cell RNA sequencing assay identifies the same number of plasmatocyte clusters as that observed in normal conditions, strongly suggesting that the plasmatocytes from the first and second hematopoietic waves share the same features.

In sum, this work characterizes the transcriptional changes occurring during hemocyte development and the hemocyte populations present in the *Drosophila* larva. It also provides the molecular signature and the initial characterization of the larval hemocyte repertoire as well as numerous novel markers in NI and in WI conditions. These first bulk and single-cell RNA-seq data pave the way to understand the role of the immune system in development and physiology.

Results

Comparing the bulk transcriptomes from embryonic (E16) and larval (WL) hemocytes

In the embryo, insulated from most immune challenges by the eggshell, the hemocytes main functions are developmental. They

clear the organism from apoptotic bodies issued from organogenesis and secrete extracellular components. In the larva, the hemocytes display new properties to respond to the microorganism-rich environment in which they grow. To identify the changes occurring in the hemocytes during development, we compared the hemocytes' transcriptomes from mature, stage 16 (E16) embryos and from third-instar wandering larvae (WL).

The comparison shows 3,396 genes significantly up-regulated in E16 and 1,593 up-regulated in WL hemocytes (Fig 1A, data in Dataset EV1). Most plasmatocyte markers such as Hemese (He; Kurucz *et al*, 2003), Singed (Sn; Zanet *et al*, 2009), Eater (Kocks *et al*, 2005), Hemolectin (Hml; Goto *et al*, 2001), Serpent (Srp; Shlyakhover *et al*, 2018), Nimrod C1 (NimC1, also called P1; Kurucz *et al*, 2007), Croquemort (Crq; Franc *et al*, 1996), and Pxn (Nelson *et al*, 1994) are strongly expressed at both stages but enriched in WL hemocytes (Fig 1C). Crystal cell markers are also present in the transcriptome: Pebbled (Peb) and Lozenge (Lz) are detected at relatively low levels, in agreement with the small number of crystal cells in the E16 and WL hemolymph (Rizki & Rizki, 1959). The crystal cell-specific markers PPO1 and PPO2, on the other hand, are among the genes expressed at the highest levels, highlighting their key function and the sharp specialization of the crystal cells (Bingeli *et al*, 2014).

Surprisingly, most lamellocyte markers such as myspheroid (Mys or L4; Irving *et al*, 2005), Misshapen (Msn; Braun *et al*, 1997), Cher (or L5; Rus *et al*, 2006), and Atilla (or L1; Honti *et al*, 2009) were also detected at significant levels in the hemocytes from both stages. This suggests that they are expressed at basal levels in normal hemocytes and are strongly induced in lamellocytes and/or that few lamellocytes are present in basal conditions. At last, Gcm is involved in hemocyte development in the early embryo (stages 8–10; Bernardoni *et al*, 1997) and is no longer expressed by E16 (Bazzi *et al*, 2018). Accordingly, Gcm transcripts are barely detected in E16 and WL transcriptomes (levels < 40 normalized read count). Overall, these data prove the efficiency of the experimental design to purify hemocytes.

Embryonic hemocytes express ECM components

We next carried out a GO term enrichment analysis on the genes up-regulated in either population ($|\log_2$ fold change WL/E16| > 1, adjusted *P*-value < 0.01; Dataset EV1). The E16 hemocytes display a striking enrichment for gene coding for extracellular matrix components (ECM; Fig 1B and D). Out of 162 gene coding for ECM proteins, 138 are enriched in E16 hemocytes. To confirm the expression pattern of the ECM genes, we compared these data with two *in situ* hybridization databases (Berkeley *Drosophila* Genome Project (Hammonds *et al*, 2013; Tomancak *et al*, 2002, 2007) and Fly-FISH (Lecuyer *et al*, 2007; Wilk *et al*, 2016); Appendix Fig S1D and E). Most genes for which we could find data are specifically expressed in hemocytes in the embryo (Appendix Fig S1D and E).

The expression/secretion of few specific ECM compounds by the hemocytes during embryonic development was previously described. The integrins alphaPS1 (Mew) and Mys as well as the integrin ligand Tiggrin (Tig) are secreted by the hemocytes at the level of muscle insertion to stabilize strong attachment between the cells (Fogerty *et al*, 1994; Bunch *et al*, 1998). The laminins LanA, LanB1, LanB2, and Wb are secreted by the hemocytes for them to

migrate efficiently throughout the embryo (Sanchez-Sanchez *et al*, 2017). Pxn and the collagen Vkg and Col4a1 secretion by the hemocytes are essential for the condensation of the ventral nerve cord (Olofsson & Page, 2005). Finally, SPARC is produced by the hemocytes and is necessary for basal lamina assembly (Martinek *et al*, 2008). These 11 compounds are expressed at extremely high levels

in the embryo and remain highly expressed in the larva (Fig 1D), suggesting that the role of these specific genes is preserved throughout development.

Among the remaining ECM genes enriched in E16, we distinguished a large group of ECM compounds described as constituent of the cuticle: 23 Tweedles (Twdl), 56 Cuticular Proteins (Cpr and

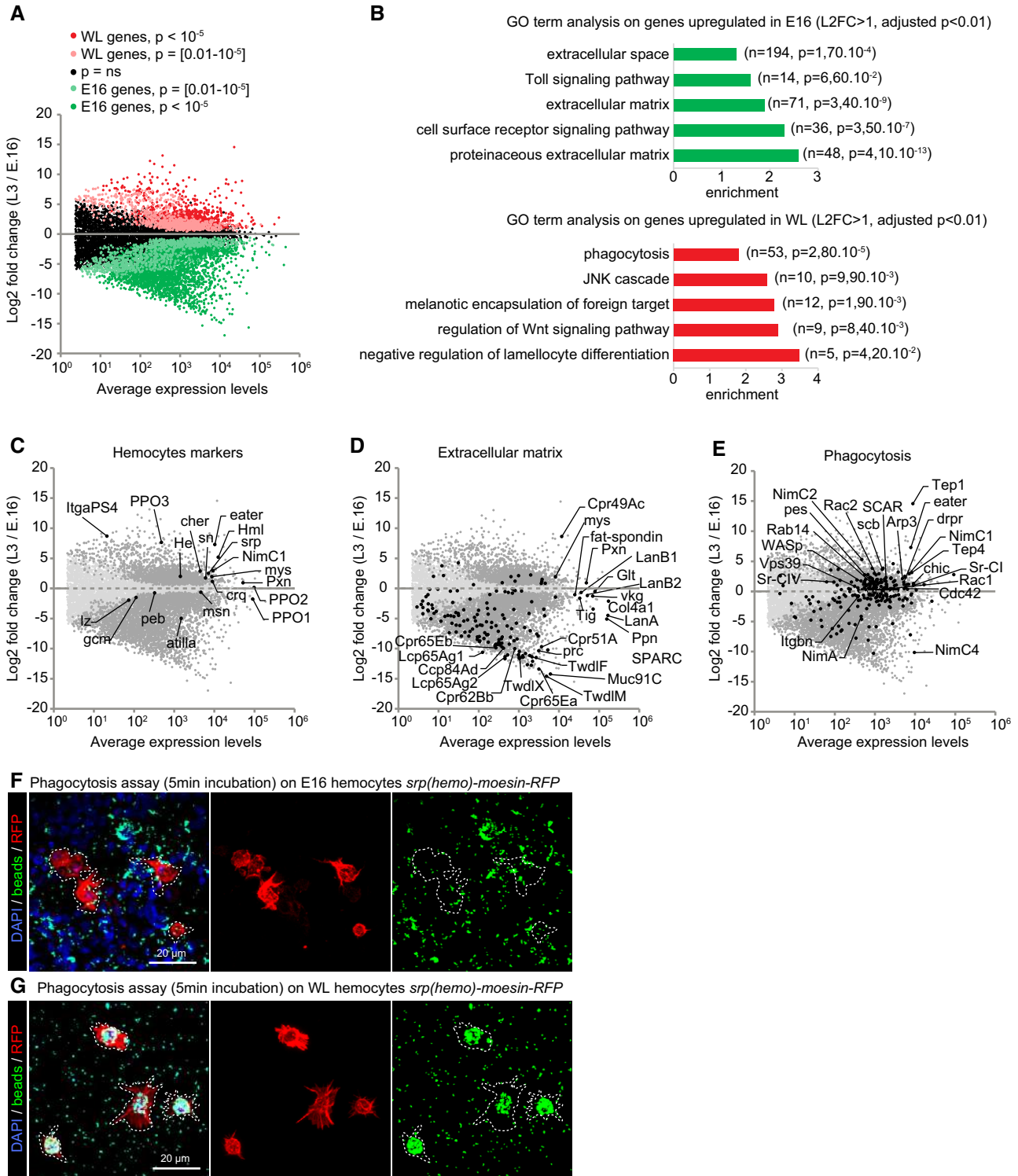


Figure 1.

Figure 1. Hemocytes display distinct properties at E16 and WL stage.

- A Transcriptome comparison of hemocytes from stage 16 (E16) embryos and wandering 3rd-instar larvae (WL). The x-axis is the average gene expression levels ($n = 3$), and the y-axis is the \log_2 fold change WL/E16. P -values are indicated with the color code.
- B Gene Ontology (GO) term enrichment analysis in E16 (green) and WL (red) hemocytes. The fold enrichments for a subset of significant GO terms are displayed; the number of genes and the P -value of the GO term enrichment are indicated in brackets.
- C–E Scatter plots as in (A) highlighting in black subsets of known genes expressed in hemocytes (C) or genes associated with the GO term extracellular matrix (D) and phagocytosis (E).
- F, G Phagocytosis assay on E16 (F) and WL hemocytes (G) *srp(hemo)-moesin-RFP*. The beads (in green) are phagocytosed by the hemocytes (in red). The WL hemocytes show greater phagocytic capacity compared to the embryonic ones after 5 min of exposure. Full stacks are displayed, and the scale bars represent 20 μm .
- Data information: Related to Appendix Figs S1 and S2, and Datasets EV1 and EV4.

Ccp), nine Larval Cuticle Proteins (Lcp), and nine Mucins (Muc; Fig 1D, annotated in Dataset EV1). This calls for a role of the embryonic hemocytes in cuticle deposition. We also identified 21 ECM genes strongly up-regulated in the embryo ($\log_2\text{FC} < -3$, P -value < 0.01 , annotated in Dataset EV1). These include the two heart-specific ECM compounds Pericardin (Prc) and Lonely heart (Loh; Maroy *et al*, 1988; Chavez *et al*, 2000; Charles, 2010), Thrombospondin (Tsp), which interacts with the integrins Mew, Mys, and If at the tendon-muscle attachment sites (Chanana *et al*, 2007) and Shifted (Shf) that modulate Hedgehog diffusion (Gorfinkiel *et al*, 2005; not exhaustive list). This strongly calls for additional embryo-specific pathways for the deposition of the ECM, in which future studies will elucidate.

Larval hemocytes express specific scavenger receptors

The GO terms enriched in WL compared to E16 hemocytes highlight phagocytosis and, to a lower extent, signaling pathways involved in the immune response (JNK and Wnt; Fig 1B and E, and Dataset EV1).

Among the genes involved in phagocytosis, a large panel is coding for transmembrane phagocytic receptors involved in pathogen recognition, such as the Nimrod family (Eater (Kocks *et al*, 2005), NimC1 (Kurucz *et al*, 2007) and NimC2), several scavenger receptors (Sr-CI and Sr-CIV (Lazzaro *et al*, 2004), He, Peste (Cuttell *et al*, 2008; Hashimoto *et al*, 2009) as well as the integrins Scab (α -PS3) and Integrin beta- ν (Itg β n; Nonaka *et al*, 2013). Noteworthy, the E16 embryonic hemocytes are specifically enriched for NimC4 (also called Simu), a receptor of the Nimrod family that is involved in the phagocytosis of apoptotic bodies (Fig 1E; Kurant *et al*, 2008; Roddie *et al*, 2019).

The WL hemocytes are also enriched for opsonins. These secreted molecules bind to the pathogens and promote their phagocytosis by the macrophages. Tep1 and Tep4 (Dostalova *et al*, 2017; Haller *et al*, 2018) are among the genes expressed at the highest levels in WL hemocytes, and Tep1 presents the strongest enrichment. Most of the genes involved in phagosome formation are also enriched at this stage: Arp3, Rac1, Rac2, SCAR, WASP, Chic, and Cdc42 (Pearson *et al*, 2003). Finally, genes involved in phagosome maturation (Rab14) and phagolysosome formation (Vps39) are enriched as well (Fig 1E; Garg & Wu, 2014; Jiang *et al*, 2014).

The scavenger receptors and the opsonins cover a large panel of pathogens (for review, see Melcarne *et al*, 2019), indicating an overall switch for hemocytes' function from apoptotic body scavenging and cuticle production at embryonic stages to pathogen scavenging at the WL stage. Since it was previously shown that the hemocytes

present in the embryo are able of phagocytosis (Vlisidou *et al*, 2009; Tan *et al*, 2014), we compared the phagocytic capacity of E16 and WL hemocytes upon exposing them to fluorescent beads. The results clearly show that the larval hemocytes phagocytose faster and more than the embryonic ones (Fig 1F and G).

In sum, the transcriptome analysis reveals a change in the function of the hemocytes during development, from building the ECM and the cuticle to adopting a defense profile against immune challenges.

Metabolic shift between embryonic and larval hemocytes

The properties of the immune cells are directly dependent on their metabolic state, which is constrained by their micro-environment (reviewed in Sieow *et al*, 2018). We hypothesized that the hemocytes display distinct metabolic states according to the nutritional environment present in the two developmental stages, as embryos are closed systems, whereas larvae have been feeding for most of their life. To address this hypothesis, we analyzed the expression profiles of the energy metabolic pathways in E16 and WL hemocytes.

The transcriptome data comparison reveals that the larval hemocytes are most likely internalizing and metabolizing lipids through the beta oxidation pathway to generate acetyl CoA and drive the TCA cycle (Appendix Fig S2A–C). This notion is supported by the up-regulation of genes encoding lipid-scavenging receptors, and the down-regulation of genes is involved in lipid biosynthetic (TAG) pathway (Appendix Fig S2A and B).

The down-regulation of genes involved in glycolysis, mainly phosphofructokinase and pyruvate dehydrogenase (Appendix Fig S2B), implies that the larval hemocytes do not rely on this process to drive the TCA cycle. The transcriptional down-regulation of gluconeogenic genes (phosphoenolpyruvate carboxykinase and fructose 1, six bisphosphatase) suggests the absence of gluconeogenesis in these cells. However, a significant up-regulation of the Glut1 sugar transporter suggests active uptake of glucose by the larval hemocytes. The down-regulation of glycolytic genes downstream of G6P and up-regulation of genes of the pentose phosphate pathway (PPP) imply that the internalized glucose could be potentially used to generate pentose sugars for ribonucleotide synthesis and redox homeostasis through the generation of NADPH. Corroborating this observation is also the strong up-regulation of redox homeostatic enzymes (Appendix Fig S2A).

In contrast to the larval hemocytes, the E16 hemocytes are glycolytic and rely less on oxidative metabolism (Appendix Fig S2B). This is supported by the strong up-regulation of a key

glycolytic enzyme, lactate dehydrogenase, which is essential for the conversion of pyruvate to lactate. Furthermore, these cells likely metabolize lipids at a lower level, as enzymes of the beta oxidation pathway are transcriptionally down-regulated compared to the larval hemocytes.

Generation of single-cell RNA-seq datasets from NI and WI larvae

The *Drosophila* larva contains plasmatocytes and crystal cells that are resident or in circulation. Upon wasp infestation, the lamellocytes are produced from precursors (Anderl *et al*, 2016) or by plasmatocyte trans-differentiation (Stofanko *et al*, 2010). To obtain a comprehensive repertoire of the hemocyte populations present in the larva, we generated two single-cell libraries on the hemocytes from not-infested WL (NI dataset) and from WL infested by the parasitoid wasp *L. bouleardi* (WI dataset). The NI cells comprise the resident and the circulating embryonic-derived hemocytes, and the WI cells include in addition the hemocytes released from the lymph gland.

The hemocytes were collected from pools of 20 female larvae. The libraries were produced using the Chromium single-cell 3'mRNA-seq protocol (10 × Genomics). The NI library contains 7,606 cells (mean read per cell = 37,288; median genes per cell = 959) and the WI library 8,058 cells (mean read per cell = 32,365; median genes per cell = 1,250). The libraries were merged to cluster the hemocytes presenting similar expression profiles using the Seurat toolkit (Butler *et al*, 2018; Stuart *et al*, 2019; Appendix Fig S3A). Subclustering was then applied to refine the grouping of the cells leading to the identification of 16 clusters of hemocytes (Appendix Fig S3A' and C–D"). The identity of each cluster was assigned using the list of known markers for the crystal cells (Lz, Peb, PPO1, PPO2), for the lamellocytes (Mys, Msn, Cher, Atilla, ItgaPS4, PPO3), and for the plasmatocytes (Sn, Pxn, Hml, Eater, NimC1, Crq, He, Srp; Appendix Fig S3B). Of note, the single-cell data show that the lamellocyte markers Mys, Msn, Cher, and Atilla detected in the bulk RNA-seq on WL and E16 are expressed in the plasmatocytes and enriched in the lamellocytes (Appendix Fig S3B).

We identified 13 clusters of plasmatocytes and one cluster of crystal cells in both the NI and the WI larvae and two clusters of lamellocytes specifically found in the WI larvae. The name of each cluster corresponds to the name of one of the main markers or to specific biological features (Fig 2A and B). Importantly, all cells analyzed in these datasets present known hemocyte markers, which indicate a high purity of the samples.

Characterization of the transcriptomic profile in normal conditions

Following the identification of the clusters, our first aim was to characterize the properties of the clusters in the NI dataset. Thus, we carried out GO term analyses on the genes enriched in each of them (Dataset EV2, Fig 2C) using DAVID (Huang da *et al*, 2009). In addition, to estimate whether the clusters are enriched/specifically localized in the circulating or in the resident compartments, we performed qPCR assays on hemocytes from either compartment to measure the expression levels of the strong markers of the different clusters (Fig 3A).

The plasmatocyte clusters PL-0, PL-1, PL-2, and PL-3 encompass more than 60% of all the hemocytes. These clusters express most of the plasmatocyte markers (Appendix Fig S4A) but do not display strong distinct signatures (avg_logFC of the strongest markers < 0.93; Fig 2D); therefore, they can only be distinguished by combining several markers. The nine remaining plasmatocyte clusters present very specific molecular signatures in addition to the main plasmatocyte markers (Fig 2D) and are organized at the periphery of the four clusters on the graphical representation generated with the UMAP dimension reduction technique (Becht *et al*, 2018; Fig 2A).

PL-Rel

The PL-Rel cluster includes 12.6% of the total hemocyte population, with more than 100 strong markers (Dataset EV2), most of which are involved in the immune response (Fig 2C). The cluster expresses the main transcription factors of the Imd pathway (i.e., Relish, Rel) and of the Toll pathway (i.e., Dorsal, Df), Cactus (Cact), and the secreted protein PGRP-SA (Govind, 1999; Valanne *et al*, 2011; Zhai *et al*, 2018; Dataset EV2). In addition, it expresses proteins associated with the JNK pathway such as Jra and Puc (Martin-Blanco *et al*, 1998; Zheng *et al*, 2017). The qPCR assay on resident and circulating hemocytes indicates that PL-Rel hemocytes are present in both compartments (Fig 3A).

PL-vir1

The PL-vir1 cluster contains 4.5% of the total hemocytes and expresses the same strong markers as PL-Rel, including Rel, Jra, and Puc (Fig 2D, Dataset EV2). Compared to PL-Rel, however, the marker of viral infection Vir1 (Dostert *et al*, 2005), the protein Pastrel involved in resistance to virus infection (Magwire *et al*, 2012; Martins *et al*, 2014), the predicted peptidase Ance-5, and the apolipoprotein Nplp2 (Rommelaere *et al*, 2019) are all up-regulated. PL-vir1 also presents the same GO terms as PL-Rel, with respect to the defense response to bacterium and to the Toll signaling pathway (Fig 2C). The qPCR assay suggests that PL-vir1 is present in both resident and circulating compartments.

PL-robo2

The PL-robo2 cluster represents 6.5% of the total hemocyte population. It does not express unique markers (Fig 2D), but displays a strong enrichment for GO terms related to migration and phagocytosis (Fig 2C). It expresses the actin-regulatory protein enable (Tucker *et al*, 2011; Stedden *et al*, 2019) and transmembrane proteins that participate in the migration of multiple cell types. It also presents the strongest up-regulation of the phagocytic receptors Crq and Drpr (Franc *et al*, 1999; Manaka *et al*, 2004). In addition, Crq is the main receptor involved in lipid scavenging and is a major actor of the induction of the inflammatory response to high-fat diet initiated by the hemocytes (Woodcock *et al*, 2015). In line with this, PL-robo2 is enriched in the lipid droplet-associated protein Jabba involved in the regulation of lipid metabolism (McMillan *et al*, 2018). PL-robo2 is present in both circulating and resident compartments (Fig 3A).

PL-Pcd

The PL-Pcd cluster contains 4.7% of the total hemocyte population and is mostly linked to translation and Golgi organization (Fig 2C): Half of the proteins present in the GO term-enriched functions are

Figure 2. Fourteen hemocyte populations can be distinguished in WL by single-cell RNA-seq.

- A UMAP projection representing the 14 clusters of cells identified in the hemocyte pools from *OregonR* WL (NI dataset).
 B Number of cells and proportion of each cluster in the NI dataset.
 C GO term enrichment analysis for each cluster. The x-axis is the GO term enrichment, the color gradient (black to light blue) indicates the *P*-value, and the number of genes and the GO term category (CC: cellular component, BP: biological process, MF: molecular function) are indicated between brackets.
 D Top 5 markers of each cluster. The expression levels are represented by the gradient of purple levels and the percentage of cells with the size of the dots.
- Data information: Related to Appendix Figs S3 and S4, Datasets EV2 and EV3.

The qPCR data highlight one marker (Ham) enriched in the resident compartment and one marker (Obp99a) enriched in circulation. These ambiguous results may be due to the fact that the markers are expressed in other clusters as well (PL-AMP and PL-ImpL2).

PL-AMP

The PL-AMP cluster (0.5% of the hemocytes) presents strong similarities with PL-Rel, as they share the same markers related to the Imd pathway (Fig 2D), but distinguishes itself by the expression of the antimicrobial peptides (AMP) Cecropin A1 (CecA1), Cecropin A2 (CecA2), Cecropin C (CecC), Attacin-A (AttA), Attacin-B (AttB), and Attacin-D (AttD; Fig 2D and Dataset EV2) as well as of the PL-Pcd cluster markers Pcd, Ance, CG31431, and CG34296 (Fig 2D). The AMP are usually induced and secreted primarily by the fat body after septic wounds that trigger the Imd pathway (Govind, 1999; Zhai *et al*, 2018) and by a small percentage of hemocytes (Sama-kovlis *et al*, 1990; Meister *et al*, 1994).

The expression of CecC, CecA1, and CecA2 was not detected by qPCR in the resident nor in the circulating hemocytes. This is likely due to the low representation of these cells combined with the small size of the Cecropin transcripts (less than 400nt) that prevent the optimal design of primers and affect PCR efficiency. Therefore, we could not conclude on the localization of the PL-AMP hemocytes in the larvae.

PL-Inos and PL-prolif

The clusters PL-Inos and PL-prolif express several common markers and represent approximately 3 and 0.6% of the total hemocyte population, respectively (Fig 2B). Initially, PL-Inos and PL-prolif were clustered together and were splitted upon subclustering (Appendix Fig S3A and C), which indicates that they present strong similarities and may represent two states of the same cell population.

The PL-Inos cluster is enriched in GO terms associated with multiple functions including the response to bacteria, the ECM, cytoplasmic translation, and centrosome organization.

The PL-prolif cluster is specifically characterized by genes involved in mitosis (Fig 2C and Dataset EV2). Klp61F, Klp67A, and Ncd, which are linked to mitotic centrosome separation (Sharp *et al*, 1999; Gandhi *et al*, 2004), as well as Ncd80 and Nuf2, which are part of the NCD80 complex, are all up-regulated. Like their mammalian counterparts, these proteins are essential for mitotic metaphase plate congregation (Przewloka *et al*, 2007). Finally, PL-prolif hemocytes express two cyclins (CycB and CycE), the nuclear protein transporter Pen and cell cycle-related enzymes (String (Stg), the cyclin-dependent kinases Cdk1 and Cdk2), which are linked to the G2/M and G1/S transition (Kussel & Frasch, 1995; Yuan *et al*, 2016).

The qPCR assays indicate that the clusters PL-Inos and PL-prolif are enriched in the resident compartment (Fig 3A and D). This is

concordant with a previous analysis, indicating that the resident hemocytes are more proliferative than the circulating ones (Makhijani *et al*, 2011).

PL-Lsp

The PL-Lsp cluster contains approximately 3% of the total hemocyte population and is strongly associated with the GO term larval serum protein complex, nutrient reservoir activity, and lipid particle (Fig 2C and Dataset EV2). This is due to the expression of the larval serum proteins (LSP), which serve as a nutrient pool that will be used during metamorphosis (Telfer & Kunkel, 1991). The PL-Lsp cluster also expresses the receptor responsible for the incorporation of the LSPs (i.e., Fbp1), proteins associated with lipid transport (Rfabg; Kutty *et al*, 1996; Massey *et al*, 1997; Burmester *et al*, 1999), and the odorant binding protein Obp99b that is considered as a storage protein (Handke *et al*, 2013). These proteins are usually described as secreted by the fat body, suggesting shared features and role in metabolism between this tissue and PL-Lsp.

The qPCR on resident and circulating plasmatocytes reveals that the PL-Lsp hemocytes are mostly in circulation (Fig 3A). This localization is supported by labeling of two independent LSP transgenic reporters (Fig 3B and C, Appendix Fig S5A–C).

PL-ImpL2

The PL-ImpL2 cluster comprises less than 0.3% of the hemocytes, but displays the most distinctive molecular signature (49 genes presenting an enrichment $\text{avg_logFC} > 1$; Dataset EV2). This includes genes involved in glutathione metabolism (GstD1, GstD3, GstE12) and specific transcription factors (Ham, Kn, Antp, Eip93F, Noc, and ElB; Fig 2C, and Appendix Fig S5D and E).

Many of these markers are usually associated with the postsignaling center (PSC) that regulates the differentiation of lamellocytes within the lymph gland (Crozatier *et al*, 2004; Mandal *et al*, 2007; Benmimoun *et al*, 2015). The low abundance of these cells renders them hard to track in the larva; however, the GstD reporter *GstD-LacZ* (Sykietis & Bohmann, 2008) labels subsets of WL hemocytes that may correspond to the PL-ImpL2 cluster (Appendix Fig S5E).

CC

The CC cluster expresses the two well-known crystal cell markers PPO1 and PPO2 (Dudzic *et al*, 2015). In addition, we identify new potential markers: Metallothionein A (MtnA), Malic enzyme (Men), and CG9119. Further analysis of the GO terms highlights the response to starvation (Lipin (Lpin), Mthl10) as well as enzymes essential for the biosynthesis of proteoglycans (Sugarless, sgl) and glucose homeostasis (Pfk, 6-phosphofructo-2-kinase (pfrx), and Aldolase (ald); Hacker *et al*, 1997; Flowers *et al*, 2007; Ugrankar *et al*, 2011; Dudzic *et al*, 2015; Enzo *et al*, 2015; Sung *et al*, 2017; Wong *et al*, 2019).

Finally, GO terms related to “extracellular region” are enriched recurrently in almost every cluster (Fig 2C). Further analyses of all the genes expressed in the NI dataset and associated with the term extracellular region show that each cluster expresses different proteins (Appendix Fig S4B).

Characterization of the molecular pathways active in the clusters

To identify which regulatory networks characterize the clusters, we performed a regulon analysis using SCENIC (Aibar et al, 2017;

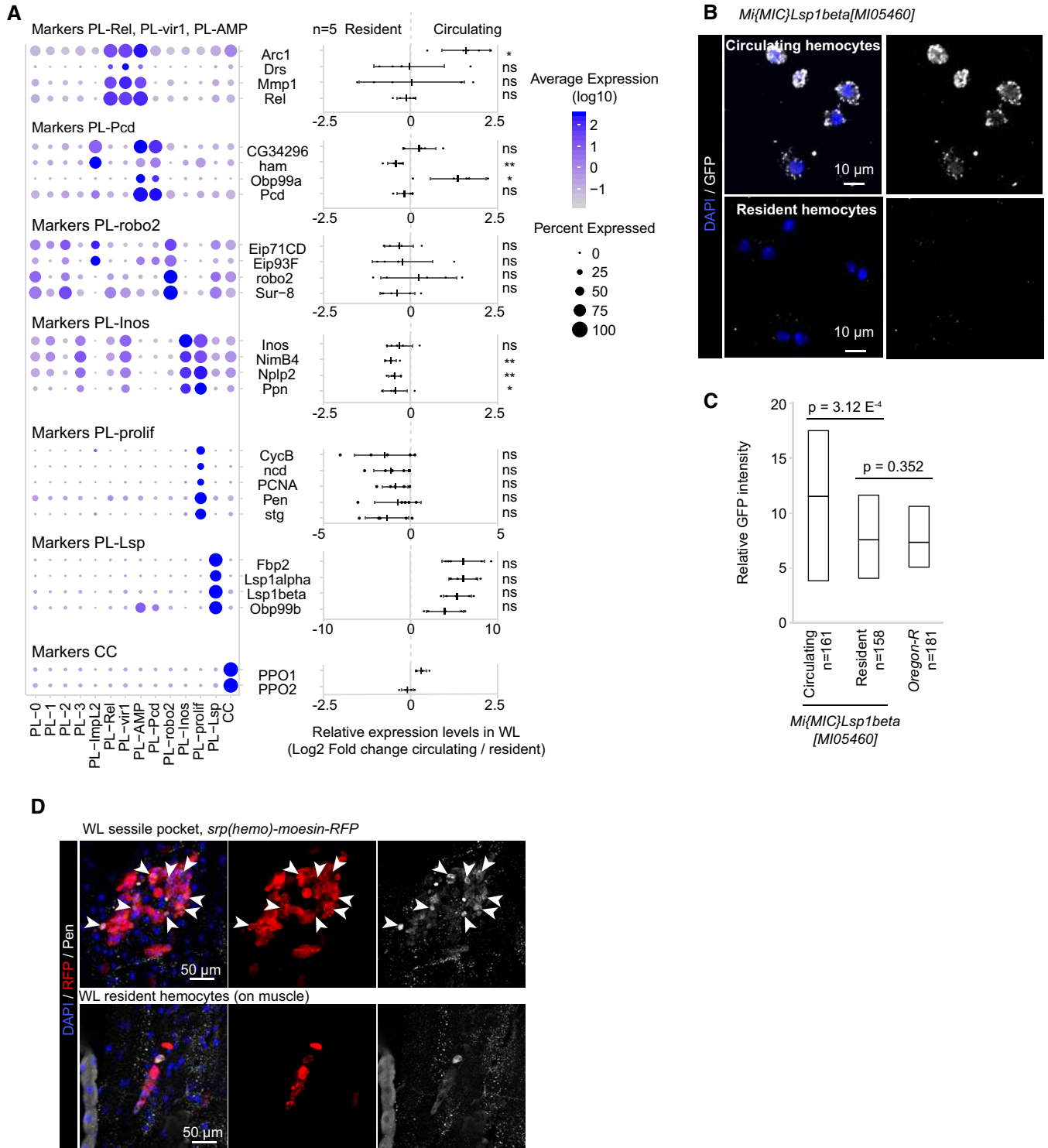


Figure 3.

Figure 3. Localization of the NI hemocyte clusters.

- A Identification of the position (circulating/resident) of the clusters within the larva by qPCR. The left panel indicates the distribution of each marker across all clusters (as in Fig 2D), and the right panel indicates the \log_2 of the ratio between the expression level in the circulating versus the resident compartment. Positive values indicate an enrichment in the circulating compartment and negative values in the resident compartment ($n = 5$, mean \pm SD is represented on the graph). The P -values are estimated by bilateral paired Student's t -test and indicated as follow: ns = non-significant (> 0.05), "*" = $P[0.05-0.01]$, "***" = $P[0.01-0.001]$.
- B Circulating and resident hemocytes (top and bottom panels, respectively) from *Mimic-Lsp1beta-MIO5460* WL, which express *Lsp1beta* tagged with GFP. The immunolabeling was done using anti-GFP (in gray), and the nuclei were marked with DAPI (blue). Full stacks are displayed, the left panels show the overlay of DAPI and GFP, and the right panels show the GFP alone. The scale bars represent 10 μ m.
- C Quantification of the GFP intensity in circulating and resident hemocytes from *MiMIC-Lsp1beta-MIO5460* larvae. The *OregonR* value indicates the background level. The number of cells included in the analysis is displayed on the x-axis label and is quantified from two independent preparation; P -values were estimated after variance analysis with bilateral student test for equal variance.
- D Resident hemocytes located around the oenocytes or along the muscles (top and bottom panels, respectively) from WL *srp(hemo)-moesin-RFP* that express *moesin* tagged with RFP in hemocytes. The immunolabeling was done using anti-RFP (in red) and anti-pendulin (Pen, in gray), and the nuclei were marked with DAPI (blue). Full stacks are displayed; the left panels show the overlay of DAPI, Pen, and RFP; the middle panels show RFP alone; and the right panels show Pen alone. Arrowheads in the top panels indicate cells co-expressing RFP and Pen. The scale bars represent 50 μ m.

Data information: Related to Appendix Fig S5 and Table EV1.

Fig 4A). SCENIC defines the regulon as an ensemble of genes coregulated by a single transcription factor and determines the regulon(s) active in single cells in three steps. First, covariation of the expression levels of the genes is estimated in the single-cell dataset. Then, each group of genes displaying covariation is screened for common cis-regulatory motifs present in the group. This defines groups of genes regulated by a specific transcription factor (=regulon). Finally, the activity of each regulon is estimated in each cell of the dataset (Aibar *et al*, 2017). Of note, this analysis was done independently of our initial clustering based on the expression levels. The clustering of the WT NI cells based on the regulons is highly comparable to the expression-based clustering, with a high overlap between the two clustering approaches, as estimated by the Rand index or RI (Rand, 1971; RI = 0.83; see the Materials and Methods section). This overlap highlights the robustness of our initial clustering.

The SCENIC analysis allowed us to associate specific regulons to each cluster (Fig 4A). Concordant with previous reports, the analysis highlighted a positive correlation between the regulon *Iz* and the crystal cells. *Iz* is a Runx transcription factor essential for the differentiation of these cells (Lebestky *et al*, 2000). The PL-Rel, PL-AMP, and PL-vir1 clusters are characterized by the regulons *Jra* (JNK cascade), *Rel* (IMD pathway), and *Ets21C* (which cooperates with the JNK pathway). The regulon activating transcription factor 3 (ATF3) involved in anti-viral response in mammals (Labzin *et al*, 2015) is specific to PL-vir1 and PL-Rel, whereas the regulon *CrebA* regulating the secretory pathway is specific to the PL-AMP cluster, which expresses most of the antimicrobial peptides. The PL-prolif cluster and the closely related cluster PL-Inos (Fig 4B) are enriched for the regulons *EcR* and *E2F1* that are involved in the regulation of hemocyte proliferation (Sinenko *et al*, 2010). PL-Lsp is associated with the *Tbp* regulon that is involved in the canonical transcriptional machinery. Such enrichment may indicate a higher rate of transcription, which would be concordant with the function of this cluster in producing storage proteins in preparation for pupariation. PL-robo2 is enriched for the regulons of the GATA factors *Pnr* and *Srp*, which is known to regulate the expression of scavenger receptors in the hemocytes (Shlyakhover *et al*, 2018; Valanne *et al*, 2018). At last, PL-ImpL2 is enriched in *Ham*, *Kn*, *CG9609*, and *Nf-YB*. *Ham* is shown to limit amplifying divisions in neural stem cells (Eroglu *et al*, 2014). *CG9609* is a zinc finger transcription factor poorly described, expressed mostly in ovaries (Robinson *et al*, 2013), and *Nf-YB* regulates cell death and proliferation (Ly *et al*, 2013).

Developmental links between the different hemocyte populations in NI animals

The GO term and the regulon analyses reveal distinct functions and properties for specific hemocyte clusters. The identification of the proliferative cluster prompted us to ask whether there is a filiation among the clusters and, if so, to define their hierarchical organization. We adopted two distinct strategies to predict the hierarchy between the clusters: RNA velocity (La Manno *et al*, 2018) and Monocle (Trapnell *et al*, 2014; Qiu *et al*, 2017a,b).

RNA velocity compares unspliced and spliced transcripts in the single-cell dataset, to evaluate the developmental direction of single cells and to generate a UMAP displaying the link between cells (La Manno *et al*, 2018). Following this, the cluster identities were appended to the RNA velocity map (Fig 4C). The map suggests that PL-prolif/PL-Inos is at the origin of most clusters, that PL-0, PL-1, PL-2, and PL-3 are derived from PL-Inos, and that PL-vir1, PL-Rel, and PL-robo2 are issued from PL-3, PL-0, and PL-2 (Fig 4C). The comparison of the RNA velocity results with the regulons (Fig 3C) suggests the pathways involved in the acquisition of the specific properties. First, from PL-prolif to PL-Inos and then to PL-1/PL-3, we observe a gradual reduction in the regulons *EcR* and *E2f1*. Then, the JNK-associated regulons (*Jra*, *Ets21C*) and the regulon *Rel* become progressively enriched starting from PL-3 to PL-Rel and PL-vir1 clusters. For the PL-robo2 branch, we observe a gradual enrichment of the regulons associated with the GATA factors *Srp* and *Pnr* and with the Hedgehog pathway (*Ci*) from PL-1/PL-3 to PL-2/PL-0. Concerning the remaining clusters, PL-Lsp is scattered over the clusters PL-0/PL-1/PL-2/PL-3, suggesting that it is also issued from PL-prolif/PL-Inos, but the directionality is unclear. At last, no clear directionality could be drawn for PL-AMP, PL-Pcd, CC, and PL-ImpL2, which suggests that their direct progenitors are not detected in our dataset (Fig 4C).

The second approach, Monocle, estimates the cell trajectories by first defining the sequences of gene expression changes required to adopt distinct cell states and then by positioning the cells on the trajectories according to their transcriptomes (Trapnell *et al*, 2014; Qiu *et al*, 2017a,b). The Monocle analysis identified trajectories in line with the branches observed with RNA velocity (Fig 4D). The PL-prolif/PL-Inos clusters are at one extremity, followed by PL-1/PL-3, then PL-2/PL-0, with PL-robo2

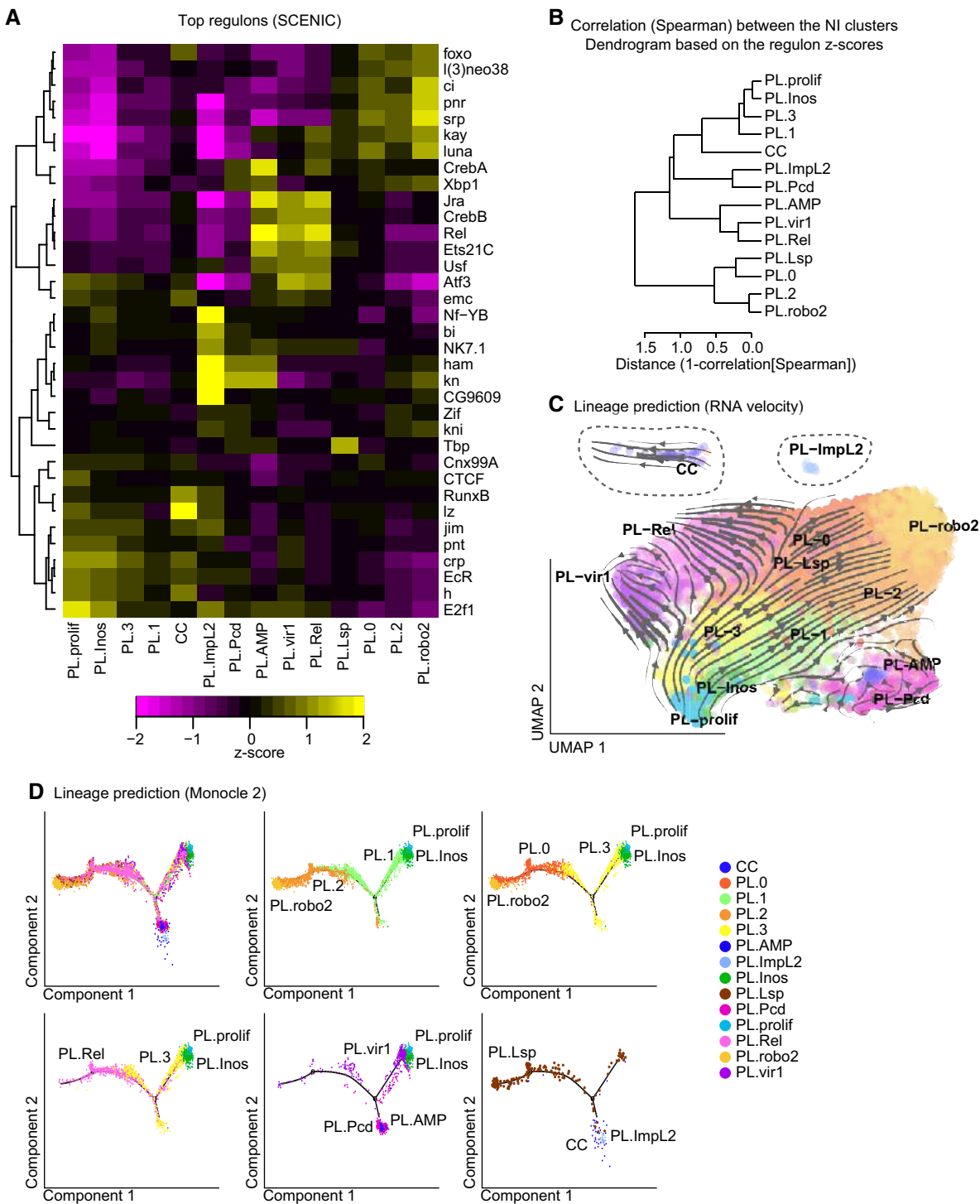


Figure 4. Identification of the cluster-specific molecular pathways and of the filiation between the NI clusters.

A Heatmap representing the z-score for the top 5 regulons of each cluster determined with SCENIC. The dendrogram on the left side of the panel indicates the correlation between the regulons across the dataset. The z-score is indicated with a gradient from magenta (z-score < 0, the regulon is repressed) to yellow (z-score > 0, the regulon is active).

B Dendrogram representing the distance among the clusters. The tree was built on the correlation (Spearman) calculated on the regulon matrix from the NI dataset.

C Lineage prediction using RNA velocity. The arrows and lines on the UMAP predict the “direction” taken by the cells of each cluster, based on the comparison between the levels of mRNA and pre-mRNA. Note that the clusters CC and PL-Impl2 (dashed lines) have been moved from their original position to fit in the graph.

D Single-cell trajectory reconstructed with Monocle 2 on the NI dataset. The first panel shows the overlap of all clusters, and subsequent panels show restricted number of clusters for which the RNA velocity analysis suggested a filiation.

at the other extremity. PL-Rel follows the PL-3 > PL-0 axis, and PL-vir1 follows the same direction as PL-Inos > PL-3.

Overall, these two distinct approaches return concordant results in terms of biological interpretation of the relationship between the clusters. We infer from these data that PL-prolif is at the origin of PL-0 to PL-3, PL-vir1, PL-Rel, and PL-robo2. In this model, PL-0 to PL-3 would represent the bulk of the plasmacytes that may then specialize into PL-vir1, PL-Rel, and PL-robo2.

Clusters' dynamics upon wasp infestation

In response to wasp infestation, the *Drosophila* larva displays a strong immune reaction involving multiple organs such as the muscle, the fat body, the lymph gland, and the hemocytes (Banerjee et al, 2019). A key response is triggered by the hemocytes, with the production of the lamellocytes, a fraction of whose aggregate around the wasp egg and encapsulate it to prevent its hatching. During this process, the hemocytes present in the resident compartment and in the lymph gland are recruited through cytokine secretion by the circulating hemocytes, the fat body, and the muscles (reviewed in Banerjee et al, 2019; Kim-Jo et al, 2019; Letourneau et al, 2016). To characterize the diversity of hemocytes generated by this systemic immune response, including the hemocytes released from the lymph gland, we produced single-cell RNA-seq data on the cells of the hemolymph from infested larvae.

The efficiency of the immune response of *Drosophila* larvae to wasp infestation critically depends on multiple parameters including the intensity of exposure (number of wasps, duration of the infestation), the genetic background of the *Drosophila* larvae, and the developmental stage and the temperature at which the infestation occurs (personal observations). To obtain a uniform response, we developed a protocol of mild infestation that maximizes the number of larvae containing a single wasp egg (Bazzi et al, 2018) and the survival rate of the *Drosophila OregonR* hosts (see Materials and Methods, Appendix Fig S6A). In these optimized conditions, we observe first the production of lamellocytes and a decrease in plasmacytes, which suggests that the plasmacytes trans-differentiate into lamellocytes from the resident and circulating pool of hemocytes (24 h after infestation). Following this, the lymph glands histolyse (> 90% of the lymph glands histolysed 48 h after infestation) and the hemocytes proliferate (Appendix Fig S6B–D). By 72 h after infestation (which corresponds to the time of hemocyte collection for the scRNA-seq), all lymph glands are histolysed and the hemolymph contains hemocytes (plasmacytes, crystal cells, and lamellocytes) from the two hematopoietic waves (Appendix Fig S7A–F; Bazzi et al, 2018). It is important to note that the WI dataset covers only the cells that have not encapsulated the wasp egg.

Compared to the NI dataset, the single-cell data on the WI hemolymph display two novel cell populations (LM-1 and LM-2) expressing the lamellocyte markers (Fig 5A and Appendix Fig S3B). The other clusters are already present in the NI dataset. PL-Inos, PL-prolif, PL-vir1, and PL-0 to PL-3 clusters increase in cell number, and the size of the PL-Lsp and PL-robo2 clusters remains constant, whereas that of the CC, PL-Pcd, and PL-Rel clusters decreases after wasp infestation (Fig 5B).

Comparisons between NI and WI data were carried out for each cluster but did not reveal strong transcriptomic modifications induced by the infestation. Each NI cluster is highly correlated with its WI counterpart (Appendix Fig S6E), and the markers and the GO terms remain rather similar (Fig 5C and D).

Characterization of the two lamellocyte clusters and their developmental links to the other clusters

To characterize further the two lamellocyte clusters, we compared first their transcriptomes to all the other clusters and carried out GO term enrichment analyses (Fig 6A and B). This comparison indicates an enrichment for genes involved in melanotic encapsulation, which is the primary role of the lamellocytes, a strong implication of the JNK pathway, which was previously implicated in lamellocytes production (Zettervall et al, 2004), and several GO terms related to cytoskeleton reorganization and integrin-mediated cell adhesion, two processes that are necessary for the formation of the capsule around the wasp egg (Irving et al, 2005).

We then compared the LM-1 and LM-2 clusters and found 157 genes up-regulated in LM-1 and 58 genes up-regulated in LM-2 (Fig 6A). Only few GO terms are enriched specifically in one or the other cluster: The LM-1-specific genes are involved in integrin processing, while the LM-2-specific genes are involved in cytoskeleton and mitochondrial processes (Fig 6B). The analysis of the top 10 markers for each population shows that the markers common to LM-1 and LM-2 include known and novel lamellocyte-specific markers (including Atilla, ItgaPS4, Rhea, Shot; in black in Fig 6C and D; listed in Dataset EV6). The markers enriched in LM-1 are expressed at low levels in LM-2 and in the other hemocyte clusters, whereas the markers enriched in LM-2 are also expressed in most hemocyte clusters (Fig 6C). This suggests that the LM-1 cluster represents the mature lamellocytes and LM-2 represents cells at a plasmacyte/lamellocyte intermediate state.

To investigate the link between the two lamellocyte populations and the plasmacytes, we carried out RNA velocity and Monocle analyses. The two analyses place LM-2 as intermediate between the plasmacytes and LM-1, and also suggest that the main cluster producing the lamellocytes is PL-vir1. Otherwise, the same major

Figure 5. Two additional hemocyte populations are produced after wasp infestation.

- UMAP projection representing the 16 clusters of cells identified in the WI sample. Note the presence of two additional clusters, LM-1 and LM-2, compared to the NI sample. The two clusters correspond to the lamellocytes.
- Estimation of the number of cells of each cluster per larva in normal condition (NI, orange) and after wasp infestation (WI, blue). For each cluster, the cell number was deduced from the total number of plasmacytes and lamellocytes enumerated in Appendix Fig S5D, and the proportion of each cluster in the single-cell datasets.
- GO term enrichment analysis for each cluster of the WI dataset. Represented as in Fig 2C.
- Dot plot representing the expression levels (gradient of red levels) and the percentage of cells (size of the dots) that express the top 5 markers of each cluster in the WI dataset.

Data information: Related to Appendix Figs S6 and S7.

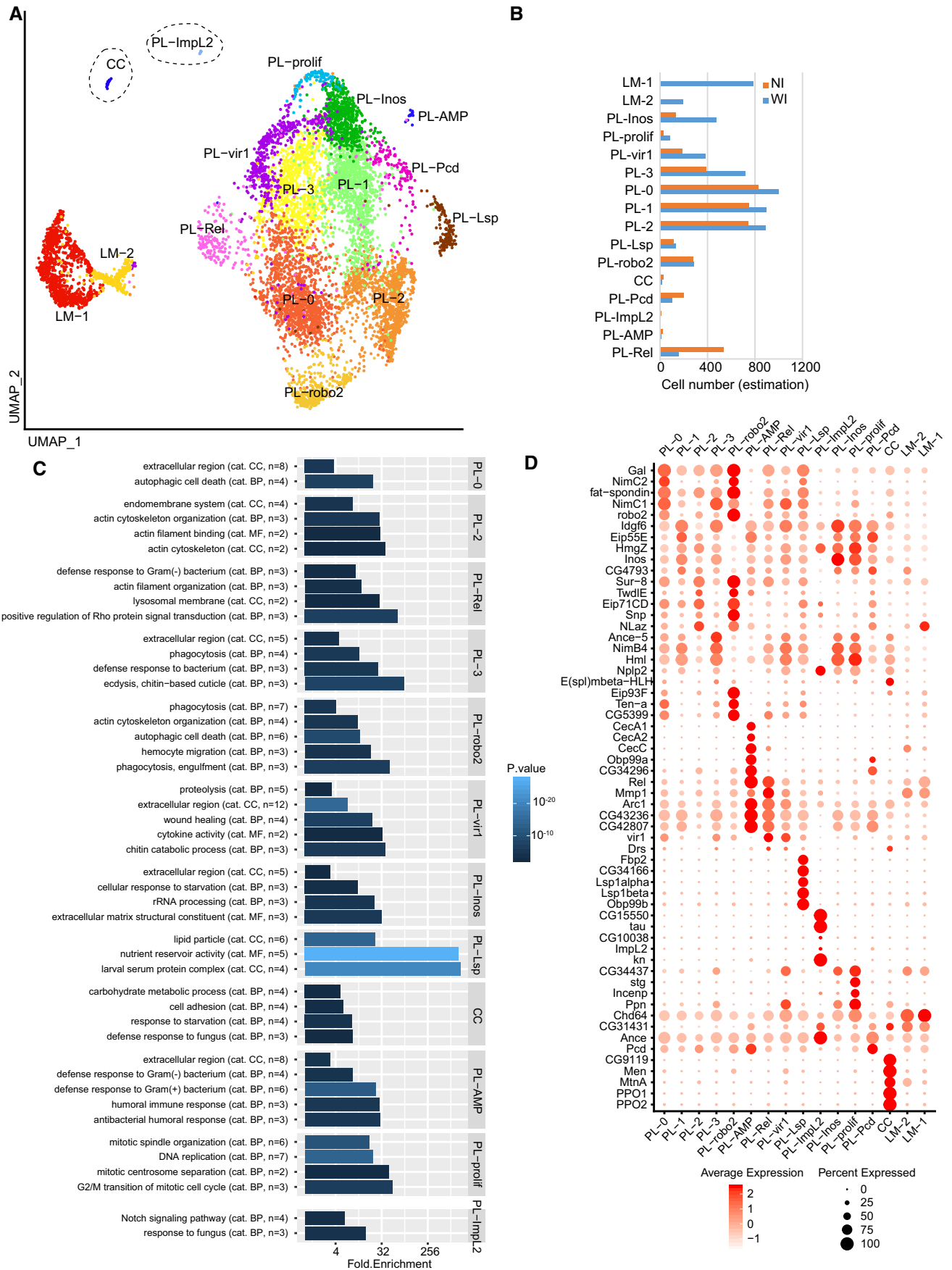


Figure 5.

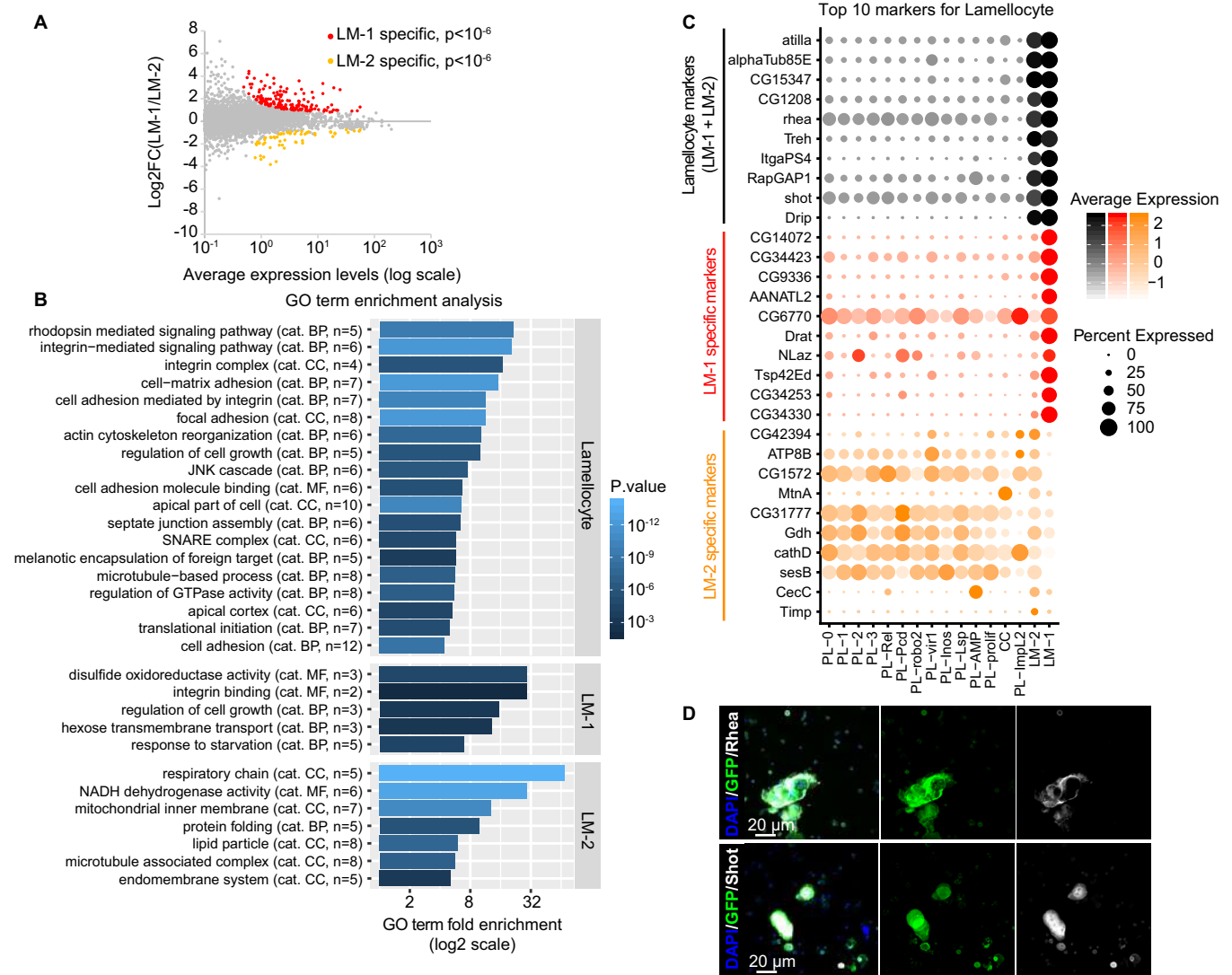


Figure 6. Characterization of the two lamellocyte clusters.

A Scatter plot comparing the transcriptome of the two lamellocyte clusters, deduced from the WI dataset. The x-axis is the average expression levels of the genes and the y-axis the log_2 fold change (LM-1/LM-2). The genes significantly enriched in the LM-1 cluster are highlighted in red ($P < 10^{-6}$), those significantly enriched in the LM-2 cluster in orange ($P < 10^{-6}$).

B GO term enrichment analysis on the genes enriched in lamellocytes compared to all other clusters (top panel) and on the genes specific to LM-1 (middle panel) or LM-2 (lower panel). The bars represent the fold enrichment, and the color gradient indicates the P-value of the GO term enrichment (as in Fig 2C).

C Expression levels (gradient of color) and the percentage of cells (size of the dots) for the top 10 markers of lamellocytes (in black), of markers specific to LM-1 compared to LM-2 (in red) and specific to LM-2 compared to LM-1 (in orange). Note that most markers enriched in LM-1 compared to LM-2 are exclusively expressed in LM-1, while most markers enriched in LM-2 compared to LM-1 are also expressed in the plasmatocyte and crystal cell clusters.

D Hemocytes from WL *OregonR* infested by wasp. The immunolabeling was done with antibodies targeting the new lamellocyte markers identified in this study Rhea (in gray, top panels) and Shot (in gray, lower panels). Phalloidin-FITC (in green) labels the actin filament particularly abundant in lamellocytes (Tokusumi *et al*, 2009), and the nuclei were marked with DAPI (blue). Full stacks are displayed; the left panels show the overlay of DAPI, FITC, and the lamellocyte markers; the middle panels show the FITC alone; and the right panels show the lamellocyte markers alone. The scale bars represent 20 μm .

branches from PL-prolif/PL-Inos to PL-rob2, PL-Rel, and PL-vir1 as those identified in the NI larvae are observed (Fig 7A and B).

Markers' dynamics upon WI

Considering the strong immune response induced by the WI, we expected a very robust modification of the transcriptional landscape of most hemocytes; however, the transcriptome of the plasmatocyte

clusters remains overall similar in WI compared to NI (see above and Appendix Fig S6E). To rule out that this observation is due to the low depth of the scRNA-seq, we used qPCR to quantify the main clusters' markers in NI and WI hemocytes from WL (Fig 8A). In agreement with the scRNA-seq data, the large majority of the NI plasmatocyte markers maintain the same expression profile upon WI. As expected, the lamellocyte markers are strongly up-regulated in WI (Fig 8A). In addition to the lamellocyte markers, the following

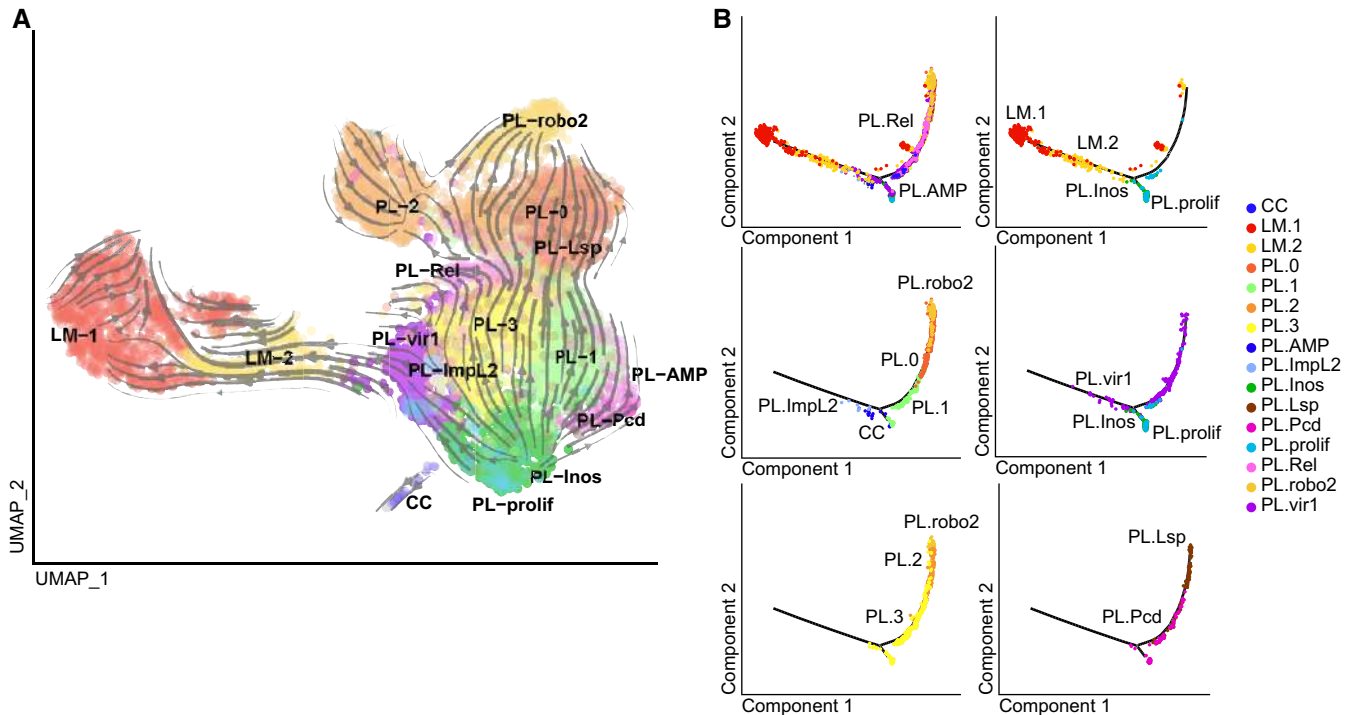


Figure 7. Identification of the filiation between the WI clusters.

A Lineage prediction for the clusters from the WI sample using RNA velocity, as in Fig 4C.

B Single-cell trajectory reconstructed with Monocle 2 on the WI dataset. The panels show restricted number of clusters for which the RNA velocity analysis suggested a filiation.

markers display significant up-regulation: NimB4 (marker of PL-Inos), CecC (PL-AMP), Hml and Sr-C1 (PL-prolif), and Lz (CC). This increase can reflect a modification of the size of their affiliated clusters, which is the case for PL-Inos and PL-prolif (Fig 5B). It also reflects the molecular response to the WI, which is likely the case for CC and PL-AMP whose size remains low upon WI.

To characterize the progression of the immune response to the infestation, we collected the hemocytes 24, 48 and 72 h after WI and quantified the expression levels of specific markers by qPCR (Fig 8B–D). CecC and the lamellocyte markers undergo strong up-regulation in the 24 h following the WI. Within this timeframe, the lymph gland is still intact (Appendix Fig S6C), indicating that this early response is produced by the hemocytes of embryonic origin. The high expression levels of the markers are then maintained until 72 h, suggesting that they are also expressed by the hemocytes released from the lymph gland (Fig 8C). The other markers (i.e., NimB4, Sr-C1, Lz, and Hml) do not display a strong modulation during the response (Fig 8B). We also characterized the expression levels of the PL-prolif markers *CycB*, *PCNA*, *Stg*, and *NCD*. The four markers display stable expression at 24 h and up-regulation at 48 h, which is maintained at 72 h after WI (Fig 8D). This suggests that the number of dividing cells stays constant at 24 h and increases later on. These data are concordant with the hemocyte counts at the different stages of infestation (Appendix Fig S6D). Within 24 h of infestation, the number of hemocytes remains the same, with lamellocytes being produced upon plasmatocyte trans-differentiation. In the following

time points, there is an increase in plasmatocyte number, which can be explained by the combination of the release of hemocytes from the lymph gland and increased proliferation (Fig 8D and Appendix Fig S6D).

Finally, to determine the origin of the hemocytes, we analyzed the expression levels of the main clusters' markers in the hemocytes originating from the lymph gland or from the embryo in WI conditions (Fig 8E). The hemocytes were traced using the lymph gland-specific driver *DotGal4* or the embryonic hemocyte driver *Srp(hemo)Gal4* combined with two lineage tracing transgenes (*gtrace*, see Materials and Methods section and Appendix Fig S7B, D and F). The hemocytes were sorted by FACS before quantification by qPCR. Of note, the filtration steps necessary for the FACS sorting removed most lamellocytes from the samples, which explains the low levels of lamellocyte markers in these data (personal observation). The analysis reveals enrichment for the markers of PL-prolif and CC in the embryonic-derived hemocytes. All other clusters display markers in the hemocytes from both origins. This suggests that the lymph gland produces hemocytes highly similar to the embryonic-derived hemocytes upon WI. It also suggests that the lymph gland releases only few crystal cells and proliferating cells in the hemolymph after WI.

Overall, this analysis indicates that the hemocytes from the lymph gland express most markers found in embryonic-derived hemocytes (in the NI dataset). Thus, at the present level of resolution of the scRNA-seq data, we cannot identify markers specific to the origin (i.e., embryonic or lymph gland) of the hemocytes.

Metabolic properties of the clusters

To observe the potential metabolic differences among the clusters, we analyzed the expression profile of the main actors of energy metabolism across the NI and WI datasets (Appendix Fig S8) in the same fashion as it was done on the bulk transcriptomes (Appendix Fig S2). Although the analyses carried out on the single cell are not as precise as the ones on the bulk transcriptome, most plasmatocyte clusters display metabolic markers in line with the

observations made with the bulk RNA-seq. We can hence use these data to draw first conclusions.

In the larva, the hemocytes import and metabolize lipids to drive the TCA cycle. Lipid-scavenging receptors and the genes of the fatty acid degradation pathway are expressed in most of them. The three exceptions are PL-AMP, PL-Pcd, and PL-Impl2 that express low levels of lipid-scavenging receptors and fatty acid degradation genes as well as low levels of TCA genes, suggesting a lower metabolism for these clusters (Appendix Fig S8 left panel).

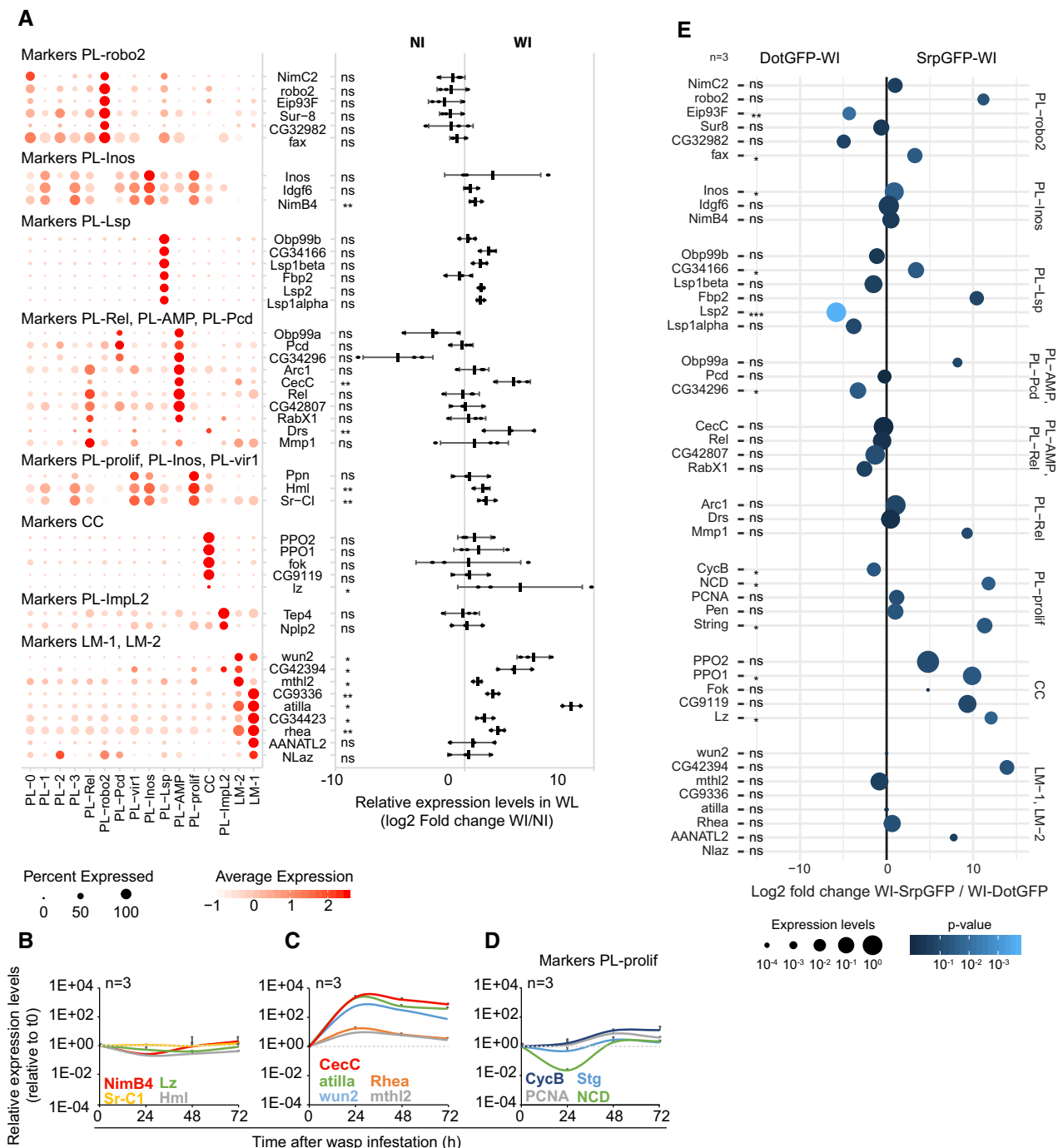


Figure 8.

Figure 8. Timing of the production of the different clusters in the hemolymph of WI larvae.

- A Expression levels of the cluster markers in the hemolymph of WI larvae compared to NI larvae. The left panel indicates the distribution of each marker across all clusters (as in Fig 2D), and the graph on the right panel indicates the \log_2 of the ratio between the expression level in WI versus NI. Positive values indicate an up-regulation upon wasp infestation and negative values a down-regulation ($n = 3$, pool of 10 larvae per replicate, mean \pm SD is represented on the graph). The P -value are estimated by bilateral Student's t -test and indicated as follow: ns = non-significant (> 0.05), ****** = $P[0.05-0.01]$, ******* = $P[0.01-0.001]$.
- B, C Expression levels of the cluster markers increasing in WI compared to NI according to (A) during the progression of the immune response to wasp infestation. Collections were carried out at t_0 (time of infestation, L2), 24 h (early L3), 48 h (mid L3), and 72 h (WL) after wasp infestation ($n = 3$). The timeline is on the x-axis and the normalized expression levels on the y-axis. The expression levels were normalized to the levels at t_0 . The dotted lines indicate t_0 relative level (=1). The markers that do not display strong variability during the timeline are presented in (B), and the ones showing a strong up-regulation are in (C).
- D Expression levels during the infestation timeline as in (B, C) for the markers of proliferation.
- E Weighted dot plot representing the enrichment (\log_2 fold change) of the markers in hemocytes originating from the lymph gland (DotGFP-WI) compared to embryonic hemocytes (srpGFP-WI) from WI larva. The lymph gland hemocytes and embryonic hemocytes were traced using the lymph gland driver DotGal4 and the embryonic driver Srp(hemo)Gal4, respectively, combined with a lineage tracing construct. The relative expression levels are indicated by the size of the dots and the P -value of the \log_2 fold change with the gradient dark blue (not significant) to light blue ($P < 10^{-3}$). The P -value is estimated by bilateral Student's t -test and indicated as follow: ns = non-significant (> 0.05), ****** = $P[0.05-0.01]$, ******* = $P[0.01-0.001]$, ******** = $P < 0.001$.

Data information: Related to Appendix Figs S6 and S8, and Table EV1.

The crystal cells distinguish themselves by the expression of the glucose transporters (Sut1 and Glut1) and genes involved in gluconeogenesis (fbp, Ald) and lipid biosynthesis (Lpin), suggesting a metabolism involving glucose and lipid uptake (Appendix Fig S8 left panel).

The wasp infestation enhances the expression levels of the lipid-scavenging receptors and of the fatty acid degradation genes in the plasmatocytes, including in the clusters PL-Pcd and PL-AMP, which suggests a stronger metabolic activity (Appendix Fig S8 right panel). We also noticed increased levels of the glucose transporter Glut1 and of the genes involved in glycolysis in PL- robo2 hemocytes, suggesting that the infestation induces a diversification of the energy source for this cluster (Appendix Fig S8 right panel). Finally, the lamellocyte clusters display a strong expression of the glucose transporter sut1. In addition, LM-1 displays a prominent glycolysis pathway, which may indicate that lamellocyte metabolism relies mostly on glucose (Appendix Fig S8 right panel).

The wasp infestation induces a strong metabolic shift in the larvae where the resources are deviated from development toward the immune response (Rauw, 2012). This shift, mediated by the hemocytes through the production of extracellular adenosine, increases considerably the sugar levels in the hemolymph (Bajgar et al, 2015). Our data suggest that this additional sugar is mostly used by the lamellocytes and by the PL- robo2 clusters to respond to the wasp infestation, while the other hemocyte clusters keep using lipids.

Discussion

The immune cells provide the first line of defense against the non-self, and accumulating evidence strongly suggests that their function exceeds the immune response. Due to their ability to communicate with the other organs and tissues, immune cells provide ideal sensors for the internal state and homeostasis during development and ontogeny. This raises the issue of immune cell heterogeneity; that is, can we identify subpopulations with specific potentials? The understanding of immune cell biology heavily relies on the thorough characterization of these cells as well as on the identification of specific markers and subpopulations. This work provides the first atlas of the *Drosophila* hemocytes, by specifically focusing on those that originate from the first hematopoietic wave. We show that

these hemocytes undergo a molecular and metabolic shift during development. We show the existence of distinct hemocyte populations and identify a large panel of novel markers specific to the different populations. Monitoring the larval response against the wasp *L. boulandi* reveals the hemocyte behavior upon challenge and defines intermediate and mature lamellocyte populations. Finally, we use multiple bioinformatics tools to predict a temporal progression among the different hemocyte clusters in control and in challenged conditions.

The developmental shift between the embryonic and the larval stages

Immune cells are considered as static components of our defense system; however, these cells constantly interact with the ever-changing environment. In addition, the cells that are born in the early embryo experience the extensive rearrangements that occur during development, including tissue and organ formation. We here show that the *Drosophila* hemocytes undergo a significant transcriptional shift that fully complies with the requirements of the embryonic and larval stages.

The highly migratory hemocytes present in the differentiated embryo display a strong developmental role: They allow tissue reshaping by secreting several constituents of the extracellular matrix and by engulfing dead cells through specific scavenger receptors such as NimC4. They display high levels of gluconeogenesis and TAG synthesis, processes that provide adequate levels of glucose and fatty acid for tissue/organ development. They secrete cuticle proteins. The larval hemocytes, on the other hand, express high levels of transcripts that are linked to the immune response, in accordance with the exposure to pathogens occurring after hatching, and are highly phagocytic. Moreover, they express fewer molecules associated with the extracellular matrix as compared to those observed in the embryo. Finally, they strongly express the molecular pathways that release stored energy (beta oxidation, TCA cycle), most likely in preparation for the metamorphosis and to help building the adult tissues.

Different types of hemocytes in wild-type larvae

The single-cell analysis on the NI animals reveals the presence of 14 different hemocyte clusters, based on the profile of gene expression,

on the enrichment in specific GO terms and regulons as well as on the *in vivo* validation. Indeed, a number of clusters are identified by a single regulon (Tbp for PL-Lsp, Lz for CC, E2f1 for PL-prolif) or by a specific combination of regulons in the case of related clusters (e.g., PL-vir1, PL-Rel, and PL-Amp). These data provide us with a battery of novel-specific markers and will make it possible to generate more targeted genetic tools. Excitingly, we can already define distinct features and functions of the different clusters.

The PL-Rel cluster likely provides a cellular reservoir for a specific immune response, and the closely related PL-AMP hemocytes seem more specifically dedicated to the humoral response, whereas PL-vir1 hemocytes seem associated with the anti-viral response. These three clusters share GO terms and regulons associated with immune functions, suggesting that they respond to a variety of challenges. These data suggest that specific hemocyte subtypes target different pathogens. This does not necessarily mean that only these hemocytes will respond to the infection, as these cells may just respond faster than others to a specific challenge.

The circulating PL-Lsp hemocytes represent the nutrient reservoir that stores amino acids and has a role in homeostasis. The PL-Lsp and PL-AMP hemocytes are associated with the major roles of the fat body, the metabolic homeostasis, and the humoral immune response, suggesting that they contribute to the fat body–hemocyte axis acting in physiological and pathological conditions. This axis is bidirectional. For example, (i) the small secreted peptide Edin produced in the fat body controls the number of plasmacytes in circulation upon wasp infestation; (ii) the hemocyte expression of the Spaetzle ligand controls the activity of Toll signaling in the fat body and affects the response to infection (Shia *et al*, 2009) as well as tumor growth (Parisi *et al*, 2014); and (iii) the metabolically induced production of the NimB5 protein from the fat body adjusts the number of hemocytes to the physiological state of the larva (preprint: Ramond *et al*, 2019).

The PL-robo2 hemocytes are associated with phagocytosis and may serve as a sensor of lipid levels in the hemolymph (Woodcock *et al*, 2015). This cluster shares features with the large PL-0 and PL-2 clusters that are mildly enriched for the regulon related to the phagocytic abilities (srp), in agreement with the finding that the vast majority of the larval hemocytes is phagocytic (Fig 1). The PL-0, PL-2, PL-1, and PL-3 clusters, which do not display strong specific molecular features, may serve different purposes, perhaps less efficiently than the more specialized hemocytes, or may express enhanced potentials in response to specific challenges.

The unexpected finding that a cluster expresses a high rate of ribosomal protein suggests that either translation is higher in PL-Pcd hemocytes compared to other clusters or that the ribosomal proteins high in this cluster act on the immune response in an uncanonical fashion. Notably, studies in mammals indicate that ribosomal protein like RPS3 selectively modulates the target genes of NF- κ B, the orthologue of Rel (Zhou *et al*, 2015).

The data on the small CC cluster validate the role of these cells in melanization and reveal a distinct metabolism as they seem to use glucose as energy source, whereas the plasmacytes mostly use lipids.

The PL-prolif cells, mostly localized in the resident compartment, likely provide the pool of mitotic precursors for most of the hemocyte clusters identified in the larva and PL-Inos the immature progenitors, respectively.

The PL-Impl2 cluster defines PSC-like cells present outside of the lymph gland in a still unknown location. These hemocytes are likely set aside in the embryo, in line with the findings that they are significantly enriched for transcripts that are specific to the E16 hemocytes (bulk transcriptome analyses, unpublished data) and that they do not seem to originate from the PL-prolif cluster.

The identification of different populations of specialized plasmacytes in the *Drosophila* larva prompts us to draw parallels with the mammalian immune cells. The closest relative to plasmacytes is the monocytes and the macrophages (Wood & Martin, 2017). Monocytes are equipped with Toll-like receptors, scavenger receptors, and their main function is to patrol as well as remove microorganisms, lipids, and dying cells via phagocytosis. Upon inflammation, they infiltrate specific tissues and differentiate into macrophages. The macrophages keep phagocytosing, induce an inflammatory response by releasing cytokines, and participate to repair of the tissue (Yang *et al*, 2014). The scRNA-seq assay reveals that hemocytes express markers such as Integrin alphaPS2 (If), EcR/Hr96, Lamp1, Rgh, Tfc/lectin-46Cb/CG34033, and Lz, which are the *Drosophila* orthologues of CD11b, PPAR γ , CD68, Dectin, CD207, and RUNX, respectively. In mammals, these proteins are responsible for migration, adhesion, phagocytosis, differentiation from monocytes to macrophages, and pathogen recognition (Ramprasad *et al*, 1996; Voon *et al*, 2015; Podolnikova *et al*, 2016; Daley *et al*, 2017; Heming *et al*, 2018).

Single-cell analyses of the kind we performed on the fly hemocytes bring about the important question of whether the differences observed between clusters are stable or transient; in other words, do the clusters represent different and stable identities or do they reflect the presence of transient, unstable, states? Based on our data, we speculate that some clusters represent specific populations (the LSP producing plasmacytes, the crystal cells, etc.), because they display very unique features. The Prolif and the Inos plasmacytes, on the other hand, share a number of markers and may represent states of the same cluster. Plasmacyte clusters 0–3, which can only be resolved using a combination of markers, may also represent developmental states, in line with the trajectories identified by the bioinformatic analyses. In this regard, investigating the similarities and differences to the adult hemocytes will shed light on some of these issues.

The larval response to wasp infestation

The single-cell analysis upon WI reveals the reduced representation of some clusters such as PL-Rel and the expanded representation of “early” clusters (e.g., PL-prolif, PL-Inos). Thus, specific hemocyte clusters may preferentially survive/proliferate upon challenge. The majority of the clusters, however, remain equally represented in the two conditions, and the correlation between the average transcriptomes in NI and WI conditions reveals strong similarity between most of the identified clusters (Pearson = 0.97). This implies that the hemocytes produced by the 1st and the 2nd hematopoietic waves share major features.

Two new populations of cells appear, LM-1 and LM-2, the second one representing an intermediate state characterized by the co-expression of lamellocyte and plasmacyte genes. Interestingly, LM-2 also expresses a specific identity that is linked to energy

supply (e.g., respiratory chain, NADH activity), whereas LM-1 cells are mostly devoted to encapsulation.

With respect to the mode of lamellocyte production, the bioinformatics predictions (RNA velocity and Monocle) could support the hypothesis of a dedicated precursor, the lamelloblast (Anderl *et al*, 2016). The PL-prolif cluster seems to rapidly branch out with one arm giving rise to lamellocytes, partly associated with the PL-vir1 cluster, and the other arm giving rise to the other plasmatocyte clusters. In this model, the 1st hematopoietic wave would produce lamellocytes through trans-differentiation (the expression of LM-2 markers already increases in the first 24 h after infestation), whereas the 2nd wave would do it (also) through the mitotically active lamelloblast. At the level of resolution provided by the scRNA-seq assay, we may have lost the lamelloblast cluster.

In sum, the different clusters identified by the scRNA-seq assay exhibit distinct features, which can be now tested functionally using the newly identified markers and the associated genetic tools that are publically available (Gal4 drivers, RNAi and overexpressing transgenes, mutations). Future technological refinements may enhance the depth of the analyses, as the current scRNA-seq assays only allow for the identification of a subset of genes for each cluster, the most expressed ones. As an example, the larval hemocytes do not all phagocytose with the same efficiency, but we cannot allocate the different potentials to specific clusters (Appendix Fig S5F). Nevertheless, our data on the bulk and single-cell transcriptomes of the *Drosophila* hemocytes provide a powerful framework to understand the role of immune cells in physiological and pathological conditions.

Materials and Methods

Fly strains and genetics

All flies were raised on standard media at 25°C. For the bulk sequencing, the hemocytes from stage 16 (E16) embryos were collected from *srp(hemoGal4/+;UAS-RFP/+)* animals obtained upon crossing *srp(hemo)Gal4* (gift from K. Brückner; Bruckner *et al*, 2004) and *UAS-RFP* flies (RRID:BDSC_8547). The wandering L3 (WL) hemocytes were collected from staged *HmlARFP/+* animals upon crossing *HmlARFP* (Makhijani *et al*, 2011) with *OregonR* flies (108–117 h After Egg Laying, h AEL).

For the single-cell sequencing, *OregonR* flies were used as the wild-type (WT) strain for all the experiments and for the single-cell RNA sequencing.

Validation of the single-cell data involved the following stocks: *srp(hemo)-moesin-RFP* [stock D2244 on chr 2, gift from D. Siekhaus (Gyoergy *et al*, 2018)], *Mimic-Lsp1beta-MI05460* (RRID:BDSC_40782), *Lsp2-Gal4* (RRID:BDSC_6357), the lineage tracing line *UAS-FLP*, *Ubi-p63E(FRT.STOP)Stinger* (RRID:BDSC_28282) that was combined with *UAS-FLP*; *act5c-FRT,y+,FRT-Gal4,UASmCD8GFP* [gift from I. Ando (Honti *et al*, 2010)], and *Dot-Gal4* (RRID:BDSC_6903) and *GstD-LacZ* [gift from D. Bohmann (Sykietis & Bohmann, 2008)].

FACS sorting of embryonic and larval hemocytes

Staged egg laying was carried out to produce E16 embryos as follows. The cross to produce *srp(hemo)Gal4/+;UAS-RFP/+* embryos

(with at least 100 females) was transferred to egg laying cages on a yeasted apple juice agar at 25°C. After a pre-lay period of 30 min, the agar plates containing yeast were replaced with fresh plates and flies were left to lay for 3 h at 25°C. Agar plates were then removed, and the embryos were raised for 11 h and 40 min at 25°C until they reached stage 16. Embryos were then isolated from the medium and washed on a 100- μ m mesh. The collected embryos were transferred into a cold solution of phosphate-buffered saline (PBS) in a Dounce Homogeniser on ice. The embryos were dissociated using the large clearance pestle than the small clearance pestle, and then, the cells were filtered through a 70- μ m filter to prepare them for FACS sorting. The cells were sorted using FACS Aria II (BD Biosciences) at 4°C in three independent biological replicates. Live cells were first selected based on the forward scatter and side scatter, and only single cells were taken into account. *OregonR* cells were used as a negative control to set the gate for the sorting of RFP-positive cells only (Appendix Fig S1). RFP-positive hemocytes were collected in 1 ml of TRI reagent (MRC) for RNA extraction.

For the wandering L3, *HmlARFP/+* hemocytes, staged lay of 3 h, were carried out at 25°C to prevent overcrowding of the vials (between 50 and 100 embryos per vial) and wandering larvae were collected 108–117 h AEL, bled in cold PBS containing PTU (Sigma-Aldrich P7629) to prevent hemocyte melanization (Lerner & Fitzpatrick, 1950), filtered through a 70- μ m filter to isolate them, and sorted by FACS as described for the embryonic hemocytes.

The purity of the sorted populations was assessed prior to the collection of the sample for RNA extraction by carrying out a post-sort step. The FACS sorter was set up to produce hemocyte pools displaying at least 80% of purity on the post-sort analysis.

RNA extraction and bulk RNA sequencing

The sorted cells were homogenized then left at room temperature (RT) for 5 min to ensure complete dissociation of nucleoprotein complexes. 0.2 ml of chloroform was added to each sample followed by centrifugation at 12,000 *g* for 15 min at 4°C. The upper aqueous phase containing the RNA was collected and transferred to a fresh autoclaved tube. 0.5 ml of 2-propanol was added, and the samples were incubated for 5–10 min at RT. The RNA was precipitated by centrifugation, washed with 1 ml of 75% ethanol, precipitated again, and air-dried. 20 μ l of RNase-free water was added to each sample before incubation at 55°C for 15 min. Single-end mRNA-seq libraries were prepared using the SMARTer (Takara) Low Input RNA Kit for Illumina sequencing. All samples were sequenced in 50-length single read. At least 40 \times 10⁶ reads were produced for each replicate (Appendix Fig S1).

Analysis of bulk RNA-seq data

The data analysis was performed using the GalaxEast platform, the Galaxy instance of east of France (<http://www.galaxeast.fr/>, RRID:SCR_006281; Afgan *et al*, 2018). First, summary statistics was computed on the raw FastQ Illumina files of the dataset using the quality control tool for high-throughput sequence data FastQC (Babraham Bioinformatics, RRID:SCR_014583). FastQ Illumina files were converted to FastQ Sanger using the FastQ Groomer tool after assessing the quality of the sequencing. The FastQ Sanger files were then mapped onto the *D. melanogaster* reference genome Dm6

using TopHat (RRID:SCR_013035; Trapnell *et al*, 2009). As for the expression levels, the analysis of differential gene expression was based on the number of reads per annotated gene. This was done by using Htseq-Count (RRID:SCR_011867; Anders *et al*, 2015), and the comparison and normalization of the data between the different cell types were done in Deseq2 (Appendix Fig S1; RRID:SCR_015687; Anders & Huber, 2010). The gene ontology studies presented in Fig 1B and Dataset EV1 were done using the Database for Annotation, Visualisation and Integrated Discovery (DAVID) v6.8 (<https://david.ncifcrf.gov/>, RRID:SCR_001881; Huang *et al*, 2009) for the identification of biological processes.

The metabolic pathway analysis (Appendix Fig S2) was done as follows. Genes that showed a fold change ≥ 2 with an adjusted *P*-value of less than 0.05 were considered for gene set enrichment analysis. Gene ontology and KEGG pathway enrichment analysis of the differentially expressed genes were done in ShinyGO v0.60 webserver (preprint: Ge & Jung, 2018). Genes associated with metabolic pathways considered in this study were retrieved from the KEGG database (<http://www.genome.jp/>, RRID:SCR_012773; Kanehisa & Goto, 2000). The \log_2FC values of the metabolic genes ($q < 0.05$) in the hemocytes were then plotted using R (version 3.4.0; R Core Team, 2017). The corresponding expression data for these genes in the “Embryo_16-18 hr” and “larva_L3_puffstage_7-9” developmental stages from modENCODE database (RRID:SCR_006206; Graveley *et al*, 2011) were downloaded using the webtool DGET (Hu *et al*, 2017; <https://www.flyrnai.org/tools/dget/web/>). These data were used to calculate the fold change and are represented as bar-plots. For genes with paralogs, the paralog with highest fold change has been considered for the analysis. The details of all the genes (including all the paralogs) from these pathways are present in Table EV1, and the genes represented in the bar-plots (Appendix Fig S2) are highlighted in yellow.

Phagocytosis assay

Hemocytes from E16 embryos and wandering larvae underwent the phagocytosis assay with latex beads. Briefly, *srp(hemo)-moesin-RFP* flies were staged for 3 h at 25°C, and then, the embryos were incubated at 25°C for 12 h in order to reach stage 16. Then, the embryos were collected and dechorionated in 25% bleach for 5 min at RT. Upon that the embryos were washed, homogenized with Dounce Homogeniser in Schneider medium complemented with 10% fetal calf serum (FCS), 0.5% penicillin, 0.5% streptomycin (PS), and few crystals of N-phenylthiourea $\geq 98\%$ (PTU) (Sigma-Aldrich P7629) to prevent hemocyte melanization (Lerner & Fitzpatrick, 1950), and filtered with a 70- μm filter. Twenty third-instar larvae were bled in Schneider medium. Hemocytes for both stages were treated at the same time with latex beads 0.50 μm (Polysciences Inc., cat 17152) for 5 and 20 min, cytospinned at 700 rpm for 3 min, fixed for 10 min in 4% paraformaldehyde/PBS at RT, incubated for 30 min with DAPI to label nuclei (Sigma-Aldrich) (diluted to 10–3 g/l in blocking reagent) and phalloidin Cy3 (only for the WL3 hemocytes due to low moesin-RFP signal), and then mounted in Aqua-Poly/Mount (Polysciences, Inc.). The slides were analyzed by confocal microscopy (Leica Spinning Disk) using identical settings.

For the phagocytosis assay on NimC1/P1-negative hemocytes, 20 third-instar larvae were bled in Schneider medium supplemented with PTU and were treated with latex beads 0.50 μm diluted 1/500

for 2, 5, or 10 min. Cells were then fixed and labeled with rabbit anti-Srp(Bazzi *et al*, 2018) and mouse anti-P1(Vilmos *et al*, 2004). We then used the secondary antibodies Cy5 goat anti-mouse IgG (Jackson ImmunoResearch Labs Cat# 115-177-003, RRID:AB_2338719) and Cy3 goat anti-rabbit IgG (Jackson ImmunoResearch Labs Cat# 111-165-144, RRID:AB_2338006) and DAPI. Images were acquired using Leica Spinning Disk microscope. Images produced were analyzed in Fiji (RRID:SCR_002285; Schindelin *et al*, 2012).

Imaging

The images produced for this paper were acquired on a Leica Spinning Disk from the Imaging center of the IGBMC (<http://ici.igbmc.fr/>). The acquisition step was 0.5 μm with a 40 \times magnification. For the quantifications, three or more fields per sample were used with more than 50 cells in total. The intensity of latex beads or protein levels was measured with the Imaris software (version 9.5).

Hemocyte immunolabeling

Ten 3rd-instar larvae per sample were bled in Schneider medium complemented with 10% fetal calf serum (FCS), 0.5% penicillin, 0.5% streptomycin (PS), and few crystals of N-phenylthiourea $\geq 98\%$ (PTU). For the collection of circulating hemocytes, the hemolymph was gently allowed to exit, while resident hemocytes were scraped and/or jabbed off the carcass in a second well as described in Petraki *et al* (2015). For the infested larvae, there was no separation of circulating from resident hemocytes and we used five larvae per sample. The cells were cytospinned at 700 rpm for 3 min; then, the samples were fixed for 10 min in 4% paraformaldehyde/PBS at RT, incubated with blocking reagent (Roche) for 1 h at RT, incubated overnight at 4°C with primary antibodies diluted in blocking reagent, washed three times for 10 min with PTX (PBS, 0.1% Triton X-100), incubated for 1 h with secondary antibodies, washed twice for 10 min with PTX, incubated for 30 min with DAPI and phalloidin GFP, and then mounted Aqua-Poly/Mount (Polysciences, Inc.). The slides were analyzed by confocal microscopy (Leica Spinning Disk) using identical settings between control and infested samples. The following combination of primary antibodies was used to determine the fraction of lamellocytes: mouse anti-Relish [1:40; supernatant from the Developmental Studies Hybridoma Bank (DSHB Cat# anti-Relish-C 21F3, RRID:AB_1553772)], mouse anti-Shot (1:40; supernatant, DSHB Cat# anti-Shot mAbRod1, RRID:AB_528467), mouse anti-Talin (Rhea) (1:40; DSHB Cat# Talin A22A, RRID:AB_10660289) mouse anti-Talin (Rhea) (1:40, DSHB Cat# Talin E16B, RRID:AB_10683995), and rat anti-Elav (1:200; DSHB Cat# Rat-Elav-7E8A10 anti-elav, RRID:AB_528218). The secondary antibodies, Cy3 donkey anti-mouse IgG (Jackson ImmunoResearch Labs Cat# 715-165-151, RRID:AB_2315777), Cy3 goat anti-rat IgG (Jackson ImmunoResearch Labs Cat# 112-165-167, RRID:AB_2338251), Cy5 goat anti-mouse IgG (Jackson ImmunoResearch Labs Cat# 115-177-003, RRID:AB_2338719), and Cy5-AffiniPure goat anti-rat IgG (H+L) (Jackson ImmunoResearch Labs Cat# 112-175-167, RRID:AB_2338264), were used at 1:500.

Quantitative PCR

For the comparison between resident and circulating hemocytes, 20 3rd-instar larvae per sample were bled on ice-cold PBS and

the circulating hemocytes were separated from the resident ones as described above. The cells were then centrifuged at 300 g, 4°C, and RNA isolation was performed with the RNeasy Mini Kit (Qiagen) by following the manufacture's protocol. The DNase treatment was performed with the TURBO DNA-free Kit (Invitrogen), and the reverse transcription (RT) was done by using the Super-Script IV (Invitrogen) with random primers. The cycle program is used for the RT 65°C for 10 min, 55°C for 20 min, 80°C for 10 min. The qPCR we used is FastStart Essential DNA Green Master (Roche). The primers are listed in Dataset EV5. The *P*-values and statistical test used are indicated in Table EV1.

For the quantitative PCR done on *UAS-FLP/+;srp(hemo)Gal4/gtrace-mCD8-GFP;gtrace-nls-GFP/+* and *UAS-FLP/+;DotGal4/gtrace-mCD8-GFP;gtrace-nls-GFP/+*, 30 wandering third-instar larvae were collected per replicate, the larvae were bled in PBS supplemented with PTU, and the cells were filtered through a 70- μ m filter to prepare them for FACS sorting. The cells were sorted using FACS Aria II (BD Biosciences) at 4°C in three independent biological replicates. Live cells were first selected based on the forward scatter and side scatter, and only single cells were taken into account. *UAS-FLP/+;gtrace-mCD8-GFP/+;gtrace-nls-GFP/+* cells were used as a negative control to set the gate for the sorting of GFP-positive cells only. GFP-positive hemocytes were collected, and the RNA isolation and qPCR were done as mentioned above.

Single-cell sample preparation, sequencing, and analysis

OregonR females were used for the generation of the single-cell data. For the NI sample, 20 female larvae were collected at the wandering L3 stage (108–117 h AEL at 25°C) and bled in Schneider medium complemented with PTU on ice. Both circulating and resident pools of hemocytes were collected as described in Petraki *et al* (2015). Briefly, the larval cuticle was first punctured to release the circulating hemocytes and then scrapped with fine forceps to release the resident hemocytes. The efficiency of the method was assessed with the *HmlARFP* strain by inspecting visually the larval carcass for remaining hemocytes.

For the WI sample, staged larvae were infested at the L2 stage (48–56 h AEL) for 2 h at 20°C with 20 female wasps (*L. bouhardi*) per 100 *Drosophila* larvae. Following infestation, the larvae were raised at 25°C until the wandering L3 stage. Of note, the wasp infestation induces a developmental delay, as infested larvae reach the wandering stage at ~120 h AEL. In an effort to obtain reproducible results, the infestation conditions were optimized so that the majority of the larvae carry a single wasp egg (Bazzi *et al*, 2018). Twenty female larvae were processed as described above for the NI condition.

After bleeding, the hemolymph from NI and WI larvae was filtered on a 100- μ m mesh to remove cell aggregates and wasp eggs. The cell viability was assessed with trypan blue (over 90%), and cell concentration was estimated with a hemocytometer. 10,000 cells of each condition were used to prepare the 3'mRNA-seq libraries with the Chromium Single Cell 3' Reagent Kits v2 (10 \times Genomics). The libraries were then sequenced on the sequencer Illumina HiSeq 4000, on two lanes using paired sequencing of 2 \times 100nt. The raw data were analyzed using Cell Ranger v3.0.1 (pipeline from 10 \times Genomics) and mapped to the *Drosophila*

genome assembly BDGP6_ens95. Cells with low unique molecular identifiers (< 200) were removed.

Clustering the single-cell data

The single-cell data were further analyzed using the R based toolkit Seurat v3 (RRID:SCR_016341; Butler *et al*, 2018; Stuart *et al*, 2019). Following this, both NI and WI datasets were combined following the standard workflow for data integration (Stuart *et al*, 2019). Briefly, first the datasets were normalized using log-normalization and the variable features (set up to 2,000 with the variance stabilizing transformation method) were determined for each dataset individually. Then, the anchors common between the two datasets were determined (dimensionality set up to 50) and the two datasets were corrected for batch effect before integration. The integrated data were clustered using PCA and visualized with UMAP. The optimal number of dimensions for the generation of the UMAP was determined using the tools DimHeatmap and Elbowplots, and the clustering was done on 20 dimensions with a resolution of 0.55. These parameters returned 14 clusters. Further clustering was then attempted on each cluster separately (manual curation). If the manual curation returned more than 10 distinct markers ($|\text{avg_logFC}| > 1$, ROC analysis returning AUC > 0.75), the cluster was subsequently subdivided. This protocol led to the redefinition of the PL-Rel and PL-Inos clusters (see Appendix Fig S3).

The GO term enrichment analysis was carried out based on gene expression levels in NI condition to identify the main features of the clusters. The number of lamellocytes being negligible in the NI dataset (eight cells), they were excluded from this analysis. The genes enriched in each cluster ($\log_2\text{FC} > 0.25$, adjusted *P*-value < 0.01, determined with FindAllMarkers from Seurat, Dataset EV2) were analyzed using DAVID. The list of cluster-specific genes was compared to the list of genes expressed in the whole dataset. The whole GO term results are available in Dataset EV3, and for each hemocyte cluster, the hemocyte-related GO terms displaying the strongest enrichment are presented in Fig 2C.

RNA velocity analysis

To visualize the ongoing transcriptional changes in single cell, we adopted the approach described in La Manno *et al* (2018); i.e., we calculated the “velocity” of each cell in the high-dimensional gene expression space. We started by generating the loom file, containing spliced and unspliced reads with velocity, version 0.17.17 (<http://velocity.org/velocity.py>; La Manno *et al*, 2018). As input to velocity, we gave the “run10x” option (specific for 10 \times data), the Cell Ranger output, and Ensembl annotation v95 (ftp://ftp.ensembl.org/pub/release-95/gtf/drosophila_melanogaster/). Our NI dataset includes 4.2% intronic sequences, on which velocity analysis was based. The representation of the data was done with the package scVelo (<https://scvelo.readthedocs.io/>; preprint: Bergen *et al*, 2019) that implements UMAP representations.

Monocle graph reconstruction

To complement the RNA velocity analysis, we run also Monocle 2 (Trapnell *et al*, 2014; Qiu *et al*, 2017a,b). We use the R version 3.5.1. The CellDataSet has been built using

“expressionFamily=negbinomial.size()”. We adopted “DDRTree” method for dimensionality reduction, and a maximum number of components equals 2.

Regulon analysis

To identify the regulons involved in the hematopoietic system, we ran Single-Cell regulatory Network Inference and Clustering (SCENIC, RRID:SCR_017247; Aibar *et al*, 2017) through its Python implementation pySCENIC, version 0.9.19 (<https://pyscenic.readthedocs.io/en/latest/>). The source code was downloaded from the GitHub repository <https://github.com/aertslab/pySCENIC.git>. The supplemental files necessary to run SCENIC were obtained from <https://resources-mirror.aertslab.org/cistarget/>. For the analysis, we chose the motifs version 8 (<http://cistarget/motif2tf/motifs-v8-nr.flybase-m0.001-o0.0.tbl>) and the regulatory elements within 5 kb upstream the TSS and the transcript introns (http://cistarget/databases/drosophila_melanogaster/dm6/flybase_r6.02/mc8nr/gene_based/dm6-5-kb-upstream-full-tx-11species.mc8nr.feather). Finally, to identify the most significant regulons showing a different activity among clusters, we performed a Wilcoxon rank-sum test (Mann & Whitney, 1947), between the AUC scores given by SCENIC in a specific cluster versus all the rest of the clusters.

Comparison of regulon-based and gene-based clusters

We performed clustering based on the regulon AUC scores per cell, by adopting the “Louvain” algorithm with a resolution equal to 1.3 in Scanpy (Wolf *et al*, 2018) version 1.4.4, in order to obtain the same number of clusters (=16) than in the previous gene-based analysis. To compare the results from gene-based and the regulon-based clustering, we calculated the Rand index (Rand, 1971), obtaining a value of 0.83. Rand index (RI) = 0 means no overlaps between the clusters; RI = 1 means perfect overlap.

Data availability

The datasets produced in this study are available in the following databases:

- The scRNA-seq data have been deposited in the ArrayExpress database at EMBL-EBI (www.ebi.ac.uk/arrayexpress) under accession number E-MTAB-8698.
- The RNA-seq data have been deposited in the ArrayExpress database at EMBL-EBI (www.ebi.ac.uk/arrayexpress) under accession number E-MTAB-8702.

Expanded View for this article is available online.

Acknowledgements

We thank the Imaging Center of the IGBMC for technical assistance. This study was supported by the grant ANR-10-LABX-0030-INRT, a French State fund managed by the Agence Nationale de la Recherche under the frame program Investissements d’Avenir ANR-10-IDEX-0002-02. The sequencing was performed by the GenomEast platform, a member of the “France Génomique” consortium (ANR-10-INBS-0009). We thank C. Thibault-Carpentier, V. Alunni, and C. Keime for handling the single-cell library preparation, the sequencing,

and the initial analysis on Cell Ranger. We thank I. Ando, K. Bruckner, M. Crozatier, M. Meister, D. Siekhaus, and D. Bohmann for providing fly and wasp stocks. In addition, stocks obtained from the Bloomington Drosophila Stock Center (NIH P400D018537) and antibodies obtained from the Developmental Studies Hybridoma Bank created by the NICHD of the NIH and maintained at The University of Iowa (Department of Biology, Iowa City, IA 52242) were used in this study. We thank Dasaradhi Palakodeti for useful discussion on transcriptome analysis. This work was supported by INSERM, CNRS, UDS, Ligue Régionale contre le Cancer, Hôpital de Strasbourg, ARC, CEFIPRA, ANR grants, and by the CNRS/University LIA Calim. T. Mukherjee and Nivedita Hariharan are funded by the Council for Scientific and Industrial Research fellowship. A. Pavlidaki is an IGBMC International PhD Programme fellow supported by LabEx INRT funds. The IGBMC was also supported by a French state fund through the ANR labex.

Author contributions

Conceptualization, PBC and AG; Methodology, PBC, AG, RS, AP, CD, NM, AR, TM, and NH; Investigation, PBC, AG, RS, AP, CD, NM, AR, TM, and NH; Writing—Original Draft, PBC, AG, RS, and AP; Writing—Review and Editing, PBC, AG, RS, and AP; Funding Acquisition, AG, NM, and TM; Resources, AG; Supervision, PBC and AG.

Conflict of interest

The authors declare that they have no conflict of interest.

References

- Afgan E, Baker D, Batut B, van den Beek M, Bouvier D, Cech M, Chilton J, Clements D, Coraor N, Gruning BA *et al* (2018) The Galaxy platform for accessible, reproducible and collaborative biomedical analyses: 2018 update. *Nucleic Acids Res* 46: W537–W544
- Aibar S, Gonzalez-Blas CB, Moerman T, Huynh-Thu VA, Imrichova H, Hulselmans G, Rambow F, Marine JC, Geurts P, Aerts J *et al* (2017) SCENIC: single-cell regulatory network inference and clustering. *Nat Methods* 14: 1083–1086
- Akira S, Uematsu S, Takeuchi O (2006) Pathogen recognition and innate immunity. *Cell* 124: 783–801
- Anderl I, Vesala L, Ihalainen TO, Vanha-Aho LM, Ando I, Ramet M, Hultmark D (2016) Transdifferentiation and proliferation in two distinct hemocyte lineages in *Drosophila melanogaster* larvae after wasp infection. *PLoS Pathog* 12: e1005746
- Anders S, Huber W (2010) Differential expression analysis for sequence count data. *Genome Biol* 11: R106
- Anders S, Pyl PT, Huber W (2015) HTSeq—a Python framework to work with high-throughput sequencing data. *Bioinformatics (Oxford, England)* 31: 166–169
- Baer MM, Bilstein A, Caussinus E, Csiszar A, Affolter M, Leptin M (2010) The role of apoptosis in shaping the tracheal system in the *Drosophila* embryo. *Mech Dev* 127: 28–35
- Bajgar A, Kucerova K, Jonatova L, Tomcala A, Schneedorferova I, Okrouhlik J, Dolezal T (2015) Extracellular adenosine mediates a systemic metabolic switch during immune response. *PLoS Biol* 13: e1002135
- Banerjee U, Girard JR, Goins LM, Spratford CM (2019) *Drosophila* as a genetic model for hematopoiesis. *Genetics* 211: 367–417
- Basset A, Khush RS, Braun A, Gardan L, Boccard F, Hoffmann JA, Lemaitre B (2000) The phytopathogenic bacteria *Erwinia carotovora* infects *Drosophila* and activates an immune response. *Proc Natl Acad Sci USA* 97: 3376–3381
- Bazzi W, Cattenoz PB, Delaporte C, Dasari V, Sakr R, Yuasa Y, Giangrande A (2018) Embryonic hematopoiesis modulates the inflammatory response and larval hematopoiesis in *Drosophila*. *Elife* 7: e34890

- Becht E, McInnes L, Healy J, Dutertre CA, Kwok IWH, Ng LG, Ginhoux F, Newell EW (2018) Dimensionality reduction for visualizing single-cell data using UMAP. *Nat Biotechnol* 37: 38–44
- Benmimoun B, Polesello C, Haenlin M, Waltzer L (2015) The EBF transcription factor Collier directly promotes *Drosophila* blood cell progenitor maintenance independently of the niche. *Proc Natl Acad Sci USA* 112: 9052–9057
- Bergen V, Lange M, Peidli S, Wolf FA, Theis FJ (2019) Generalizing RNA velocity to transient cell states through dynamical modeling. *bioRxiv* <https://doi.org/10.1101/820936> [PREPRINT]
- Bernardoni R, Vivancos V, Giangrande A (1997) glide/gcm is expressed and required in the scavenger cell lineage. *Dev Biol* 191: 118–130
- Binggeli O, Neyen C, Poidevin M, Lemaitre B (2014) Prophenoloxidase activation is required for survival to microbial infections in *Drosophila*. *PLoS Pathog* 10: e1004067
- Braun A, Lemaitre B, Lanot R, Zachary D, Meister M (1997) *Drosophila* immunity: analysis of larval hemocytes by P-element-mediated enhancer trap. *Genetics* 147: 623–634
- Bruckner K, Kockel L, Duchek P, Luque CM, Rorth P, Perrimon N (2004) The PDGF/VEGF receptor controls blood cell survival in *Drosophila*. *Dev Cell* 7: 73–84
- Bunch TA, Graner MW, Fessler LI, Fessler JH, Schneider KD, Kerschen A, Choy LP, Burgess BW, Brower DL (1998) The PS2 integrin ligand tiggriin is required for proper muscle function in *Drosophila*. *Development* 125: 1679–1689
- Burmester T, Antoniewski C, Lepesant JA (1999) Ecdysone-regulation of synthesis and processing of fat body protein 1, the larval serum protein receptor of *Drosophila melanogaster*. *Eur J Biochem* 262: 49–55
- Butler A, Hoffman P, Smibert P, Papalexis E, Satija R (2018) Integrating single-cell transcriptomic data across different conditions, technologies, and species. *Nat Biotechnol* 36: 411–420
- Chanana B, Graf R, Koledachkina T, Pflanz R, Vorbruggen G (2007) AlphaPS2 integrin-mediated muscle attachment in *Drosophila* requires the ECM protein Thrombospondin. *Mech Dev* 124: 463–475
- Charles JP (2010) The regulation of expression of insect cuticle protein genes. *Insect Biochem Mol Biol* 40: 205–213
- Chavez VM, Marques G, Delbecque JP, Kobayashi K, Hollingsworth M, Burr J, Natzle JE, O'Connor MB (2000) The *Drosophila* disembodied gene controls late embryonic morphogenesis and codes for a cytochrome P450 enzyme that regulates embryonic ecdysone levels. *Development* 127: 4115–4126
- Crozatier M, Ubeda JM, Vincent A, Meister M (2004) Cellular immune response to parasitization in *Drosophila* requires the EBF orthologue collier. *PLoS Biol* 2: E196
- Cuttell L, Vaughan A, Silva E, Escaron CJ, Lavine M, Van Goethem E, Eid JP, Quirin M, Franc NC (2008) Undertaker, a *Drosophila* junctophilin, links draper-mediated phagocytosis and calcium homeostasis. *Cell* 135: 524–534
- Daley D, Mani VR, Mohan N, Akkad N, Ochi A, Heindel DW, Lee KB, Zambirinis CP, Pandian GSB, Savadkar S et al (2017) Dectin 1 activation on macrophages by galectin 9 promotes pancreatic carcinoma and peritumoral immune tolerance. *Nat Med* 23: 556–567
- Dostalova A, Rommelaere S, Poidevin M, Lemaitre B (2017) Thioester-containing proteins regulate the Toll pathway and play a role in *Drosophila* defence against microbial pathogens and parasitoid wasps. *BMC Biol* 15: 79
- Dostert C, Jouanguy E, Irving P, Troxler L, Galiana-Arnoux D, Hetru C, Hoffmann JA, Imler JL (2005) The Jak-STAT signaling pathway is required but not sufficient for the antiviral response of *Drosophila*. *Nat Immunol* 6: 946–953
- Dragojlovic-Munther M, Martinez-Agosto JA (2012) Multifaceted roles of PTEN and TSC orchestrate growth and differentiation of *Drosophila* blood progenitors. *Development* 139: 3752–3763
- Dudzic JP, Kondo S, Ueda R, Bergman CM, Lemaitre B (2015) *Drosophila* innate immunity: regional and functional specialization of prophenoloxidases. *BMC Biol* 13: 81
- Enzo E, Santinon G, Pocaterra A, Aragona M, Bresolin S, Forcato M, Grifoni D, Pession A, Zanconato F, Guzzo G et al (2015) Aerobic glycolysis tunes YAP/TAZ transcriptional activity. *EMBO J* 34: 1349–1370
- Eroglu E, Burkard TR, Jiang Y, Saini N, Homem CCF, Reichert H, Knoblich JA (2014) SWI/SNF complex prevents lineage reversion and induces temporal patterning in neural stem cells. *Cell* 156: 1259–1273
- Ferrandon D, Imler JL, Hoffmann JA (2004) Sensing infection in *Drosophila*: toll and beyond. *Semin Immunol* 16: 43–53
- Flowers JM, Sezgin E, Kumagai S, Duvernell DD, Matzkin LM, Schmidt PS, Eanes WF (2007) Adaptive evolution of metabolic pathways in *Drosophila*. *Mol Biol Evol* 24: 1347–1354
- Fogerty FJ, Fessler LI, Bunch TA, Yaron Y, Parker CG, Nelson RE, Brower DL, Gullberg D, Fessler JH (1994) Tiggriin, a novel *Drosophila* extracellular matrix protein that functions as a ligand for *Drosophila* alpha PS2 beta PS integrins. *Development* 120: 1747–1758
- Franc NC, Dimarcq JL, Lagueux M, Hoffmann J, Ezekowitz RA (1996) Croquemort, a novel *Drosophila* hemocyte/macrophage receptor that recognizes apoptotic cells. *Immunity* 4: 431–443
- Franc NC, Heitzler P, Ezekowitz RA, White K (1999) Requirement for croquemort in phagocytosis of apoptotic cells in *Drosophila*. *Science* 284: 1991–1994
- Friggi-Grelin F, Rabouille C, Therond P (2006) The cis-Golgi *Drosophila* GMAP has a role in anterograde transport and Golgi organization *in vivo*, similar to its mammalian ortholog in tissue culture cells. *Eur J Cell Biol* 85: 1155–1166
- Gandhi R, Bonaccorsi S, Wentworth D, Doxsey S, Gatti M, Pereira A (2004) The *Drosophila* kinesin-like protein KLP67A is essential for mitotic and male meiotic spindle assembly. *Mol Biol Cell* 15: 121–131
- Garg A, Wu LP (2014) *Drosophila* Rab14 mediates phagocytosis in the immune response to *Staphylococcus aureus*. *Cell Microbiol* 16: 296–310
- Ge SX, Jung D (2018) ShinyGO: a graphical enrichment tool for animals and plants. *bioRxiv* <https://doi.org/10.1101/315150> [PREPRINT]
- Gold KS, Bruckner K (2015) Macrophages and cellular immunity in *Drosophila melanogaster*. *Semin Immunol* 27: 357–368
- Gorfinkiel N, Sierra J, Callejo A, Ibanez C, Guerrero I (2005) The *Drosophila* ortholog of the human Wnt inhibitor factor Shifted controls the diffusion of lipid-modified Hedgehog. *Dev Cell* 8: 241–253
- Goto A, Kumagai T, Kumagai C, Hirose J, Narita H, Mori H, Kadowaki T, Beck K, Kitagawa Y (2001) A *Drosophila* haemocyte-specific protein, hemolectin, similar to human von Willebrand factor. *Biochem J* 359: 99–108
- Govind S (1999) Control of development and immunity by rel transcription factors in *Drosophila*. *Oncogene* 18: 6875–6887
- Graveley BR, Brooks AN, Carlson JW, Duff MO, Landolin JM, Yang L, Artieri CG, van Baren MJ, Boley N, Booth BW et al (2011) The developmental transcriptome of *Drosophila melanogaster*. *Nature* 471: 473–479

- Gyoergy A, Roblek M, Ratheesh A, Valoskova K, Belyaeva V, Wachner S, Matsubayashi Y, Sanchez-Sanchez BJ, Stramer B, Siekhaus DE (2018) Tools allowing independent visualization and genetic manipulation of *Drosophila melanogaster* macrophages and surrounding tissues. *G3 (Bethesda)* 8: 845–857
- Hacker U, Lin X, Perrimon N (1997) The *Drosophila* sugarless gene modulates Wingless signaling and encodes an enzyme involved in polysaccharide biosynthesis. *Development* 124: 3565–3573
- Haller S, Franchet A, Hakkim A, Chen J, Drenkard E, Yu S, Schirmeier S, Li Z, Martins N, Ausubel FM et al (2018) Quorum-sensing regulator RhIR but not its autoinducer RhII enables *Pseudomonas* to evade opsonization. *EMBO Rep* 19: e44880
- Hammonds AS, Bristow CA, Fisher WW, Weiszmann R, Wu S, Hartenstein V, Kellis M, Yu B, Frise E, Celniker SE (2013) Spatial expression of transcription factors in *Drosophila* embryonic organ development. *Genome Biol* 14: R140
- Handke B, Poernbacher I, Goetze S, Ahrens CH, Omasits U, Marty F, Simigdala N, Meyer I, Wollscheid B, Brunner E et al (2013) The hemolymph proteome of fed and starved *Drosophila* larvae. *PLoS One* 8: e67208
- Hashimoto Y, Tabuchi Y, Sakurai K, Kutsuna M, Kurokawa K, Awasaki T, Sekimizu K, Nakanishi Y, Shiratsuchi A (2009) Identification of lipoteichoic acid as a ligand for draper in the phagocytosis of *Staphylococcus aureus* by *Drosophila* hemocytes. *J Immunol* 183: 7451–7460
- Heming M, Gran S, Jauch S-L, Fischer-Riepe L, Russo A, Klotz L, Hermann S, Schäfers M, Roth J, Barczyk-Kahlert K (2018) Peroxisome proliferator-activated receptor- γ modulates the response of macrophages to lipopolysaccharide and glucocorticoids. *Front Immunol* 9: 893
- Honti V, Kurucz E, Csordas G, Laurinyecz B, Markus R, Ando I (2009) *In vivo* detection of lamellocytes in *Drosophila melanogaster*. *Immunol Lett* 126: 83–84
- Honti V, Csordas G, Markus R, Kurucz E, Jankovics F, Ando I (2010) Cell lineage tracing reveals the plasticity of the hemocyte lineages and of the hematopoietic compartments in *Drosophila melanogaster*. *Mol Immunol* 47: 1997–2004
- Honti V, Csordas G, Kurucz E, Markus R, Ando I (2014) The cell-mediated immunity of *Drosophila melanogaster*: hemocyte lineages, immune compartments, microanatomy and regulation. *Dev Comp Immunol* 42: 47–56
- Hu Y, Comjean A, Perrimon N, Mohr SE (2017) The *Drosophila* Gene Expression Tool (DGET) for expression analyses. *BMC Bioinformatics* 18: 98
- Huang da W, Sherman BT, Lempicki RA (2009) Systematic and integrative analysis of large gene lists using DAVID bioinformatics resources. *Nat Protoc* 4: 44–57
- Irving P, Ubeda JM, Doucet D, Troxler L, Lagueux M, Zachary D, Hoffmann JA, Hetru C, Meister M (2005) New insights into *Drosophila* larval haemocyte functions through genome-wide analysis. *Cell Microbiol* 7: 335–350
- Jiang P, Nishimura T, Sakamaki Y, Itakura E, Hatta T, Natsume T, Mizushima N (2014) The HOPS complex mediates autophagosome-lysosome fusion through interaction with syntaxin 17. *Mol Biol Cell* 25: 1327–1337
- Kanehisa M, Goto S (2000) KEGG: kyoto encyclopedia of genes and genomes. *Nucleic Acids Res* 28: 27–30
- Kim-jo C, Gatti JL, Poirie M (2019) *Drosophila* cellular immunity against parasitoid wasps: a complex and time-dependent process. *Front Physiol* 10: 603
- Kleino A, Silverman N (2014) The *Drosophila* IMD pathway in the activation of the humoral immune response. *Dev Comp Immunol* 42: 25–35
- Kocks C, Cho JH, Nehme N, Ulvila J, Pearson AM, Meister M, Strom C, Conto SL, Hetru C, Stuart LM et al (2005) Eater, a transmembrane protein mediating phagocytosis of bacterial pathogens in *Drosophila*. *Cell* 123: 335–346
- Kurucz E, Axelrod S, Leaman D, Gaul U (2008) Six-microns-under acts upstream of Draper in the glial phagocytosis of apoptotic neurons. *Cell* 133: 498–509
- Kurucz E, Zettervall CJ, Sinka R, Vilmos P, Pivarcsi A, Ekengren S, Hegedus Z, Ando I, Hultmark D (2003) Hemese, a hemocyte-specific transmembrane protein, affects the cellular immune response in *Drosophila*. *Proc Natl Acad Sci USA* 100: 2622–2627
- Kurucz E, Markus R, Zsomboki J, Folkl-Medzihradzsky K, Darula Z, Vilmos P, Udvardy A, Krausz I, Lukacsovich T, Gateff E et al (2007) Nimrod, a putative phagocytosis receptor with EGF repeats in *Drosophila* plasmatocytes. *Curr Biol* 17: 649–654
- Kussel P, Frasch M (1995) Pendulin, a *Drosophila* protein with cell cycle-dependent nuclear localization, is required for normal cell proliferation. *J Cell Biol* 129: 1491–1507
- Kutty RK, Kutty G, Kambadur R, Duncan T, Koonin EV, Rodriguez IR, Odenwald WF, Wiggert B (1996) Molecular characterization and developmental expression of a retinoid- and fatty acid-binding glycoprotein from *Drosophila*. A putative lipophorin. *J Biol Chem* 271: 20641–20649
- La Manno G, Soldatov R, Zeisel A, Braun E, Hochgerner H, Petukhov V, Lidschreiber K, Kastriiti ME, Lonnerberg P, Furlan A et al (2018) RNA velocity of single cells. *Nature* 560: 494–498
- Labzin LI, Schmidt SV, Masters SL, Beyer M, Krebs W, Klee K, Stahl R, Lutjohann D, Schultze JL, Latz E et al (2015) ATF3 is a key regulator of macrophage IFN responses. *J Immunol* 195: 4446–4455
- Lazzaro BP, Scurman BK, Clark AG (2004) Genetic basis of natural variation in *D. melanogaster* antibacterial immunity. *Science* 303: 1873–1876
- Lebestky T, Chang T, Hartenstein V, Banerjee U (2000) Specification of *Drosophila* hematopoietic lineage by conserved transcription factors. *Science* 288: 146–149
- Lecuyer E, Yoshida H, Parthasarathy N, Alm C, Babak T, Cerovina T, Hughes TR, Tomancak P, Krause HM (2007) Global analysis of mRNA localization reveals a prominent role in organizing cellular architecture and function. *Cell* 131: 174–187
- Lerner AB, Fitzpatrick TB (1950) Biochemistry of melanin formation. *Physiol Rev* 30: 91–126
- Letourneau M, Lapraz F, Sharma A, Vanzo N, Waltzer L, Crozatier M (2016) *Drosophila* hematopoiesis under normal conditions and in response to immune stress. *FEBS Lett* 590: 4034–4051
- Ly LL, Suyari O, Yoshioka Y, Tue NT, Yoshida H, Yamaguchi M (2013) dNF-YB plays dual roles in cell death and cell differentiation during *Drosophila* eye development. *Gene* 520: 106–118
- Magwire MM, Fabian DK, Schweyen H, Cao C, Longdon B, Bayer F, Jiggins FM (2012) Genome-wide association studies reveal a simple genetic basis of resistance to naturally coevolving viruses in *Drosophila melanogaster*. *PLoS Genet* 8: e1003057
- Makhijani K, Alexander B, Tanaka T, Rulifson E, Bruckner K (2011) The peripheral nervous system supports blood cell homing and survival in the *Drosophila* larva. *Development* 138: 5379–5391
- Manaka J, Kuraishi T, Shiratsuchi A, Nakai Y, Higashida H, Henson P, Nakanishi Y (2004) Draper-mediated and phosphatidylinositol-independent phagocytosis of apoptotic cells by *Drosophila* hemocytes/macrophages. *J Biol Chem* 279: 48466–48476
- Mandal L, Martinez-Agosto JA, Evans CJ, Hartenstein V, Banerjee U (2007) A Hedgehog- and Antennapedia-dependent niche maintains *Drosophila* haematopoietic precursors. *Nature* 446: 320–324

- Mann HB, Whitney DR (1947) On a test of whether one of two random variables is stochastically larger than the other. *Ann Math Stat* 18: 50–60
- Markus R, Laurinyecz B, Kurucz E, Honti V, Bajusz I, Sipos B, Somogyi K, Kronhamn J, Hultmark D, Ando I (2009) Sessile hemocytes as a hematopoietic compartment in *Drosophila melanogaster*. *Proc Natl Acad Sci USA* 106: 4805–4809
- Maroy P, Kaufmann G, Dubendorfer A (1988) Embryonic ecdysteroids of *Drosophila-melanogaster*. *J Insect Physiol* 34: 633–637
- Martin-Blanco E, Gampel A, Ring J, Virdee K, Kirov N, Tolkovsky AM, Martinez-Arias A (1998) puckered encodes a phosphatase that mediates a feedback loop regulating JNK activity during dorsal closure in *Drosophila*. *Genes Dev* 12: 557–570
- Martinek N, Shahab J, Saathoff M, Ringuette M (2008) Haemocyte-derived SPARC is required for collagen-IV-dependent stability of basal laminae in *Drosophila* embryos. *J Cell Sci* 121: 1671–1680
- Martins NE, Faria VG, Nolte V, Schlotterer C, Teixeira L, Sucena E, Magalhães S (2014) Host adaptation to viruses relies on few genes with different cross-resistance properties. *Proc Natl Acad Sci USA* 111: 5938–5943
- Massey HC Jr, Kejzlarova-Lepesant J, Willis RL, Castleberry AB, Benes H (1997) The *Drosophila* Lsp-1 beta gene. A structural and phylogenetic analysis. *Eur J Biochem* 245: 199–207
- McMillan EA, Longo SM, Smith MD, Broskin S, Lin B, Singh NK, Strochlic TI (2018) The protein kinase CK2 substrate Jabba modulates lipid metabolism during *Drosophila* oogenesis. *J Biol Chem* 293: 2990–3002
- Meister M, Braun A, Kappler C, Reichhart JM, Hoffmann JA (1994) Insect immunity. A transgenic analysis in *Drosophila* defines several functional domains in the dipterin promoter. *EMBO J* 13: 5958–5966
- Melcarne C, Lemaitre B, Kurant E (2019) Phagocytosis in *Drosophila*: from molecules and cellular machinery to physiology. *Insect Biochem Mol Biol* 109: 1–12
- Nelson RE, Fessler LI, Takagi Y, Blumberg B, Keene DR, Olson PF, Parker CG, Fessler JH (1994) Peroxidase: a novel enzyme-matrix protein of *Drosophila* development. *EMBO J* 13: 3438–3447
- Nonaka S, Nagaosa K, Mori T, Shiratsuchi A, Nakanishi Y (2013) Integrin alphaPS3/betacru-mediated phagocytosis of apoptotic cells and bacteria in *Drosophila*. *J Biol Chem* 288: 10374–10380
- Norum M, Tang E, Chavoshi T, Schwarz H, Linke D, Uv A, Moussian B (2010) Trafficking through COPII stabilises cell polarity and drives secretion during *Drosophila* epidermal differentiation. *PLoS One* 5: e10802
- Olofsson B, Page DT (2005) Condensation of the central nervous system in embryonic *Drosophila* is inhibited by blocking hemocyte migration or neural activity. *Dev Biol* 279: 233–243
- Owusu-Ansah E, Banerjee U (2009) Reactive oxygen species prime *Drosophila* haematopoietic progenitors for differentiation. *Nature* 461: 537–541
- Parisi F, Stefanatos RK, Strathdee K, Yu Y, Vidal M (2014) Transformed epithelia trigger non-tissue-autonomous tumor suppressor response by adipocytes via activation of Toll and Eiger/TNF signaling. *Cell Rep* 6: 855–867
- Pearson AM, Baksa K, Ramet M, Protas M, McKee M, Brown D, Ezekowitz RA (2003) Identification of cytoskeletal regulatory proteins required for efficient phagocytosis in *Drosophila*. *Microbes Infect* 5: 815–824
- Petraki S, Alexander B, Bruckner K (2015) Assaying blood cell populations of the *Drosophila melanogaster* larva. *J Vis Exp* e52733
- Podolnikova NP, Kushchayeva YS, Wu Y, Faust J, Ugarova TP (2016) The role of integrins $\alpha M\beta 2$ (Mac-1, CD11b/CD18) and $\alpha D\beta 2$ (CD11d/CD18) in macrophage fusion. *Am J Pathol* 186: 2105–2116
- Przewloka MR, Zhang W, Costa P, Archambault V, D'Avino PP, Lilley KS, Laue ED, McAinsh AD, Glover DM (2007) Molecular analysis of core kinetochore composition and assembly in *Drosophila melanogaster*. *PLoS One* 2: e478
- Qiu X, Hill A, Packer J, Lin D, Ma YA, Trapnell C (2017a) Single-cell mRNA quantification and differential analysis with census. *Nat Methods* 14: 309–315
- Qiu X, Mao Q, Tang Y, Wang L, Chawla R, Pliner HA, Trapnell C (2017b) Reversed graph embedding resolves complex single-cell trajectories. *Nat Methods* 14: 979–982
- R Core Team (2017) *R: a language and environment for statistical computing*
- Ramond E, Petrigiani B, Dudzic JP, Boquete J-P, Poidevin M, Kondo S, Lemaitre B (2019) Metabolic adjustment of *Drosophila* hemocyte number and sessility by an adipokine. *bioRxiv* <https://doi.org/10.1101/648626> [PREPRINT]
- Ramprasad MP, Terpstra V, Kondratenko N, Quehenberger O, Steinberg D (1996) Cell surface expression of mouse macrosialin and human CD68 and their role as macrophage receptors for oxidized low density lipoprotein. *Proc Natl Acad Sci USA* 93: 14833–14838
- Rand WM (1971) Objective criteria for the evaluation of clustering methods. *J Am Stat Assoc* 66: 846–850
- Ratheesh A, Belyaeva V, Siekhaus DE (2015) *Drosophila* immune cell migration and adhesion during embryonic development and larval immune responses. *Curr Opin Cell Biol* 36: 71–79
- Rauw WM (2012) Immune response from a resource allocation perspective. *Front Genet* 3: 267
- Rizki MT, Rizki RM (1959) Functional significance of the crystal cells in the larva of *Drosophila melanogaster*. *J Biophys Biochem Cytol* 5: 235–240
- Robinson SW, Herzyk P, Dow JA, Leader DP (2013) FlyAtlas: database of gene expression in the tissues of *Drosophila melanogaster*. *Nucleic Acids Res* 41: D744–D750
- Roddie HG, Armitage EL, Coates JA, Johnston SA, Evans IR (2019) Simu-dependent clearance of dying cells regulates macrophage function and inflammation resolution. *PLoS Biol* 17: e2006741
- Rommelaere S, Boquete JP, Piton J, Kondo S, Lemaitre B (2019) The exchangeable apolipoprotein Nplp2 sustains lipid flow and heat acclimation in *Drosophila*. *Cell Rep* 27: 886–899 e6
- Rus F, Kurucz E, Markus R, Sinenko SA, Laurinyecz B, Pataki C, Gausz J, Hegedus Z, Udvardy A, Hultmark D et al (2006) Expression pattern of Filamin-240 in *Drosophila* blood cells. *Gene Expr Patterns* 6: 928–934
- Samakovlis C, Kimbrell DA, Kylsten P, Engstrom A, Hultmark D (1990) The immune response in *Drosophila*: pattern of cecropin expression and biological activity. *EMBO J* 9: 2969–2976
- Sanchez-Sanchez BJ, Urbano JM, Comber K, Dragu A, Wood W, Stramer B, Martin-Bermudo MD (2017) *Drosophila* embryonic hemocytes produce laminins to strengthen migratory response. *Cell Rep* 21: 1461–1470
- Schindelin J, Arganda-Carreras I, Frise E, Kaynig V, Longair M, Pietzsch T, Preibisch S, Rueden C, Saalfeld S, Schmid B et al (2012) Fiji: an open-source platform for biological-image analysis. *Nat Methods* 9: 676–682
- Sears HC, Kennedy CJ, Garrity PA (2003) Macrophage-mediated corpse engulfment is required for normal *Drosophila* CNS morphogenesis. *Development* 130: 3557–3565
- Sharp DJ, Yu KR, Sisson JC, Sullivan W, Scholey JM (1999) Antagonistic microtubule-sliding motors position mitotic centrosomes in *Drosophila* early embryos. *Nat Cell Biol* 1: 51–54
- Shia AK, Glittenberg M, Thompson G, Weber AN, Reichhart JM, Ligoxygakis P (2009) Toll-dependent antimicrobial responses in *Drosophila* larval fat body require Spatzle secreted by haemocytes. *J Cell Sci* 122: 4505–4515

- Shlyakhover E, Shklyar B, Hakim-Mishnaevski K, Levy-Adam F, Kurant E (2018) *Drosophila* GATA factor serpent establishes phagocytic ability of embryonic macrophages. *Front Immunol* 9: 266
- Sieow JL, Gun SY, Wong SC (2018) The sweet surrender: how myeloid cell metabolic plasticity shapes the tumor microenvironment. *Front Cell Dev Biol* 6: 168
- Sinenko SA, Hung T, Moroz T, Tran QM, Sidhu S, Cheney MD, Speck NA, Banerjee U (2010) Genetic manipulation of AML1-ETO-induced expansion of hematopoietic precursors in a *Drosophila* model. *Blood* 116: 4612–4620
- Stedden CG, Menegas W, Zajac AL, Williams AM, Cheng S, Ozkan E, Horne-Badovinac S (2019) Planar-polarized semaphorin-5c and plexin A promote the collective migration of epithelial cells in *Drosophila*. *Curr Biol* 29: 908–920 e6
- Stofanko M, Kwon SY, Badenhorst P (2010) Lineage tracing of lamellocytes demonstrates *Drosophila* macrophage plasticity. *PLoS One* 5: e14051
- Stuart T, Butler A, Hoffman P, Hafemeister C, Papalexi E, Mauck WM III, Hao Y, Stoeckius M, Smibert P, Satija R (2019) Comprehensive integration of single-cell data. *Cell* 177: 1888–1902.e21
- Sung EJ, Ryuda M, Matsumoto H, Uryu O, Ochiai M, Cook ME, Yi NY, Wang H, Putney JW, Bird GS et al (2017) Cytokine signaling through *Drosophila* Mthl10 ties lifespan to environmental stress. *Proc Natl Acad Sci USA* 114: 13786–13791
- Sykitis GP, Bohmann D (2008) Keap1/Nrf2 signaling regulates oxidative stress tolerance and lifespan in *Drosophila*. *Dev Cell* 14: 76–85
- Tan KL, Vlisidou I, Wood W (2014) Ecdysone mediates the development of immunity in the *Drosophila* embryo. *Curr Biol* 24: 1145–1152
- Telfer WH, Kunkel JG (1991) The function and evolution of insect storage hexamers. *Annu Rev Entomol* 36: 205–228
- Tepass U, Fessler LI, Aziz A, Hartenstein V (1994) Embryonic origin of hemocytes and their relationship to cell-death in *Drosophila*. *Development* 120: 1829–1837
- Tokusumi T, Sorrentino RP, Russell M, Ferrarese R, Govind S, Schulz RA (2009) Characterization of a lamellocyte transcriptional enhancer located within the misshapen gene of *Drosophila melanogaster*. *PLoS One* 4: e6429
- Tomancak P, Beaton A, Weiszmam R, Kwan E, Shu S, Lewis SE, Richards S, Ashburner M, Hartenstein V, Celniker SE et al (2002) Systematic determination of patterns of gene expression during *Drosophila* embryogenesis. *Genome Biol* 3: RESEARCH0088
- Tomancak P, Berman BP, Beaton A, Weiszmam R, Kwan E, Hartenstein V, Celniker SE, Rubin GM (2007) Global analysis of patterns of gene expression during *Drosophila* embryogenesis. *Genome Biol* 8: R145
- Trapnell C, Pachter L, Salzberg SL (2009) TopHat: discovering splice junctions with RNA-Seq. *Bioinformatics (Oxford, England)* 25: 1105–1111
- Trapnell C, Cacchiarelli D, Grimsby J, Pokharel P, Li S, Morse M, Lennon NJ, Livak KJ, Mikkelsen TS, Rinn JL (2014) The dynamics and regulators of cell fate decisions are revealed by pseudotemporal ordering of single cells. *Nat Biotechnol* 32: 381–386
- Tucker PK, Evans IR, Wood W (2011) Ena drives invasive macrophage migration in *Drosophila* embryos. *Dis Model Mech* 4: 126–134
- Ugrankar R, Liu Y, Provaznik J, Schmitt S, Lehmann M (2011) Lipin is a central regulator of adipose tissue development and function in *Drosophila melanogaster*. *Mol Cell Biol* 31: 1646–1656
- Valanne S, Wang JH, Ramet M (2011) The *Drosophila* toll signaling pathway. *J Immunol* 186: 649–656
- Valanne S, Vesala L, Ramet M (2018) Commentary: *Drosophila* GATA Factor serpent establishes phagocytic ability of embryonic macrophages. *Front Immunol* 9: 1582
- Vilmos P, Nagy I, Kurucz E, Hultmark D, Gateff E, Ando I (2004) A rapid rosetting method for separation of hemocyte sub-populations of *Drosophila melanogaster*. *Dev Comp Immunol* 28: 555–563
- Vlisidou I, Dowling AJ, Evans IR, Waterfield N, French-Constant RH, Wood W (2009) *Drosophila* embryos as model systems for monitoring bacterial infection in real time. *PLoS Pathog* 5: e1000518
- Voon DC-C, Hor YT, Ito Y (2015) The RUNX complex: reaching beyond haematopoiesis into immunity. *Immunology* 146: 523–536
- Wilk R, Hu J, Blotsky D, Krause HM (2016) Diverse and pervasive subcellular distributions for both coding and long noncoding RNAs. *Genes Dev* 30: 594–609
- Wolf FA, Angerer P, Theis FJ (2018) SCANPY: large-scale single-cell gene expression data analysis. *Genome Biol* 19: 15
- Wong KKL, Liao JZ, Verheyen EM (2019) A positive feedback loop between Myc and aerobic glycolysis sustains tumor growth in a *Drosophila* tumor model. *Elife* 8: e46315
- Wood W, Martin P (2017) Macrophage functions in tissue patterning and disease: new insights from the fly. *Dev Cell* 40: 221–233
- Woodcock KJ, Kierdorf K, Pouchelon CA, Vivancos V, Dionne MS, Geissmann F (2015) Macrophage-derived upd3 cytokine causes impaired glucose homeostasis and reduced lifespan in *Drosophila* fed a lipid-rich diet. *Immunity* 42: 133–144
- Yang J, Zhang L, Yu C, Yang X-F, Wang H (2014) Monocyte and macrophage differentiation: circulation inflammatory monocyte as biomarker for inflammatory diseases. *Biomark Res* 2: 1
- Yasothornsrikul S, Davis WJ, Cramer G, Kimbrell DA, Dearolf CR (1997) viking: Identification and characterization of a second type IV collagen in *Drosophila*. *Gene* 198: 17–25
- Yuan K, Sella CA, Shermoen AW, O'Farrell PH (2016) Timing the *Drosophila* mid-blastula transition: a cell cycle-centered view. *Trends Genet* 32: 496–507
- Zacharogianni M, Kondylis V, Tang Y, Farhan H, Xanthakis D, Fuchs F, Boutros M, Rabouille C (2011) ERK7 is a negative regulator of protein secretion in response to amino-acid starvation by modulating Sec16 membrane association. *EMBO J* 30: 3684–3700
- Zanet J, Stramer B, Millard T, Martin P, Payre F, Plaza S (2009) Fascin is required for blood cell migration during *Drosophila* embryogenesis. *Development* 136: 2557–2565
- Zettervall CJ, Anderl I, Williams MJ, Palmer R, Kurucz E, Ando I, Hultmark D (2004) A directed screen for genes involved in *Drosophila* blood cell activation. *Proc Natl Acad Sci USA* 101: 14192–14197
- Zhai Z, Huang X, Yin Y (2018) Beyond immunity: the Imd pathway as a coordinator of host defense, organismal physiology and behavior. *Dev Comp Immunol* 83: 51–59
- Zheng Q, Ma A, Yuan L, Gao N, Feng Q, Franc NC, Xiao H (2017) Apoptotic cell clearance in *Drosophila melanogaster*. *Front Immunol* 8: 1881
- Zhou X, Liao WJ, Liao JM, Liao P, Lu H (2015) Ribosomal proteins: functions beyond the ribosome. *J Mol Cell Biol* 7: 92–104



Toward a Consensus in the Repertoire of Hemocytes Identified in *Drosophila*

Pierre B. Cattenoz^{1,2,3,4*}, Sara Monticelli^{1,2,3,4}, Alexia Pavlidaki^{1,2,3,4} and Angela Giangrande^{1,2,3,4*}

¹ Institut de Génétique et de Biologie Moléculaire et Cellulaire, Illkirch, France, ² Centre National de la Recherche Scientifique, UMR 7104, Illkirch, France, ³ Institut National de la Santé et de la Recherche Médicale, U1258, Illkirch, France, ⁴ Université de Strasbourg, Illkirch, France

OPEN ACCESS

Edited by:

Marc S. Dionne,
Imperial College London,
United Kingdom

Reviewed by:

Iwan Robert Evans,
The University of Sheffield,
United Kingdom
Ioannis Eleftherianos,
George Washington University,
United States

*Correspondence:

Pierre B. Cattenoz
cattenoz@igbmc.fr
orcid.org/0000-0001-5301-1975
Angela Giangrande
angela@igbmc.fr
orcid.org/0000-0001-6278-5120

Specialty section:

This article was submitted to
Cell Death and Survival,
a section of the journal
Frontiers in Cell and Developmental
Biology

Received: 18 December 2020

Accepted: 12 February 2021

Published: 04 March 2021

Citation:

Cattenoz PB, Monticelli S,
Pavlidaki A and Giangrande A (2021)
Toward a Consensus in the Repertoire
of Hemocytes Identified in *Drosophila*.
Front. Cell Dev. Biol. 9:643712.
doi: 10.3389/fcell.2021.643712

The catalog of the *Drosophila* immune cells was until recently limited to three major cell types, based on morphology, function and few molecular markers. Three recent single cell studies highlight the presence of several subgroups, revealing a large diversity in the molecular signature of the larval immune cells. Since these studies rely on somewhat different experimental and analytical approaches, we here compare the datasets and identify eight common, robust subgroups associated to distinct functions such as proliferation, immune response, phagocytosis or secretion. Similar comparative analyses with datasets from different stages and tissues disclose the presence of larval immune cells resembling embryonic hemocyte progenitors and the expression of specific properties in larval immune cells associated with peripheral tissues.

Keywords: macrophage, single cell RNA seq, drosophila, lamellocyte, innate immunity

INTRODUCTION

Immune cells are able to move and connect distant tissues and organs. This feature likely accounts for their pleiotropic role as sensors and regulators of the internal state in homeostatic, challenged and pathological conditions. While pleiotropy seems to arise from immune cell heterogeneity, the cause and nature of cell diversity is still poorly understood. How much does it depend on intrinsic differences dictated by cell autonomous cues vs. environmental conditions met by these cells during their life? To address the longstanding question on the impact of nature vs. nurture, of cell identity vs. cell state, we first need to characterize the different subtypes in depth.

Beside a lower complexity of the immune cell lineages, *Drosophila* shares with vertebrates several factors controlling the differentiation of the myeloid lineage [e.g., GATA and Runx proteins (Wood and Jacinto, 2007)], immune cell migration [e.g., integrins and Rho GTPases (Paladi and Tepass, 2004; Siekhaus et al., 2010; Comber et al., 2013)], phagocytosis [e.g., the CED-1 family member Draper and the CD36-related receptor Croquemort (Franc et al., 1996; Manaka et al., 2004)] and immune response [i.e., JAK/STAT, IMD, and Toll pathways (Buchon et al., 2014)]. Hence, it represents a simple yet evolutionary conserved model to address the origin of the immune cell diversity.

The immune cells of *Drosophila*, the hemocytes, have been classically subdivided in three types: the plasmatocytes, the crystal cells and the lamellocytes, which are thought to derive from the same lineage, similar to the myeloid cells in mammals (Banerjee et al., 2019). The plasmatocytes are macrophage-like cells that phagocytose pathogens as well as cell debris and constitute ~95% of the hemocytes. The remaining hemocytes are the crystal cells, platelet-like cells in charge of melanization, a process that is necessary for wound closure and immune response to pathogens. The third type of immune cells, the lamellocytes, appears only after immune/inflammatory challenge from progenitors or by plasmatocyte transdifferentiation (Banerjee et al., 2019).

Until recently, the hemocytes were identified using distinctive morphological features and a handful of molecular markers. The plasmatocytes are small cells of ~10 μm of diameter. They can be round or present cytoplasmic projections [i.e., podocytes (Rizki and Rizki, 1980)]. They express several markers such as the transmembrane receptors Nimrod C1 (NimC1), Eater, Hemese (He) and Croquemort (Crq), the fascin Singed (Sn) and the secreted proteins Hemolectin (Hml), Peroxidase (Pxn), and Collagen type IV alpha 1 (Col4a1) (Nelson et al., 1994; Franc et al., 1996; Goto et al., 2001; Kurucz et al., 2003; Kocks et al., 2005; Zanet et al., 2009). The crystal cells have the same size than the plasmatocytes and are characterized by the presence of crystals. They express the transcription factors Lozenge (Lz) and Pebbled (Peb) as well as Prophenoloxidases 1 and 2 (PPO1 and PPO2) (Rizki and Rizki, 1959; Binggeli et al., 2014). PPO2 is a major constituent of the crystals, which are released upon wounding to initiate the melanization reaction (Binggeli et al., 2014). The lamellocytes are large melanized cells (>60 μm of diameter) with heterogeneous shapes. They are strongly labeled with the actin filament probe called phalloidin and express the Prophenoloxidase 3 (PPO3), the kinase Misshapen (Msn), the integrins Myospheroid (Mys, Integrin beta or L4), and Integrin alphaPS4 subunit (ItgaPS4 or L5), the actin binding protein Cheerio (Cher, L5), and the glycosylphosphatidylinositol (GPI)-anchored protein Atilla (L1) (Braun et al., 1997; Irving et al., 2005; Rus et al., 2006; Honti et al., 2009).

The development of single cell RNA sequencing (scRNAseq) techniques has made it possible to significantly enlarge the panel of the *Drosophila* immune cells based on their transcriptional profile. ScRNAseq consists of sequencing the transcriptome of single cells in a high throughput fashion. The cells are then grouped according to their expression profiles (reviewed in Potter, 2018; See et al., 2018). Three scRNAseq studies recently revealed the diversity of the hemocytes present in the *Drosophila* larva (Cattenoz et al., 2020; Fu et al., 2020; Tattikota et al., 2020). We perform here a comparative study to refine immune cell diversity, origin and localization within the organism. Our comparison defines subgroups robustly found in the three datasets from steady state larval hemocytes, despite the different experimental and analytical approaches. The common subgroups reflect the differentiation state, intermediary vs. mature hemocytes, as well as their

main functions (phagocytosis, immune response/antimicrobial peptide (AMP) production, secretion and proliferation). Finally, we analyze the hemocytes present in available single cell datasets from larval eye discs and brains as well as from stage 6 embryos in order to link specific subgroups to distinct environments/developmental trajectories.

MATERIALS AND METHODS

Comparison of scRNAseq Data on Wandering 3rd Instar Larval Hemocytes

The list of markers for each subgroup were retrieved from the publications [Dataset_EV2 in Cattenoz et al. (2020) and **Supplementary File 2** in Tattikota et al. (2020)]. The two lists were generated with the same tool [function “FindMarkers” in Seurat R toolkit (Butler et al., 2018; Stuart et al., 2019)] and provide comparable parameters including the enrichment levels for all the subgroup markers. The two tables were compiled in R and plotted using the package ggplot2 (Villanueva and Chen, 2019). The markers described in Fu et al. (2020) dataset were retrieved from the figure of the manuscript. Of note, the PM12 cells in Tattikota et al. (2020) appear exclusively in wounding condition, an experimental set up that was not assessed by the two other studies. To keep the comparison as homogenous as possible, the markers of the subgroup PM12 were excluded from our analysis.

The dot plots were generated using the function “DotPlot” in the Seurat R toolkit (Butler et al., 2018; Stuart et al., 2019) with the non-infested data from Cattenoz et al. deposited in the ArrayExpress database at EMBL-EBI¹ under the accession number E-MTAB-8698. The list of markers for the CAH7 PM, the Lsp PM, the Ppn PM, the thanocytes, and the primocytes were retrieved from the figures in Fu et al. (2020). The top PSC markers were retrieved from the lymph gland scRNAseq data from Cho et al. (2020; **Supplementary Table S2**): the markers presenting the highest enrichment in the PSC were selected.

Comparison of the WL Hemocyte scRNAseq Data With Stage 6 Embryo, Larval Eye Disc and Larval Brain scRNAseq Data

The normalized expression matrix of the stage 6 embryos (Karaiskos et al., 2017) was downloaded from <https://shiny.mdc-berlin.de/DVEX/> and analyzed with the standard workflow from Seurat toolkit² (Butler et al., 2018; Stuart et al., 2019). Briefly, first the data were normalized (function NormalizeData), the variable genes were identified (function FindVariableFeatures, selection method “vst,” number of feature = 2,000), the data were scaled (function ScaleData, features = all.genes), linear dimensional reduction was carried out on the variable genes (function RunPCA), the dimensionality of the dataset was determined and set

¹www.ebi.ac.uk/arrayexpress

²https://satijalab.org/seurat/v3.2/pbmc3k_tutorial.html

to 15 (function `ElbowPlot`), the cells were then clustered (functions `FindNeighbors`, `dims = 1:15` and `FindClusters`, `resolution = 1.2`), at last non-linear dimensional reductions were carried out (functions `RunUMAP` and `RunTSNE`). This pipeline generated a single subgroup enriched for all the markers of the hemocyte subgroup described in Karaïskos et al. (2017): i.e., `Gcm`, `Ham`, `Ttk`, `CrebA`, `Shep`, `RhoL`, `Fok`, `Knrl`, `Kni`, `Zfh1`, `CG33099`, `Srp`, `Btd`, and `NetB`. This subgroup was used for the downstream analyses.

The normalized expression matrix of the wild type larval eye disc (Ariss et al., 2018) was downloaded from <https://www.ebi.ac.uk/gxa/sc/experiments/E-MTAB-7195/downloads> and analyzed following the same pipeline than stage 6 embryos described above with modification: the dimensionality was set to 17 and the cells were clustered with a resolution of 0.5. The hemocyte subgroup was unambiguously identified using the hemocyte markers `Srp`, `Hml`, `Pxn`, `NimC1`, `Crq`, and `Sn` and used for the downstream analyses.

The expression matrices of the normal 1st instar larval brains (Brunet Avalos et al., 2019) were downloaded from <https://www.ncbi.nlm.nih.gov/geo/query/acc.cgi?acc=GSE134722>.

The expression matrices GSM3964166, GSM3964167, GSM3964168, and GSM4132287 were merged and integrated following Seurat standard pipeline (Butler et al., 2018; Stuart et al., 2019): each matrix was normalized (function `NormalizeData`), the variable features and the common anchors were identified (function `FindVariableFeatures`, method “vst,” function `FindIntegrationAnchors`, dimension 1:50) and the matrices were integrated (function `IntegrateData`, dimension: 1:50). The integrated matrix was analyzed following the same pipeline as described above for the stage 6 embryos with the following parameters: the dimensionality was set to 50 and the cells were clustered with a resolution of 0.4. The hemocyte subgroup was unambiguously identified using the hemocyte markers `Srp`, `Hml`, `Pxn`, `NimC1`, and `He` and used for the downstream analyses.

The expression matrices of the brains from 2nd instar larvae [24 h after larval hatching (h ALH)], feeding 3rd instar larvae (48 h ALH) and wandering 3rd instar larvae (96 h ALH) (Cocanougher et al., 2019) were downloaded from <https://www.ncbi.nlm.nih.gov/geo/query/acc.cgi?acc=GSE135810>. The following matrices were used: GSM4030602, GSM4030604, and GSM4030607 for the 2nd instar larvae, GSM4030600 and GSM4030606 for the feeding 3rd instar larvae and GSM4030623, GSM4030624, GSM4030625, and GSM4030626 for the wandering 3rd instar larvae. The matrices were integrated for each stage and analyzed as described for the 1st instar larval brain described above with the following parameters: the dimensionality was set to 30 and the cells were clustered with a resolution of 0.4 for the 2nd instar larvae and 2.4 for the feeding and wandering 3rd instar larvae. The hemocyte subgroups were unambiguously identified using the hemocyte markers `Srp`, `Hml`, `Pxn`, `NimC1`, `He`, and `Nplp2` (described by the authors) and used for the downstream analyses.

Pearson correlation were computed as follow. Pseudo-transcriptomes were generated for the hemocyte subgroups from the stage 6 embryos data (Karaïskos et al., 2017), from

the eye disc data (Ariss et al., 2018), for the brain data (Brunet Avalos et al., 2019) as well as for each subgroup of the non-infested dataset from Cattenoz et al. (2020) using the function “AverageExpression” from the Seurat R toolkit (Butler et al., 2018; Stuart et al., 2019). The correlation between the pseudo-transcriptomes were then measured using the Pearson correlation coefficient. The pseudo-transcriptomes of the hemocyte subgroups from Cattenoz et al. were compared to the pseudo-transcriptome of stage 6 embryos’ hemocytes in **Supplementary Figure S3G**, to the pseudo-transcriptome of the eye disc associated hemocytes in **Supplementary Figure S3C** and to the pseudo-transcriptome of the brain associated hemocytes in **Supplementary Figure S3E**.

The dot plot (**Figure 4D**) was generated using the function “DotPlot” from the Seurat R toolkit with the non-infested data from Cattenoz et al. (2020) and the expression matrices from stage 6 embryos and larval eye discs (Karaïskos et al., 2017; Ariss et al., 2018). The dot plot was compiled in Adobe Illustrator CS6.

Regulon Analysis

To identify the regulons enriched in the lamellocytes, we ran Single-Cell regulatory Network Inference and Clustering (SCENIC) (Aibar et al., 2017) through its Python implementation `pySCENIC`, version 0.9.19³. The source code was downloaded from the GitHub repository <https://github.com/aertslab/pySCENIC.git>. The **Supplementary Files** necessary to run SCENIC were obtained from <https://resources-mirror.aertslab.org/cistarget/>. The analysis was carried out on the wasp infested expression matrix from Cattenoz et al. deposited in the ArrayExpress database at EMBL-EBI⁴ under the accession number E-MTAB-8698.

The motifs version 8,⁵ the regulatory elements within 5 kb upstream the TSS and the transcript introns⁶ were used for the analysis. The most significant regulons showing differential activity among clusters were determined with Mann-Whitney *U*-test (Mann and Whitney, 1947), between the AUC scores given by SCENIC in a specific cluster versus all the rest of the clusters. The regulons displaying a *z*-score above 2 or below −2 for the lamellocytes subgroups were selected to build the heatmap shown in **Figure 3A**. The heatmap was generated with the R package “pheatmap” (Kolde, 2019).

The scatter plot (**Figure 3B**) was generated with the pseudo-transcriptomes of LM1 and LM2 subgroups from the wasp infested dataset in Cattenoz et al. (2020). The pseudo-transcriptomes were estimated with the function “AverageExpression” from the Seurat R toolkit (Butler et al., 2018; Stuart et al., 2019).

Fly Strains and Genetics

All flies were raised on standard media at 25°C. The following strains were used: *Oregon-R*, *srp(hemo)-3xmcherry*

³<https://pyscenic.readthedocs.io/en/latest/>

⁴www.ebi.ac.uk/arrayexpress

⁵cistarget/motif2tf/motifs-v8-nr.flybase-m0.001-o0.0.tbl

⁶cistarget/databases/drosophila_melanogaster/dm6/flybase_r6.02/mc8nr/gene_based/dm6-5kb-upstream-full-tx-11species.mc8nr.feather

[*srp(hemo)* > *RFP*, gift from D. Siekhaus (Gyoergy et al., 2018)], *BAC-gcm-Flag* (Laneve et al., 2013).

Immunolabelling and Image Acquisition

For hemocyte labeling, 10 wandering 3rd instar larvae were bled in Schneider medium complemented with 10% Fetal Calf Serum (FCS), 0.5% penicillin, 0.5% streptomycin (PS), and few crystals of N-phenylthiourea $\geq 98\%$ (PTU). The cells were cytospinned on a glass slide at 700 rpm for 3 min at room temperature (RT), then the samples were fixed for 10 min in 4% paraformaldehyde/PBS at RT and rinsed with PTX (PBS 1x, 0.5% triton X-100).

For the embryos, overnight collections were washed on a 100 μm mesh and dechorionated in bleach for 5 min. The fixation was carried out for 25 min at RT under agitation in a solution of 4% paraformaldehyde in PBS 1x/heptane (1/1 vol.). The vitelline membrane of the embryos was then removed by replacing the PFA solution by methanol and strong agitation for 30 s. The methanol/heptane solution was removed and the embryos were washed with PTX for 15 min at RT.

For the lymph gland and filet preparation, wandering 3rd instar larvae were dissected in cold PBS 1x, then transferred in 4% paraformaldehyde in PBS 1x for at least 30 min at RT and rinsed in PTX for 15 min.

Following the PFA fixation and PTX wash, the samples were incubated with blocking reagent (Roche) for 1 h at RT, incubated overnight at 4°C with primary antibodies diluted in blocking reagent, washed three times for 10 min with PTX, incubated for 1 h with secondary antibodies, washed twice for 10 min with PTX, incubated for 30 min with DAPI and phalloidin TRITC (1:1,000, Sigma #P1951), and then mounted in Aqua-Poly/Mount (Polysciences, Inc.). The following primary antibodies were used: rabbit anti-Srp [1:500, (Bazzi et al., 2018)], rabbit anti-Flag (1:100, Sigma S3165), chicken anti-GFP (1:500, abcam ab13970), rat anti-RFP (1:500, Chromotek 5F8-100), rabbit anti-Pxn [1:5,000; gift from J. Shim, (Yoon et al., 2017)], mouse anti-Hemese [1:50 gifts from I. Ando, (Kurucz et al., 2003)].

The following secondary antibodies were used at 1:500: FITC donkey anti-chicken IgG (Jackson ImmunoResearch Labs Cat# 703-095-155), FITC goat anti-mouse IgG (Jackson ImmunoResearch Labs Cat# 115-095-166), Cy3 donkey anti-mouse IgG (Jackson ImmunoResearch Labs Cat# 715-165-151), Cy3 goat anti-rat IgG (Jackson ImmunoResearch Labs Cat# 112-165-167), Cy3 donkey anti-rabbit IgG (Jackson ImmunoResearch Labs Cat# 711-165-152), Cy5 goat anti-mouse IgG (Jackson ImmunoResearch Labs Cat# 115-175-003) and Cy5 goat anti-rat IgG (Jackson ImmunoResearch Labs Cat# 112-175-167), Cy5 goat anti-rabbit IgG (Jackson ImmunoResearch Labs Cat# 111-175-144), Alexa Fluor 647 goat anti-mouse IgG (Jackson ImmunoResearch Labs Cat# 115-605-166).

The slides were analyzed by confocal microscopy (Leica Spinning Disk and Leica SP8) with 20x, 40x, and 63x objectives, using hybrid detectors in photon counting mode. DAPI was excited at 350 nm, the emission filters 410–510 were used to collect the signal; FITC was excited at 488 nm, the emission filters 498–551 were used to collect the signal; Cy3 was excited at 568 nm, emission filters 648–701 were used to collect the signal, and Cy5 was excited at 633 nm; emission signal was

collected at 729–800 nm. The images were analyzed with Fiji (Schindelin et al., 2012).

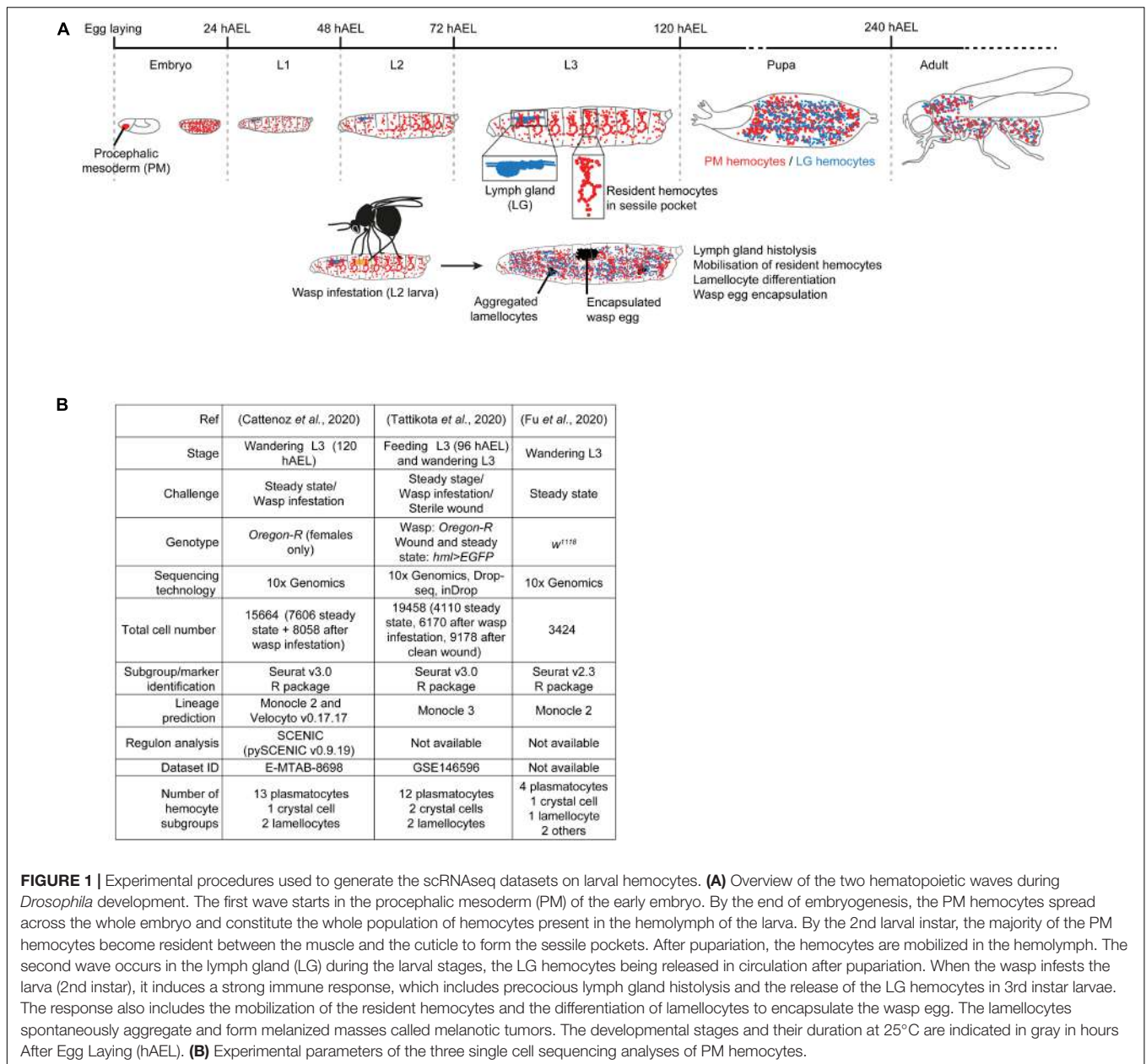
RESULTS

Characterization of the *Drosophila* Larval Hemocytes by scRNAseq

The first hematopoietic wave occurs at early embryonic stages 6–9, in the procephalic mesoderm (PM). The progenitors undergo several rounds of division, differentiate into plasmacytes and crystal cells and migrate along stereotyped routes to spread throughout the organism (PM hemocytes) (Tepass et al., 1994; Gold and Bruckner, 2014). The second hematopoietic wave occurs in the lymph gland (LG) of the larva to generate cells that are only released in the hemolymph after puparium formation, upon lymph gland histolysis (LG hemocytes) (Jung et al., 2005; reviewed by Banerjee et al., 2019). The larval infestation from parasitoid wasps such as *Leptopilina boulardi* as well as wounding triggers precocious lymph gland histolysis. These challenges also lead to the differentiation of lamellocytes that encapsulate the wasp eggs or participate to the wound closure (**Figure 1A**) and the same cell type is found upon the activation of pro-inflammatory pathways (Lemaitre et al., 1995; Luo et al., 1995; Markus et al., 2005; Fleury et al., 2009; Kim-Jo et al., 2019).

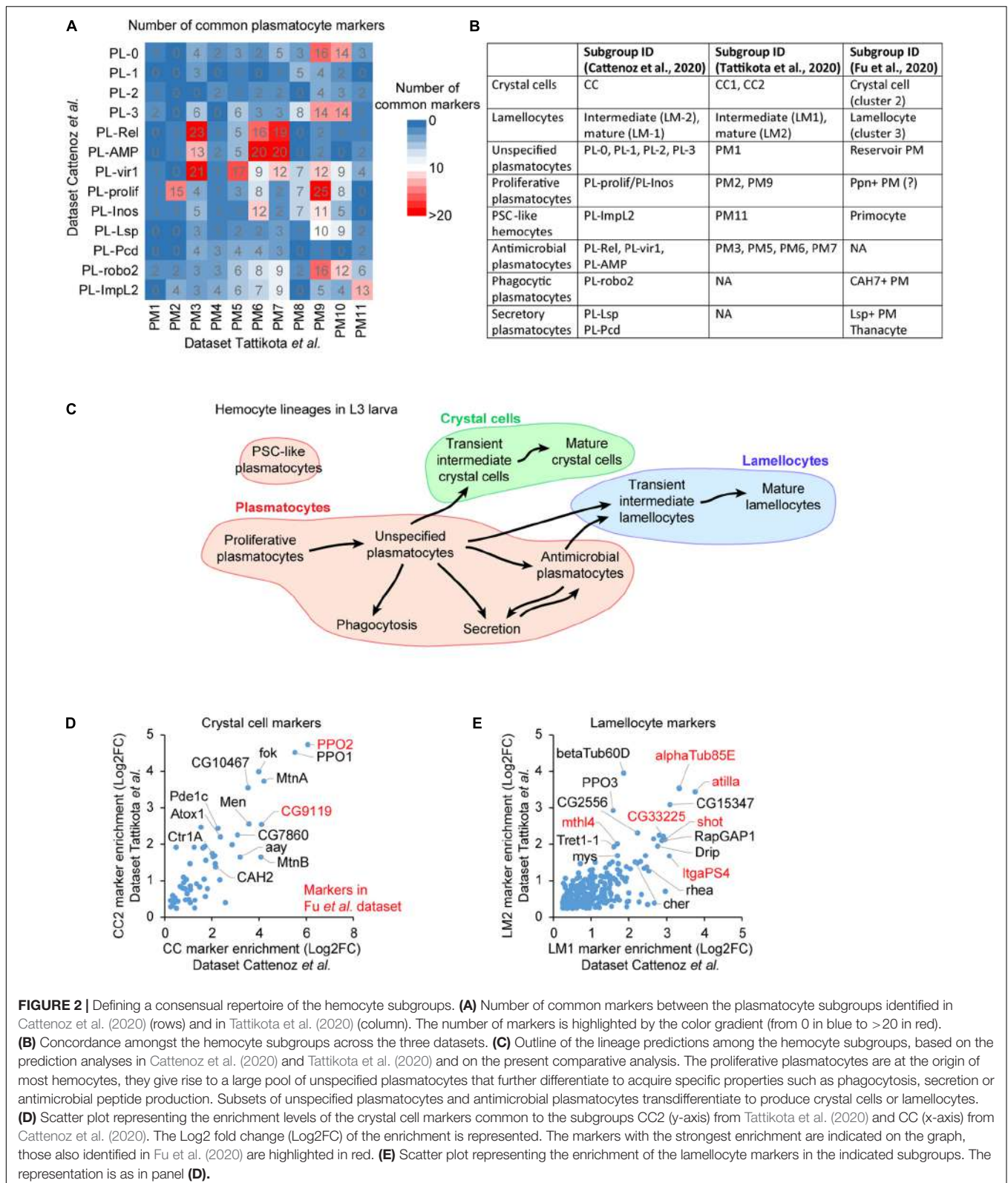
The larval PM hemocytes were recently analyzed in three scRNAseq studies (Cattenoz et al., 2020; Fu et al., 2020; Tattikota et al., 2020), following different experimental parameters (**Figure 1B**). Tattikota et al. analyzed hemocytes from feeding 3rd instar larvae and wandering 3rd instar larvae (WL) in steady state conditions or after inducing an immune reaction (clean wounding, or wasp infestation). Three sequencing technologies were used and the animals were of two genotypes. The merge of these datasets identified twelve subgroups of plasmacytes, two of crystal cells and two of lamellocytes (Tattikota et al., 2020). Fu et al. analyzed hemocytes from WL of one genotype in steady state conditions using 10x Genomics technology. They identified four subgroups of plasmacytes, one of crystal cells, one of lamellocytes and two minor cell populations called primocytes and thanocytes (Fu et al., 2020). Cattenoz et al. analyzed hemocytes from female WL of one genotype, in steady state conditions and after wasp infestations, using 10x Genomics technology. They identified thirteen subgroups of plasmacytes, one of crystal cells and two of lamellocytes, the latter ones being specifically found in the dataset from the challenged condition (Cattenoz et al., 2020). In the three datasets, the definition of the subgroups was followed by lineage prediction analyses to identify distinct developmental trajectories amongst the hemocyte subgroups. The trajectories are defined by organizing the cells along a pseudo-time axis based on the progression of the expression of the variable genes (Kester and van Oudenaarden, 2018).

The systematic comparison of the lists of markers from the three studies allows the identification of common subgroups (**Figure 2A**). The markers are defined by their levels of enrichment in a specific subgroup compared to the whole hemocyte population [$\text{Log}_2(\text{enrichment}) > 0.25$, adjusted



$p < 0.01$ in Cattenoz *et al.* (2020) and Tattikota *et al.* (2020)]. The correlation between the subgroups of each dataset is inferred from the cross-comparison of all plasmatocyte markers found in the three studies (Figure 2A). The number of markers as well as their level of enrichments are taken into consideration (Supplementary Figures S1A,B, S2A,C–E). An additional level of comparison among the datasets is the developmental trajectory. If our comparison based on markers is accurate, the developmental trajectories between the distinct subgroups should be preserved across the three studies, and we find that this is the case. Thus, the subgroups presenting the highest number of common markers, the highest levels of markers' enrichment and similar developmental trajectories likely define equivalent subgroup (Figures 2B,C).

For example, PM9 in Tattikota *et al.* dataset shares a significant number of markers with PL-0, PL-3, PL-*vir1*, PL-*prolif*, PL-*Inos*, and PL-*robo2* in Cattenoz *et al.* dataset (Figure 2A). The subgroup presenting the highest number of markers with the highest enrichments is PL-*prolif* (Supplementary Figure S1A). The second closest subgroup is PL-*robo2*, which also displays markers with relatively high enrichments. However, PL-*robo2*/PM9 markers are expressed in most hemocyte subgroups while PL-*prolif*/PM9 markers are highly specific (Supplementary Figure S1B). At last, lineage predictions carried out in both studies suggest that PM9 and PL-*prolif* are sitting at the beginning of the developmental trajectories of the hemocytes (Cattenoz *et al.*, 2020; Tattikota *et al.*, 2020). Altogether, these data suggest that PM9 and PL-*prolif* represent the same subgroup.



The marker comparison shows a large correlation across studies for crystal cells and lamellocytes: 53 crystal cell markers and 265 lamellocyte markers are commonly found by Tattikota

et al. and Cattenoz et al. (Figures 2D,E). All the markers previously used to label the crystal cells and the lamellocytes are present in the two datasets. Such tight correlation is expected

for subgroups that present strong physiological differences compared to the plasmatocytes. Fu et al. disclosed a limited list of markers for crystal cells and lamellocytes; all of them are nevertheless present in the crystal cell and lamellocyte subgroups identified in two other datasets, further confirming the identity of these subgroups. The three studies consistently found a large subgroup of “unspecified plasmatocytes” presenting no distinctive marker and encompassing more than 50% of plasmatocytes (PM1 in Tattikota et al.; PL-0, 1, 2, and 3 in Cattenoz et al.; reservoir PM in Fu et al.), as well as several smaller subgroups enriched for specific markers: the proliferative, the antimicrobial, the posterior signaling center-like, the phagocytic and the secretory plasmatocytes (Figure 2B).

Proliferative Plasmatocytes

The markers involved in mitosis, including Cyclin B (CycB) (Gavet and Pines, 2010), the phosphatase String (Stg) (Edgar and O’Farrell, 1990), the importin Pendulin (Pen) (Kussel and Frasch, 1995) and the kinase Polo (Sunkel and Glover, 1988) are enriched in clusters PM2 as well as PM9 in Tattikota et al., and in the PL-prolif cluster in Cattenoz et al. (Supplementary Figures S2A,B). These proliferative subgroups are positioned at the beginning of the developmental trajectories and give rise to the pool of unspecified plasmatocytes. The PL-prolif subgroup represents a hemocyte subset of the PL-Inos subgroup, which lacks the proliferative genes but expresses all the other markers of PL-prolif (Cattenoz et al., 2020), suggesting that PL-prolif and PL-Inos represent two states (dividing/quiescent) of the same subgroup.

Antimicrobial Plasmatocytes

Two datasets contain subgroups of plasmatocytes enriched in transcripts involved in immune pathways: PL-AMP, PL-Rel and PL-vir1 in Cattenoz et al.; PM3, PM5, PM6, and PM7 in Tattikota et al. The comparison of the markers indicates a correlation between PL-Rel/PL-AMP and PM3/PM6/PM7 as well as between PL-vir1 and PM3/PM5 (Supplementary Figures S2C,D).

PM6/7 and PL-AMP are highly enriched for AMP expression [i.e., Cecropins A1, A2, and C (CecA1, CecA2, CecC), Dipterican B (DptB), Drosomycin (Drs), Metchnikowin (Mtk), Mtk-like (Mtkl)]. Of note, the AMPs Mtk, DptB, and Drs are enriched at higher levels in the dataset from Tattikota et al. than in the one from Cattenoz et al. This is likely due to the induction of these AMPs by clean wounding, a condition specific to the dataset from Tattikota et al. All these subgroups also express high levels of Matrix metalloproteinase 1 (Mmp1), involved in wound healing (Stevens and Page-McCaw, 2012). PM3 and PL-Rel express elements of the IMD and JNK pathways and lower levels of AMP, which suggests weaker or different mode of activation of the immune response. This may reflect different microenvironments and/or different intrinsic properties compared to PM6/7 and PL-AMP.

PM5 and PL-vir1 present common expression profiles, distinctive from the other subgroups. They are not enriched in AMPs (Supplementary Figure S2D) and seem specialized in xenobiotic detoxification, as suggested by the expression of the Ferritin 1 heavy chain homolog, the Ferritin 2 light chain

homolog and the Multidrug resistance protein (Chahine and O’Donnell, 2009; Tang and Zhou, 2013).

Posterior Signaling Center-Like Plasmatocytes

The comparison of the markers consistently identifies a subgroup of cells representing less than 1% of the hemocyte population across the three studies: PL-Impl2 (Cattenoz et al., 2020), PM11 (Tattikota et al., 2020), and the primocytes (Fu et al., 2020) (Supplementary Figures S2E,F). This subgroup expresses typical markers of the posterior signaling center (PSC) present in the lymph gland, such as the transcription factors Knot (Kn) (Makki et al., 2010) and Antennapedia (Antp) (Mandal et al., 2007). The comparison of the markers of this subgroup with the PSC markers identified by the scRNAseq assay on the lymph gland (Cho et al., 2020) also identifies this subgroup as PSC-like plasmatocytes (Supplementary Figure S2G).

Phagocytic Plasmatocytes and Secretory Plasmatocytes

The datasets from Fu et al. and from Cattenoz et al. identified phagocytic plasmatocytes, plasmatocytes secreting storage proteins and plasmatocytes secreting opsonins.

Phagocytic plasmatocytes: CAH7 + PM (Fu et al.) and PL-robo2 (Cattenoz et al.) are enriched for the phagocytic receptor NimC2 (Kurucz et al., 2007), the cytoskeleton proteins Myoblast city (Erickson et al., 1997), the Tenascin accessory (Mosca et al., 2012), the transmembrane receptor Lipophorin receptor 2 (LpR2) and Mmp2 (Supplementary Figure S2H). Lineage predictions call for PL-robo2/CAH7 + PM being directly issued from the unspecified plasmatocytes and since the strongest markers for PL-robo2 are also enriched to a lower extent in a subset of unspecified plasmatocytes (PL-0/PL-2), PL-robo2 may specifically represent the phagocytic, active state, of this subset.

Secretory plasmatocytes: Lsp + PM (Fu et al.) and PL-Lsp (Cattenoz et al.) display a highly distinctive expression pattern of proteins secreted in the hemolymph such as Larval serum protein 1 alpha (Lsp1alpha), Larval serum protein 2 (Lsp2), Apolipophorin (Apolpp), and Odorant binding protein 99b (Obp99b) (Supplementary Figure S2I). All these proteins are mostly expressed by the fat body (Chintapalli et al., 2007) and serve as storage proteins (Telfer and Kunkel, 1991; Handke et al., 2013), suggesting common functions between the fat body and these secretory plasmatocytes.

At last, the thanocytes (Fu et al.) and PL-Pcd (Cattenoz et al.) express low levels of NimC1 and secrete the opsonins Thioester-containing protein 2 and 4 (Tep2 and Tep4) that promote the phagocytosis of bacteria and the activation of the Toll pathway (Dostalova et al., 2017; Supplementary Figure S2J). The thanocyte markers are consistently enriched in both PL-AMP and PL-Pcd, yet differ from PL-AMP by the lack of AMP production (Supplementary Figure S2J). Thus, PL-AMP may represent an activated state of PL-Pcd/thanocyte, in which the inflammatory pathways are triggered and antimicrobial peptides are secreted.

These three subgroups were not identified in Tattikota et al. dataset. Their markers are detected in some cells but these

cells are not clustered together and are associated with the pool of unspecified plasmatocytes, with whom they share the majority of the markers.

Lamellocytes

The datasets from Tattikota et al. and Cattenoz et al. include conditions promoting the differentiation of the lamellocytes and identify two subgroups. One of them expresses both plasmatocyte and lamellocyte markers and likely corresponds to plasmatocytes that are transdifferentiating into lamellocytes (LM1 in Tattikota et al., LM-2 in Cattenoz et al.). The second subgroup lacks most of the plasmatocyte markers and expresses the lamellocyte markers strongly (LM2 in Tattikota et al., LM-1 in Cattenoz et al.). For the sake of simplicity, we will call the first and the second subgroups intermediary and mature lamellocytes, respectively.

To identify the molecular pathways activated during lamellocyte differentiation, we carried out a regulon analysis using SCENIC (Aibar et al., 2017) on the dataset from wasp infested larvae generated by Cattenoz et al. (2020). This analysis relies on two steps. First, the genes presenting covariation are identified across the whole single cell dataset. Then, the promoters of the covarying genes are scanned for canonical transcription factor binding sites. The genes presenting similar expression profiles and carrying the same transcription factor binding site(s) are grouped in one regulon named after the transcription factor. This analysis highlights two regulons, Kayak (Kay) and Jun-related antigen (Jra), which regroup the targets of the two main transcription factors of the JNK pathway (reviewed in La Marca and Richardson, 2020; **Figure 3A**), known to promote the differentiation of lamellocytes (Tokusumi et al., 2009). We have pulled together the transcriptomes of all cells from the intermediary and mature lamellocytes from Cattenoz et al. dataset to generate pseudo-transcriptomes. The comparison of the pseudo-transcriptomes shows that the genes regulated by the JNK pathways are expressed at higher levels in the mature lamellocytes than in the intermediary ones (**Figure 3B**). Strikingly, this analysis also reveals for the first time seven novel regulons associated with lamellocyte differentiation: Cyclic-AMP response element binding protein B (CrebB), Forkhead box sub-group O (Foxo), REPTOR-binding partner (REPTOR-BP), Pannier (Pnr), Maf-S, Zinc-finger protein (Zif), and Checkpoint suppressor 1-like (CHES-1-like). These regulons are highly enriched in lamellocytes and display an enhanced activation from the intermediary lamellocytes to the mature lamellocytes (**Figure 3A**).

The regulons CrebB, Foxo and REPTOR-BP are involved in the maintenance of energy metabolism upon food restriction or molecular stress (Dionne et al., 2006; Iijima et al., 2009; Tiebe et al., 2015). They may be responsible for the induction of specific glucose transporters and the metabolic shift from lipolytic to glycolytic observed during the transdifferentiation of plasmatocytes into lamellocyte (Cattenoz et al., 2020; Tattikota et al., 2020). These pathways may also maintain the high metabolic activity of lamellocytes, while the metabolism of other organs is inhibited to privilege the immune response over the

developmental processes (Bajgar et al., 2015; Dolezal, 2015). Maf-S along with Foxo regulate oxidative stress resistance (Rahman et al., 2013; Gumeni et al., 2019) and CHES-1-like is involved in the DNA-damage response (Busygina et al., 2006). Both oxidative stress and DNA damage can be associated with the high metabolism of lamellocytes, a phenomenon usually observed in cancerous cells in mammals (Moretton and Loizou, 2020).

Hemocyte Populations in Other Single Cell Datasets

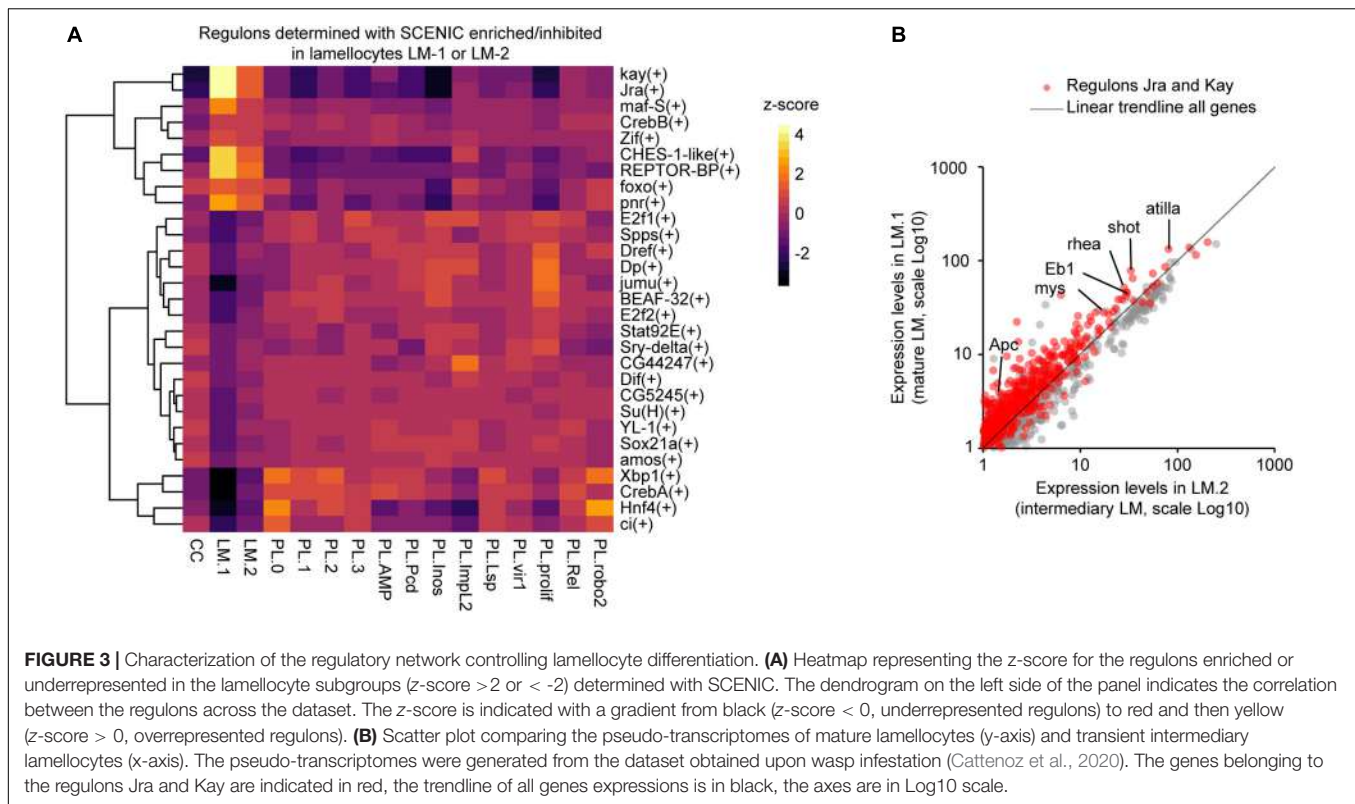
In mammals, macrophages are conditioned by their microenvironment, which leads to molecular signatures specific to the tissues in which they reside (van de Laar et al., 2016; Williams et al., 2020). To assess if specific hemocyte subgroups are associated to different tissues in *Drosophila*, we have screened tissue specific or embryonic scRNAseq datasets containing hemocytes (i.e., larval eye discs, larval brains, and stage 6 embryos) and compared their molecular signatures to the dataset of Cattenoz et al.

Hemocytes Associated With the Larval Eye Disc Resemble Unspecified Plasmatocytes

The scRNAseq analyses on larval eye discs (Ariss et al., 2018) reveal a small subgroup of cells in line with the hemocytes observed in close contact with this disc (Holz et al., 2003; **Figure 4A** and **Supplementary Figures S3A,B**). Since the eye disc associated hemocytes express a large panel of hemocyte markers, their pseudo-transcriptome was compared to the pseudo-transcriptome of each of the subgroups identified in Cattenoz et al. dataset using Pearson correlation coefficient. This analysis highlights a strong correlation between the eye disc associated hemocytes and unspecified plasmatocytes (PL-1/PL-3, **Supplementary Figure S3C**), which do not express strong markers. Moreover, the eye disc associated hemocytes do not express subgroup-exclusive markers, like *Lsp1alpha* in PL-Lsp or *Kn* and *Tau* in PL-ImpL2 (**Figure 4D**). Altogether, these evidence suggest that the eye disc associated hemocytes are unspecified plasmatocytes.

Next, to determine if the eye disc associated hemocytes represent a subgroup that was not defined in Cattenoz et al. dataset, we compared their pseudo-transcriptome to the combined pseudo-transcriptome of all subgroups from Cattenoz et al. (**Supplementary Figure S4A**). This comparison did not return a strong signature for the eye disc associated hemocytes (less than 10 genes specifically expressed in the eye disc hemocytes), which is concordant with the high correlations measured between almost all subgroups and the eye-associated hemocytes (**Supplementary Figure S3C**). Thus, at this level of resolution, the hemocytes in the eye disc cannot be distinguished from unspecified plasmatocytes.

One of the main characteristics of the unspecified plasmatocytes is the expression of Extra Cellular Matrix (ECM) components such as *Pxn*, which is necessary for the assembly of the basement membrane (Bhave et al., 2012). *Pxn* is indeed strongly expressed in the hemocytes associated to the eye disc and is detected at the basement membrane of the disc (**Figure 4A**). Similar analyses will reveal whether this feature



is common to the hemocytes associated to the other imaginal tissues. Interestingly, larval hemocytes secrete ECM compounds to build the basement membrane of the ovaries and the fat body (Shahab et al., 2015; Van De Bor et al., 2015).

Hemocytes Associated With the Brain Resemble the Proliferative Plasmatocytes (PL-Inos, PL-Prolif)

Two scRNAseq datasets on the larval brain from 1st instar to 3rd instar larvae (Brunet Avalos et al., 2019; Cocanougher et al., 2019) report the presence of hemocytes (Supplementary Figure S3D), in line with the hemocytes observed in close contact with this tissue (Figure 4B). The comparison of the pseudo-transcriptomes of hemocytes from the 1st instar brain and of Cattenoz et al. subgroups highlights the highest correlation with the PL-prolif and PL-Inos subgroups (Supplementary Figure S3E). The correlation coefficients are much weaker than in the comparison with the eye disc associated hemocytes. In addition, the comparison of the pseudo-transcriptomes of brain associated hemocytes with the pseudo-transcriptome of all subgroups from Cattenoz et al. suggests a specific molecular signature for these hemocytes (Supplementary Figure S4B). PL-prolif markers are represented in the brain associated hemocytes, together with dozens of genes that are consistently expressed from 1st instar to 3rd instar larval brains (Figure 4D, Supplementary Table S1 and Supplementary Figure S4C). Altogether, these data suggest that the brain hemocytes represent a discrete subgroup with a specific molecular signature. The strong markers of PL-Inos/PL-prolif are preserved during development as they are observed from the 1st to the 3rd instar datasets (Figure 4D).

PSC-Like Plasmatocytes and Proliferative Plasmatocytes Resemble Prohemocytes From Stage 6 Embryos

The single cell analyses suggest that the larval hemocytes originate from the proliferative subgroup. We therefore predicted that the prohemocytes present at the early embryonic stages may resemble this subgroup and compared the larval dataset from Cattenoz et al. with the one obtained from scRNAseq on embryos at stage 6 (Supplementary Figure S3F; Karaiskos et al., 2017). At this stage, the cells of the procephalic mesoderm express the earliest hemocyte-specific transcription factors Glial Cell Missing/Glial Cell Deficient (Gcm) and Serpent (Srp) (Figure 4C; Sam et al., 1996; Bernardoni et al., 1997; Waltzer et al., 2003). The comparison of the pseudo-transcriptomes indeed shows that the prohemocytes from stage 6 embryos present the highest correlation with the subgroups PL-prolif/PL-Inos (i.e., proliferative plasmatocytes) and PL-Impl2 (i.e., PSC-like plasmatocytes), and express the strongest markers of these subgroups (Figure 4D and Supplementary Figure S3G).

DISCUSSION

The comparative analysis of the scRNAseq datasets confirms the diversity of the immune cells present in the *Drosophila* larva. Molecular features consistently found across the studies allow the identification of robust plasmatocyte subgroups in addition to crystal cells and lamellocytes. The proliferative subgroup resembles the prohemocytes present in the early embryonic

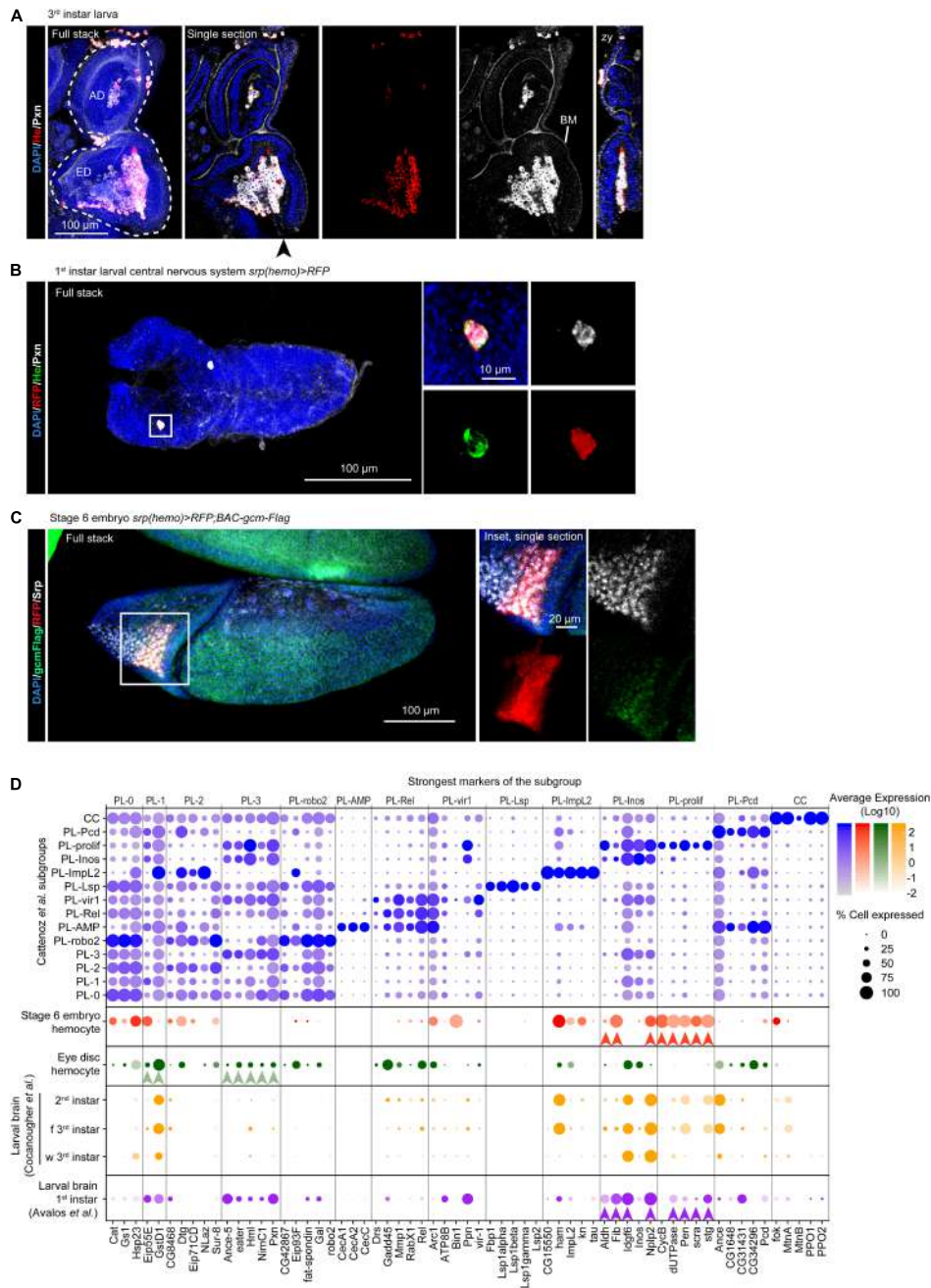


FIGURE 4 | The molecular signatures of the hemocytes from larval eye discs, larval brains and stage 6 embryos. **(A)** Eye disc from 3rd instar larva. The immunolabelling assay used anti-He (in red), anti-Pxn (in white) and the nuclei were labeled with DAPI (blue). The left panel shows the full stack, the eye disc (ED) and the antenna disc (AD) are indicated with a white dashed line, the next panels show a single section with all the channels, He labeling only and Pxn labeling only, respectively. Pxn labeling is present at the basement membrane (BM). The rightmost panel shows an orthogonal projection along the z-y axes from the position indicated by the black arrowhead. The scale bar represents 100 μ m. **(B)** Central Nervous System from 1st instar larva carrying the *srp(hemo) > RFP* transgene, which allows for hemocyte detection (Gyoergy et al., 2018). The immunolabelling assay used three hemocyte markers [anti-RFP (in red), anti-He (in green), anti-Pxn (in gray)], and the nuclei were labeled with DAPI (blue). The left panel shows the full stack, the right panels (partial stacks) show the inset at high magnification (merged and individual channels). The scale bars represent 100 μ m in the full stack and 10 μ m in the inset. The hemocyte lays on the surface of the nervous system. **(C)** Stage 6 embryo *srp(hemo) > RFP; BAC-gcm-Flag*. The BAC was used to reveal the Gcm protein (Laneve et al., 2013). The immunolabelling assay used anti-RFP (in red), anti-Flag (in green), anti-Srp (in gray), and the nuclei were labeled with DAPI (blue). The left panel shows the full stack, the right panels show a single section of the inset at high magnification (merged and individual channels). The scale bars represent 100 μ m in the stack and 20 μ m in the inset. **(D)** Dot plot representing the expression levels and percentage of cells expressing the top markers of each subgroup identified by Cattenoz et al. (2020). The violet dots represent the expression in Cattenoz et al. (2020) subgroups, the red dots, expression in the hemocytes from stage 6 embryos (E6 embryos), the green dots in the hemocytes from larval eye discs, the purple and orange dots in the hemocytes from larval brains at the indicated stages (f 3rd instar: feeding 3rd instar larvae; w 3rd instar: wandering 3rd instar larvae). The arrowheads (red, green, purple) indicate the strongest markers linking the tissue-specific hemocytes with the subgroups from Cattenoz et al. (2020).

stages and the plasmatocytes associated with different larval tissues seem to present specific features.

Identification of Robust Subgroups

The present analysis identifies common subgroups with specific potentials (proliferation, AMP production, PSC-like, phagocytosis, secretion, crystal cells and lamellocytes) or lacking specific properties (unspecified plasmatocytes) (summarized in **Figures 2B,C**).

The proliferative plasmatocytes seem the sole source of larval hemocytes, including the crystal cells (Cattenoz et al., 2020; Tattikota et al., 2020). This subgroup may represent cells retaining a progenitor state, in line with their resemblance with the molecular signature of the hemocyte progenitors present in the early embryo. Lineage predictions suggest that the proliferative subgroup generates the unspecified plasmatocytes, which constitute more than 50% of the hemocytes and represent intermediary states between proliferative and differentiated cells (Cattenoz et al., 2020; Tattikota et al., 2020). The unspecified plasmatocytes seem to constitute the majority of the hemocytes associated with the eye discs, where they produce ECM proteins. The antimicrobial subgroup is the largest specified subgroup. It encompasses plasmatocytes enriched in transcripts coding for proteins associated to the immune response, including elements of the IMD and the Toll pathways and AMPs. The PSC-like subgroup displays a signature highly similar to that of the PSC in the lymph gland. Future studies will determine whether this subgroup plays a similar signaling role in the hemolymph and/or in specific niches. The phagocytic plasmatocytes are enriched for markers involved in engulfment, phagocytosis and actin remodeling. The secretory plasmatocytes are subdivided into two subgroups, one secreting storage proteins and the other secreting opsonins. The phagocytic and the storage protein secreting subgroups resemble strongly the unspecified plasmatocytes, as the number of specific markers is quite limited. The lack of a strong distinctive signature suggests that these cells may be associated with specific microenvironments/challenges, which would induce the expression of proteins on-demand, without drastically affecting hemocyte properties and identity. In other terms, we hypothesize that these two clusters are of common nature and that their differences rely on different “nurture.”

In addition to the plasmatocyte subgroups, the three studies identified lamellocyte and crystal cell subgroups. Both subgroups are characterized by a specific list of markers, suggesting a well-defined nature of these cells. Some markers are already known (Rizki and Rizki, 1959; Braun et al., 1997; Irving et al., 2005; Rus et al., 2006; Honti et al., 2009; Binggeli et al., 2014), some are new. The datasets from Tattikota et al. and Cattenoz et al. include similar experimental immune challenges (i.e., wasp infestation) to activate the production of lamellocytes and display two subgroups of lamellocytes, one intermediary and one mature. The regulons analysis identifies the transcription factors involved in lamellocyte transdifferentiation/functions. These include the transcription factors of the JNK pathway known to promote lamellocyte differentiation and seven novel transcription factors potentially required for lamellocytes maturation. Further investigations

will determine the roles of these transcription factors in the differentiation of the lamellocytes.

Advantages and Biases of the Computational Approach

The comparison of the different hemocyte scRNAseq datasets allows the identification of common molecular signatures, despite the heterogeneity of the experimental procedures. This straightforward approach is based on the marker lists provided by each study and is not computationally demanding. The downside is that it highlights only the subgroups presenting the strongest markers and biologically relevant minor variations can be hidden by the differences between the parameters chosen for the computational analysis. This is the case of the secretory and phagocytic subgroups, which were not identified in Tattikota et al. (2020). In addition to the different analytic parameters, the absence of these subgroups may also be explained by the different experimental conditions. Tattikota et al. dataset includes three experimental conditions with a majority of the cells coming from wounded larvae. Such set up may favor the identification of subgroups specific to wounded conditions at the expense of subgroups present in steady state conditions.

The molecular signature of the subgroups defined in Cattenoz et al. have been used to determine the identity of hemocytes present in the scRNAseq from larval eye discs and brains as well as from stage 6 embryos. The strong molecular signature of the hemocytes permits a clear distinction of these cells within each dataset and then the comparison with the hemocyte subgroups' signatures allows the identification of the closest subgroups. Typically, the hemocytes associated with the brain display the distinctive profile of the small, proliferative, subgroup. The main caveat of this analysis is related to the limited number of hemocytes recovered in assay (<100 cells in each dataset). We cannot exclude that discrete subgroups were not found because of their low frequencies in the specific tissue. This may notably be the case of the hemocytes associated with the eye discs, which display markers of the large subgroup of unspecified plasmatocytes. In addition, the dissection procedure may remove the less tightly associated cells, rendering our interpretation incomplete. The development of *ad hoc* protocols to analyze the hemocytes in the whole animal will help significantly.

The comparison of scRNAseq datasets brings robustness to the precise information on the cellular diversity gained with a single dataset. However, this approach is highly dependent on the analysis pipelines followed within each study. Since the number of studies using scRNAseq are currently booming and in parallel, new analytical tools are constantly generated, the comparability between datasets is not always straightforward (Vieth et al., 2019; Gao et al., 2020). Generating a universal pipeline of scRNAseq analysis will be highly valuable as it will facilitate the comparison between datasets.

In sum, the comparison of the three scRNAseq datasets allows the definition of common features and robust subgroups, an important asset to understand the biology of hemocyte heterogeneity. Some subgroups show a distinctive transcriptomic signature, while others present many shared

markers, suggesting an origin according to nature and nurture, respectively. Increasing evidence highlight the influence of the microenvironment in governing the gene expression profile in mammalian tissue-specific macrophages, despite their common embryonic origin (Gautier et al., 2012; Lavin et al., 2014). We expect that similar mechanisms in *Drosophila* lead to the differentiation of specific subgroups. Future lineage tracing assays will help assessing the relative impact of intrinsic and environmental cues on the presence of the different subgroups as well as their stability. The generation of subgroup specific drivers will make it possible to assess the role of the different subgroups in physiological and pathological conditions. Finally, bulk RNAseq of distinct subgroups (sorted according to the markers from the scRNAseq) will generate deeper molecular signatures. The combination of more refined experimental and analytical approaches will determine with higher precision the similarities and differences between subgroups and reveal the function of the subgroups. This will contribute to unravel the heterogeneity and the biology of the macrophage populations.

DATA AVAILABILITY STATEMENT

The data was deposited in the ArrayExpress database at EMBLEBI (www.ebi.ac.uk/arrayexpress) under the accession number E-MTAB-8698.

AUTHOR CONTRIBUTIONS

PC and AG: conceptualization, investigation, writing—original draft, funding acquisition, and supervision. PC, AG, AP, and SM: methodology and writing—review and editing. AG: resources. All authors contributed to the article and approved the submitted version.

REFERENCES

- Aibar, S., Gonzalez-Blas, C. B., Moerman, T., Huynh-Thu, V. A., Imrichova, H., Hulselmans, G., et al. (2017). SCENIC: single-cell regulatory network inference and clustering. *Nat. Methods* 14, 1083–1086. doi: 10.1038/nmeth.4463
- Ariss, M. M., Islam, A., Critcher, M., Zappia, M. P., and Frolov, M. V. (2018). Single cell RNA-sequencing identifies a metabolic aspect of apoptosis in Rbf mutant. *Nat. Commun.* 9:5024.
- Bajgar, A., Kucerova, K., Jonatova, L., Tomcala, A., Schneedorferova, I., Okrouhlik, J., et al. (2015). Extracellular adenosine mediates a systemic metabolic switch during immune response. *PLoS Biol.* 13:e1002135. doi: 10.1371/journal.pbio.1002135
- Banerjee, U., Girard, J. R., Goins, L. M., and Spratford, C. M. (2019). *Drosophila* as a genetic model for hematopoiesis. *Genetics* 211, 367–417.
- Bazzi, W., Cattenoz, P. B., Delaporte, C., Dasari, V., Sakr, R., Yuasa, Y., et al. (2018). Embryonic hematopoiesis modulates the inflammatory response and larval hematopoiesis in *Drosophila*. *Elife* 7:e34890.
- Bernardoni, R., Vivancos, V., and Giangrande, A. (1997). glide/gcm is expressed and required in the scavenger cell lineage. *Dev. Biol.* 191, 118–130. doi: 10.1006/dbio.1997.8702
- Bhave, G., Cummings, C. F., Vanacore, R. M., Kumagai-Cresse, C., Ero-Tolliver, I. A., Rafi, M., et al. (2012). Peroxidase forms sulfilimine chemical bonds using hypohalous acids in tissue genesis. *Nat. Chem. Biol.* 8, 784–790. doi: 10.1038/nchembio.1038
- Binggeli, O., Neyen, C., Poidevin, M., and Lemaitre, B. (2014). Prophenoxidase activation is required for survival to microbial infections in *Drosophila*. *PLoS Pathogens* 10:e1004067. doi: 10.1371/journal.ppat.1004067
- Braun, A., Lemaitre, B., Lanot, R., Zachary, D., and Meister, M. (1997). *Drosophila* immunity: analysis of larval hemocytes by P-element-mediated enhancer trap. *Genetics* 147, 623–634. doi: 10.1093/genetics/147.2.623
- Brunet Avalos, C., Maier, G. L., Bruggmann, R., and Sprecher, S. G. (2019). Single cell transcriptome atlas of the *Drosophila* larval brain. *Elife* 8:e50354.
- Buchon, N., Silverman, N., and Cherry, S. (2014). Immunity in *Drosophila melanogaster*—from microbial recognition to whole-organism physiology. *Nat. Rev. Immunol.* 14, 796–810. doi: 10.1038/nri3763
- Busygina, V., Kottemann, M. C., Scott, K. L., Plon, S. E., and Bale, A. E. (2006). Multiple endocrine neoplasia type 1 interacts with forkhead transcription factor CHES1 in DNA damage response. *Cancer Res.* 66, 8397–8403. doi: 10.1158/0008-5472.can-06-0061
- Butler, A., Hoffman, P., Smibert, P., Papalexis, E., and Satija, R. (2018). Integrating single-cell transcriptomic data across different conditions, technologies, and species. *Nat. Biotechnol.* 36, 411–420. doi: 10.1038/nbt.4096
- Cattenoz, P. B., Sakr, R., Pavlidaki, A., Delaporte, C., Riba, A., Molina, N., et al. (2020). Temporal specificity and heterogeneity of *Drosophila* immune cells. *EMBO J.* 39:e104486.
- Chahine, S., and O'Donnell, M. J. (2009). Physiological and molecular characterization of methotrexate transport by Malpighian tubules of adult

FUNDING

This work was supported by INSERM, CNRS, UDS, Ligue Régionale contre le Cancer, Hôpital de Strasbourg, ARC, CEFIPRA, ANR grants and by the CNRS/University LIA Calim. AP was an IGBMC International Ph.D. Program fellow supported by LabEx INRT funds. SM benefits from a CEFIPRA fellowship. The IGBMC was also supported by a French state fund through the ANR labex.

ACKNOWLEDGMENTS

We thank the Imaging Center of the IGBMC for technical assistance. This study was supported by the grant ANR-10-LABX-0030-INRT, a French State fund managed by the Agence Nationale de la Recherche under the frame program Investissements d'Avenir ANR-10-IDEX-0002-02. We thank I. Ando, J. Shim, D. Siekhaus for providing fly stocks and antibodies. In addition, stocks obtained from the Bloomington *Drosophila* Stock Center (NIH P40D018537) as well as antibodies obtained from the Developmental Studies Hybridoma Bank created by the NICHD of the NIH and maintained at The University of Iowa (Department of Biology, Iowa City, IA 52242) were used in this study. We thank Dr. A. Riba for his assistance in the regulon analysis, C. Delaporte for technical assistance, R. Sakr, T. Boutet, and C. Riet for critical reading of the manuscript.

SUPPLEMENTARY MATERIAL

The Supplementary Material for this article can be found online at: <https://www.frontiersin.org/articles/10.3389/fcell.2021.643712/full#supplementary-material>

- Drosophila melanogaster*. *J. Insect Physiol.* 55, 927–935. doi: 10.1016/j.jinsectphys.2009.06.005
- Chintapalli, V. R., Wang, J., and Dow, J. A. (2007). Using FlyAtlas to identify better *Drosophila melanogaster* models of human disease. *Nat. Genet.* 39, 715–720. doi: 10.1038/ng2049
- Cho, B., Yoon, S. H., Lee, D., Koranteng, F., Tattikota, S. G., Cha, N., et al. (2020). Single-cell transcriptome maps of myeloid blood cell lineages in *Drosophila*. *Nat. Commun.* 11:4483.
- Cocanougher, B., Wittenbach, J., Long, X. S., Kohn, A., Norekian, T., Yan, J., et al. (2019). Comparative single-cell transcriptomics of complete insect nervous systems. *bioRxiv [Preprint]* doi: 10.1101/785931
- Comber, K., Huelsmann, S., Evans, I., Sanchez-Sanchez, B. J., Chalmers, A., Reuter, R., et al. (2013). A dual role for the betaPS integrin myospheroid in mediating *Drosophila embryonic* macrophage migration. *J. Cell Sci.* 126(Pt 15), 3475–3484. doi: 10.1242/jcs.129700
- Dionne, M. S., Pham, L. N., Shirasu-Hiza, M., and Schneider, D. S. (2006). Akt and FOXO dysregulation contribute to infection-induced wasting in *Drosophila*. *Curr. Biol.* 16, 1977–1985. doi: 10.1016/j.cub.2006.08.052
- Dolezal, T. (2015). Adenosine: a selfish-immunity signal? *Oncotarget* 6, 32307–32308. doi: 10.18632/oncotarget.4685
- Dostalova, A., Rommelaere, S., Poidevin, M., and Lemaitre, B. (2017). Thioester-containing proteins regulate the Toll pathway and play a role in *Drosophila* defence against microbial pathogens and parasitoid wasps. *BMC Biol.* 15:79.
- Edgar, B. A., and O'Farrell, P. H. (1990). The three postblastoderm cell cycles of *Drosophila* embryogenesis are regulated in G2 by string. *Cell* 62, 469–480. doi: 10.1016/0092-8674(90)90012-4
- Erickson, M. R. S., Galletta, B. J., and Abmayr, S. M. (1997). *Drosophila* myoblast city encodes a conserved protein that is essential for myoblast fusion, dorsal closure, and cytoskeletal organization. *J. Cell Biol.* 138, 589–603. doi: 10.1083/jcb.138.3.589
- Fleury, F., Gibert, P., Ris, N., and Allemand, R. (2009). Ecology and life history evolution of frugivorous *drosophila* parasitoids. *Adv. Parasitol.* 70, 3–44. doi: 10.1016/S0065-308X(09)70001-6
- Franc, N. C., Dimarçq, J. L., Lagueux, M., Hoffmann, J., and Ezekowitz, R. A. (1996). Croquemort, a novel *Drosophila* hemocyte/macrophage receptor that recognizes apoptotic cells. *Immunity* 4, 431–443. doi: 10.1016/S1074-7613(00)80410-0
- Fu, Y., Huang, X., Zhang, P., van de Leemput, J., and Han, Z. (2020). Single-cell RNA sequencing identifies novel cell types in *Drosophila* blood. *J. Genet. Genomics* 47, 175–186. doi: 10.1016/j.jgg.2020.02.004
- Gao, M., Ling, M., Tang, X., Wang, S., Xiao, X., Qiao, Y., et al. (2020). Comparison of high-throughput single-cell RNA sequencing data processing pipelines. *bioRxiv [Preprint]* doi: 10.1101/2020.02.09.940221
- Gautier, E. L., Shay, T., Miller, J., Greter, M., Jakubzick, C., Ivanov, S., et al. (2012). Gene-expression profiles and transcriptional regulatory pathways that underlie the identity and diversity of mouse tissue macrophages. *Nat. Immunol.* 13, 1118–1128. doi: 10.1038/ni.2419
- Gavet, O., and Pines, J. (2010). Activation of cyclin B1-Cdk1 synchronizes events in the nucleus and the cytoplasm at mitosis. *J. Cell Biol.* 189, 247–259. doi: 10.1083/jcb.200909144
- Gold, K. S., and Bruckner, K. (2014). *Drosophila* as a model for the two myeloid blood cell systems in vertebrates. *Exp. Hematol.* 42, 717–727. doi: 10.1016/j.exphem.2014.06.002
- Goto, A., Kumagai, T., Kumagai, C., Hirose, J., Narita, H., Mori, H., et al. (2001). A *Drosophila* haemocyte-specific protein, hemolectin, similar to human von willebrand factor. *Biochem. J.* 359(Pt 1), 99–108. doi: 10.1042/0264-6021:3590099
- Guilliams, M., Thierry, G. R., Bonnardel, J., and Bajenoff, M. (2020). Establishment and maintenance of the macrophage niche. *Immunity* 52, 434–451. doi: 10.1016/j.immuni.2020.02.015
- Gumeni, S., Evangelakou, Z., Tsakiri, E. N., Scorrano, L., and Trougakos, I. P. (2019). Functional wiring of proteostatic and mitostatic modules ensures transient organismal survival during imbalanced mitochondrial dynamics. *Redox Biol.* 24:101219. doi: 10.1016/j.redox.2019.101219
- Gyoergy, A., Roblek, M., Ratheesh, A., Valoskova, K., Belyaeva, V., Wachner, S., et al. (2018). Tools allowing independent visualization and genetic manipulation of *Drosophila melanogaster* macrophages and surrounding tissues. *G3* 8, 845–857. doi: 10.1534/g3.117.300452
- Handke, B., Poernbacher, I., Goetze, S., Ahrens, C. H., Omasits, U., Marty, F., et al. (2013). The hemolymph proteome of fed and starved *Drosophila larvae*. *PLoS One* 8:e67208. doi: 10.1371/journal.pone.0067208
- Holz, A., Bossinger, B., Strasser, T., Janning, W., and Klapper, R. (2003). The two origins of hemocytes in *Drosophila*. *Development* 130, 4955–4962. doi: 10.1242/dev.00702
- Honti, V., Kurucz, E., Csordas, G., Laurinyecz, B., Markus, R., and Ando, I. (2009). In vivo detection of lamellocytes in *Drosophila melanogaster*. *Immunol. Lett.* 126, 83–84. doi: 10.1016/j.imlet.2009.08.004
- Iijima, K., Zhao, L., Shenton, C., and Iijima-Ando, K. (2009). Regulation of energy stores and feeding by neuronal and peripheral CREB activity in *Drosophila*. *PLoS One* 4:e8498. doi: 10.1371/journal.pone.0008498
- Irving, P., Ubeda, J. M., Doucet, D., Troxler, L., Lagueux, M., Zachary, D., et al. (2005). New insights into *Drosophila larval* haemocyte functions through genome-wide analysis. *Cell Microbiol.* 7, 335–350. doi: 10.1111/j.1462-5822.2004.00462.x
- Jung, S. H., Evans, C. J., Uemura, C., and Banerjee, U. (2005). The *Drosophila* lymph gland as a developmental model of hematopoiesis. *Development* 132, 2521–2533. doi: 10.1242/dev.01837
- Karaiskos, N., Wahle, P., Alles, J., Boltengagen, A., Ayoub, S., Kipar, C., et al. (2017). The *Drosophila* embryo at single-cell transcriptome resolution. *Science* 358, 194–199.
- Kester, L., and van Oudenaarden, A. (2018). Single-cell transcriptomics meets lineage tracing. *Cell Stem Cell* 23, 166–179. doi: 10.1016/j.stem.2018.04.014
- Kim-Jo, C., Gatti, J. L., and Poirie, M. (2019). *Drosophila* cellular immunity against parasitoid wasps: a complex and time-dependent process. *Front. Physiol.* 10:603.
- Kocks, C., Cho, J. H., Nehme, N., Ulvila, J., Pearson, A. M., Meister, M., et al. (2005). Eater, a transmembrane protein mediating phagocytosis of bacterial pathogens in *Drosophila*. *Cell* 123, 335–346. doi: 10.1016/j.cell.2005.08.034
- Kolde, R. (2019). *heatmap: Pretty Heatmaps*. Available online at: <https://CRAN.R-project.org/package=heatmap>
- Kurucz, E., Markus, R., Zsamboki, J., Folk-Medzihradzsky, K., Darula, Z., Vilmos, P., et al. (2007). Nimrod, a putative phagocytosis receptor with EGF repeats in *Drosophila* plasmotocytes. *Curr. Biol.* 17, 649–654. doi: 10.1016/j.cub.2007.02.041
- Kurucz, E., Zettervall, C. J., Sinka, R., Vilmos, P., Pivarsci, A., Ekengren, S., et al. (2003). Hemese, a hemocyte-specific transmembrane protein, affects the cellular immune response in *Drosophila*. *Proc. Natl. Acad. Sci. U.S.A.* 100, 2622–2627.
- Kussel, P., and Frasch, M. (1995). Pendulin, a *drosophila* protein with cell cycle-dependent nuclear-localization, is required for normal-cell proliferation. *J. Cell Biol.* 129, 1491–1507.
- La Marca, J. E., and Richardson, H. E. (2020). Two-faced: roles of JNK signalling during tumorigenesis in the *drosophila* model. *Front. Cell Dev. Biol.* 8:42.
- Laneve, P., Delaporte, C., Trebuchet, G., Komonyi, O., Flici, H., Popkova, A., et al. (2013). The Gcm/Glide molecular and cellular pathway: new actors and new lineages. *Dev. Biol.* 375, 65–78.
- Lavin, Y., Winter, D., Blecher-Gonen, R., David, E., Keren-Shaul, H., Merad, M., et al. (2014). Tissue-resident macrophage enhancer landscapes are shaped by the local microenvironment. *Cell* 159, 1312–1326.
- Lemaitre, B., Meister, M., Govind, S., Georgel, P., Steward, R., Reichhart, J. M., et al. (1995). Functional-analysis and regulation of nuclear import of dorsal during the immune-response in *Drosophila*. *Embo J.* 14, 536–545.
- Luo, H., Hanratty, W. P., and Dearolf, C. R. (1995). An amino-acid substitution in the *drosophila* hop(Tum-L) jak kinase causes leukemia-like hematopoietic defects. *Embo J.* 14, 1412–1420.
- Makki, R., Meister, M., Pennetier, D., Ubeda, J. M., Braun, A., Daburon, V., et al. (2010). A short receptor downregulates JAK/STAT signalling to control the *Drosophila* cellular immune response. *PLoS Biol.* 8:e1000441.
- Manaka, J., Kuraishi, T., Shiratsuchi, A., Nakai, Y., Higashida, H., Henson, P., et al. (2004). Draper-mediated and phosphatidylserine-independent phagocytosis of apoptotic cells by *Drosophila* hemocytes/macrophages. *J. Biol. Chem.* 279, 48466–48476.
- Mandal, L., Martinez-Agosto, J. A., Evans, C. J., Hartenstein, V., and Banerjee, U. (2007). A Hedgehog- and Antennapedia-dependent niche maintains *Drosophila* haematopoietic precursors. *Nature* 446, 320–324.

- Mann, H. B., and Whitney, D. R. (1947). On a test of whether one of two random variables is stochastically larger than the other. *Ann. Math. Stat.* 18, 50–60.
- Markus, R., Kurucz, T., Rus, F., and Ando, I. (2005). Sterile wounding is a minimal and sufficient trigger for a cellular immune response in *Drosophila melanogaster*. *Immunol. Lett.* 101, 108–111.
- Moretton, A., and Loizou, J. I. (2020). Interplay between cellular metabolism and the DNA damage response in cancer. *Cancers* 12:2051.
- Mosca, T. J., Hong, W., Dani, V. S., Favaloro, V., and Luo, L. (2012). Trans-synaptic Teneurin signalling in neuromuscular synapse organization and target choice. *Nature* 484, 237–241.
- Nelson, R. E., Fessler, L. I., Takagi, Y., Blumberg, B., Keene, D. R., Olson, P. F., et al. (1994). Peroxidase: a novel enzyme-matrix protein of *Drosophila* development. *EMBO J.* 13, 3438–3447.
- Paladi, M., and Tepass, U. (2004). Function of Rho GTPases in embryonic blood cell migration in *Drosophila*. *J. Cell Sci.* 117(Pt 26), 6313–6326.
- Potter, S. S. (2018). Single-cell RNA sequencing for the study of development, physiology and disease. *Nat. Rev. Nephrol.* 14, 479–492.
- Rahman, M. M., Sykiotis, G. P., Nishimura, M., Bodmer, R., and Bohmann, D. (2013). Declining signal dependence of Nrf2-MafS-regulated gene expression correlates with aging phenotypes. *Aging Cell* 12, 554–562.
- Rizki, M. T., and Rizki, R. M. (1959). Functional significance of the crystal cells in the larva of *Drosophila melanogaster*. *J. Biophys. Biochem. Cytol.* 5, 235–240.
- Rizki, T. M., and Rizki, R. M. (1980). Properties of the larval hemocytes of *Drosophila melanogaster*. *Experientia* 36, 1223–1226.
- Rus, F., Kurucz, E., Markus, R., Sinenko, S. A., Laurinyecz, B., Pataki, C., et al. (2006). Expression pattern of Filamin-240 in *Drosophila* blood cells. *Gene Expr. Patterns* 6, 928–934.
- Sam, S., Leise, W., and Hoshizaki, D. K. (1996). The serpent gene is necessary for progression through the early stages of fat-body development. *Mech. Dev.* 60, 197–205. doi: 10.1016/S0925-4773(96)00615-6
- Schindelin, J., Arganda-Carreras, I., Frise, E., Kaynig, V., Longair, M., Pietzsch, T., et al. (2012). Fiji: an open-source platform for biological-image analysis. *Nat. Methods* 9, 676–682. doi: 10.1038/nmeth.2019
- See, P., Lum, J., Chen, J. M., and Ginhoux, F. (2018). A single-cell sequencing guide for immunologists. *Front. Immunol.* 9:2425. doi: 10.3389/fimmu.2018.02425
- Shahab, J., Baratta, C., Scuric, B., Godt, D., Venken, K. J., and Ringuette, M. J. (2015). Loss of SPARC dysregulates basal lamina assembly to disrupt larval fat body homeostasis in *Drosophila melanogaster*. *Dev. Dyn.* 244, 540–552. doi: 10.1002/dvdy.24243
- Siekhaus, D., Haesemeyer, M., Moffitt, O., and Lehmann, R. (2010). RhoL controls invasion and Rap1 localization during immune cell transmigration in *Drosophila*. *Nat. Cell Biol.* 12, 605–610. doi: 10.1038/ncb2063
- Stevens, L. J., and Page-McCaw, A. (2012). A secreted MMP is required for reepithelialization during wound healing. *Mol. Biol. Cell* 23, 1068–1079. doi: 10.1091/mbc.e11-09-0745
- Stuart, T., Butler, A., Hoffman, P., Hafemeister, C., Papalexi, E., Mauck, W. M., et al. (2019). Comprehensive integration of single-cell data. *Cell* 188:e1821. doi: 10.1016/j.cell.2019.05.031
- Sunkel, C. E., and Glover, D. M. (1988). polo, a mitotic mutant of *Drosophila* displaying abnormal spindle poles. *J. Cell Sci.* 89(Pt 1), 25–38.
- Tang, X., and Zhou, B. (2013). Ferritin is the key to dietary iron absorption and tissue iron detoxification in *Drosophila melanogaster*. *FASEB J.* 27, 288–298. doi: 10.1096/fj.12-213595
- Tattikota, S. G., Cho, B., Liu, Y., Hu, Y., Barrera, V., Steinbaugh, M. J., et al. (2020). A single-cell survey of *Drosophila* blood. *Elife* 9:e54818. doi: 10.7554/eLife.54818.sa2
- Telfer, W. H., and Kunkel, J. G. (1991). The function and evolution of insect storage hexamers. *Annu. Rev. Entomol.* 36, 205–228. doi: 10.1146/annurev.en.36.010191.001225
- Tepass, U., Fessler, L. I., Aziz, A., and Hartenstein, V. (1994). Embryonic origin of hemocytes and their relationship to cell-death in *Drosophila*. *Development* 120, 1829–1837.
- Tiebe, M., Lutz, M., De La Garza, A., Buechling, T., Boutros, M., and Teleman, A. A. (2015). REPTOR and REPTOR-BP regulate organismal metabolism and transcription downstream of TORC1. *Dev. Cell* 33, 272–284. doi: 10.1016/j.devcel.2015.03.013
- Tokusumi, T., Sorrentino, R. P., Russell, M., Ferrarese, R., Govind, S., and Schulz, R. A. (2009). Characterization of a lamellocyte transcriptional enhancer located within the misshapen gene of *Drosophila melanogaster*. *PLoS One* 4:e6429. doi: 10.1371/journal.pone.0006429
- Van De Bor, V., Zimniak, G., Papone, L., Cerezo, D., Malbouyres, M., Juan, T., et al. (2015). Companion blood cells control ovarian stem cell niche microenvironment and homeostasis. *Cell Rep.* 13, 546–560. doi: 10.1016/j.celrep.2015.09.008
- van de Laar, L., Saelens, W., De Prijck, S., Martens, L., Scott, C. L., Van Isterdael, G., et al. (2016). Yolk sac macrophages, fetal liver, and adult monocytes can colonize an empty niche and develop into functional tissue-resident macrophages. *Immunity* 44, 755–768. doi: 10.1016/j.immuni.2016.02.017
- Vieth, B., Parekh, S., Ziegenhain, C., Enard, W., and Hellmann, I. (2019). A systematic evaluation of single cell RNA-seq analysis pipelines. *Nat. Commun.* 10:4667. doi: 10.1038/s41467-019-12266-7
- Villanueva, R. A. M., and Chen, Z. J. (2019). ggplot2: elegant graphics for data analysis, 2nd edition. *Meas. Interdisciplinary Res. Perspect.* 17, 160–167. doi: 10.1080/15366367.2019.1565254
- Waltzer, L., Ferjoux, G., Bataille, L., and Haenlin, M. (2003). Cooperation between the GATA and RUNX factors serpent and lozenge during *Drosophila* hematopoiesis. *EMBO J.* 22, 6516–6525. doi: 10.1093/emboj/cdg622
- Wood, W., and Jacinto, A. (2007). *Drosophila melanogaster* embryonic haemocytes: masters of multitasking. *Nat. Rev. Mol. Cell Biol.* 8, 542–551. doi: 10.1038/nrm2202
- Yoon, S., Cho, B., Shin, M., Koranteng, F., Cha, N., and Shim, J. (2017). Iron homeostasis controls myeloid blood cell differentiation in *Drosophila*. *Mol. Cells* 40, 976–985.
- Zanet, J., Stramer, B., Millard, T., Martin, P., Payre, F., and Plaza, S. (2009). Fascin is required for blood cell migration during *Drosophila* embryogenesis. *Development* 136, 2557–2565. doi: 10.1242/dev.036517

Conflict of Interest: The authors declare that the research was conducted in the absence of any commercial or financial relationships that could be construed as a potential conflict of interest.

Copyright © 2021 Cattenoz, Monticelli, Pavlidaki and Giangrande. This is an open-access article distributed under the terms of the Creative Commons Attribution License (CC BY). The use, distribution or reproduction in other forums is permitted, provided the original author(s) and the copyright owner(s) are credited and that the original publication in this journal is cited, in accordance with accepted academic practice. No use, distribution or reproduction is permitted which does not comply with these terms.

Résumé en français suivi des mots-clés en français

Insérer votre résumé en français (1000 caractères maximum) suivi des mots-clés en français

La réponse immunitaire est un mécanisme ancestral des organismes vivants et les voies moléculaires contrôlant l'hématopoïèse sont conservées. Le facteur de transcription Gcm est exprimé et requis dans la glie et les hémocytes des mouches, les cellules charognards agissant à l'intérieur et à l'extérieur du système nerveux central (SNC). Notre laboratoire a montré que dans les hémocytes, Gcm agit comme un inhibiteur de la voie JAK/STAT. Mon objectif était d'évaluer le rôle et la conservation évolutive du gène gcm dans le système immunitaire des mammifères. J'ai utilisé un modèle de souris mutant pour mGcm2 des cellules immunitaires du SNC, microglies. Mes résultats ont montré que mGcm2 est exprimé dans le cerveau âgé de souris. De plus, la microglie mutante mGcm2 montre une morphologie pro-inflammatoire et une expression de gènes pro-inflammatoires accrues par rapport au témoin. Ces résultats suggèrent que chez les mammifères, le Gcm possède de propriétés anti-inflammatoires.

Mots clés : microglie, inflammation, vieillissement, conservation évolutive

Résumé en anglais suivi des mots-clés en anglais

Insérer votre résumé en anglais (1000 caractères maximum) suivi des mots-clés en anglais

The immune response is an ancestral mechanism of living organisms and the molecular pathways controlling hematopoiesis are extremely conserved. The transcription factor Gcm is expressed and required in fly glia as well as in hemocytes, the scavenger cells acting within and outside the Central Nervous System (CNS). Our lab previously showed that in hemocytes Gcm acts as an inhibitor of the JAK/STAT and of the TOLL pathway, the latter through a novel mechanism. My aim was to assess the role and the evolutionary conservation of the gcm gene in the immune system of mammals. For this reason, I used a conditional knock out mouse model to specifically delete mGcm2 from the immune cells of the CNS, called microglia. My results showed that mGcm2 is expressed in the aged brain of mice. Furthermore, mGcm2 mutant microglia show increased pro-inflammatory morphology and expression of pro-inflammatory genes compared to the control. These results suggest that as in the flies also in mammals Gcm has important anti-inflammatory properties.

Keywords : microglia, inflammation, aging, evolutionary conservation